9.1 RESERVOIR SIMULATION

Saibal Bhattacharya, Martin K. Dubois and Alan P. Byrnes

Overview

Reservoir simulations were performed in four areas in the Hugoton-Panoma fields in southwest Kansas and northwest Oklahoma: Alexander, Flower, Graskell, and Hoobler (Figure 9.1.1 and Table 9.1.1). The only two other Hugoton simulation studies that have been published in the entire 6,000 square mile area are by Phillips (Fetkovich et al., 1994) and Mobil (Oberst et al., 1994), also shown in Figure 9.1.1 and Table 9.1.1. Our work is the first to treat the Hugoton (Chase Group) and Panoma (Council Grove Group), as one large reservoir system, something we feel is especially critical in correctly simulating the Council Grove. Both earlier simulations treated the reservoirs as layered flow units (marine carbonate formation or members of the Chase Group) separated by no-flow layers (continental siltstone formations or members). Both concluded that the "pay" zones, the marine carbonates, were differentially depleted.

The principal objectives to the simulation studies were threefold:

1. Validate properties in the static model for the Chase and Council Grove reservoir system.
2. Characterize and quantify remaining gas.
3. Project and estimate production forward.

Our static modeling and simulation techniques evolved over a two-year period as we embarked on an ambitious project to build a multilayer lithofacies-specific reservoir property model for the Hugoton and Panoma in Kansas and Oklahoma. One of the primary goals for the simulation exercises was to validate the static model. The simulation and model building exercises were, therefore, intertwined and iterative.

It became readily apparent that performance history of the Council Grove well could not be effectively simulated until the Chase and Council Grove reservoirs were modeled as one system (Bhattacharya et al., 2004). In this study, we used a simple one-section model (one square mile) with core-derived lithofacies and properties for the Council Grove that were extended uniformly in layers across the entire section. No core was available in the Chase. For geomodel development, we utilized neural networks trained (Geomod 2 version) only on Council Grove lithofacies to estimate lithofacies in the Chase. Log porosity was upscaled from the Alexander D-2 and porosity-permeability and water saturation estimation algorithms were used to populate the Chase layers with uniform properties.

The Flower model and simulation was chosen next to take advantage of its very high quality core and pressure test data. In this 3 by 3 mile (9-square-mile) area simulation study we used a more rigorously built static model where lithofacies were estimated at node wells using neural networks trained on Council Grove and a limited amount of Chase core (Geomod 3 version). A finely layered static model (234 layers) covering 70 square miles was constructed in Petrel and the 3 by 3 mile Flower simulation model was

cut out of the larger model. We experimented with upscaling in this simulation by first upscaling to 69 layers and then to 25 layers. The latter is one layer per zone (formation or member) in the Chase and Council Grove. This study showed that simulation results were the same, giving us confidence in the upscaling methods employed. The model was successfully simulated with relatively good history matches for all but a few edge wells.

We employed similar static model and simulation strategy for the Graskell area, covering 12 square miles and involving 39 wells. Here again, a 70-square-mile area was modeled using a later version of Geomod 3 neural networks. The simulation area was cut out of the static model and upscaled to 25 layers for simulation. We were not as successful in this model and simulation exercise with roughly 40% of the wells being poorly matched, all of them falling in the southwest quadrant of the model. We attribute the shortfall being due primarily to less than adequate lithofacies and properties in the static model.

Our ultimate goal was to build a single static geomodel for the entire Wolfcamp system that is sufficiently robust to be accurate on a local scale. Ideally, areas to be simulated could then be extracted from any area in the model, upscaled, and simulated. This procedure was employed for the Hoobler simulation model where a 12-square-mile area was extracted from the 269-layer Geomod 4, a full-field, 109-million-cell model. The Hoobler study area differed from the other models because it is outside the Panoma field and where only the Hugoton (Chase) reservoir is productive. Although there is Council Grove production on the east side of the area simulated, it is separate from the Panoma and is associated with a downdip, closed structure rather than the Panoma stratigraphic trap.

The simulation exercises met their objectives. History matches were attained at most wells by modification of completion intervals and productivity gains as a result of hydraulic fracturing except in a portion of the Graskell area. Reservoir properties such as porosity, pay thickness, and initial saturations were not modified during the history-matching process. Figures 9.1.2 though 9.1.4 demonstrate the differential depletion phenomena noted by Fetkovich et al. (1994) and Oberst et al. (1994). However, when comparing the Flower and Hoobler with the Graskell, it is evident that the degree of depletion is not correlated with stratigraphic interval (zone). In the Flower area the zones with the lowest depletion include the Towanda, Fort Riley, Wreford, and several Council Grove zones, while zones with high permeability such as the Herington, Krider, and Winfield may be more than 90% depleted. In the Flower area, initially 85% of GIP was in the upper half of the Chase, but presently over 70% of the remaining gas resides in the lower half of the Chase and the upper half of the Council Grove, if our modeling and simulations are correct (Figure 9.1.5). In the Graskell area the relationships are reversed with the upper Chase being less depleted than the lower Chase (Figure 9.1.4). Table 9.1.2 summarizes overall production efficiency to the present time in the model areas. The Hoobler appears to have significantly more remaining gas as a percentage of original than the other two areas. Most of this “excess” gas is in the Towanda and Fort Riley that have not been completed in the Hoobler area. Simulated production projections suggest that the Hugoton-Panoma wells should be able to sustain economic levels of production for

many decades to come (Table 9.1.3). In the Flower model, production decline is hyperbolic as lower permeability zones contribute a higher and higher proportion of the produced gas. In the year 2050, the 28 wells in the model are projected to be producing a combined 600 mcfpd for an average 21 mcfpd per well. If the model is correct, the current wells could yield an additional 21 BCF over the nine-section area over a 45-year period, provided the well bore integrity can be maintained over that period for wells that are as much as 70 years old at present. Although 21 BCF is substantial, the present value of this gas spread over 45 years is not as impressive.

Relative Permeability

The relative permeability properties of Hugoton carbonates and siliciclastics are discussed in the Relative Permeability section of Chapter 4. To provide relative-permeability models for the geomodel construction, gas-water drainage relative-permeability data were compiled for 32 samples representing a range of lithofacies. These data did not test the relative permeability for rocks with absolute permeability k_{ik}<0.1 md and did not include an adequate population of continental fine- to coarse-grained siltstones. To model the continental and marine clastics, equations developed for other low-permeability clastics and summarized recently (Byrnes, 2005) were used.

In general, gas and water drainage relative permeability curves for the Hugoton samples reveal several characteristics similar to other low-permeability rocks. Table 4.2.9 summarizes measured drainage gas-water relative-permeability data for Hugoton rocks. The data primarily represent measurements on cores with absolute permeability greater than 0.5 md and half have permeability greater than 3 md. Figure 4.2.80 shows a summary of all the drainage gas relative-permeability curves. These curves exhibit similar subparallel trends. To model the gas relative-permeability, a modified Corey (1954) equation was used:

$$k_{rg} = (1 - (S_w\text{-}S_{wc,g})/(1\text{-}S_{gc}\text{-}S_{wc,g}))^{p} \, (1\text{-}((S_w\text{-}S_{wc,g})/(1\text{-}S_{wc,g}))^{q})$$

where S_w is fractional water saturation, S_{gc} is the fractional critical gas saturation, $S_{wc,g}$ is the fractional critical water saturation with respect to gas drainage (discussed below), and p and q are empirical exponents expressing the influence of pore-size distribution. For the Hugoton rock samples studied, the gas relative-permeability curves could be modeled using exponents of $\boldsymbol{p}$ = 1.3$\pm$0.4 (1 s.d.), $\boldsymbol{q}$ = 2, and $S_{wc,g}$ = 0.

To model gas relative permeability in the low-permeability sandstones and siltstones (k_{ik} < 1 md), trends developed for low-permeability rocks in other regions were used with the following empirical parameters:

$S_{wc,g} = 0.16 + 0.053*\log_{10}k_{ik}$ (for $k_{ik} \geq 0.001$ md)
$S_{wc,g} = 0$ (for k_{ik} <0.001 md)
$S_{gc} = 0.15 - 0.05*\log_{10}k_{ik}$
$\boldsymbol{p}$ = 1.7
$\boldsymbol{q}$ = 2

where $S_{wc,g}$ and S_{gc} are expressed in fractions and k_{ik} is expressed in md.

To model water relative-permeability, the following modified Corey (1954) equation was used:

$$k_{rw} = ((S_w - S_{wc})/(1 - S_{wc}))^q \, (k_w/k_{ik})$$

where q = 8.3 in the rocks with k > 0.01 md and q = 4 in rocks with k < 0.01 md.

For geomodel development in each of the four simulation studies (described in Sections 9.2 through 9.5) five relative permeability rock-types (RT) were defined: RT1 ($k \leq 0.0001$ md), RT2 ($0.0001 < k < 0.001$ md), RT3 ($0.001 < k < 0.01$ md), RT4 ($0.01 < k < 0.1$ md), and RT5 ($k > 0.1$ md) (Figures 9.1.6A to 9.1.6E). For rocks with k > 0.01 md, the carbonate parameters were used in the relative permeability equations for gas (***p*** = 1.3) and water (***q*** = 8.3). For rocks with k < 0.01 md the siliciclastic parameters were used for gas (***p*** = 1.7) and water (***q*** = 4). Rock-type and the corresponding relative-permeability table (Figures 9.1.6A to 9.1.6E) were assigned to each grid cell based on the absolute permeability of the cell. The same ***p*** parameter was used for both siliciclastics and carbonates with k < 0.01 md because a large number of data exist for siliciclastics and little relative permeability data were available for carbonates and an assumed ***p*** value equal to 1.7 is within one standard deviation of the ***p*** value measured for higher permeability carbonates (***p*** = 1.3±0.4, 1 s.d.). The use of the same ***p*** value for k > 0.1 md (***p*** = 1.3) was consistent with data measured on both siliciclastics and carbonates from the Hugoton, as discussed in Chapter 4. Figure 9.1.7 illustrates the different k_{rg} and k_{rw} curves for each rock type.

5 rock-types were selected to represent the basic classes of relative permeability. Rock-types 4 and 5 are identical for gas relative permeability but differ slightly in water relative-permeability properties. Rock-types 1, 2, and 3 exhibit a shift to lower k_{rg} with decreasing permeability at any given Sw consistent with low-permeability gas sandstone trends reported by Byrnes (2005). For rocks with k < 0.01 md the variance in gas relative-permeability is small for error in permeability assignment within approximately one order of magnitude. For rocks with k > 0.1 md, error in permeability assignment results in no change in k_{rg}. For these rocks the error in k_{rg} associated with uncertainty in the relative-permeability curve parameter ***p*** is greater than the error associated with permeability assignment and resulting rock-type assignment. Given the uncertainty in the gas relative permeability exponent, p, Figure 9.1.8 illustrates the range in possible k_{rg} for the first standard deviation (i.e., ***p*** = 0.9 and ***p*** = 1.7) and for the second standard deviation (***p*** = 0.5 and ***p*** = 2.1). The variance in k_{rg} decreases with decreasing water saturation.

Initial Saturation Estimation

A known and pervasive problem in the Hugoton and Panoma fields is the difficulty in estimating initial fluid saturations from wireline logs due to invasion effects. Thus, a set of facies- and porosity-specific capillary-pressure curves (refer to Figures

4.2.68 to 4.2.78 in Section 4) were developed using available core data to estimate the initial water saturations given a free-water-level (FWL). The above-mentioned capillary pressures were used to assign an initial S_w to each grid cell based on the estimated porosity, lithofacies, and height above FWL at the given location.

References:

Fetkovich, M. J., Ebbs, Jr., D. J., and Voelker, J. J., 1994, Multiwell, multilayer model to evaluate infill-drilling potential in the Oklahoma Hugoton field, SPE Reservoir Engineering, Aug. 1994, p. 162 – 168.

Oberst, R. J., Bansal P. P., Cohen M. F., and Ryan T. C., 1994, 3-D reservoir simulation results of a 25-square-mile study area in the Kansas Hugoton gas field, SPE 27931, SPE Mid continent Gas Symposium, Amarillo, TX.

Bhattacharya, S., Dubois M.K., and Byrnes A.P., 2004, Multi-well characterization and simulation – Chase and Council Grove reservoir systems, Kansas Geological Survey, Open-file Report 2004-67.

Byrnes, A.P., 2005, Permeability, capillary pressure, and relative permeability properties in low-permeability reservoirs and the influence of thin, high-permeability beds on production, *in* Gas in Low Permeability Reservoirs of the Rocky Mountain Region, Rocky Mountain Assoc. of Geologists 2005 Guidebook CD, M.G. Bishop, S.P. Cumella, J.W. Robinson, and M.R. Silverman eds., p. 69-108.

Corey, A. T., 1954, The interrelations between gas and oil relative permeabilities, Producers Monthly, v. 19 (Nov 1954), p. 38-41.

Area	County	Size (sq mi)	Wells	Reservoirs Simulated
Alexander	Grant	1	3	Chase and Council Grove
Flower	Stevens	9	28	Chase and Council Grove
Graskell	Grant-Haskell	12	39	Chase and Council Grove
Hoobler	Texas	12	14	Chase (no Council Grove production below)
Phillips	Texas	12	14	Chase (no Council Grove production below)
Mobil	Stevens	25	28	Chase (Council Grove production below)

Table 9.1.1. Simulations of record in the Hugoton-Panoma fields. The first four are part of the Hugoton Asset Management Project and were conducted over a two-year period (2004-2006). They are listed in order of completion. The next two are earlier published work.

Model	OGIP	Cum Gas	% Produced
Flower	179.3	123.7	69.0%
Graskell	170.6	109.1	64.0%
Hoobler	131.3	69.8	53.1%

Table 9.1.2 Overall production efficiency to present for the three multi section simulation models.

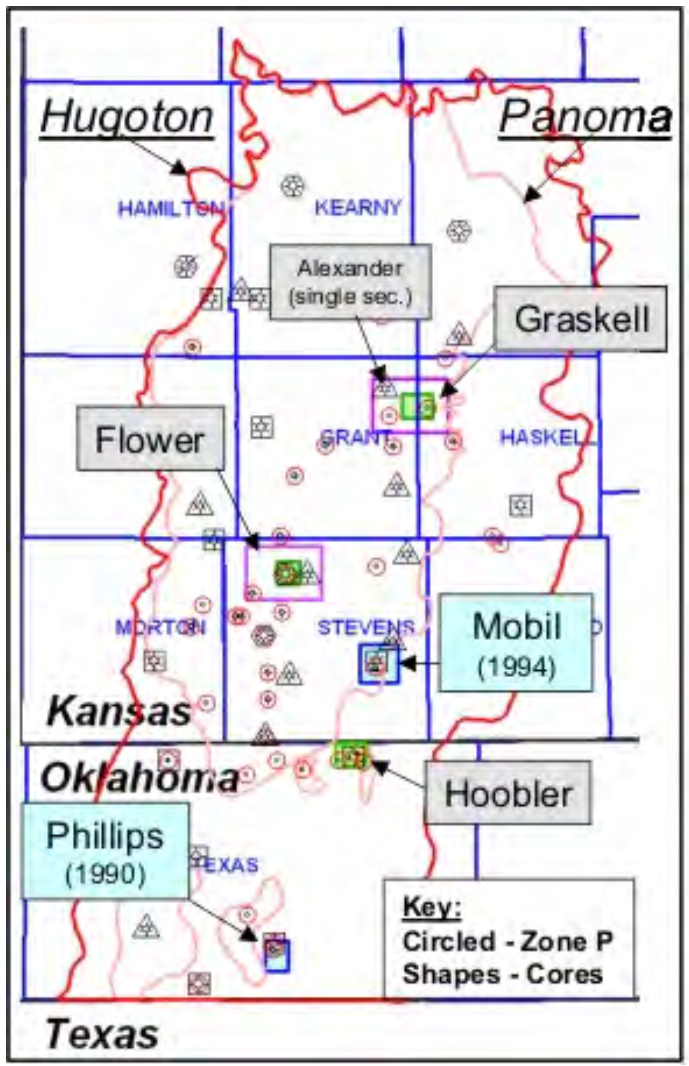

Figure 9.1.1. Simulations of record in the Hugoton-Panoma fields. The four in gray are part of the Hugoton Asset Management Project and were conducted over a two-year period (2004-2006). The other two are earlier published work.

	Formation / Member	LAYER	1937 Model P	1937 OGIP (BCF)	2005 Model P	2005 GIP (BCF)	2005 % Prod	2050 Model P	2050 GIP (BCF)	2050 % Prod
Chase	HRNGTN	1	423	**8.71**	58	1.04	88%	25	0.44	95%
	KRIDER	2	423	**41.7**	24	2.2	95%	15	1.4	97%
	ODELL	3	423	1.1	195	0.75	32%	110	0.5	55%
	WINF	4	423	**21.5**	68	**3.2**	85%	33	1.5	93%
	GAGE	5	423	**7.9**	130	2.2	72%	62	1.03	87%
	TOWANDA	6	423	**28.5**	122	**7.8**	73%	58	**3.6**	87%
	HOLMESVILLE	7	423	2.02	207	0.96	52%	124	0.64	68%
	FT RILEY	8	423	**21.3**	178	**8.4**	61%	92	**4.3**	80%
	L/FT RILEY	9	423	**7.3**	201	**3.2**	56%	105	**1.7**	77%
	MATFIELD	10	423	2.02	355	1.7	16%	259	1.2	41%
	WREFORD	11	423	**10.1**	285	**6.6**	35%	181	**4**	60%
Council Grove	A1_SH	12	423	0.3	377	0.3	0%	318	0.3	0%
	A1_LM	13	423	**4.9**	412	**4.8**	2%	380	**4.4**	10%
	B1_SH	14	423	0.55	359	0.51	7%	300	0.52	5%
	B1_LM	15	423	**4.5**	324	**3.3**	27%	247	**2.4**	47%
	B2_SH	16	423	0.18	311	0.41	NA*	235	0.49	NA*
	B2_LM	17	423	**5.2**	188	1.9	63%	135	1.18	77%
	B3_SH	18	423	0.0067	280	0.21	NA*	197	0.26	NA*
	B3_LM	19	423	1.02	296	0.69	32%	208	0.48	53%
	B4_SH	20	423	0.049	288	0.105	NA*	198	0.153	NA*
	B4_LM	21	423	1.4	239	0.72	49%	144	0.37	74%
	B5_SH	22	423	0.007	232	0.197	NA*	141	0.183	NA
	B5_LM	23	423	**7.3**	181	**2.7**	63%	105	1.5	79%
	C_SH	24	423	0.02	322	0.102	NA*	263	0.211	NA*
	C_LM	25	423	1.7	386	1.63	4%	326	1.5	12%
				179.3		**55.6**			**34.3**	***Remaining***
						69.0%			**80.9%**	***% Produced***

Dominately Silt NA* Silts desaturate and gain minor amount of gas

Figure 9.1.2 Pressures and GIP for the Flower simulation model through time.

	Formation / Member	LAYER	1941 Model P	1941 OGIP (BCF)	2005 Model P	2005 GIP (BCF)	2005 % Prod
Chase	HRNGTN	1	450	4.2	215	1.65	61%
	KRIDER	2	450	**30.9**	63.4	3.99	87%
	ODELL	3	450	0.012	136	0.079	NA*
	WINF	4	450	**23.1**	118	5.23	77%
	GAGE	5	450	1.9	291	2.38	NA*
	TOWANDA	6	450	**42.9**	300	**27.3**	36%
	HOLMESVILLE	7	450	3.04	325	2.07	32%
	FT RILEY	8	450	**25.2**	353	**18.8**	25%
	MATFIELD	9	450	0.009	370	0.009	0%
	WREFORD	10	450	0.0097	385	0.009	7%
Council Grove	A1_SH	11	450	0	391	0	0%
				131.3		**61.5**	***Remaining***
						53.1%	***% Produced***

Dominately Silt

NA* Silts desaturate and gain minor amount of gas

Figure 9.1.3 Pressures and GIP for the Hoobler simulation model through time.

	Formation / Member	LAYER	1946 Model P	1946 OGIP (BCF)	May 2004 Model P	May 2004 GIP (BCF)	May 2004 % Prod
Chase	HRNGTN	1	440	3.6	401	3.09	14%
	KRIDER	2	440	**12.1**	335	**9.05**	25%
	ODELL	3	440	3.6	346	2.7	25%
	WINF	4	440	**9.2**	263	**5.2**	43%
	GAGE	5	440	**9.3**	239	**4.7**	49%
	TOWANDA	6	440	**29.9**	136	**8.6**	71%
	HOLMESVILLE	7	440	2.9	165	1.02	65%
	FT RILEY	8	440	**43.9**	97	**9.1**	79%
	L/FT RILEY	9	440	**17.8**	95	**3.5**	80%
	MATFIELD	10	440	2.6	236	1.6	38%
	WREFORD	11	440	**17.6**	229	**8.7**	51%
Council Grove	A1_SH	12	440	1.5	252	0.93	38%
	A1_LM	13	440	**12.9**	154	**4.2**	67%
	B1_SH	14	440	0.2	347	0.3	NA*
	B1_LM	15	440	1.3	378	1.1	15%
	B2_SH	16	440	0.03	409	0.08	NA*
	B2_LM	17	440	0.9	421	0.85	6%
	B3_SH	18	440	0.07	431	0.11	NA*
	B3_LM	19	440	0.4	435	0.33	18%
	B4_SH	20	440	0.5	438	0.49	NA*
	B4_LM	21	440	0.07	442	0.09	NA*
	B5_SH	22	440	0.04	444	0.019	NA*
	B5_LM	23	440	0.2	448	0.193	4%
				170.6		**66.0**	***Remaining***
	Dominately Silt		**Model produced**	**104.7**		**61.3%**	***% Produced***
			Cum Gas May 2004	**109.1**		**63.9%**	***% Produced***

Note: Model was short on gas

NA* Silts desaturate and gain minor amount of gas

Figure 9.1.4 Pressures and GIP for the Flower simulation model through time. Since there were difficulties in well history matches the volumes and numbers should only be used in a relative sense.

	Formation / Member	LAYER	1937 %GIP	2005 %GIP	2050 %GIP	*1937-2005* Prod (BCF)	*2005-2050* Prod (BCF)
Chase	HRNGTN	1				**7.7**	0.6
	KRIDER	2				**39.5**	0.8
	ODELL	3				0.4	0.3
	WINF	4				**18.3**	**1.7**
	GAGE	5	**45%**	17%	14%	5.7	1.2
	TOWANDA	6				**20.7**	**4.2**
	HOLMESVILLE	7				1.1	0.3
	FT RILEY	8				**12.9**	**4.1**
	L/FT RILEY	9				4.1	**1.5**
	MATFIELD	10				0.3	0.5
	WREFORD	11	**40%**	**52%**	**45%**	3.5	**2.6**
Council Grove	A1_SH	12				0.0	0.0
	A1_LM	13				0.1	0.4
	B1_SH	14				0.0	0.0
	B1_LM	15				1.2	0.9
	B2_SH	16				-0.2	-0.1
	B2_LM	17				3.3	0.7
	B3_SH	18	9%	**21%**	**28%**	-0.2	-0.1
	B3_LM	19				0.3	0.2
	B4_SH	20				-0.1	0.0
	B4_LM	21				0.7	0.4
	B5_SH	22				-0.2	0.0
	B5_LM	23				4.6	1.2
	C_SH	24				-0.1	-0.1
	C_LM	25	6%	11%	13%	0.1	0.1
						123.7	**21.4**

Silts desaturate and gain minor amount of gas

Figure 9.1.5 Gas in place and gas produced through time for the Flower model.

A.

SW	KRW	KRG
0.2511	0.000000	0.4088
0.3000	0.000001	0.3179
0.3500	0.000016	0.2359
0.4000	0.000082	0.1657
0.4500	0.000262	0.1077
0.5000	0.000643	0.0622
0.5500	0.001337	0.0291
0.6000	0.002483	0.0082
0.6500	0.004242	0.0000
0.7000	0.006802	0.0000
0.7500	0.010378	0.0000
0.8000	0.015206	0.0000
0.8500	0.021550	0.0000
0.9000	0.029698	0.0000
0.9500	0.039963	0.0000
1.0000	0.052685	0.0000

Rock Type 1

K ≤ 0.0001 md

B.

SW	KRW	KRG
0.1285	0.000000	0.6986
0.1500	0.000000	0.6505
0.2000	0.000005	0.5434
0.2500	0.000041	0.4437
0.3000	0.000164	0.3525
0.3500	0.000458	0.2709
0.4000	0.001033	0.1996
0.4500	0.002031	0.1390
0.5000	0.003622	0.0895
0.5500	0.006001	0.0510
0.6000	0.009397	0.0235
0.6500	0.014063	0.0065
0.7000	0.020283	0.0000
0.7500	0.028369	0.0000
0.8000	0.038660	0.0000
0.8500	0.051527	0.0000
0.9000	0.067365	0.0000
0.9500	0.086600	0.0000
1.0000	0.109688	0.0000

Rock Type 2

0.0001 < K < 0.001 md

C.

SW	KRW	KRG
0.0657	0.000000	0.9714
0.1000	0.000000	0.8880
0.1500	0.000015	0.7688
0.2000	0.000098	0.6540
0.2500	0.000347	0.5453
0.3000	0.000906	0.4441
0.3500	0.001963	0.3517
0.4000	0.003753	0.2691
0.4500	0.006553	0.1972
0.5000	0.010688	0.1364
0.5500	0.016526	0.0870
0.6000	0.024481	0.0490
0.6500	0.035013	0.0223
0.7000	0.048624	0.0061
0.7500	0.065864	0.0000
0.8000	0.087327	0.0000
0.8500	0.113652	0.0000
0.9000	0.145523	0.0000
0.9500	0.183669	0.0000
1.0000	0.228865	0.0000

Rock Type 3

0.001 < K < 0.01 md

D.

SW	KRW	KRG
0.0150	0.000000	0.980323
0.0500	0.000000	0.933155
0.1000	0.000000	0.863278
0.1500	0.000000	0.791337
0.2000	0.000001	0.718271
0.2500	0.000004	0.644987
0.3000	0.000019	0.572359
0.3500	0.000070	0.501227
0.4000	0.000212	0.432390
0.4500	0.000563	0.366608
0.5000	0.001350	0.304595
0.5500	0.002978	0.247013
0.6000	0.006133	0.194472
0.6500	0.011917	0.147516
0.7000	0.022044	0.106617
0.7500	0.039083	0.072161
0.8000	0.066777	0.044426
0.8500	0.110449	0.023560
0.9000	0.177499	0.009523
0.9500	0.278028	0.001985
1.0000	0.425582	0.000001

Rock Type 4

0.01 < K < 0.1 md

Table 9.1.3. Relative-permeability tables for respective rock-types used in single- and multi-section simulation studies.

E.

SW	KRW	KRG
0.0150	0.000000	0.980323
0.0500	0.000000	0.933155
0.1000	0.000000	0.863278
0.1500	0.000000	0.791337
0.2000	0.000001	0.718271
0.2500	0.000005	0.644987
0.3000	0.000023	0.572359
0.3500	0.000082	0.501227
0.4000	0.000249	0.432390
0.4500	0.000662	0.366608
0.5000	0.001586	0.304595
0.5500	0.003499	0.247013
0.6000	0.007205	0.194472
0.6500	0.014001	0.147516
0.7000	0.025899	0.106617
0.7500	0.045917	0.072161
0.8000	0.078454	0.044426
0.8500	0.129761	0.023560
0.9000	0.208535	0.009523
0.9500	0.326643	0.001985
1.0000	0.499997	0.000001

Rock Type 5

K > 0.1 md

Table 9.1.3. Relative-permeability tables for respective rock-types used in single- and multi-section simulation studies.

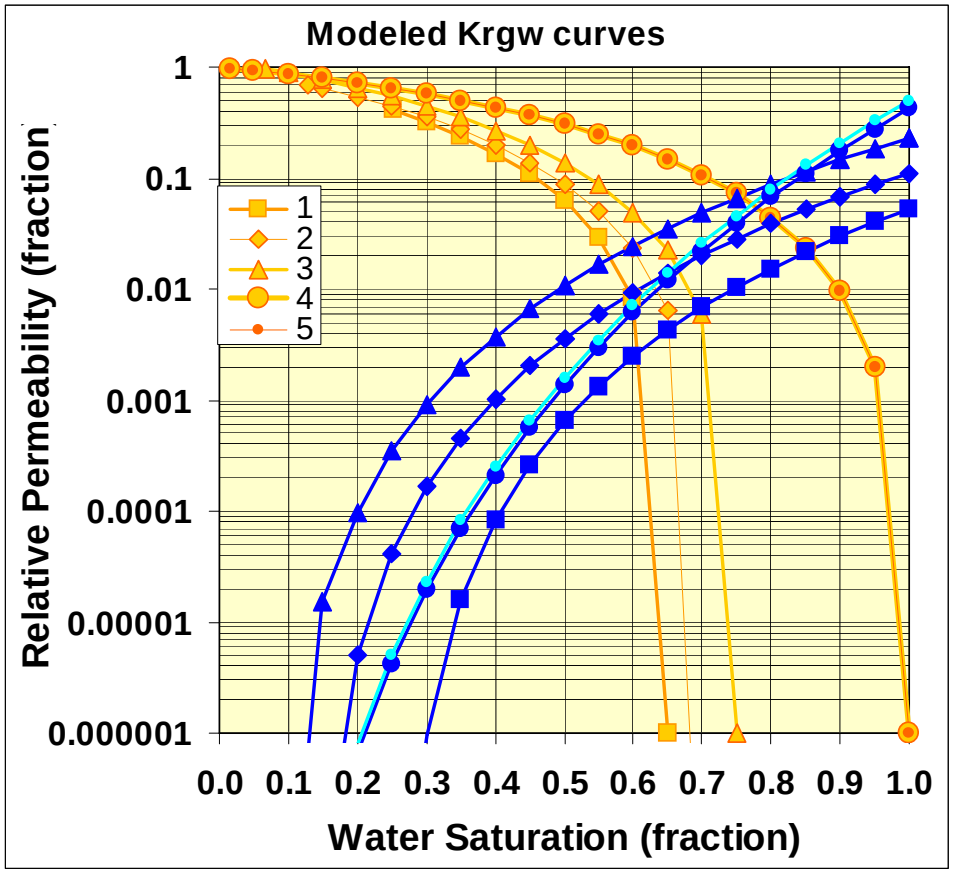

Figure 9.1.7. Gas and water relative-permeability curves for different rock-types.

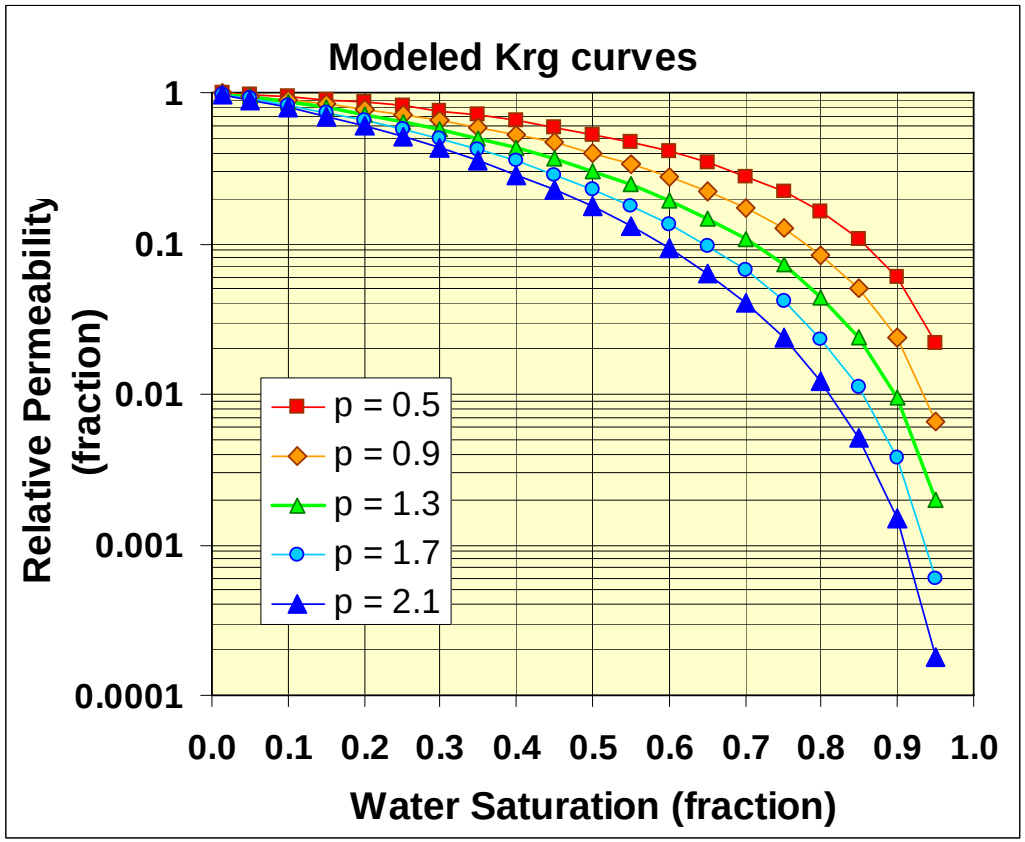

Figure 9.1.8. Range of possible gas relative-permeability values for first and second standard deviation.

9.2 SINGLE-SECTION SIMULATION – ALEXANDER D2

Saibal Bhattacharya, Martin K. Dubois and Alan P. Byrnes

Introduction

The Alexander D2 (D2) well (Figure 9.2.1A), is located in sec. 29, T. 27 S, R. 35 W., Grant County, Kansas. The well profile (Figure 9.2.1B) from D2 shows that the Chase reservoir overlies the Council Grove reservoir. In most producing sections of the Hugoton and Panoma fields, two wells produce from the Chase Group (Hugoton field) and a third produces from the Council Grove Group (Panoma field). Though the Chase (Hugoton) directly overlies the Council Grove (Panoma), the two fields are regulated as separate fields. Three stages of development that followed in these fields also can be traced in our study area and consist of the initial Hugoton well, the Alexander D1 well Hugoton "parent" followed by the Alexander D2, the Panoma well, and finally the Alexander D3, a Hugoton infill well.

The estimated bottom-hole shut-in pressures (BHSPs), calculated from surface buildups, at Alexander D1 (referred to here onward as D1) and Alexander D2 (referred to here onward as D2) wells are compared in Figure 9.2.2. The plot shows that only during the initial year-and-a-half did D2 record BHSPs that were slightly higher than recorded at D1. Thereafter, the BHSPs at D1 and D2 almost march in lock-step until 1991, when Alexander D3 came online. This type of congruence between bottom-hole shut-in pressures recorded in the Chase and Council Grove wells has been observed in other wells around D2 and over other parts of the Hugoton and Panoma fields leading to the speculation that these reservoirs are in hydraulic communication. This report summarizes the reservoir simulation studies carried out on 640 acres around the D1 and D2 wells, and models both the Chase and Council Grove reservoirs as one system.

Static Model

The principal properties required for reservoir simulation studies are porosity, permeability, and initial water saturation (Sw). However, because Sw cannot be accurately estimated from wireline logs due to deep filtrate invasion during drilling, Sw must be estimated based on lithofacies-dependent capillary-pressure relationships. Thus, projecting lithofacies in the 3D model space is a critical first step. For these exercises we have assumed that the layered flow-units of both the Council Grove and Chase are laterally continuous across the entire unit. Properties in the model vary between layers but not within layers. This assumption is based upon the general observation that the lateral scale of major lithofacies bodies is much greater than the scale of the production unit being modeled.

The main flow-units are relatively thin (2-10 m) marine carbonates that are separated by thin (2-10 m) nonmarine siltstones that have low permeability. The alternating layers were deposited as a series of stacked marine-nonmarine sedimentary cycles (Figure 9.2.1B). In the combined model (Chase and Council Grove), the 281 ft thick Chase Group was divided into 1-ft layers, but because the Chase interval was not

cored, lithofacies were predicted using a neural network model that was developed earlier (Dubois et al., 2003). Porosity at a 1-ft scale was derived from wireline logs and was corrected based upon empirical relationships to core data. Permeability and water saturations were estimated at the 1-ft scale given porosity and lithofacies using core-derived empirical relationships. Figure 9.2.1B shows the stratigraphic section for the Chase and Council Grove Groups with wireline log curves. Lithofacies are shown by color fill in this section. Original gas in place (OGIP) is property-based volumetric for a free water level = 55 ft above sea level and bottomhole pressure = 456 psi (calculated from an initial surface shut-in pressure of 420 psi).

Scale Dependency of Permeability

Permeability in both horizontal and vertical directions is very much scale dependent and the scale at which matrix permeability is measured, the 1-inch diameter plug scale, is at the low end of the scale. Matrix (core plug) permeability is the starting point for the static 3D model because these data are readily available and also because facies-specific capillary-pressure correlations used in water saturation estimates were developed from measurements taken on core plugs. Early in our simulation exercises, we discovered that plug-scale matrix permeability was insufficient for history matching reservoir performance and up to eight times matrix permeability was required. We have made some initial steps to provide geological explanations for the phenomena and a possible solution based on empirical data.

Available permeability measurements were at three scales: plug (Kp), whole-core (Kwc) cylinders (approximately 4 inches in diameter and 6 inches in length), and drill-stem-test flow-based permeability (Kdst). Kp is generally less than Kwc in low-permeability ranges and is equal to or lower than Kwc in high-permeability ranges. Figure 9.2.3 shows examples of two Council Grove lithofacies having both Kp and Kwc for the same sample. The very fine-grained nonmarine sandstone has relatively low permeability and Kwc is 4.5 times greater than Kp while the more permeable grainstone Kwc is only 1.2 times Kp. Unfortunately we currently have insufficient data to make direct comparisons of Kwc and Kp on like samples. A method for developing an equation for estimating a multiplier for the transformation of Kp to Kwc is illustrated in Figures 9.2.4 to 9.2.6. In Figure 9.2.4, permeability is plotted against porosity for both Kp and Kwc and an exponentially fitted trend line was generated for each set. The two lines intersect at approximately 16% porosity and 1 millidarcy (md) permeability, while at 10% porosity Kwc is 0.5 md, 8.3 times Kpc of 0.06 md. At very low permeability, Kwc is more than two orders of magnitude greater than Kp.

It would appear from work to date that whole-core permeability could be more appropriate than plug permeability, but this would imply that the microfracturing that is required for higher permeability in whole core is also present in the reservoir in all lithofacies and is pervasive and not merely induced in the whole core by the coring operation. Though not obvious or pervasive in core, some micro- and large-scale fractures are seen in the available cores. Figure 9.2.7 shows microfractures in a nonmarine siltstone paleosols. The 1994 photo is of the core very soon after being cored

using an underbalanced foam system to minimize filtrate invasion. Small microfractures, which may be outlines of peds, are barely visible in the 1994 photo but are readily apparent in the 2004 photo. Time (weathering) and handling have aided the disintegration. These microfractures may be natural and may have contributed to permeability at scales larger than plugs. Larger-scale vertical fractures partially filled with cement are common, though not abundant in nearly every carbonate layer in every core, but much less abundant in the nonmarine siltstones. These fractures likely provide additional permeability at scales larger than whole core.

A plot (Figure 9.2.8) of Kdst versus whole-core and plug permeability for the same interval shows consistently lower permeability than would be suggested by whole core. Further investigation is needed on this subject. In early models vertical permeability (Kv or Kz) was estimated at 0.1 times the horizontal permeability (Kxy). A plot of the ratio of Kv to maximum horizontal permeability (Kmax) versus Kmax for whole core is shown in Figure 9.2.9. The available core data suggest that a Kv/Kmax ratio of 0.25 may be more appropriate.

Reservoir Engineering Studies

Figure 9.2.10A shows the upscaled layer Sw, porosity, and permeability in Chase and Council Grove (CG) estimated by using plug-based permeability data. It becomes apparent from initial layer saturations that the Chase layers have more gas than the CG. Also, the significant Chase production is driven by higher prevalent layer permeabilities in the Chase layers than those in the CG layers. Following observations between whole-core permeability and plug-permeability data (Figure 9.2.6), the horizontal permeability (Kxy) over a ½ ft interval was multiplied by 100 if its plug-derived permeability was less than 0.00245 md, while a multiplier was calculated, using the formula $y=0.9401*x^{(-0.7759)}$ [where y is the multiplier and x is the plug-derived permeability], when the plug-based permeability varied between 0.00245 md and 0.922 md. For plug-based permeability values greater than 0.922 md, a multiplier of 1 was used. Also, based on available whole core data, the vertical permeability for each ½ ft layer was assumed to be 0.25 times the Kxy. The resultant layer permeabilities are summarized in Figure 9.2.10B.

Hydraulic Fractures

The D1 well entered production in August 1951. Current records indicate that this well was hydraulically fractured some time during its production life. However, the exact date on which the D1 well was fractured is not available. Fracturing technology came into use in the study area in the 1960's. In this study, it was assumed that Chase Parent wells such as the D1 were fractured as of January 1, 1960. Later Council Grove wells such as the D2, drilled in the 1970's or later, were assumed to be fractured upon completion.

No information or test data are available which would enable one to estimate the physical characterization of these hydraulic fractures. Also, wells might have undergone

repeat stimulation treatments. The intent of the hydraulic fracturing was to enhance the well productivity. Lacking physical descriptions of hydraulic fractures, the enhanced well productivities were modeled in this study using the well-productivity (ff) factor greater than 1 with the ff set to 1.0 for an unfractured well. Based on previously reported studies, an initial assumption of ff = 6.0 was made to model the enhanced productivity as a result of hydraulic fracturing in D1 as of January 1, 1960.

Initial Reservoir Pressure

The initial reservoir pressure in the drainage area of D1 was estimated by converting the first recorded surface shut-in pressure of 420 psi to a subsurface depth of 3,000 ft (Figure 9.2.11) using standard formulations (Lee and Wattenburger, 1996). The resultant initial reservoir pressure in the modeled area was estimated at 456 psi. Based on the initial pressure of 456 psi, the modeled area in the simulator is charged with 15.84 bcf of gas.

Reservoir Simulation Studies

Figure 9.2.12 shows the location of the two wells, D1 and D2, in the modeled area. Grid-cell sizes are 330 ft by 330 ft and the area modeled is 640 acres. The intent of this study is to use a simple geo-model for 640 acres around D2 and define minimum modifications necessary to obtain performance matches at the Chase Parent (D1) and a Council Grove (D2) wells. The 3D volume for the model area has 25 layers, with each layer having uniform petrophysical properties as tabulated in Figure 9.2.10B. Actual locations for D1 and D2 have not been used. These wells have been located in the modeled area such that they are as close to the center of the 640 acres as possible without one overlapping the other location-wise. Figure 9.2.13 summarizes some of the major PVT parameters that are part of the simulation-input file. This simulation study ends in February 1991, i.e., before the drilling of Alexander D3 (D3) well – a Chase Infill well. Given the physical location of the D3 well, it is reasonable to assume that its drainage area extends into the neighboring and adjacent 640 acres. Therefore, D3 well has not been included as a part of this study which is limited to one 640-acre unit.

In the simulator, the D1 and D2 wells were produced under historic flow constraints until February 1991. From March 1991, the wells are produced free of rate constraints but under flowing bottom-hole pressures (Pwf, assumed to be same as historically recorded flowing-surface pressures in absence of down hole recorded pressure data) prevalent during 1991-92 period. Thus post February 1991, D1 was flowed under Pwf = 87.5 psi while D2 was produced at Pwf = 102 psi for two additional years (until March 1993).

RUN 1

In the first Run, the D1 well was completed within the Chase layers (L1 to L11) while the completion for D2 well was constrained within the Council Grove layers (L12 to L23). As mentioned earlier, hydraulic fractures were put in place at the D1 well as of

January 1, 1960, using ff = 6.0. The D2 well was hydraulically fractured before onset of production and was modeled using ff = 6.0. Figures 9.2.14A and 9.2.14B compare the simulator-calculated production (lines) from D1 and D2 against their respective historic volumes (points). The results from this run show that the current model is sufficient to match the production history at D1. However, when the well is released of flow constraints (on March 1991), a significant production spike occurs indicating the presence of excess flow capacity in the drainage area of D1. Also, the current model is insufficient to obtain a production-history match at D2.

Figure 9.2.15 shows the differential-pressure depletion, as of November 1, 1975, in the simulated area as a result of production from D1 only. The first recorded surface shut-in pressure at D2, upon its completion in July 1975, was 240 psi. It becomes apparent from the above figure that as of November 1, 1975, the pressures prevalent in the Council Grove layers exceeded 350 psi. Thus a Council Grove well such as D2, if completed within Council Grove interval in the simulator, will result in an initial shut-in pressure far in excess of 240 psi as of 1975. However, if completions of such a well were extended up to Chase intervals, as a result of hydraulic fracturing carried out on all such wells at the onset of production, commingled shut-in pressures at the Council Grove well would be affected by the lower pressures prevalent in the depleted Chase layers.

RUN 2

The input parameters for this run remained the same as in Run 1 except that the D2 well was completed to L6 (Towanda) in Chase. Figures 9.2.16A and 9.2.16B plot the simulator-calculated production against historic volumes from D1 and D2 respectively. It is evident from the above plots that extending D2 completions to Towanda (L6) in Chase resulted in a match between the simulator-calculated production rates with history at the D2 well. Also, a production match was attained at the D1 well. However, when both D1 and D2 wells were freed of rate constraints as of March 1, 1991, significant production spikes occurred in the simulation output indicating presence of excess flow capacity in the modeled area.

The presence of excess flow capacity was further confirmed by Figure 9.2.17, which plots the simulator-calculated flowing bottom-hole pressure against the recorded tubing-head flowing pressures at D1 and D2. The simulator-calculated flowing bottom-hole pressures are higher than the surface-flowing pressures at both D1 and D2.

RUN 3

To address the issue of excess flow capacity, the ff factor value was reduced from 6 to 3 for both D1 and D2 in this run. Figures 9.2.18A and 9.2.18B display the results of this run. It appears that the simulator-calculated production rates matched historic values at both D1 and D2, and that the production spikes, though present, have declined from that obtained in Run 2 for both the wells. However, the presence of production spikes indicated that there still remained excess flow-capacity in the model despite lowering of the ff factor to 3.0.

RUN 4

The Sw in each layer where the initial water saturation was less than 0.99 was adjusted (increased) so that the gas saturation (i.e., Sg = 1- Sw) was reduced by a factor of 7.5% in order to do away with the excess flow capacity prevalent in the model. Other input parameters remained unchanged from Run 3. Figures 9.2.19A and 9.2.19B plot the simulator-calculated production rates for D1 and D2 against respective historic rates. It appears from the above figures that not only have the simulator-calculated flow rates matched the historic volumes, but that there was no excess flow capacity in the model when the wells were freed of their flow constraints in March 1991. Figure 9.2.20A compares the simulator-calculated flowing bottom-hole pressures with flowing pressures recorded at the surface for D1 and D2. This figure shows, as expected, that the simulator-calculated bottom-hole pressures closely followed the trend of recorded surface pressures and were slightly higher than the surface pressures. Thus, it is apparent from this run that an original-gas-in-place (OGIP) charge of 14.64 bcf in the model area was sufficient to obtain production and pressure history-matches at Alexander D1 and D2 wells without any excess flow capacity. Figure 9.2.20B shows the differential-pressure depletion occurring in the model area as of February 1991, i.e., just before the completion of the Chase infill well Alexander D3.

The OGIP reduction factor of 0.925 (relative to the geomodel charge) was found to best match the well-performance histories without showing evidence of excess flow capacity after a series of trial simulation runs using different reduction factors. The model OGIP is dependent on facies-specific capillary pressure correlations and an assumed free-water level. However, some uncertainty related to facies-prediction, FWL estimation, and variability in the saturation-height (capillary pressure) correlations exists. Thus, the volumetric OGIP may be considered as the best estimate under data-limited circumstances and not an exact number.

Published literature (Fetkovich et al., 1990) reported on previously conducted single-well multi-layer simulation studies in Hugoton field. However, these single-well studies modeled only the Chase Parent well without mentioning presence or effects of a Council Grove well in the same section as the parent well. The above-mentioned reference states that volumetric OGIPs needed to be reduced (by as much as 20%) in order to history match the Chase Parent well performance. Reduction of volumetric OGIP in these single-well simulation studies have been attributed to assumptions such as equal drainage areas for layers with significant permeability variation and arbitrarily imposed no-flow boundaries at the edges of the simulated volume, especially when there was significant evidence of intra-layer communication across multi-section areas in the Hugoton field.

RUN 5

Figure 9.2.21A compares the cumulative production from D2 when its completion was restrained within Council Grove against production from the same well when it was

completed to L6 (Towanda) in Chase. All other input parameters have been kept the same as in Run 4 including an OGIP reduction by 7.5%. When D2 completion was constrained to the Council Grove, the simulator-calculated cumulative production was 0.16 bcf as of February 1991. However, the simulator-calculated cumulative production from D2 as of February 1991 was 1.098 bcf, matching historic records, when the well completions were extended to L6 in Chase. Thus, the volume of Chase gas produced by D2 when completed to L6 was 0.938 bcf (= 1.098 - 0.16). The original volume of OGIP in the Chase layers in the modeled area was 13.34 bcf. However, the Chase OGIP was reduced to 12.34 bcf (i.e., by 1 bcf) when the Sg (gas saturations) in the pay layers were reduce by 7.5% (i.e., by using a reduction factor of 0.925). Thus, to obtain performance matches at both D1 and D2 with no remaining excess flow-capacity, the Chase OGIP got reduced by 1.938 bcf (= 1 + 0.938), which was about 14.5% of the Chase OGIP of 13.34 bcf (Figure 9.2.21B).

RUN 6

It is apparent from Run 3 that there was excess flow capacity in the modeled volume for both the D1 and D2 wells because of production spikes at these wells when flowed free of rate constraints. One way to remedy the presence of excess flow capacity was to reduce the OGIP in place by 7.5% as done in Run 4. In Run 6, the D1 was completed in Chase while D2 was completed to L8 (Fort Riley) in Chase. Figures 9.2.22A and 9.2.22B plot the simulator-calculated production rates for D1 and D2 respectively and compare them against the historic rates. The OGIP in this run had not been reduced from the original volumes and ff = 6.0 had been used for the both D1 and D2. Completing D2 to L8 resulted in a history match until May 2004. However, when released from rate constraints, the simulator-calculated production rate fell below the previously established decline trend for D2 (Figure 9.2.22B). For D1, a history match was obtained until May 2004. However, evidence of excess flow capacity at D1 (Figure 9.2.22A) surfaced when released of flow constraints. Figure 9.2.23 compares the simulator-calculated BHFPs for D1 and D2 with the historic surface-flowing pressures. The simulator-calculated flowing pressures for D1 were higher than the historic surface pressures indicating excess flow capacity. Also, the simulator-calculated flowing pressures for D2 hovered around the historic flowing pressures. However, presence of pressure spikes indicated presence of flow limitations given the completion scenario in this run and distribution of permeability and gas volumes in the drainage area of D2.

RUN 7

The input parameters for this run were the same as in Run 6 except that the ff factor for D1 was decreased to 3 while that of D2 was increased to 9. Figures 9.2.24A and 9.2.24B plot the simulator-calculated production rates for D1 and D2. The production spike in D1 remained, though reduced, when released of rate constraints. Despite attaining a history match at D2 until February 1991, the simulator-calculated production rate fell below the previously established decline trend indicating that limiting D2 completion to L8 (Fort Riley) instead of L6 (Towanda) resulted in delivery limitations in the later part of the production life of the well. Figure 9.2.25 plots the simulator-

calculated bottom-hole flowing pressures for D1 and D2 against historically recorded surface-flowing pressures at these wells. It was apparent from this plot that D1 had excess flow capacity because the BHFP was higher than the surface pressure, while D2 was beset with deliverability limitations due to presence of pressure spikes.

Conclusions

A 640-acre area around the Alexander D2 (D2), a Council Grove well, was simulated using a 25-layer model. Alexander D1 (D1), a Chase Parent well, located in the same section as D2, also was modeled in this study under the assumption that both D1 and D2 drainage was limited to 640 acres. The simulation study was carried out until February 1991, i.e., before the completion of Alexander D3 (D3) – a Chase infill well. Each layer in the model was populated with petrophysical properties obtained from wireline logs (recorded at Alexander D2) and from core-analysis data available from the Hugoton and Panoma fields. Within the area simulated, each layer was assumed to have uniform porosity, thickness, and saturation values as recorded by the wireline logs recorded at Alexander D2. The Alexander D1 and D2 wells were located centrally in the model area.

1. Matches with production and pressure histories at D1 and D2 were obtained when the D1 well was completed in the Chase layers and D2 completions were extended to L6 (Towanda) and when the volumetric OGIP was reduced by 7.25%. Also, such a model did not show excess flow capacity when D1 and D2 were flowed free of rate constraints.

2. When D2 completions were extended to L8 (Fort Riley), D1 showed excess flow capacity while D2 showed less than the required flow capacity to match previously established decline trends particularly in the post-1991 period.

3. This study shows that completions of Council Grove wells have to be extended into Chase layers to history-match recorded production from these wells. Thus, the Council Grove well produced gas from the Chase intervals.

4. Previously reported single-well simulation studies appear to have modeled only the Chase Parent well in the Hugoton field. These studies reported that a 20% reduction in volumetric original-gas-in-place (OGIP) was necessary to history match Chase Parent well performance. It appears from this study, that such a high-percentage reduction of volumetric OGIP was necessary because these studies did not take into account the drainage of Chase gas by Council Grove wells.

References:

1. Dubois, M. K., Byrnes, A. P., Bohling, G. C., Seals, S.C., and Doveton, J.H., 2003, Statistically-based lithofacies predictions for 3-D reservoir modeling: examples from the Panoma (Council Grove) field, Hugoton embayment, southwest Kansas (abs): Proceedings American Association of Petroleum Geologists 2003 Annual Convention, Salt Lake City, Utah, v.12, p. A44, /and// /Kansas Geological Survey Open-file Report 2003-30, 3 panels, http://www.kgs.ku.edu/PRS/publication/2003/ofr2003-30/index.html

<http://www.kgs.ku.edu/PRS/publication/2003/ofr2003-30/index.html> (accessed August 23, 2006).

2. Lee, J., and Wattenbarger, R. A., 1996, Gas reservoir engineering, Society of Petroleum Engineers Textbook Series, Richardson, Texas, p 349.

3. Fetkovich, M. J., Ebbs, D. J., and Voelker, J. J., 1990, Development of a multiwell, multilayer model to evaluate infill drilling potential in the Oklahoma Hugoton field, SPE 20778, 65th Annual Technical Conference, New Orleans.

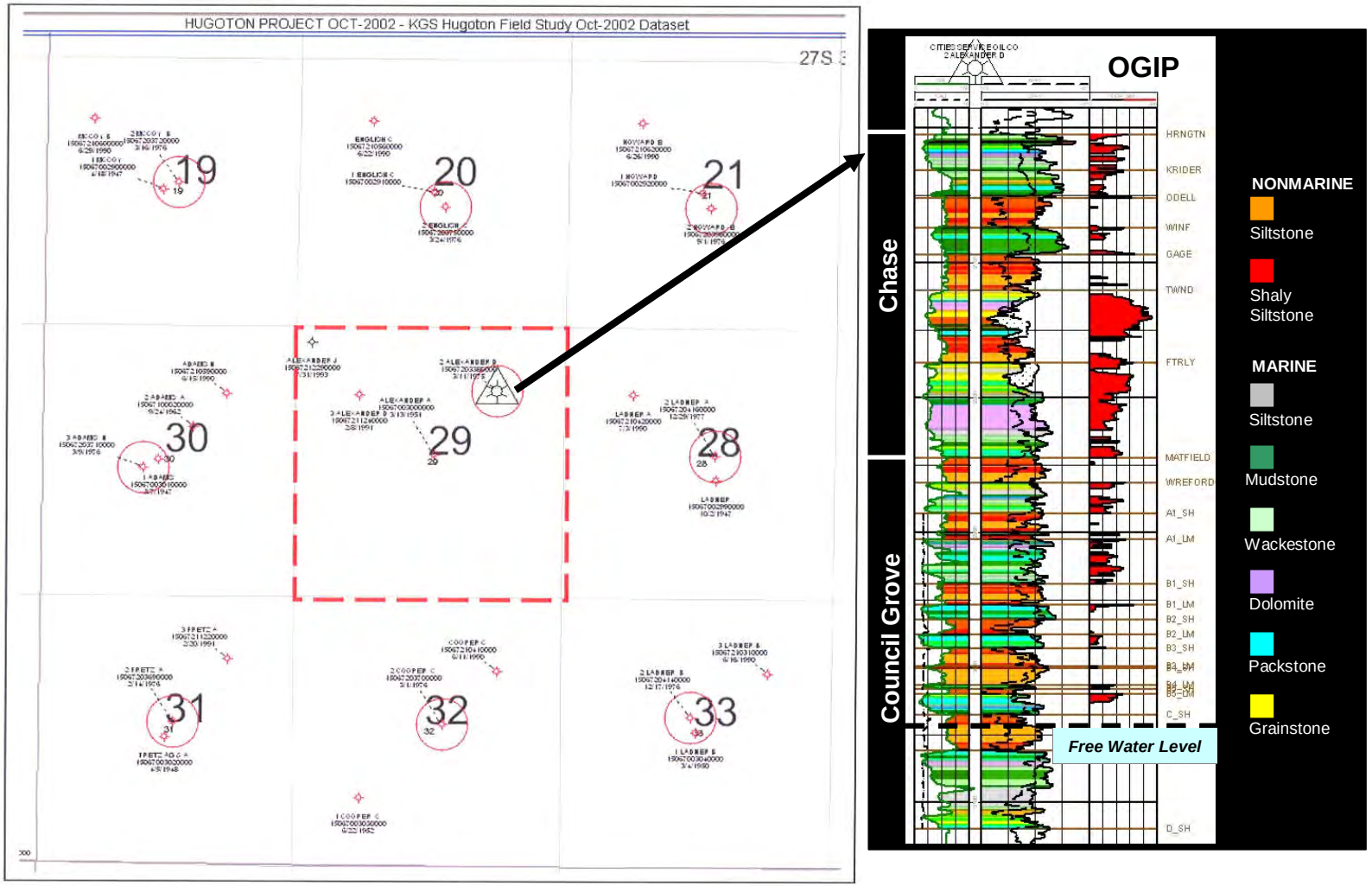

A.

B.

Figure 9.2.1. A) Map showing location of Alexander D1 and D2 wells. B) Well profile for the type well Alexander D2.

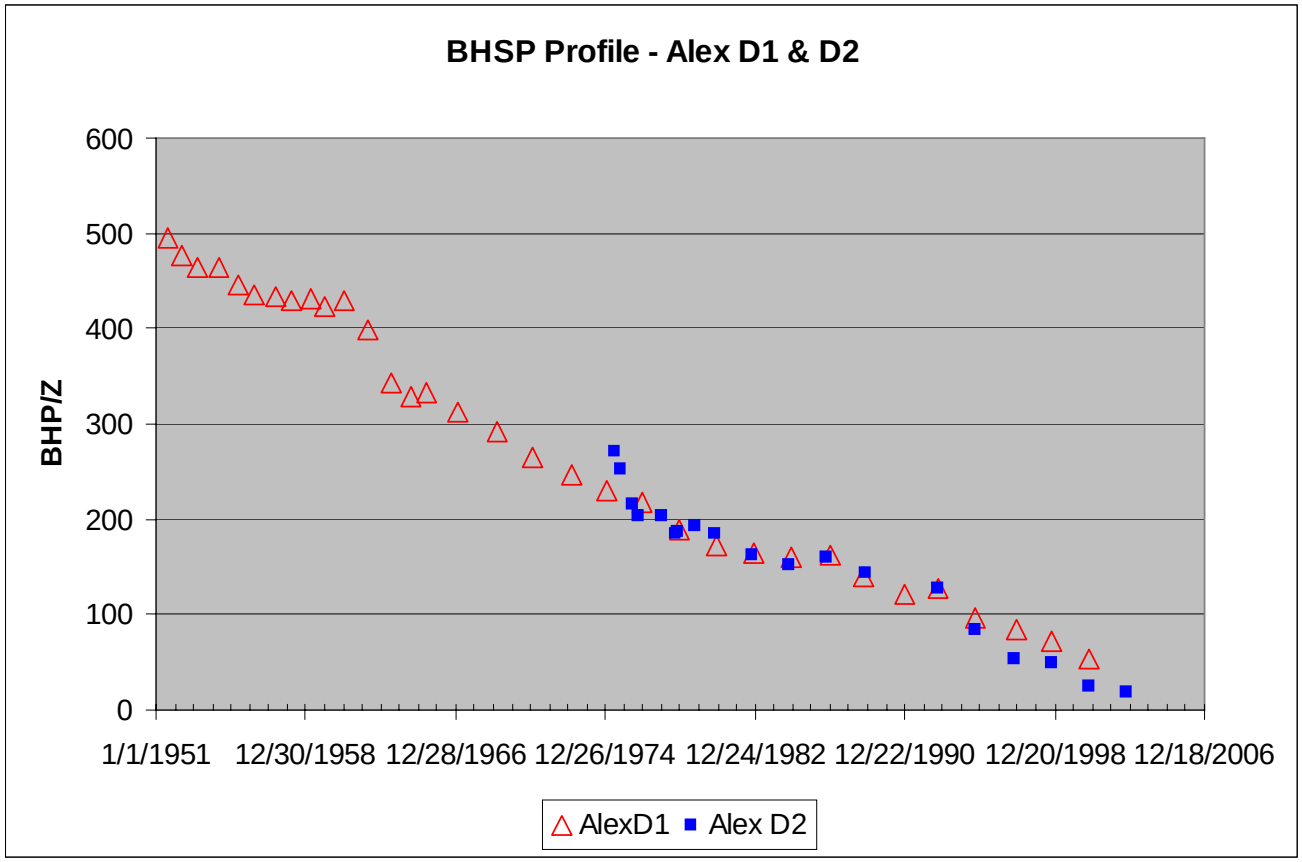

Figure 9.2.2. Plot comparing bottom hole shut-in pressures recorded at D1 and D2. Overlap of pressures indicative of communication between Chase and Council Grove reservoirs.

Plug & Whole-core Permeability

Permeability multiplier is a function of lithofacies and plug to matrix permeability

Permeability multiplier is inversely proportional to plug to matrix permeability

- **Multiplier is 10 times (or more) at very low k**
- **Near 1 at very high k**

L-1 Nonmarine Siltstone and Sandstone

Whole Core Porosity (%) 10.8
Perm Max (md) 0.30

Plug $Porosity_{in}$(%) 11.9
Perm (md) 0.0667

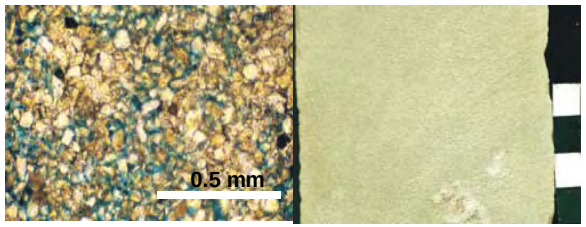

Thin Section Photomicrograph — Close-up Core Slab

Amoco Beaty E-2
Core Slab, 2694',
Blue Rapids Shale (B1sh)

Very Fine Grained Sandstone

L- 8 Grainstones

Whole Core Porosity (%) 18.8
Perm Max (md) 39.0

Plug Porosity (%) 21.2
Perm (md) 32.3

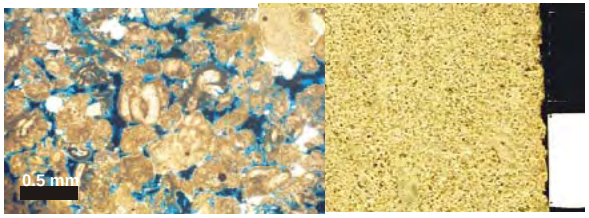

Thin Section Photomicrograph — Close-up Core Slab

Alexander D-2
Core Slab, 3024
Cottonwood Limestone (B5)

M-CG Oncoid-Pellet Packstone-Grainstone

Figure 9.2.3. Thin sections from two Council Grove lithofacies related to plug and whole-core permeability measurements.

Plug and Whole-core Permeability

These data are from Chase and Council Grove P&P dataset. Fractured samples and those samples with very low perms were removed. This plot includes all facies.

- Plug K is consistently lower than whole core at phi <15%.
- Difference between core and plug K at lower phi increases.
- Exponential fit trend-line equations were used to generate a plug to whole-core multiplication factor.

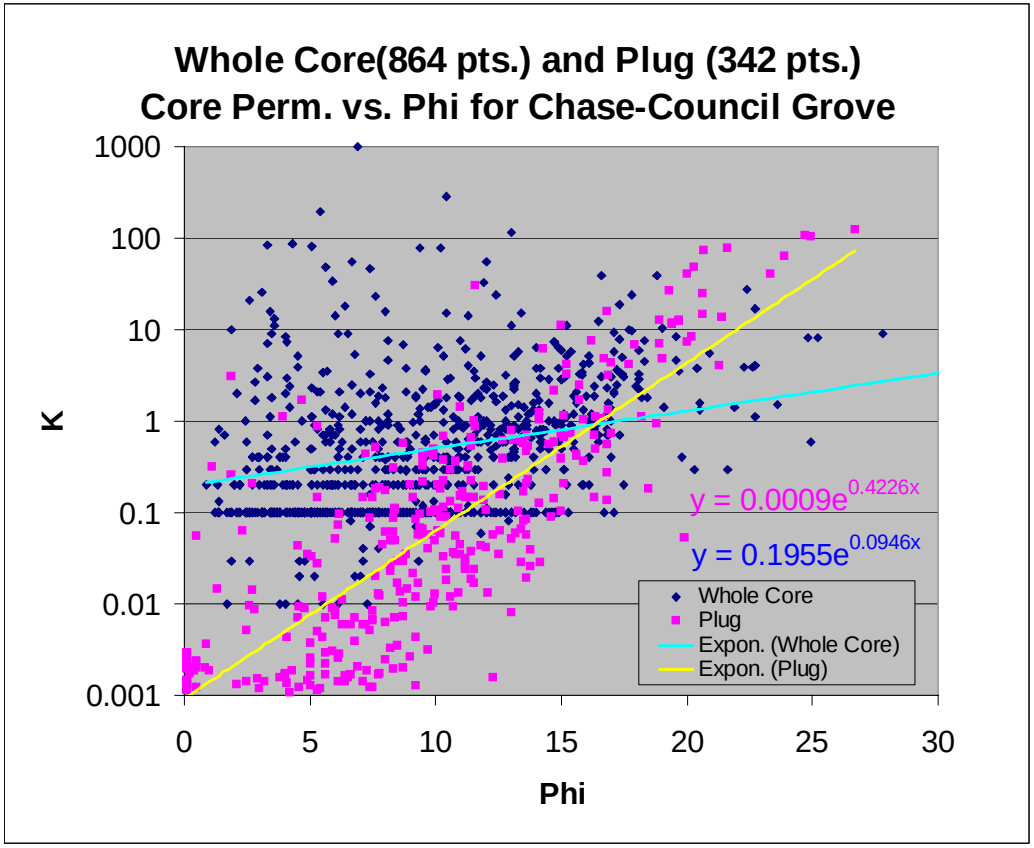

Figure 9.2.4. Comparison of permeability-porosity recorded on plugs and whole cores from Chase and Council Grove intervals.

Multiplier for Plug to Whole Core

Procedure to estimate K multipliers:

1. **Used "Goal Seek" function (in Microsoft Excel) to obtain phi required for given plug k (0.0005, 0.001, 0.005, 0.01, 0.05, 0.1, 0.5, 1, and 5) using $y = 0.0009e^{0.4226x}$**
2. **Using $y = 0.1955e^{0.0946x}$, calculated a whole core k for each phi.**
3. **Determined multiplication factor for plug to whole core.**
4. **Plotted multiplier vs. plug and generated a fitted power curve and equation.**
5. **Checked the equation against the data**

   $y = 0.9401x^{-0.7759}$

(y = multiplier and x = plug K)

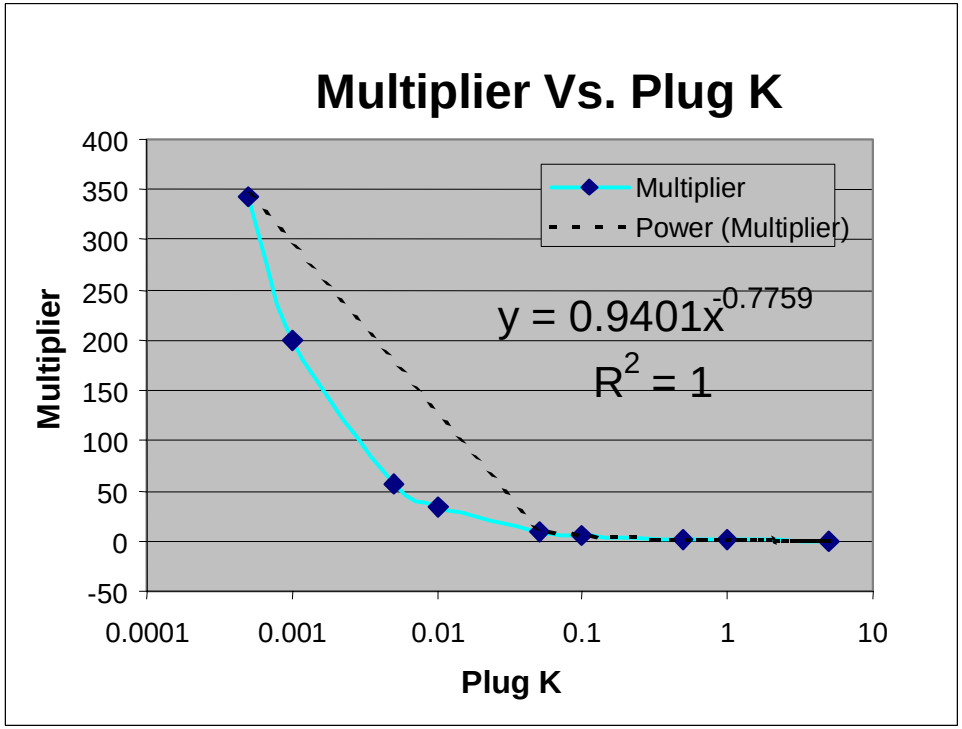

Figure 9.2.5. Development of permeability multiplier to convert plug permeability to those measured on whole cores.

Multiplier Calculation

	K (y)	Constant	Phi (x)	Constant	e^x	Equation
Plug	0.005005	0.0009	4.06	0.4226	5.560878	$y = 0.0009e^{0.4226x}$
WC	0.287044	0.1955	4.06	0.0946	1.468257	$y = 0.1955e^{0.0946x}$

Use Goal Seek for a given Kplug by changing phi to get WC perm

Given Plug	*Calculated* WC	*Calculated* Multiplier	*Fitted Power Equation* $y = 0.9401x^{-0.7759}$
0.0005	0.171	342	342.3286334
0.001	0.2	200	199.9281985
0.005	0.287	57.4	57.35129468
0.01	0.335	33.5	33.49454269
0.05	0.481	9.62	9.608226366
0.1	0.561	5.61	5.611436499
0.5	0.804	1.608	1.609693633
1	0.939	0.939	0.9401
5	1.35	0.27	0.269676577

RECOMMENDATION

Plug k < 0.00245, K = 100 * Plug k

0.00245 < Plug k < 0.922, K = y * Plug k
(use $y = 0.9401x^{-0.7759}$ where y = multiplier and x = plug k)

Plug perm >0.922, Plug = Whole Core

Figure 9.2.6. Multipliers used to convert plug permeability to whole-core permeability for different ranges of plug permeabilities.

Permeability at Varying Scales

Core-plug matrix K is minimum permeability

Whole-core K is up to 1 order of magnitude higher than plug due to microfractures, either natural or induced

Youngren; Council Grove 2784

(photo in 2004) (photo in 1994)

Figure 9.2.7. Example of siltstone deposited in continental to marginal marine marsh in Council Grove Youngren well. Microfractures barely evident in the 1994 photo are more apparent in the 2004 photo due to expansion/contraction (atmospheric conditions) and mechanical disturbance during handling. Partings follow what may be thin clay to very fine silt cutans that coat 2-3 cm peds. Whether the microfractures contributed to *in situ* permeability has not been determined.

Comparison of Core K with DST K

Arithmetic average core k (39 whole core and 6 plug k) cross plotted with average DST k (45 DST's).

Average core k is for the entire cored interval, not the DST interval (not available at the time). Fractured core and missing intervals are not estimated, thus leaving out a few intervals within the cored interval.

- **Core k is consistently lower than DST k.**
- **Variance from the DST k is greatest at low permeability (< 1md) and Core k ~= DST k at high permeablity (>10)**

Possible factors:

- **Skin (damage) may lower DST k**
- **Natural heterogeneity may lower DST k**

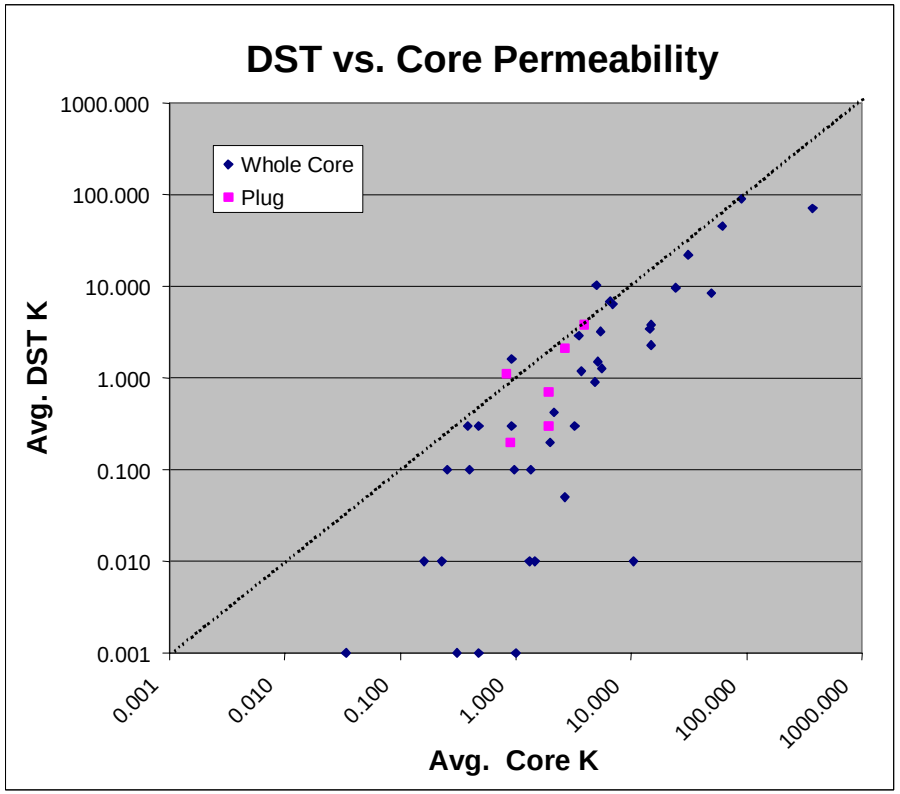

Figure 9.2.8. Comparison of permeability from drill-stem tests with that from Chase and Council Grove core from multiple wells in Stevens County, Kansas.

Vertical Permeability Based on Core Data

Kz/Kxy used to date is 0.1. Preliminary work on limited core data suggests that 0.25 may be more appropriate.

Procedure:

Kv/Kmax calculated from 89 whole-core samples having a Kv and then plotted against Kmax

Median and mean values were calculated for all and then with outliers removed (Kv/Kmax > 1 or < 0.01 were removed)

Recommended Kv factor, 0.25, is the median value after outliers removed

***Additional work:* "Harvest" more Kv data and relate Kv to facies and/or Kxy**

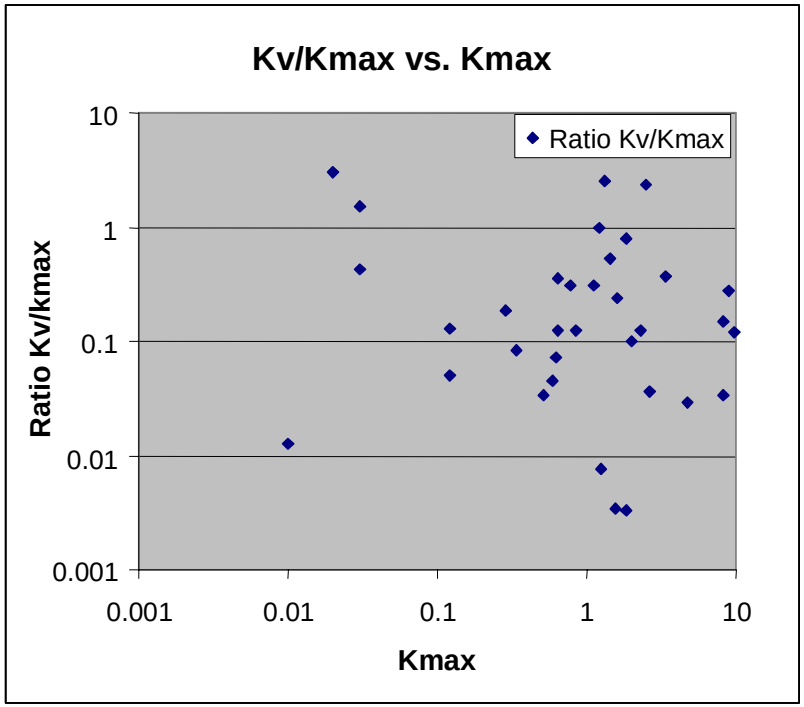

	Median	Mean	Count
Kz/Kxy (all)	0.273	8.141	89
Kz/Kxy (no value >1)	0.231	0.318	77
Kz/Kxy (no value >1 or <0.01)	0.254	0.354	66

Figure 9.2.9. Ratio of vertical to horizontal (maximum) permeability plotted against the maximum horizontal permeability.

No permeability multiplier applied

						Kv/Kxy multiplier =
						0.1
		Upscl H	Upscl Phi	UpScl Sw	UpScl K hor	UpScl Kv
		ft			md	md
1	HRNGTN	26.5	0.089	0.33	1.182	3.34794E-07
2	KRIDER	19.5	0.069	0.46	0.042	1.34307E-07
3	ODELL	21.5	0.071	0.99	0.002	0.000125028
4	WINF	19.5	0.058	0.41	0.356	1.19645E-13
5	GAGE	26.5	0.076	0.99	0.054	0.000159669
6	TWND	33.5	0.169	0.38	55.238	0.004026007
7	HOLMESVILLE	18.5	0.099	0.99	0.250	0.000192849
8	FTRLY	22.5	0.144	0.28	11.822	0.013852189
9	L_FTRLY	47.5	0.109	0.43	0.289	1.04493E-05
10	MATFIELD	17.5	0.076	0.99	0.004	0.000172546
11	WREFORD	22.5	0.096	0.51	0.259	5.09112E-05
12	A1_SH	19	0.079	0.91	0.220	0.000146295
13	A1_LM	32	0.103	0.54	0.457	4.77417E-05
14	B1_SH	15.5	0.080	0.99	0.007	0.000274647
15	B1_LM	10	0.071	0.78	0.824	1.90486E-06
16	B2_SH	11	0.073	0.99	0.017	0.000112545
17	B2_LM	9.5	0.091	0.79	0.160	0.003293057
18	B3_SH	13	0.084	0.99	0.016	0.000239957
19	B3_LM	1	0.086	0.72	0.189	0.012473465
20	B4_SH	11.5	0.080	0.99	0.027	0.000192878
21	B4_LM	2.5	0.134	0.63	5.211	0.12593811
22	B5_SH	3.5	0.070	0.99	0.001	0.000122015
23	B5_LM	14.5	0.138	0.77	7.063	0.005252614
24	C_SH	26	0.070	0.99	0.002	0.000148729
25	C_LM	57.5	0.094	1.00	2.795	7.23571E-05

A.

Selective permeability multiplier applied

						Kv/Kxy multiplier =
						0.25
		Upscl H	Upscl Phi	UpScl Sw	UpScl K hor	UpScl Kv
		ft			md	md
1	HRNGTN	27	0.089	0.33	1.401	8.52512E-05
2	KRIDER	20	0.069	0.46	0.261	3.44329E-05
3	ODELL	22	0.071	0.97	0.151	0.031445022
4	WINF	20	0.058	0.41	0.481	3.06782E-11
5	GAGE	27	0.076	0.90	0.213	0.039828652
6	TWND	34	0.169	0.19	55.345	0.280904773
7	HOLMESVILLE	19	0.099	0.64	0.422	0.045080797
8	FTRLY	23	0.144	0.28	11.900	0.416917007
9	L_FTRLY	48	0.109	0.43	0.583	0.002607391
10	MATFIELD	18	0.076	0.98	0.202	0.040509001
11	WREFORD	23	0.096	0.51	0.523	0.012327338
12	A1_SH	19.5	0.079	0.90	0.392	0.035447834
13	A1_LM	32.5	0.103	0.54	0.760	0.011493021
14	B1_SH	16	0.080	0.99	0.254	0.055176391
15	B1_LM	10.5	0.071	0.78	1.078	0.000498971
16	B2_SH	11.5	0.073	0.98	0.169	0.028966931
17	B2_LM	10	0.091	0.79	0.558	0.128446483
18	B3_SH	13.5	0.084	0.99	0.270	0.050936456
19	B3_LM	1.5	0.086	0.72	0.646	0.161548365
20	B4_SH	12	0.080	0.99	0.250	0.04467553
21	B4_LM	3	0.134	0.63	5.286	0.491584825
22	B5_SH	4	0.070	0.99	0.139	0.034861456
23	B5_LM	15	0.138	0.77	7.217	0.256295099
24	C_SH	26.5	0.070	0.99	0.153	0.037897379
25	C_LM	58	0.094	1.00	3.041	0.016952937

B.

Chase layers

Council Grove layers

Figure 9.2.10. A) Tabulation of upscaled layer porosity, permeability derived from plug-based permeability-porosity relationship, and initial water saturation for Chase and Council Grove layers. B) Layer-specific permeability estimated by use of multipliers to convert plug permeability to whole-core permeability. These layer specific values were input to the simulator.

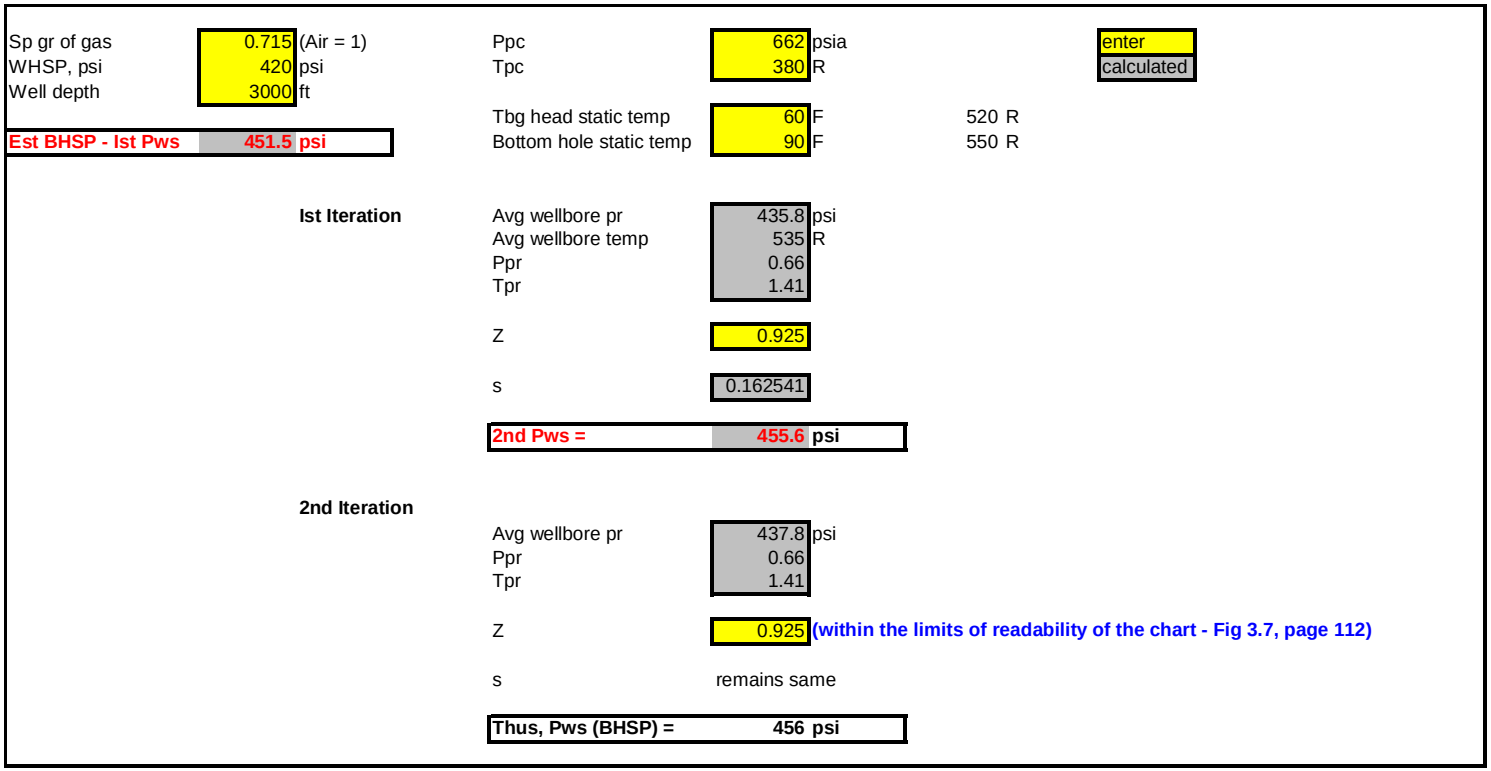

Figure 9.2.11. Calculation process to convert surface shut-in pressure to bottom-hole shut-in condition.

Location of Alexander D1 (D1) and Alexander D2 (D2) in Modeled Area

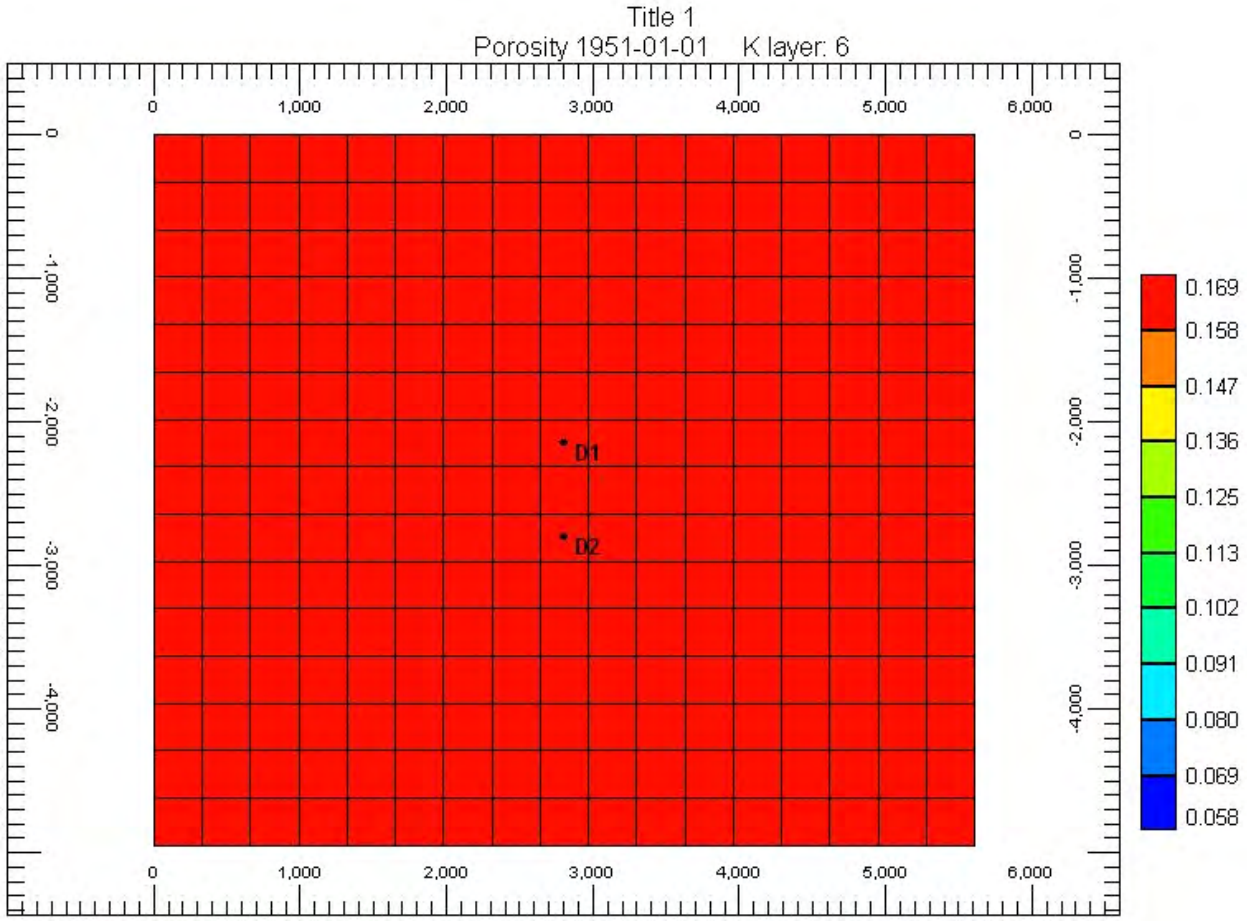

Figure 9.2.12. Location of D1 and D2 wells within the simulation study area.

Assumed PVT properties:				
Reference pressure	465	psi		
Rock compressibility	0.000002	1/psi	(assumed)	
Reservoir temp	90	F		
Gas gravity (Air = 1.0)	0.715			
Water salinity	110,000	ppm		

Figure 9.2.13. Summary of PVT properties used for simulation.

Alex D1 completed in Chase. Alex D2 completed in CG. Ff = 6.0. Pi = 456 psi, OGIP = 15.84 bcf

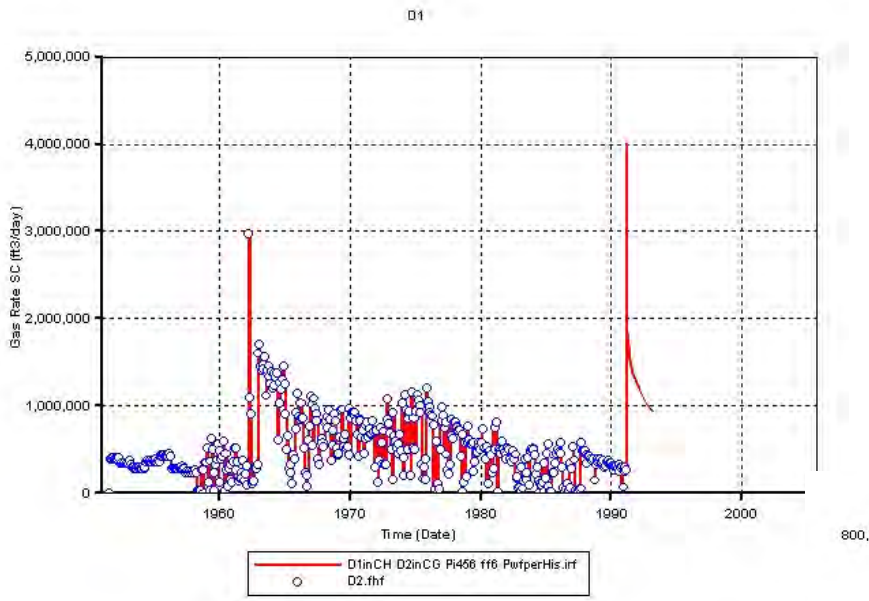

A.

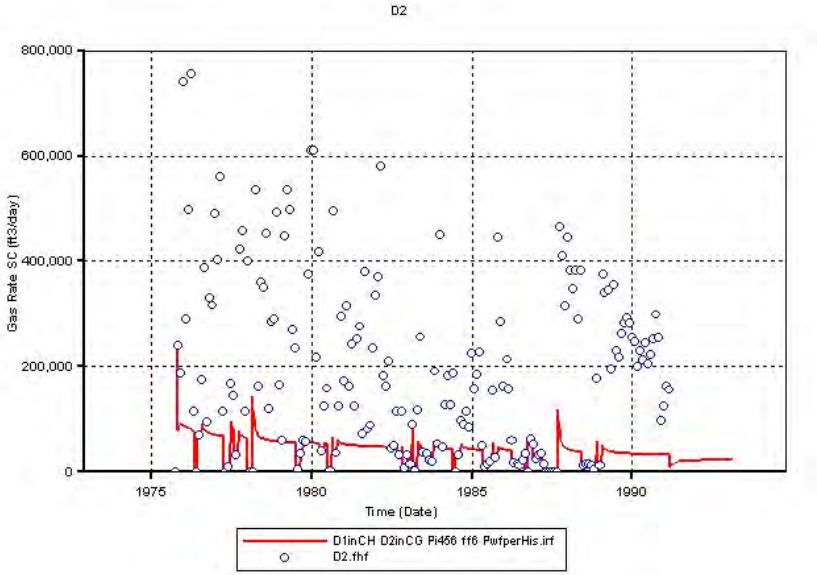

B.

Figure 9.2.14. RUN 1 results – Comparison of simulator-calculated production (line) from D1 (A) and D2 (B) with their respective historic rates (points).

Alex D1 completed in Chase. Alex D2 completed in CG. Ff = 6.0. Pi = 456 psi, OGIP = 15.84 bcf

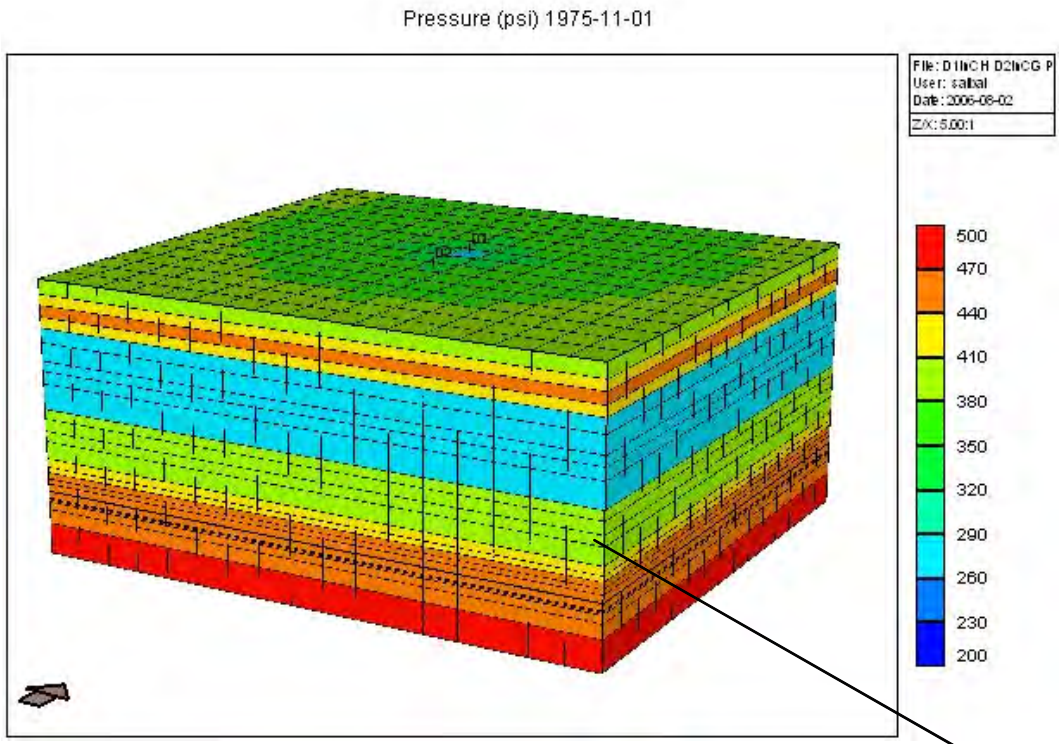

Figure 9.2.15. RUN 1 results – Simulator-calculated pressure distribution in the study area as of November 1975 as a result of production from D1 shows differential depletion.

Alex D1 completed in Chase. Alex D2 completed to L6 (Towanda). Ff = 6.0. Pi = 456 psi

Post Feb1991 – D1 Pwf = 87.5 psi & D2 Pwf = 102 psi

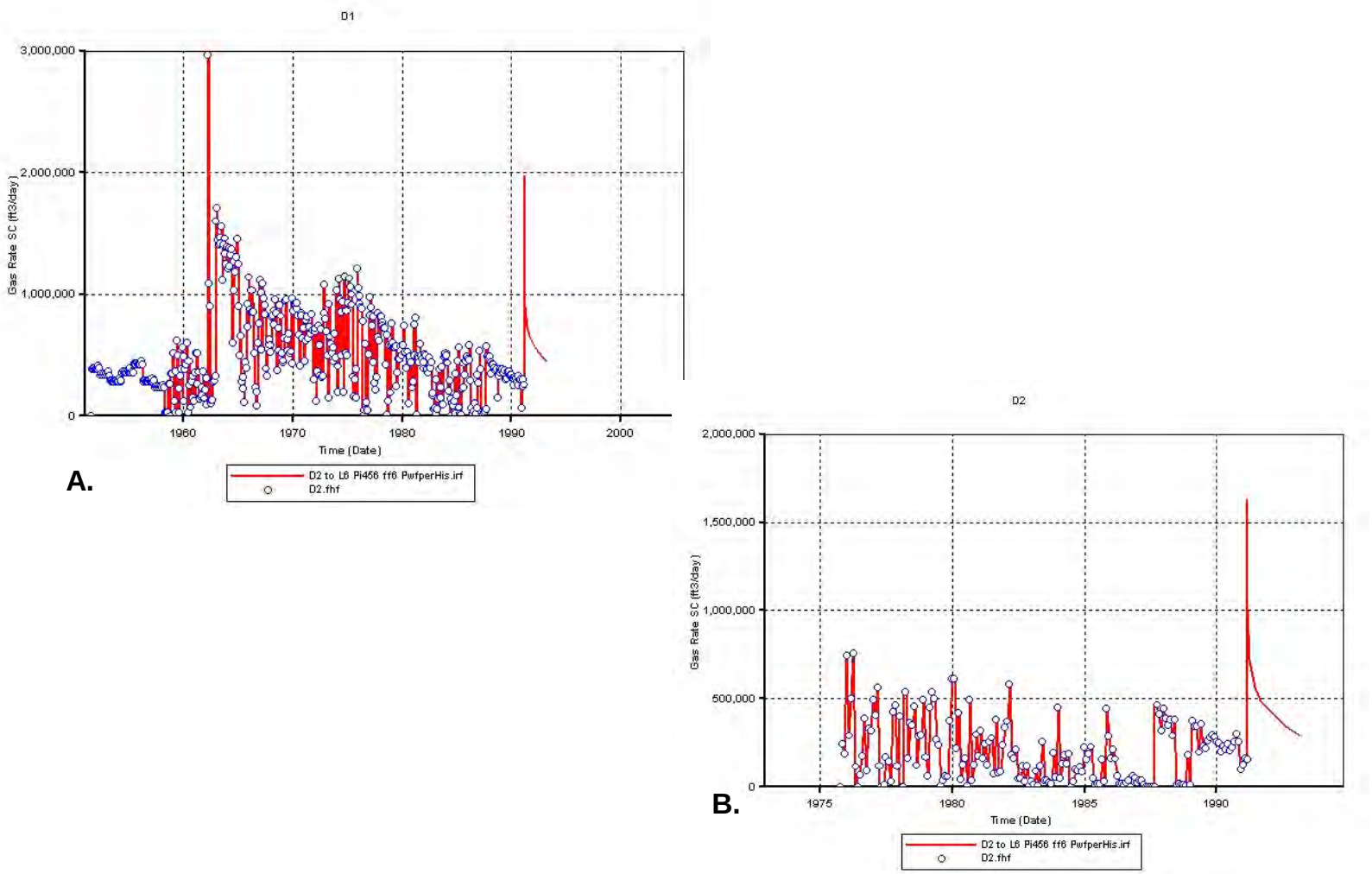

Figure 9.2.16. RUN 2 results - Comparison of simulator-calculated production (line) from D1 (A) and D2 (B) with their respective historic rates (points).

Alex D1 completed in Chase. Alex D2 completed to L6 (Towanda). Ff = 6.0. Pi = 456 psi

Post Feb1991 – D1 Pwf = 87.5 psi & D2 Pwf = 102 psi

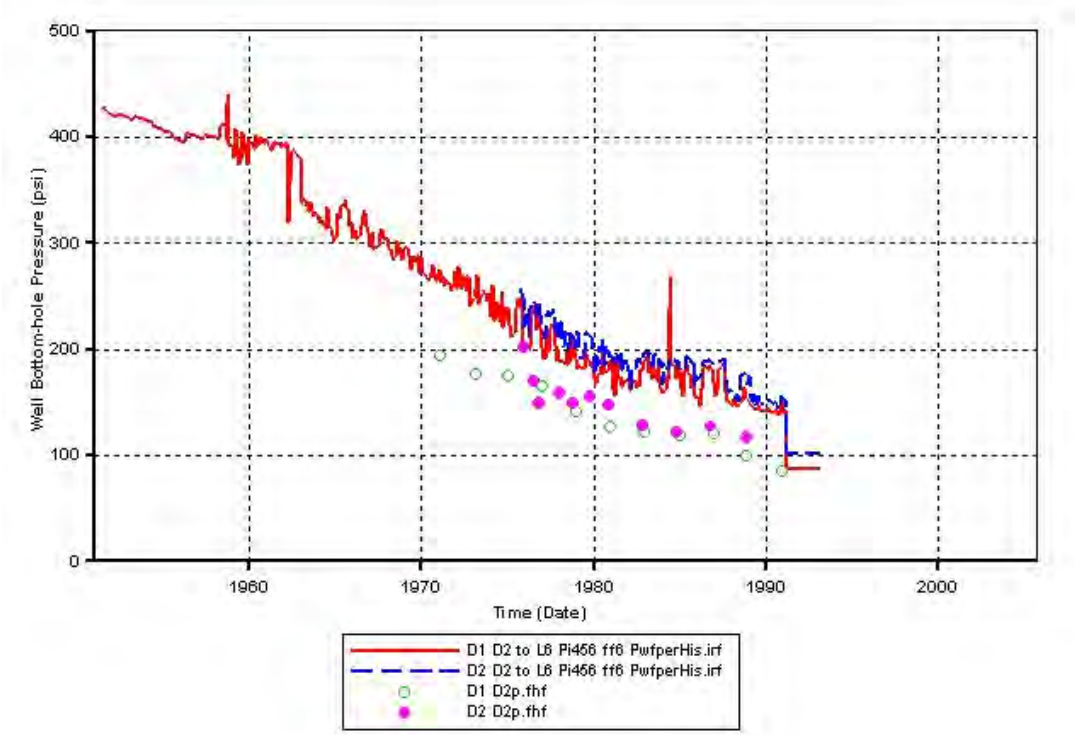

Figure 9.2.17. RUN 2 Results - Simulator-calculated bottom-hole flowing pressure at D1 and D2 wells compared to corresponding historic values show presence of excess flow capacity.

Alex D1 completed in Chase. Alex D2 completed to L6 (Towanda). Ff = 3.0. Pi = 456 psi

Post Feb1991 – D1 Pwf = 87.5 psi & D2 Pwf = 102 psi

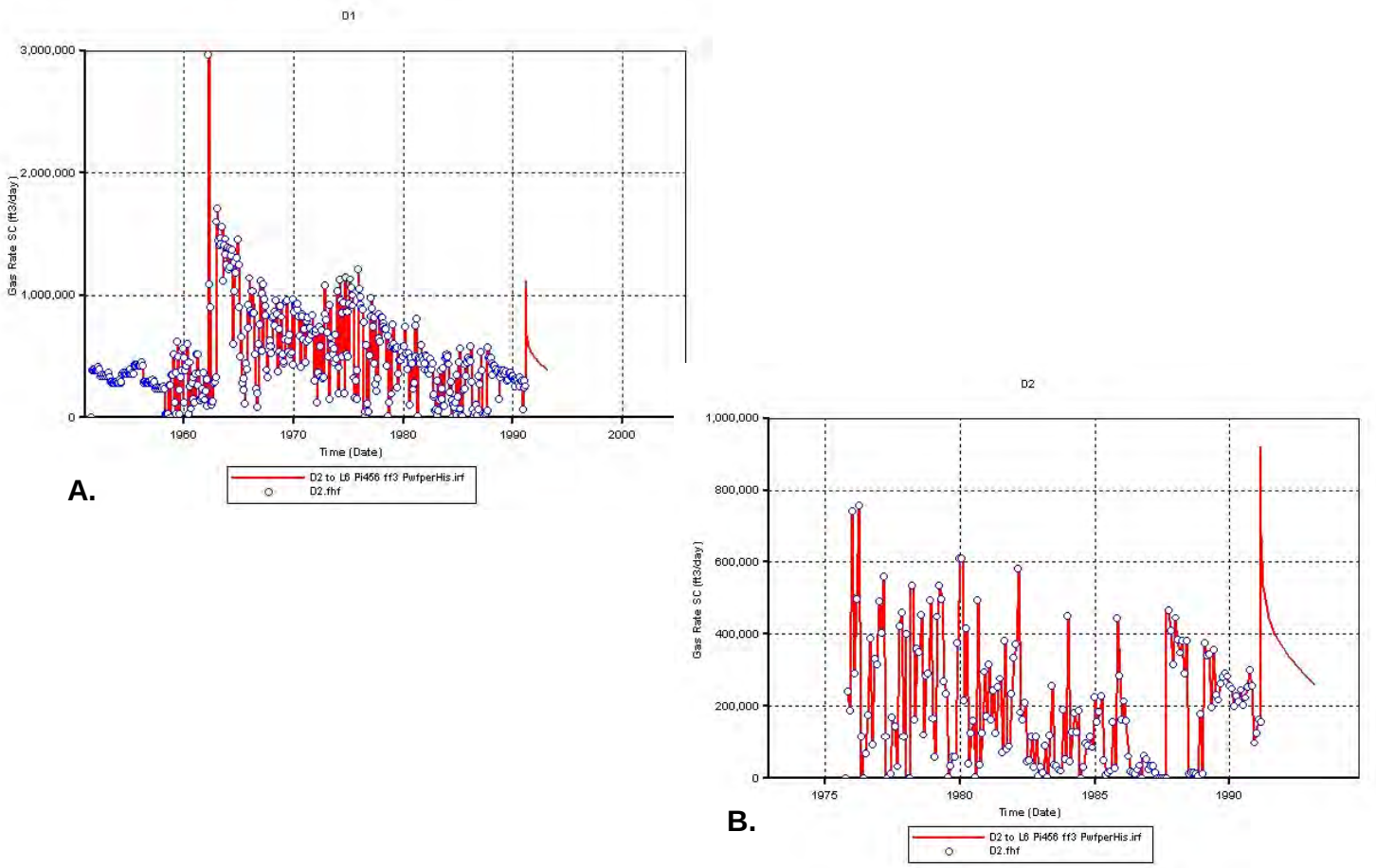

Figure 9.2.18. RUN 3 Results – Simulator-calculated flow rates at D1 and D2 wells compared with historic volumes.

Alex D1 completed in Chase. Alex D2 completed to L6 (Towanda). Ff = 3.0. Pi = 456 psi

Post Feb1991 – D1 Pwf = 87.5 psi & D2 Pwf = 102 psi. OGIP*0.925, i.e. 14.64 bcf

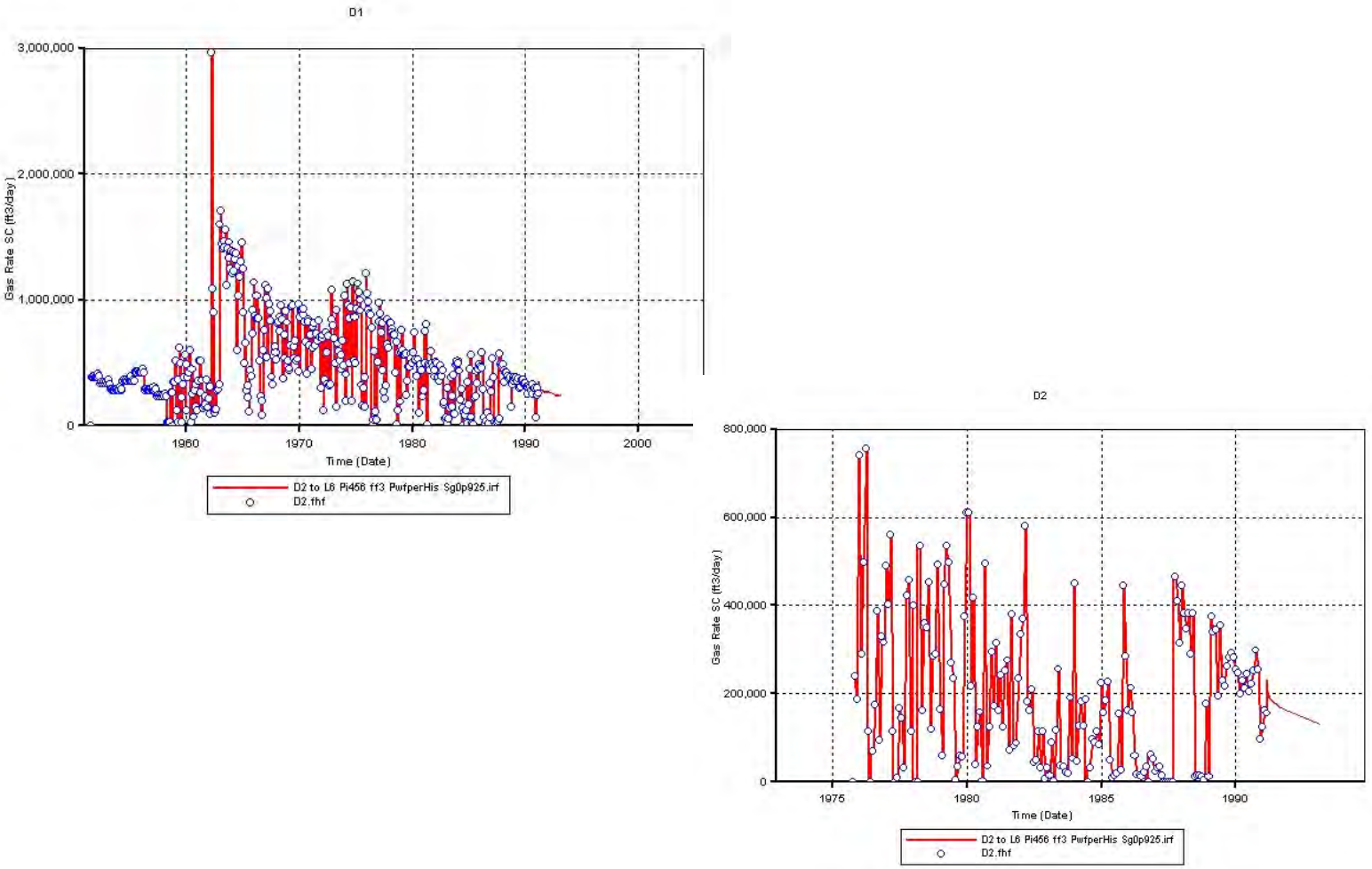

Figure 9.2.19. RUN 4 Results - Simulator-calculated flow rates at D1 and D2 wells compared with historic volumes.

Alex D1 completed in Chase. Alex D2 completed to L6 (Towanda). Ff = 3.0. Pi = 456 psi

Post Feb1991 – D1 Pwf = 87.5 psi & D2 Pwf = 102 psi. OGIP*0.925, i.e., 14.64 bcf

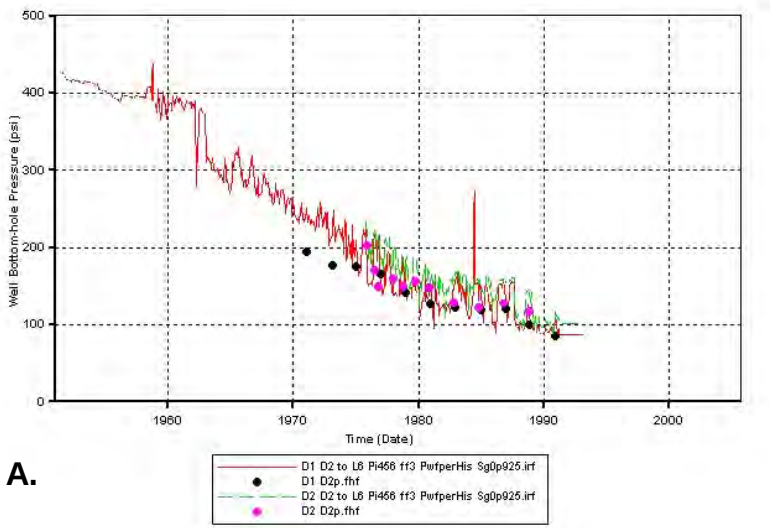

A.

Differential depletion in Hugoton/Panoma

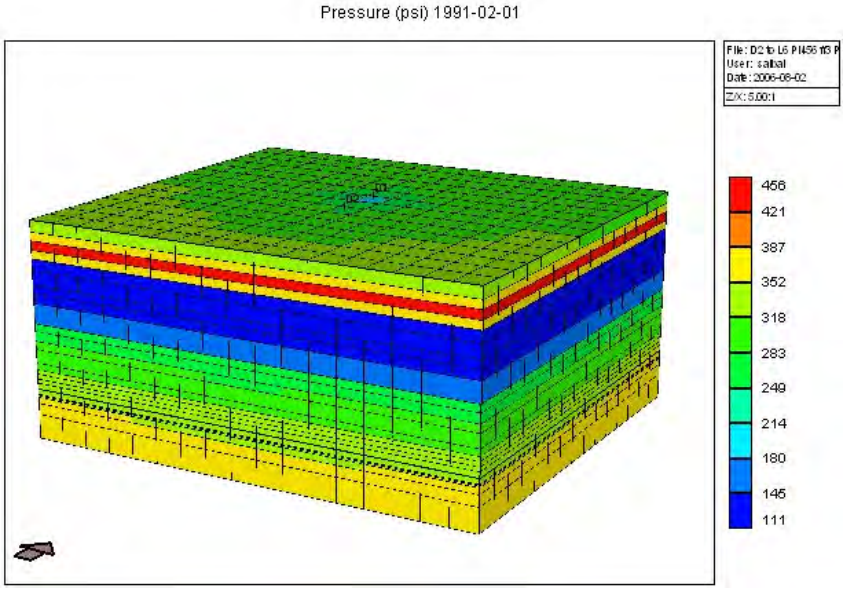

B.

Figure 9.2.20. RUN 4 Results – A) Simulator-calculated bottom-hole flowing pressure at D1 and D2 wells compared to historically recorded surface-flowing pressures. B) Simulator-calculated pressure distribution in study area as of February 1991.

Alex D1 completed in Chase. Alex D2 completed in CG. Ff = 3.0. Pi = 456 psi

Post Feb1991 – D1 Pwf = 87.5 psi & D2 Pwf = 102 psi. OGIP*0.925, i.e., 14.64 bcf

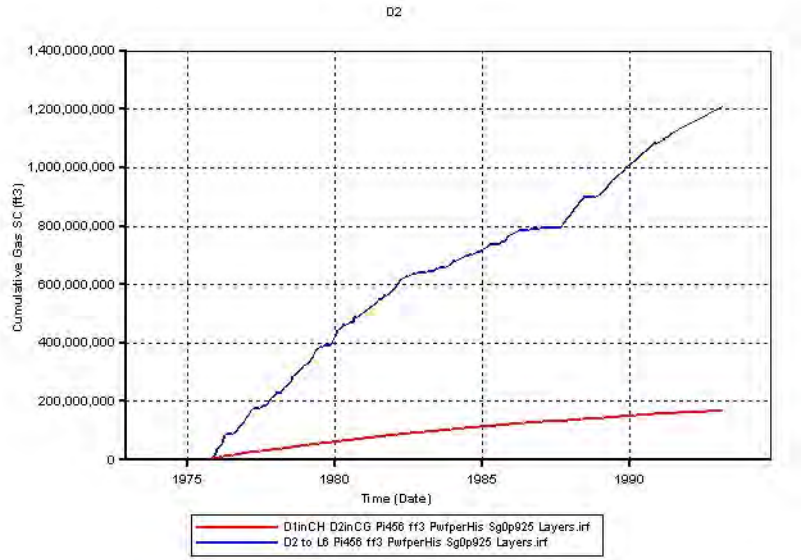

A.

B.

When D2 completed in CG						
	Cum D2 as of Feb 1991			**0.16**	bcf	
	Cum D2 his prod - Feb 1991			**1.098**	bcf	
	CH gas prod by D2			**0.938**	bcf	
CH OGIP*.925				**12.34**	bcf	
Original CH OGIP				**13.34**	bcf	
Chase OGIP reduction						
	Reduction is gas volume - OGIP adjustment			**1.00**	bcf	
	CH gas prod by D2			**0.938**	bcf	
	Total volume not made available to D1			**1.94**	bcf	
				14.5	% of original CH OGIP	

Figure 9.2.21. RUN 5 Results – A) Simulator-calculated cumulative production from D2 with its completion restrained within Council Grove (red line) compared with that when its completions extended to Towanda in Chase (blue line). B) Calculation showing volume of Chase gas that was not available to D1 well for production.

Alex D1 completed in Chase. Alex D2 completed to L8 (Fort Riley). Ff = 6.0. Pi = 456 psi

Post Feb1991 – D1 Pwf = 87.5 psi & D2 Pwf = 102 psi.

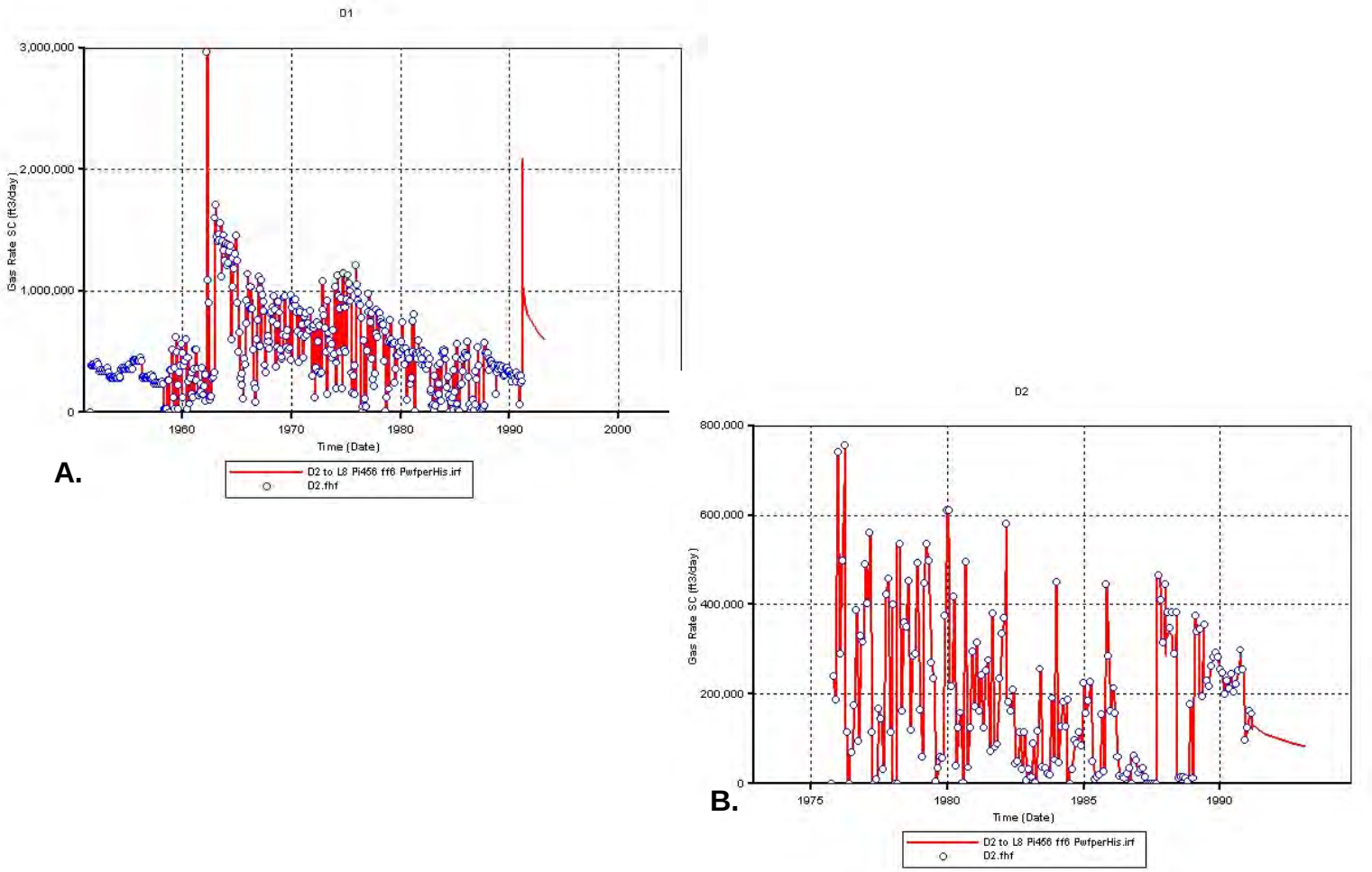

Figure 9.2.22. RUN 6 Results - Simulator-calculated flow rates at D1 and D2 wells compared with historic volumes.

Alex D1 completed in Chase. Alex D2 completed to L8 (Towanda). Ff = 6.0. Pi = 456 psi

Post Feb1991 – D1 Pwf = 87.5 psi & D2 Pwf = 102 psi.

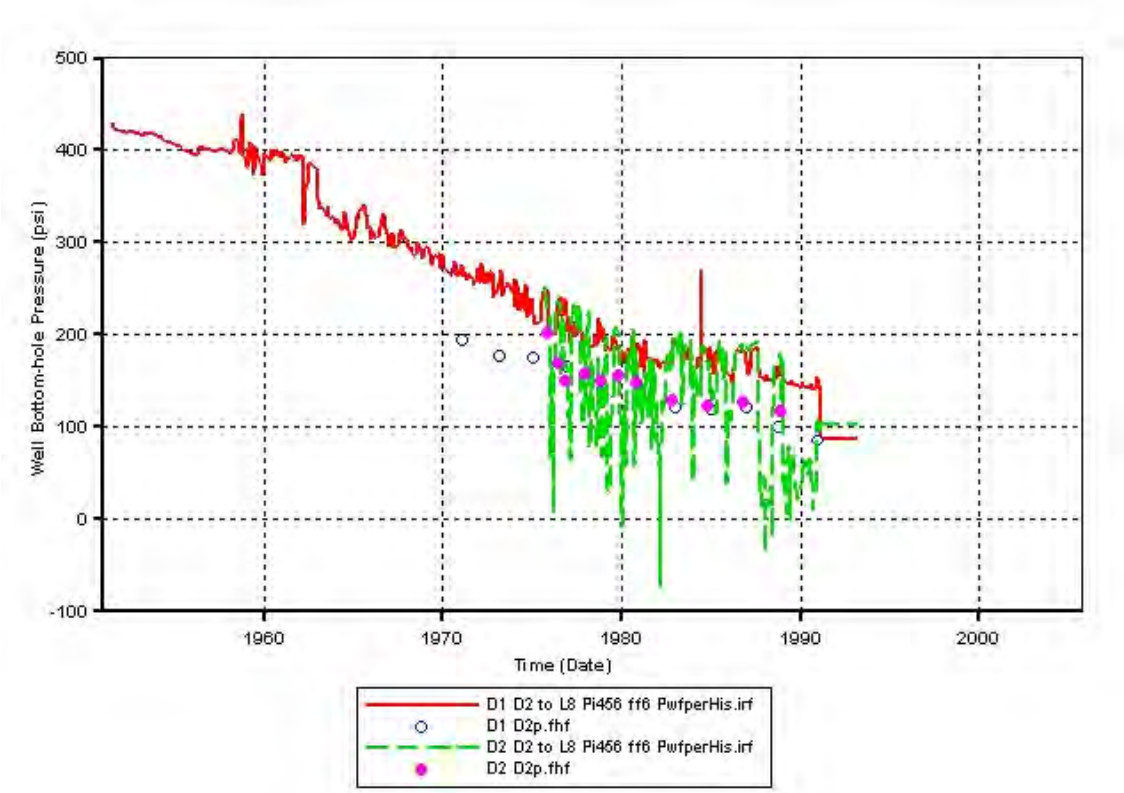

Figure 9.2.23. RUN 6 Results - Simulator-calculated bottom-hole flowing pressure at D1 and D2 wells compared to corresponding historic values recorded at the surface.

Alex D1 completed in Chase. Alex D2 completed to L8 (Towanda). Pi = 456 psi. D1 ff = 3.0 & D2 ff = 9.0. Post Feb1991 – D1 Pwf = 87.5 psi & D2 Pwf = 102 psi.

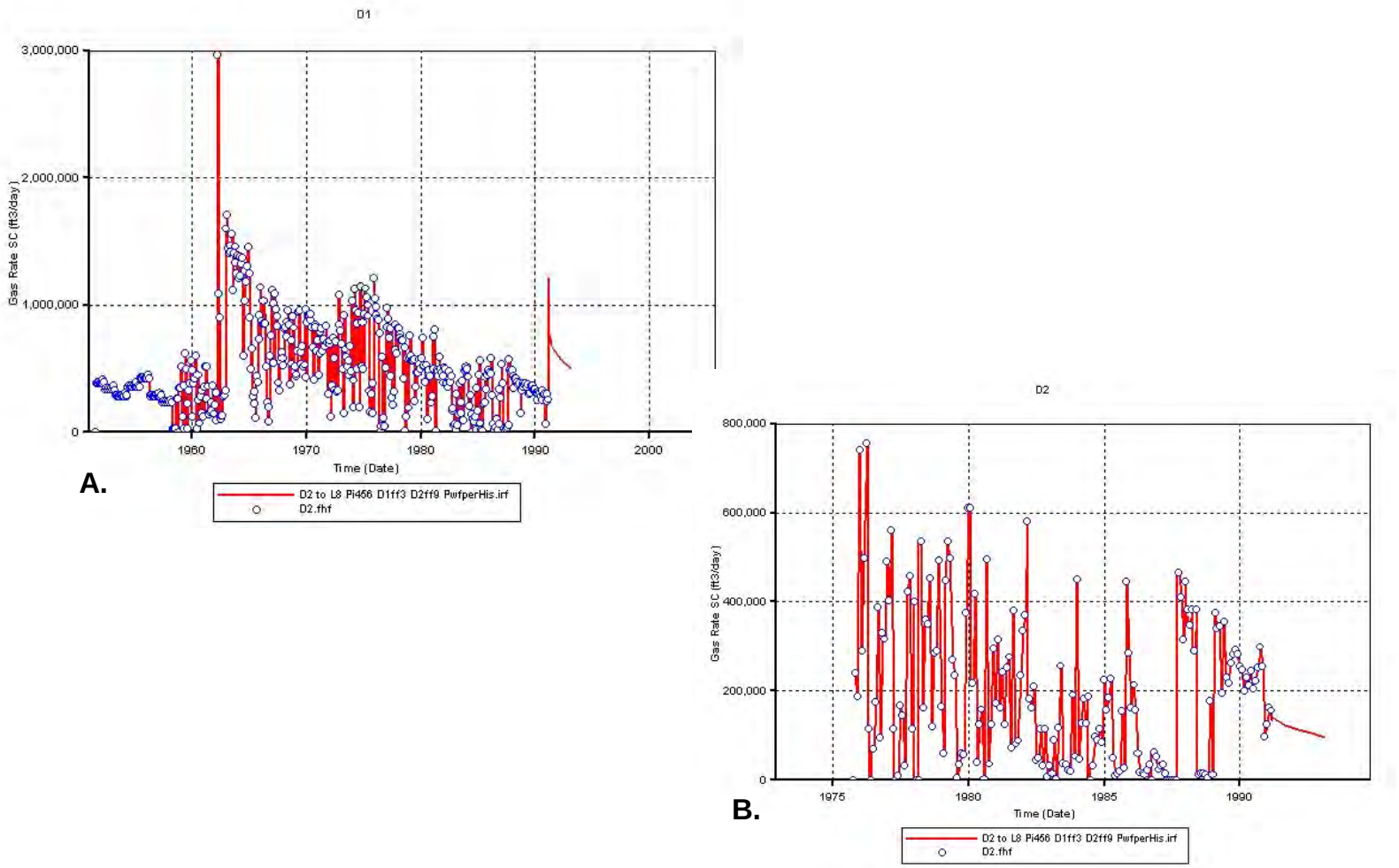

Figure 9.2.24. RUN 7 Results - Simulator-calculated flow rates at D1 and D2 wells compared with historic volumes.

Alex D1 completed in Chase. Alex D2 completed to L8 (Towanda). Pi = 456 psi. D1 ff = 3.0 & D2 ff = 9.0. Post Feb1991 – D1 Pwf = 87.5 psi & D2 Pwf = 102 psi.

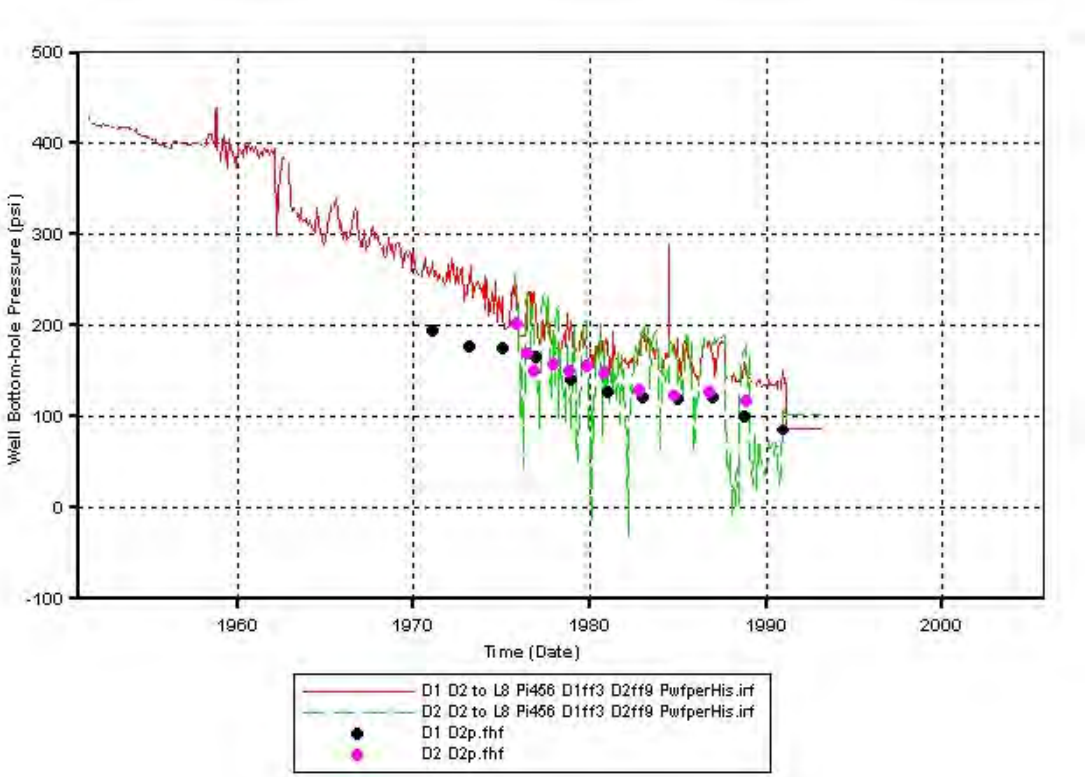

Figure 9.2.25. RUN 7 Results - Simulator-calculated bottom-hole flowing pressure at D1 and D2 wells compared to corresponding historic values recorded at the surface.

9.3 MULTI-SECTION SIMULATION – FLOWER AREA

Saibal Bhattacharya, Martin K. Dubois and Alan P. Byrnes

Introduction

The Hugoton and Panoma gas fields (Figure 9.3.1), North America's largest, produce from 13 fourth-order marine-nonmarine sedimentary cycles of the Wolfcampian Chase and Council Grove Groups, respectively. A fine-layered cellular geomodel was constructed for these fields using a four-step workflow: 1) define lithofacies in core and correlate to wireline log curves and geologic variables (depositional environment and relative cycle-position), 2) train a neural network and predict lithofacies at non-cored wells, 3) populate a 3D-cellular model with lithofacies using stochastic methods, and 4) populate the model with petrophysical properties and fluid saturations using facies-specific equations based on core data. The fine-scale model was upscaled to 25 layers for simulation.

Objective

The objective of this study was to validate the geomodel by simulating the production/pressure performance of wells located in select multi-section areas in the Hugoton field. The intent of this exercise is to see how closely the simulator-calculated pressure/production performances of individual wells match with respective histories with minimum modifications of the geomodel. The focus is not to obtain exact matches of pressure/production histories at individual wells with localized model modifications. Computer Modeling Group's (CMG's) IMEX simulator was used in this study.

This report details the simulation studies carried out at one such area – nine sections around the Flower Science well. The location of the Flower simulation within the context of the Hugoton-Panoma fields is shown in Figure 9.3.1, while Figure 9.3.2 shows the locations of the wells within this study area.

Geomodel Inputs

Flower Area Geologic Model

The Flower area is located near the very center of the Hugoton and Panoma gas fields where the gas column is thickest (500 ft, 150 m) and is continuous from the top of the Chase through the lower part of the Council Grove, through the Cottonwood Limestone Member (B5_LM). Thin-bedded (2-10 m), marine carbonate mudstone to grainstone and siltstone to very fine sandstone siliciclastics in 13 fourth-order marine-continental cycles, illustrated in core, are the main pay zones separated by eolian and sabkha redbeds of low reservoir quality (Figure 9.3.3). The heterolithic system is a classic example of sedimentary response to rapid glacio-eustatic sea-level fluctuations on an extremely gently sloped ramp of an asymmetric foreland basin (Anadarko) on a craton. Petrophysical properties vary among 11 major lithofacies classes. Water saturations cannot be interpreted from logs due to deep filtrate invasion (Dubois, Brynes, et al.,

2003). Neural-network procedures, stochastic modeling, and data-analysis automation facilitated building a detailed 3D cellular reservoir model that is part of the Hugoton Asset Management Project (http://www.kgs.ku.edu/HAMP/index.html), a Kansas Geological Survey – industry consortium. In building the Flower static model, we used a four-step workflow: 1) define lithofacies in core and correlate to electric log curves (training set), 2) train a neural network and predict lithofacies at non-cored wells, 3) populate a 3D cellular model with lithofacies using stochastic methods, and 4) populate model with lithofacies-specific petrophysical properties and fluid saturations. A portion of the static model was then upscaled for simulation

Reservoir Lithofacies

The main pay zones in the Hugoton consist of 13 thin (mean thickness varying from 6 to 70 ft) marine, mainly carbonate intervals (with six intervals located in the Chase section and seven intervals located in the Council Grove section), deposited during sea-level high stands. These are separated by continental, mainly siltstone (redbed) intervals (mean thickness 6-25 ft, 2-8 m) deposited during sea-level low stands, when most of the shelf was exposed. The siltstones generally have poor reservoir quality and vertically isolate, or restrict communication between, the 13 pay intervals (Siemers and Ahr, 1990; Ryan et al., 1994; Oberst et al., 1994; Olson et al., 1997). The principal factor in determining the reservoir storage and flow capacity (hydrocarbon pore volume and permeability) of Hugoton reservoir rock is primary depositional texture. Although diagenesis, both early and after burial, including leaching of grains and cements and early and late dolomitization, played important roles in enhancing or reducing porosity (Seimers and Ahr, 1990; Luczaj and Goldstein, 2000; Olson et al., 1997), the dominant reservoir rocks are marine carbonate with grain-supported textures and, to a lesser extent, siliciclastic sandstone (Siemers and Ahr, 1990; Caldwell, 1991; Olson et al., 1997; Heyer, 1999; Dubois et al. 2003a).

Static Model

For the Flower simulation exercise, a finely layered 70-square-mile static model (234 layers, 1,048,320 cells) was initially built and populated with lithofacies, porosity, permeability, and water saturation (Figure 9.3.4). The XY-grid dimensions are 660 by 660 ft (200 by 200 m). A nine-section portion of the model centered on the Flower A-1 well was “cut out” of the larger model and the 234-layer model was upscaled to 25 layers with porosity, permeability, and water saturation for simulation.

Well data for the larger Flower area static model included formation tops from 300 wells, and facies and porosity data from 57 node wells (Figure 9.3.5). The simulation model included six node wells, including the Flower A1 that had a continuous core through the Chase and Council Grove. Lithofacies are estimated at half-foot (0.15 m) intervals in the 57 node wells, wells having modern log curves (density and neutron porosity, deep induction log, gamma ray, and photoelectric effect), using neural networks trained on wells having core (Dubois and Byrnes et al., 2003; Dubois and Bohling et al., 2003; Dubois et al., 2005). The neural network models for the Flower model are those

referred to as the Geomod2 vintage neural networks. Corrected porosity at the node wells was estimated using algorithms developed from core to log porosity regression analysis (Figure 9.3.6).

Workflow for Static Model Construction

The following workflow was employed for building the static Flower area model:

1. Build a structural model establishing the cellular architecture based on the structural tops from the 300 wells. Model consists of 25 zones that conform to the stratigraphic nomenclature, and 234 conformable layers with an average thickness of 2 ft in the marine intervals and 4 ft in the nonmarine intervals.
2. Model the lithofacies and porosity by first "blocking" the half-foot (0.15 m) data to the layer thickness at the 57 node wells using a most-abundant lithofacies approach for facies and arithmetic average for porosity.
3. Model lithofacies between node wells using stochastic indicator simulation using variograms developed through data analysis.
4. Model porosity between node wells using sequential Gaussian simulation conditioned on lithofacies and using variograms developed through data analysis.
5. Water saturation was calculated at the cells using transform equations developed from empirical core data knowing lithofacies, porosity, and height above free-water level.
6. Free-water level was estimated to be 125 ft below the average lowest depth of perforations in the Council Grove Group.
7. Permeability in the x, y, and z directions was calculated at the cells using transform equations developed from empirical core data knowing lithofacies and porosity. Permeability x was assumed equal to permeability y while facies-specific ratios of vertical to horizontal permeability were determined from available core data.

Engineering Model

A finely layered model is necessary to adequately distribute porosity, permeability, and water saturation in the 3D model, but is cumbersome for simulation. A nine-section portion of the 234-layer model was cut out of the larger model and upscaled to 25 layers. These layers correspond to the 25 zones in the structural model that in turn correspond to the major stratigraphic units that are marine or nonmarine half cycles. In general, the result is 25 layers that alternate from relatively good reservoir properties (higher porosity and permeability) to relatively poor reservoir properties (relatively low porosity and permeability). Porosity was upscaled using an arithmetic average, conditioned on lithofacies; water saturation was upscaled using a porosity-weighted arithmetic average; and permeability upscaling utilized flow-based tensor upscaling using the PSK-solver. Figure 9.3.7 illustrates the results of the upscaling from the 234-layer static model to the 25-layer engineering model. The models were exported from Petrel in a format compatible for import directly into the CMG simulator.

A 25-layer geomodel was exported to the reservoir simulator – Computer Modeling Group's IMEX. Each layer in this 25-layer model coincides with a formation- or member-level stratigraphic interval in the Chase and Council Grove systems, respectively. Each layer represents a half-cycle of marine/non-marine sedimentary cycle. In most cases, the model layer closely approximates the DST intervals at the Flower Science well. The area simulated extends over nine sections around the Flower Science well. Grid-cells dimensions were set at 660 ft by 660 ft for all layers.

Wells have been named using an uniform convention in this study. The names of all Chase Parent wells carry a prefix "P", while those of Chase Infill and Council Grove wells carry prefixes "I" and "CG", respectively.

Figure 9.3.8 lists the basic PVT-properties input for simulation.

Permeability Modeling

Fundamental to modeling the permeability distribution in the Hugoton is the need to understand the relative role of matrix and fracture flow and the possible scale dependence of permeability. Figure 9.3.9 showed that for rocks below approximately 8% porosity, or approximately 0.5 md (0.0005 μm^2), microfractures in core significantly increased permeability. A fundamental question for these data is: are the microfractures present in the subsurface or are they a stress-release or coring-induced phenomenon? This question can only be answered by comparing upscaled matrix permeabilities with unfractured full-diameter permeabilities and with drill-stem-test (DST) or well-test calculated permeabilities. Comparing carefully examined unfractured full-diameter permeability values with that measured on plugs taken from the full-diameter cores (Figure 9.3.10) indicates that homogenously sampled matrix properties apply to the full-diameter core scale.

The ability to compare well-scale permeability with matrix permeability is limited because so few wells have DST or well-test data for thin intervals for which core data are available and which were tested prior to hydraulic fracturing, which complicates artificial fracture-enhanced permeability with reservoir permeability. In four key research wells, permeability was measured using DST for multiple intervals for which core analysis was also performed. To compare with core permeabilities, full-diameter and plug permeabilities were arithmetically averaged (representing parallel flow contribution from each depth interval) to determine average interval permeabilities. Comparison between DST, upscaled full-diameter, and plug permeabilities shows good correlation for intervals with permeability greater than ~0.5 md (0.0005 μm^2). For interval permeabilities below 0.5 (0.0005 μm^2) md, full-diameter permeabilities exhibit nearly constant permeability between 0.5 and 3 md (0.0005-0.000033 μm^2), characteristic of microfracture-influenced permeability. Matrix-scale plug permeabilities are both higher and lower than DST permeabilities (Figure 9.3.11).

Variance in the DST-matrix correlation is partially or predominantly related to the limited vertical sampling of the core plugs and difficulty in representing some pore

properties that are larger in scale than core plugs. The single phylloid algal bafflestone interval exhibits significantly lower matrix permeability because core plugs did not sample the larger-scale vuggy nature of this lithofacies, which exhibits high permeability. Because microfractures do not contribute significantly to measured permeability for rocks with permeability greater than 0.5 md (0.0005 μm^2), both full-diameter and plug data reflect matrix properties, and the good correlation with DST permeabilities indicates that the reservoir is not fractured at the scale of investigation of the DST test. The better correlation of plug and DST permeabilities for intervals with permeability below 0.5 md, and the fact that upscaled permeabilities from plug data are greater than or equal to DST permeabilities for three of the four intervals, can be interpreted to indicate that these intervals are also unfractured. These data, and less precise data from other wells, indicate that the production characteristics of many wells in the Hugoton are consistent with matrix properties without significant contribution from natural fracture system. Data and statistics on the fraction of wells that exhibit production greater than what would be predicted from matrix properties have not yet been compiled and calculated.

Facies-specific permeability-porosity co-relationships were used for an initial estimate of grid permeabilities in each layer. Layer-DSTs from the Flower well were interpreted to estimate layer permeabilities effective in the drainage area of the science well. Also, permeabilities were measured at intervals of half-feet along the length of the Chase and Council Grove core retrieved from the Flower well. The core-derived (horizontal) permeability values at half-foot intervals were arithmetically averaged (upscaled) to derive the layer (horizontal permeability).

The geomodel built in Petrel® consisted of 69 layers. The tensor-upscaling algorithm in Petrel® was used to upscale vertical and horizontal permeability to 25 layers before exporting the model to CMG. For each layer at the location of the Flower Science well, the upscaled permeability was compared with that calculated from DST. For most layers the upscaled permeability was found to be close to that calculated from DSTs. For layers where the upscaled permeability differed from DST-permeability, an appropriate multiplier was applied to the specific layer in the model area so that the layer permeability at the Flower well (in the geomodel) matched that calculated from the corresponding DST. For each layer, Figure 9.3.12 summarizes the initial upscaled permeability and the multiplier applied to each layer so that the layer-permeability matched permeability derived from DST.

Reservoir Pressure

Some uncertainty exists regarding the initial reservoir pressure that can be considered representative of the Flower area. The earliest well spudded in this area was Zimmerman 1 in November 1937 (Figure 9.3.13). Available production data consist of volumes cumulated over 9- to 12-month periods till June 1952. The first recorded cumulative production data are attributed to July 1938. Thus, it is not possible to determine the exact start date of production from Zimmerman 1. The first recorded (surface) shut-in (SI) pressure at this well is 422 psi as of December 1937 in one database

(Figure 9.3.13). No mention about initial shut-in pressure at Zimmerman 1is found in other databases.

After Zimmerman 1, a series of five wells were drilled in the study area between November 1949 and October 1950 with the initial (surface) shut-in pressures at these wells varying between 373 psi and 395 psi (Figure 9.3.13). Thus within the study area, reservoir pressure varies at least by 20 psi based on initial shut-in pressure data recorded at wells drilled within a year. The average and median of (surface) shut-in pressures recorded at these five wells are 382 and 383 psi, respectively. By the time these later five wells were drilled, Zimmerman 1 had already produced 2.18 bcf of gas (as of May 1949).

Surface shut-in pressures were converted to bottom-hole shut-in pressures. Figures 9.3.14A and 9.3.14B show the estimation of initial reservoir pressure from recorded surface shut-in pressures following the average temperature and z-factor method. The estimated initial reservoir pressures are 458 psi and 416 psi assuming WHSPs of 422 psi and 385 psi, respectively. Not knowing what the initial pressure is representative of the Flower study area, initial simulation runs were carried out using starting reservoir pressure of 460 psi which resulted in charging the input geomodel (for the area studied) with an original-gas-in-place (OGIP) of 196 bcf.

Hydraulic Fractures

All wells in the study area have been fractured. The Chase Infill and the Council Grove wells were fractured upon completion. The Chase Parent wells were drilled before fracturing technology was developed and thus produced unfractured until the 1960s. The exact dates of hydraulic fracturing the Chase Parent wells are not known. Thus, all Chase Parent wells have been assumed to be fractured on January 1960. This date approximately coincides with a visible increase in production from the Chase wells. However, there is no information or test data available which would enable one to estimate the physical characteristics of these fractures. The intent of the fracturing was to enhance the well productivity. Lacking physical descriptions of hydraulic fractures, the enhanced well productivities were modeled in this study using the well productivity (ff) factor greater than 1 with the ff set to 1.0 for an unfractured well.

Limited pressure test data were available for the Alexander D2 well located outside the study area. An approximate estimation of fracture half-length was made by analyzing these data. Sensitivity studies were carried out at individual wells in the study area by modeling the fractures with local grid-refinements using half-lengths from Alexander D2. The effects of hydraulic fractures defined by local grid refinement were replicated when ff = 6.0 was used at respective wells. Thus, each well was assigned an ff = 6.0 to model its flow behavior after hydraulic fracturing.

In this study, ff values ranging between 4 and 9 resulted in history matches at most Chase wells with minimal excess flow capacity when wells were freed of rate constraints. That hydraulic fractures resulted in an increase in well productivity by 4 to 9 times an unfractured well was found acceptable by operators of the field.

Flow Constraints

Monthly production data were available for all wells except the Chase Parent wells, for which annual production data were available for years before 1953 and bi-annual cumulative production data were available from 1953 to 1966. From 1967 onwards, monthly production data were available for the Chase Parent wells. Regular tubing head flow and shut-in pressure data were available for all wells from 1967 onwards.

In the simulation study, all wells were flowed under rate constraints until June 2003. Thereafter, all wells were flowed under a constant bottom-hole pressure (BHP) of 14.7 psi until December 2004. The intent of changing from rate constraint to pressure constraints was to see if the simulator-calculated production rates from July 2003 followed the already established decline trends without showing production spikes (or signs of excess flow capacity).

Reservoir Simulation Studies

Run 1

The initial simulation runs were carried out by confining the completion of Chase (CH) wells within the Chase layers and those of the Council Grove (CG) wells in the CG layers. Figures 9.3.15 to 9.3.17 show the resulting history matches obtained at the Chase Parent (CHP), Chase Infill (CHI), and CG wells. The ff factor was set to 6 for all wells except the PTrot24 (Trotter 1-24) well. Production is matched at all CHP wells with the simulator-calculated bottom-hole-flowing pressure (BHFP) closely matching the trend of the well-head-flowing pressure (WHFP). Though a regular record of well-head-shut-in pressures (WHSP) was available, field operators expressed doubts about whether the recorded WHSP (after 72 hrs of SI) was stabilized to be representative of the reservoir conditions and about the procedure to convert tubing-head pressures to reservoir conditions. It was thus recommended that the simulator-calculated bottom-hole-flowing pressures be matched against the flowing pressures recorded at the surface, taking into account the fact that a small discrepancy was expected to be present between flowing-surface and bottom-hole pressures. A production spike was observed in most CHP wells after the wells were flowed free of rate constraints in July 2003, indicating presence of excess flow capacity.

Figure 9.3.16 shows the history matches obtained for CHI wells. Production matches were obtained at all wells except IPer (Persinger) which is a border well. The simulator-calculated BHFPs are significantly higher than the corresponding WHFPs. Production spikes are visible after wells are released from rate constraints indicating presence of excess flow capacity. Figure 9.3.17 shows the history matches obtained for the CG wells. With CG completions constrained to CG layers, simulator-calculated

production rates could not match the historic values at any of the CG wells. Figure 9.3.18 shows the simulator-calculated pressure distribution as of January 1970, i.e., just before the CG wells came online. The simulator output indicates that the CG layers are at 460 psi. However, initial surface SI pressures at all CG wells before onset of significant production converge to 265 psi. Adjusted for gas column, this SI pressure translates to around 280 psi.

Between the start of production in the 1930's and 1940's and January 1970, the CHP wells had been in production and this resulted in lower pressures in the CH layers. Figure 9.3.18 indicates that the simulator results show differential depletion in the CH layers with Layer 2 (i.e., Krider) being at 285 psi. Thus for CG wells to show initial SI pressures in the range of 280 psi, one possibility is to extend the CG well completions into Chase layers. However, this brings forth the question as to how far into CH do the CG well completions need to extend. It appears from the pressure distribution in Figure 4.1.4 that if the CG completions were extended to Layer 2 then upon shut-in, the test will straddle all CG layers (which are above 400 psi) and most of CH layers one of which (i.e., Layer 2) is at 285 psi. The test of this assumption is to rerun the simulation with CG completions extending to Layer 2 and then analyze the simulation output to see if the CG wells record SI pressures around 280 psi upon completion, and also see if the simulator-calculated production rates at CG wells match those recorded historically.

Run 2

Completions in CG wells were extended to Layer 2 (Krider). Figure 9.3.19 shows the history matches for CHP wells. The simulator-calculated rates matched historic rates in all wells, and thus extending CG completions into Krider did not interfere with production from the CHP wells. The simulator-calculated BHFP and the recorded WHFPs are close and follow similar trends. Figure 9.3.20 compares the simulator-calculated flow rates with historic rates for the CHP wells. Upon release from rate constraints in July 2003, most wells except Persinger (PPer) show a production spike indicating the presence of excess flow capacity due to high ff values and/or excess OGIP. Figure 9.3.21 displays the history matches obtained for the CHI wells. Cumulative production is matched at all wells except Persinger (IPer), which is a border well. Thus, extending completions of CG wells to Krider (Layer 2) did not disturb the production matches at the CHI wells. The simulator-calculated BHFP is higher than the recorded WHFP in most non-border wells. The BHFP trends are similar to that of WHFP before flattening in later flow periods indicating excess flow capacity (i.e., too high ff and/or OGIP). Figures 9.3.22a and 9.3.22b show the history matches obtained for the CG wells. The cumulative production is matched in all CG wells. The BHFP is slightly higher than WHFP in most wells. However, the BHFP trends are similar to WHFP initially before flattening during the later flow period indicating excess flow capacity.

It appears from the above simulation runs that ff = 6 is perhaps too high for most CHP, CHI, and CG wells because of the presence of a production spike in July 2003 and a flattening of the simulator-calculated BHFP in the later part of the flow period. Thus, selective reduction in ff was carried out in most CHP wells. Simulation runs were carried

out with ff = 2 and 3 for CHP wells. However, such reduction in ff was not effective in doing away with the production spikes. Any further reduction in ff values in order to eliminate the production spikes would mean that hydraulic fracturing either did not improve well productivity or improved it by a minor fraction. As mentioned earlier, field operators were comfortable with the assumption that hydraulic fracturing resulted in a significant increase in well productivity such that an assumption of ff = 6 (or around 6) can be considered reasonable.

The presence of excess flow capacity can be attributed to multiple factors and/or any combination of them. Important factors that contribute to the well flow-capacity include: a) ff value, b) OGIP in the drainage area, and c) effective permeability distribution in drainage area. The above discussed simulation runs were carried out assuming that the initial reservoir pressure in the Flower study area was 460 psi (resulting in OGIP = 196 bcf) based on the initial surface SI pressure of 422 psi at one CHP well, the Zimmerman 1 (Figure 9.3.13). The surface shut-in pressure of 422 psi is at best reflective of the conditions prevailing within the drainage area of the Zimmerman 1 well. It is reasonable that production from other CHP wells drilled earlier or contemporary to Zimmerman 1 affected the average reservoir pressure in the Flower study area, or that the first recorded shut-in pressure at this well is not representative of the study area given that there is variation of 20 psi (Figure 9.3.13) in surface shut-in pressures recorded at 5 wells drilled between November 1949 and October 1950. Thus, the problem of excess flow capacity may be caused due to assuming a high initial reservoir pressure, i.e. 460 psi. Also, given the heterogeneity in reservoir permeability, some variation (within a range) in the initial reservoir pressure possibly existed over the study area.

To address the problem of excess flow capacity, the following simulation runs were carried out by assuming a lower initial reservoir pressure, i.e., 435 psi which results in an OGIP of 185 bcf.

Run 3

The initial reservoir pressure was set at 435 psi and completions of CG wells were extended to Krider (Layer 2) in this run. Figure 9.3.23 shows the history matches obtained for the CHP wells when ff values were set between 5 and 9. Production was matched at all CHP wells. Only the PBet (Betts) well shows a small production spike (compared to previous runs) when produced free of rate constraints. Figure 9.3.24 compares the simulator-calculated BHFPs with the recorded WHFPs. A close match is observed for all the CHP wells. Figure 9.3.25a and 9.3.25b show the history matches obtained at CG wells. Production is matched for all CG wells and 3 wells do not show any production spikes upon release from rate constraints. Presence of production spikes in remaining CG wells indicates need for ff adjustments.

Run 4

Figures 9.3.26a and 9.3.26b show the history matches for the CG wells when ff values in wells showing production spikes (in Run 3) are adjusted (reduced from the

initial value of 6). Despite reduction of ff value to between 2 and 3, production spikes remain in the CG wells. It appears that ff values must be reduced below 2 to reduce/eliminate the remaining production spikes. Thus, it appears that the production spikes are perhaps a result of excess OGIP rather than high ff values. Hence, the initial reservoir pressure was reduced to 423 psi (resulting in an OGIP of 179.5 bcf) for the following runs.

The OGIP in the Chase layers is 152.2 bcf when the initial reservoir pressure is assumed to be 423 psi. As mentioned earlier, until May 1949 only 1 well, Zimmerman 1, was producing from the study area. Five additional wells were drilled in the study area between November 1949 and October 1950. As of May 1949, cumulative production from Zimmerman 1 was 2.18 bcf, i.e., 1.4% of the Chase OGIP. It is important to note that early Hugoton wells produced without being fractured until hydraulic fracturing came in use in the 1960's, and communication issues between the Chase and Council Grove reservoirs do not arise until after 1960's. Using standard gas laws, the average Flower area reservoir pressure after May 1949 is expected to be 1.4% less than the starting pressure of 423 psi, i.e., 417 psi. As mentioned earlier, the mean and median surface shut-in pressures, recorded at the 5 wells completed between November 1949 and October 1950 in the Flower area, were 382 and 383 psi respectively, and Figure 9.3.14B shows that a well-head shut-in pressure of 385 psi translates to 418 psi under bottom-hole conditions. Thus based on recorded production volumes and the standard gas law, the representative initial reservoir pressure in the Flower area is around 423 psi.

Run 5

Figure 9.3.27 shows the history matches for CHP wells. Simulator-calculated well production rates match with historic rates and production spikes are eliminated (or significantly reduced) with minor adjustments to ff values in select wells. Figures 9.3.28a and 9.3.28b summarize the history matches obtained for the CG wells. Some wells still show production spikes and thus the following run incorporates ff adjustments especially for select CG wells.

Run 6

Figure 9.3.29 shows the history matches at CHP wells whose ff values vary between 5 and 9. The above figure depicts a good history match of production rates at the CHP wells with minimal or no production spikes. Figure 9.3.30 depicts a good match between the simulator-calculated BHFPs and the recorded WHFPs at CHP wells. Figure 9.3.31a and 9.3.31b display the match between simulator-calculated production and historic rates for CG wells with ff values set between 5 and 9. Production rates are matched at all CG wells during flow under rate constraints. Some CG wells still show a production spike when flowed free of rate constraints. However, the magnitudes of these remaining production spikes are significantly less than previous runs. Figures 9.3.32a and 9.3.32b compare the simulator-calculated BHFPs with the recorded WHFPs. The pressure values closely follow similar decline trends. Figure 9.3.33 production history matches for the CHI wells. Production is matched at CHI wells that are not located close to the border of the area simulated. It is reasonable to expect a lack of match at these border wells,

marked by red boxes, because part of the area drained by these wells lies outside the area simulated. Also, no significant production spikes are visible at the non-border wells. Figure 9.3.34 compares the simulator-calculated BHFPs with recorded WHFPs. The pressure values for the non-border wells closely follow similar trends. However at some of the wells, the simulator-calculated pressures flatten at later flow periods, which may indicate excess flow capacity. As expected, pressure matches are absent for the border wells.

Figure 9.3.35 displays the simulator-calculated pressure distribution in each layer as of January 1, 1970 – i.e., just prior to the drilling of the CG wells in the study area. The reservoir pressure in Krider (Layer 2) is around 250 psi, while it ranges between 350 and 380 psi for the other CH zones. As noted earlier, CG wells in the study area tested surface shut-in pressures around 265 psi upon completion. Thus to test the robustness of the reservoir model being simulated, a hypothetical CG well was placed at the center of the study area (Figure 9.3.36A) and its completion extended from Krider (Layer 2 in Chase) to B5Lime (Layer 23 in Council Grove) – similar to other CG wells in this model. This test well was named "SI Well", and was completed within the simulator input file on January 1, 1970. Available records do not clearly indicate if the initial shut-in tests at the CG wells were carried out before or after the hydraulic fracturing. Thus, ff values at this well were maintained at 1. Local grids around this test well were subjected to refinement to reduce grid-size induced errors in calculated build-up pressures. The well was flowed for a day within the simulator and then shut-in for 72 hours (following the field practice in the 1970's at the time of drilling of the CG wells). The SI pressure at this test well was found to stabilize around 238 psi (Figure 9.3.36B).

The Flower Science well was drilled in early 1995, and detailed layer-specific DST recordings are available from this test well. Figure 9.3.37 displays the simulator-calculated pressure distribution in the study area as of January 1, 1995. Figures 9.3.38A and 9.3.38B compare the simulator-calculated layer pressure at the location of the Flower Science well with that recorded in the field by DSTs carried out in early 1995. Close matches were obtained in most layers except L/FTRLY, B2LM, and B4LM where the simulator-calculated pressures were significantly higher than that recorded in DSTs. Thus despite matching production histories at the CG wells, layers such as B2LM and B4LM in this simulation model did not drain to the extent suggested by the Flower DSTs. The question that naturally arises at this juncture is if gas from the above two CG layers is being drained by non-CG wells, i.e., CH wells. Such a situation would be possible if completions at the CHP and CHI wells extended into the CG layers. Thus in the succeeding simulation runs, completions at the CHP and CHI wells were extended to Layer 23 (i.e., B5 Lime/Shale) while completions at the CG wells remained extended to Layer 2 (Krider).

Run 7

Completions at the CHP and CHI wells have been extended to Layer 23 (B5 Lime/Shale). Production and pressure matches at the CHP, CHI, and CG wells remain unchanged. Within the simulator model, a hypothetical CG well was located at the center

of the study area (Figure 9.3.39A) and completed on January 1, 1970. A 72-hr shut-in was carried out at this hypothetical CG well in January 1970 resulting in a shut-in pressure of 256 psi (Figure 9.3.39B). This simulator-calculated shut-in pressure at the CG well upon completion is closer to 265 psi – the surface pressure recorded at most CG wells in the study area upon completion. Thus, extending the CH fractures into CG results in shut-in pressures closer to those recorded in the field at CG wells upon their completion. Figure 9.3.40 compares the simulator-calculated layer pressures at the Flower Science well from Run 6 (Figure 9.3.40B) and Run 7 (Figure 9.3.40C) as of January 1995 with that recorded by DST. Extending completions at the CH wells into CG while CG completions extend into Chase appears to improve the layer pressure matches at the Flower Science well. Also, such a model results in a simulator-calculated SI pressure at a hypothetical CG well to come closer to 265 psi while not compromising the production and pressure history matches at CHP, CHI, and CG wells.

Figure 9.3.41 compares the simulator-calculated layer pressure values at the Flower Science well as of January 1, 2004, with that calculated as of January 1, 1995, to highlight layers that significantly contribute to the production between 1995 and 2004. Figure 9.3.42 compares the simulator-calculated reservoir pressures in each layer (Chase and Council Grove) at the location of the Flower Science well between January 1995 and January 2004. This plot clearly shows that per the current model, greater pressure declines occur in the Chase layers as compared with the Council Grove layers. Thus, most of the production, harvested by the existing wells in the study area (i.e., CHP, CHI, and CG wells) over this decade, originates from the Chase layers.

Figure 9.3.43 displays as a 3D volume the simulator-calculated pressure distribution in the study area as of January 1, 2004. The area modeled in this study is assumed to produce under volumetric expansion. Thus, external fluids (water) do not influx into the study-area volume. Hence, gas saturations do not change over time. Continued production from the wells results in changes in reservoir pressure depending on the gas volumes contributed by a layer or any local reservoir volume. Remaining potential, therefore, lies in areas where remaining high pressures (as of January 1, 2004) combine with better porosity, pay thickness, and effective permeability. Layers with high remaining pressures will not be prospective if their porosity, pay thickness, and effective permeability are low. Recovery volumes from future wells also depend on the type of completions, i.e., if the well is vertical or horizontal connecting one or more layers.

Figures 9.3.44A and 9.3.44B plot the annual percentage decline in simulator-calculated production from Chase Parent and Council Grove wells in the Flower area when RUN 7 is extended to 2050. These plots show that these wells decline at rates between 8 to 10% as of 2005. The simulator-estimated annual production decline rates fall to close to 2% near 2045.

Run 8

This simulation run looks at a “what if” scenario – What happens if completions in CH wells extended to B2LM (Layer 17) rather than B5LM (i.e. Layer 23) while the

completions at the CG wells extended to FTRLY (i.e. Layer 8) rather than Krider (i.e., Layer 2)? Results from this simulation run show that production matches were obtained at CHP and CHI wells. However, production spikes surfaced in case of some of these CH wells when wells flowed free of rate constraints. Also, the simulator-calculated production rates at the CG wells fall short of recorded rates (Figure 9.3.45). Figure 9.3.46 compares the simulator-calculated layer pressure data, as of January 1995, at the location of the Flower Science well from Run 7 with that from Run 8. In Run 8, the simulator-calculated production rates for CG wells fell short of recorded history while Run 7 resulted in good matches. The above figure indicates that based on the current reservoir model, completions at the CG wells have to extend up and into the Chase beyond FTRLY.

Conclusions

a) Increasing OGIP in CG layers within petrophysical constraints while using a permeability distribution that mirrors layer permeability calculated from DSTs recorded at the Flower Science well does not result in production history matches at CG wells.

b) Production matches at the CG wells are achieved only when CG wells communicate with CH gas. In this study, such communication was established by extending completions at the CG wells into CH layers.

c) CG completions need to extend up to Krider (in Chase) for CG wells to show an initial SI pressure in the vicinity of 265 psi upon well completion in January 1970.

d) An OGIP of 180 bcf (spread between the CH and CG layers) is sufficient to obtain production/pressure matches at the CH and CG wells using ff values between 5 to 9. Such a model also resulted in minimal or no production spikes when wells are set free of their rate constraints and produce under pumped-off conditions.

e) Extending CH completions into B5LM (i.e., into CG) while completions in the CG wells extended into Krider (i.e., into CH) improved the match (as of January 1995) between the simulator-calculated layer pressure at the location of the Flower well with that recorded from DST. It also resulted in a closer match between the simulator-calculated SI pressure at a hypothetical CG well, located in the center of the study area, to that recorded at CG wells upon completion in the study area.

f) Run 7 provided the best match with all available pressure and production data in the study area including:

i) Production history matches at CHP, CHI, and CG wells

ii) Close match between simulator-calculated BHFPs and recorded WHFPs at CHP, CHI, and CG wells

iii) Minor or no production spikes at the above mentioned wells when they were flowed under pumped-off conditions and free of rate constraints.

iv) SI pressures close to 265 psi at a hypothetical CG well upon completion in January 1970.

v) Good match of simulator-calculated layer pressures at the Flower Science well with that recorded by DSTs as of January 1995

vi) ff values for most wells cluster around 6.

g) Based on results from Run 7, the simulator-calculated annual production declines vary between 8 to 10% for the Chase Parent and Council Grove wells as of 2005. By 2045, the annual rate of production decline falls to about 2% for these wells.

h) Extending CH completions to B2LM while extending CG completions to FRTLY does not result in production history matches at the CG wells.

References:

Caldwell, C. D., 1991, Cyclic Deposition of the Lower Permian, Wolfcampian, Chase Group, Western Guymon-Hugoton Field, Texas County, Oklahoma, *in* Midcontinent Core Workshop: Integrated Studies of Petroleum Reservoirs in the Midcontinent: Midcontinent American Association of Petroleum Geologists Section Meeting, Wichita, Kansas, p. 57-75.

Dubois, M. K., Byrnes, A. P., Bohling,G. C., Seals, S. C., and Doveton, J. H., 2003, Statistically based lithofacies predictions for 3-D reservoir modeling: examples from the Panoma (Council Grove) field, Hugoton Embayment, Southwest Kansas (abs): Proceedings AAPG 2003 Annual Convention, Salt Lake City, Utah, v.12, p. A44, *and* Kansas Geological Survey Open-File Report 2003-30, 3 panels, http://www.kgs.ku.edu/PRS/publication/2003/ofr2003-30/index.html (accessed October 10, 2005).

Dubois, M.K., Bohling, G. C., Byrnes, A. P., and Seals, S. C., 2003, Extracting lithofacies from digital well logs using artificial intelligence, Panoma (Council Grove) Field, Hugoton Embayment, Southwest Kansas**,** (abs): Mid-continent Section AAPG Meeting, Tulsa, *and* KGS Open-file Report 2003-68, http://www.kgs.ku.edu/PRS/publication/2003/ofr2003-68/index.html (accessed December 21, 2005).

Dubois, M. K., Byrnes, A. P. and Bohling, G. C., 2005, Geologic model for the giant Hugoton and Panoma fields (abs): AAPG Midcontinent Section Meeting, Oklahoma City, Oklahoma,
http://www.kgs.ku.edu/PRS/Poster/2005/MidcontAAPG/index.html (accessed October 10, 2005).

Heyer, J. F., 1999, Reservoir characterization of the Council Grove Group, Texas County, Oklahoma, *in* D. F. Merriam, ed., Transactions of the American Association of Petroleum Geologists Midcontinent Section Meeting: Wichita, KS, p. 71-82.

Luczaj, J. A., and Goldstein, R. H., 2000, Diagenesis of the Lower Permian Krider Member, southwest Kansas, U.S.A.: fluid-inclusion, U-Pb, and fission-track evidences for reflux dolomitization during latest Permian time: Journal of Sedimentary Research, v. 70, no. 3, p. 762-773.

Oberst, R. J., Bansal, P. P., and Cohen, M. F., 1994, 3-D reservoir simulation results of a 25-square mile study area in Kansas Hugoton gas field:, SPE Mid-Continent Gas Symposium, Amarillo, TX, SPE 27931, p. 137-147.

Olson, T. M., Babcock, J. A., Prasad, K. V. K., Boughton, S. D., Wagner, P. D., Franklin, M. K., and Thompson, K. A., 1997, Reservoir characterization of the giant Hugoton gas Field, Kansas: American Association of Petroleum Geologists Bulletin, v. 81, p. 1785-1803.

Ryan, T. C., Sweeney, M. J., and Jamieson, W. H. Jr., 1994, Individual layer transient tests in low-pressure, multi-layered reservoirs: SPE Mid-Continent Gas Symposium, Amarillo, Texas, SPE 27928, p. 99-113.

Siemers, W. T., and Ahr, W. M., 1990, Reservoir facies, pore characteristics, and flow units: Lower Permian Chase Group, Guymon-Hugoton field, Oklahoma: Society of Petroleum Engineers, Proceedings 65th Annual Technical Conference and Exhibition, New Orleans, LA, September 23-26, SPE #20757, p. 417-428.

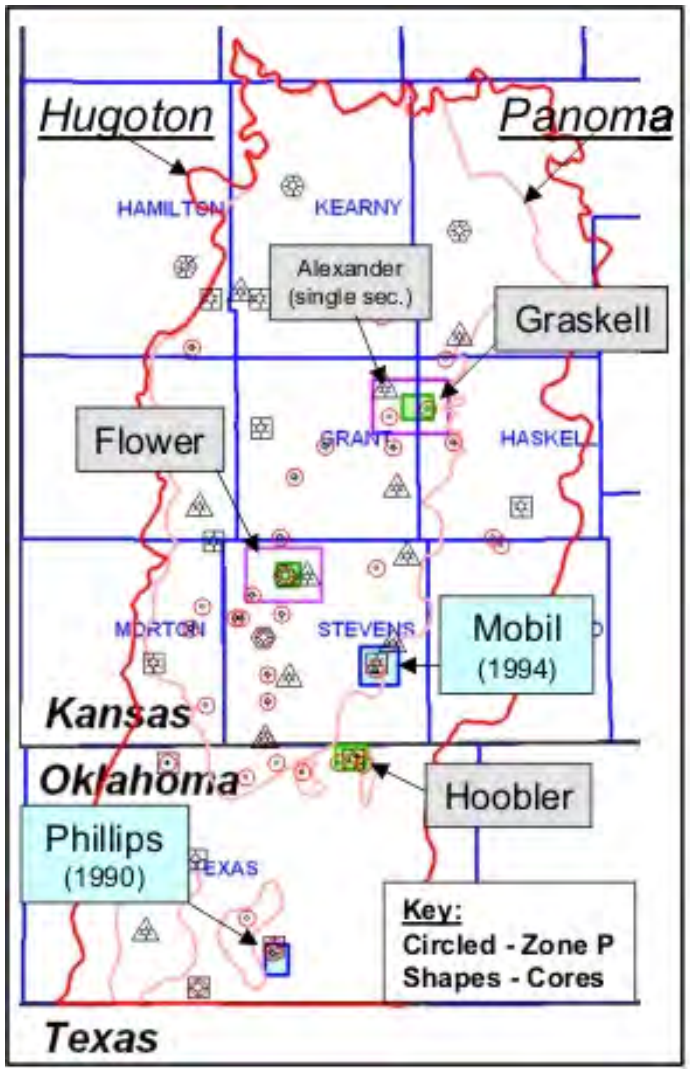

Figure 9.3.1. Map showing the location of the Flower study area in the Hugoton and Panoma fields.

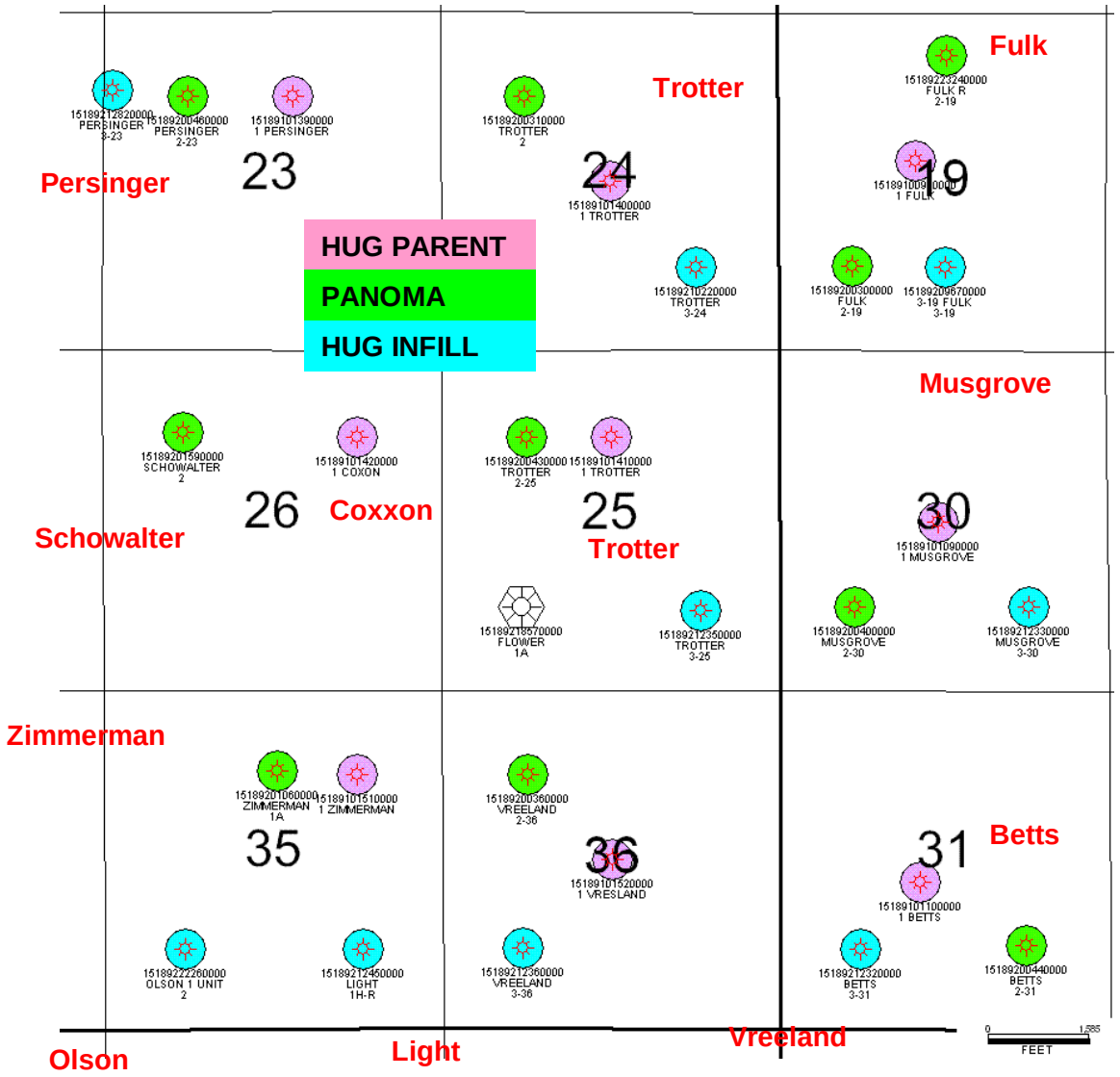

Figure 9.3.2. Map showing the location of wells in the Flower study area.

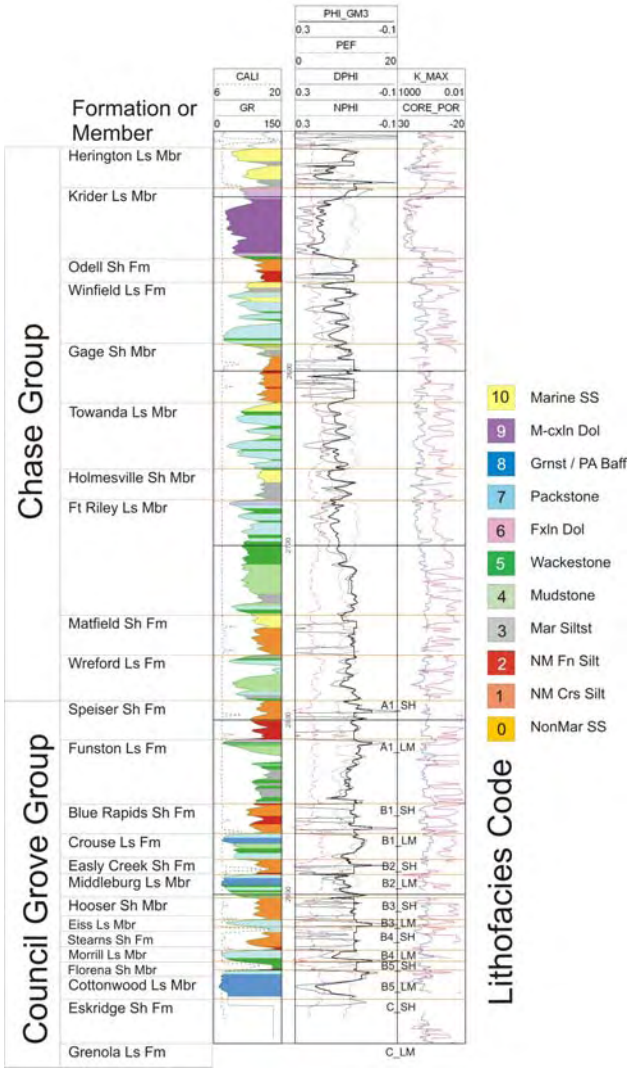

Figure 9.3.3. Profile of study area type well Flower A-1 well located in Sec 25-31S-38W, Stanton County, Kansas.

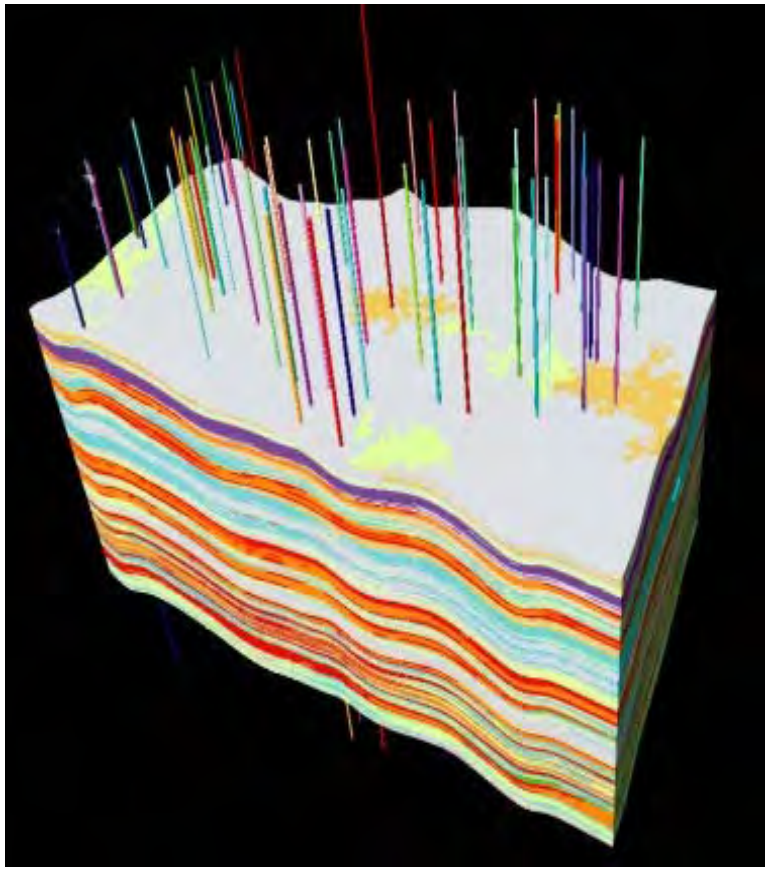

Figure 9.3.4. 234-layer 3D volume of static model showing (color-coded) lithofacies in the 70 square mile around the Flower study area. Wells with facies and porosity information are shown (node wells).

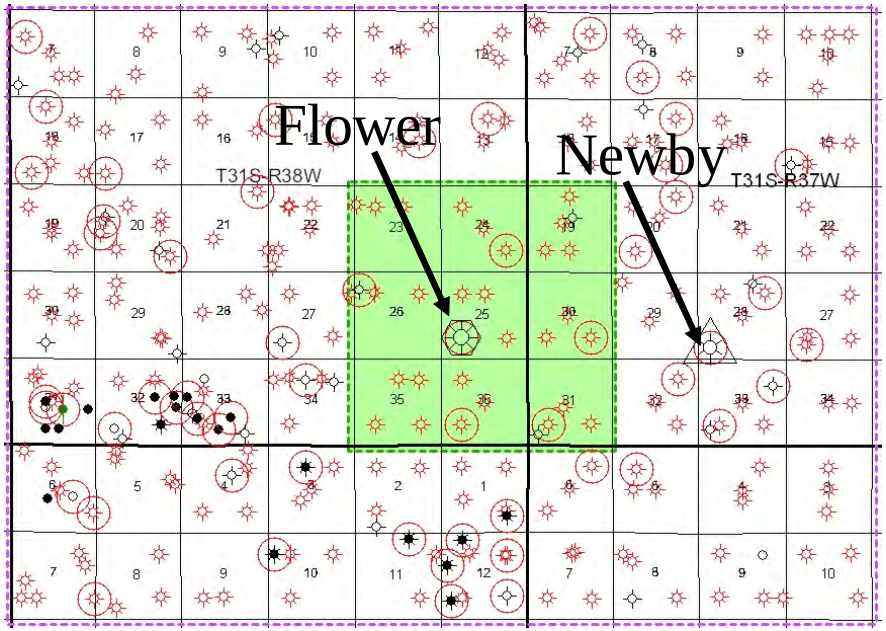

Figure 9.3.5. Data used to model the larger Flower area included formation tops from 300 wells, facies and porosity data from 57 node wells. The area simulated is shaded green has 6 node wells including the Flower A1 that had a continuous core through the Chase and Council Grove. The Newby well has continuous core in the Council Grove.

PHI_CORR = A + B*DPHI + C*NPHI

	Intercept A	PHID B	PHIN C
Facies 1 & 2	0.018	0.843	0.000
Facies 3 & 4	0.019	0.662	0.000
Facies 5 & 7 & 8	4.278	0.400	0.209
Facies 6	0.000	0.500	0.500
Facies 9	8.918	0.447	0.131
Facies 10	4.484	0.524	0.135

Figure 9.3.6. Lithofacies-specific set of constants, derived from regression analysis, to estimate porosity from wireline log data.

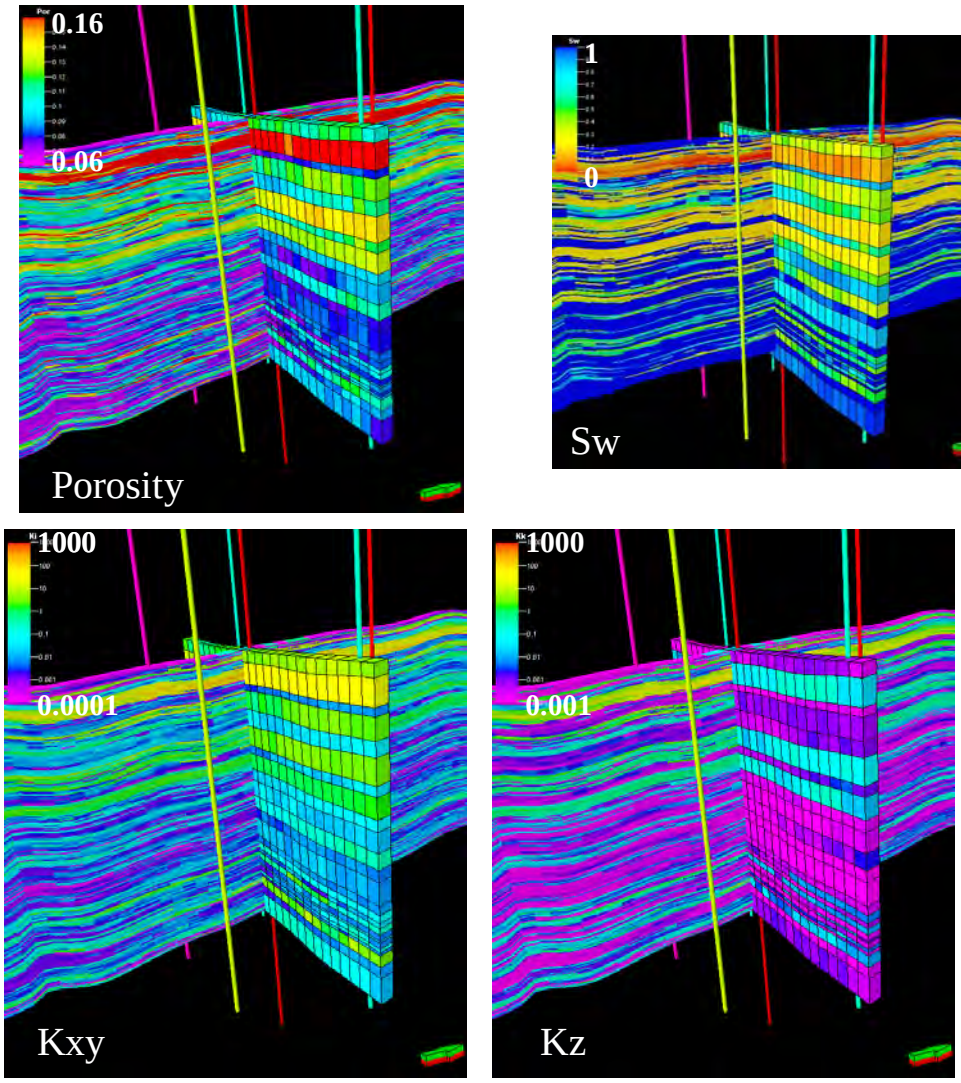

Figure 9.3.7. Layer properties in fine- and up-scaled models shown with intersecting EW (25-layer upscaled) and NS (234-layer static model) cross sections that meet at the Flower A1 well. Well trajectories are shown for the node wells.

Assumed PVT properties:					
Reference pressure			465	psi	
Rock compressibility			0.000002	1/psi	(assumed)
Reservoir temp			90	F	
Gas gravity (Air = 1.0)			0.715		
Water salinity			110,000	ppm	

Figure 9.3.8. General PVT properties input to simulation study of Flower area.

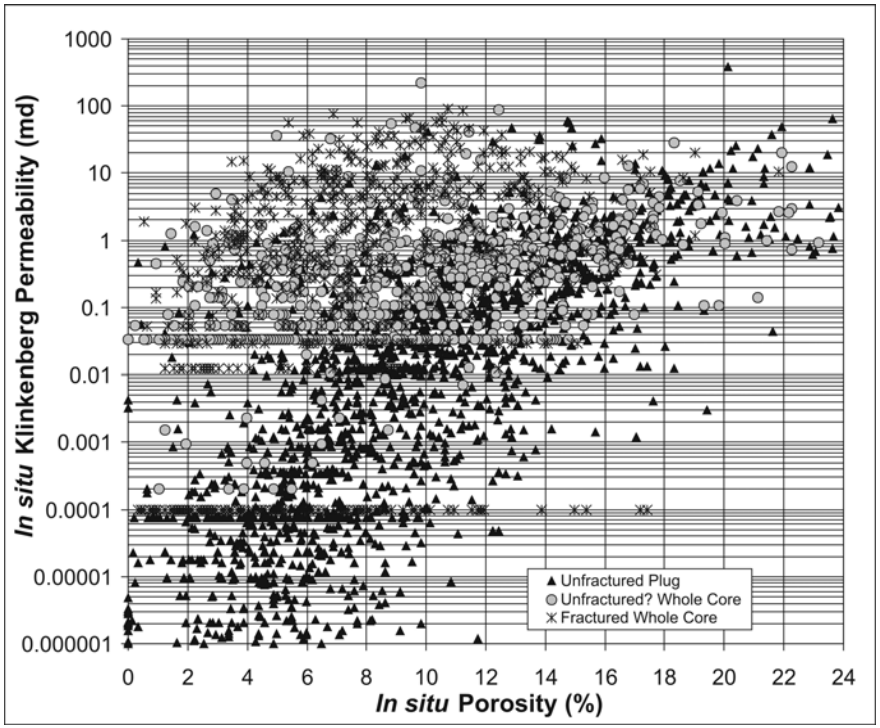

Figure 9.3.9. Crossplot of *in situ* Klinkenberg permeability versus *in situ* porosity for whole core identified as fractured (asterisks), whole core that were not identified as fractured but may contain microfractures (grey circle), and unfractured core plugs (black triangle).

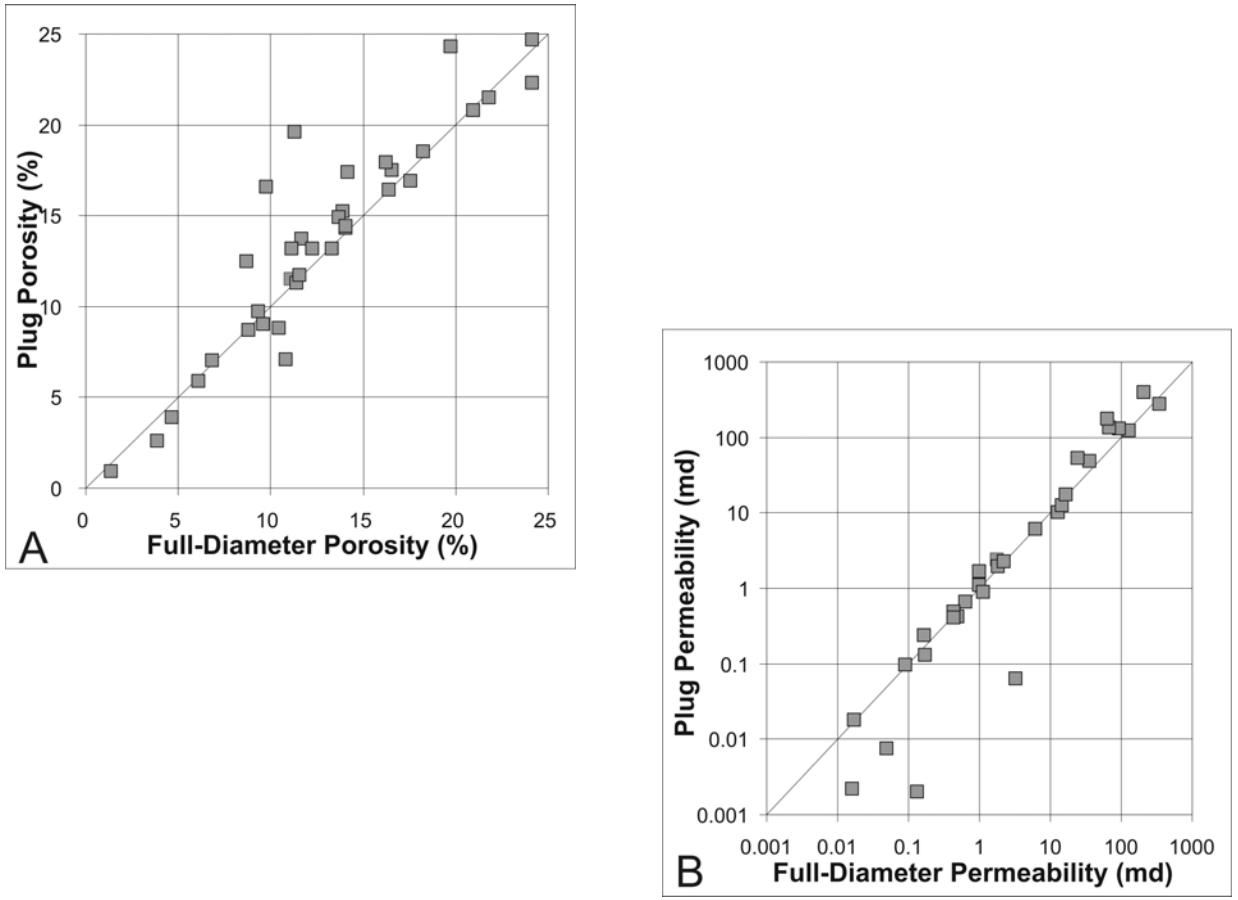

Figure 9.3.10. Crossplot of full-diameter core porosity versus plug porosity (A) and permeability (B) for samples in which the full-diameter cores did not exhibit any apparent microfracturing. Good correlation indicates that matrix-scale properties apply to full-diameter scale. Variance can be attributed to full-diameter core sampling multiple lithofaceis or a range in porosity not sampled by the corresponding core plug.

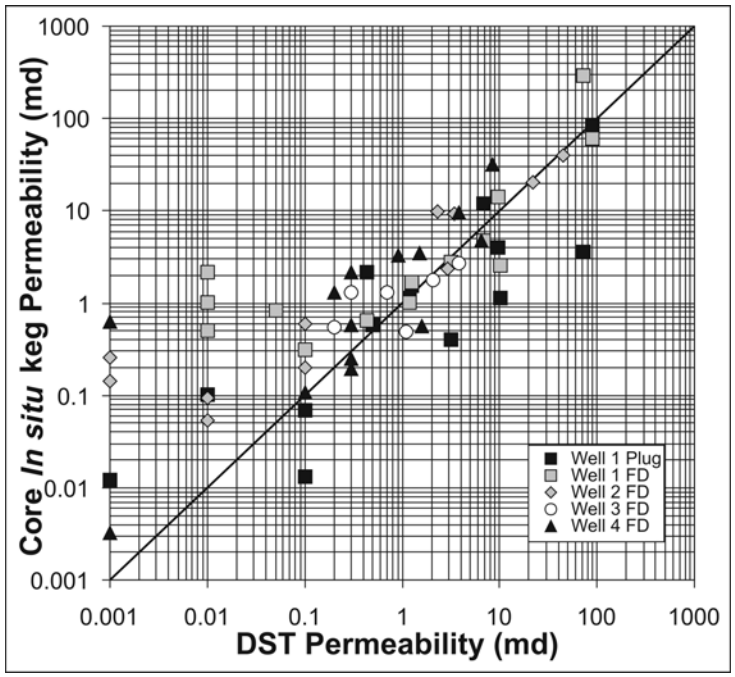

Figure 9.3.11. Crossplot of calculated interval drill stem test (DST) formation permeability versus average interval permeability calculated from full-diameter core for four wells and from core plugs in well 1. Routine core data were corrected for confining stress, Klinkenberg, and relative permeability effects so as to correspond to reservoir-condition values. Good correlation down to ~0.5 md shows matrix-scale control of flow in the region of DST investigation. Below 0.5 md microfractures in full-diameter core result in permeabilities higher than in the unfractured reservoir. Higher DST than core plug permeabilities can be interpreted to indicate that formation is not fractured in the range of investigation and that plug sampling density was probably not adequate to properly sample lower range of permeability.

Layer	Formation	Upscaled K, md	DST K, md	Multiplier
1	Hrngtn-Paddock	5.668	6.9	1
2	Krider	47.422	90.30	1.9
3	Odell	0.017	9.7*	1
	Wnf SS			
4	Wnf LS	1.620	7.60	4.7
5	Gage	0.064	Not Tested	1.0
6	Towanda	1.666	1.20	1.0
7	B/TWND	1.859	Not Tested	1.0
8	FTRLY	0.948	0.43	1.0
9	L/FTRLY	0.019	0.001	1.0
10	B/FTRLY	0.039	0.1	1.0
11	WREFORD	0.107	0.5	4.7
12	A1_SH	0.001	Not Tested	1.0
13	A1_LM	0.023	3.141**	1.0
14	B1_SH	0.002	Not Tested	1.0
15	B1_LM	0.123	0.1	1.0
16	B2_SH	0.004	Not Tested	1.0
17	B2_LM	0.755	10.2	13.5
18	B3_SH	0.002	Not Tested	1.0
19	B3_LM	0.047	0.01	1.0
20	B4_SH	0.001	Not Tested	1.0
21	B4_LM	0.676	3.2	4.7
22	B5_SH	0.002	Not Tested	1.0
23	B5_LM	11.558	72.1	6.2
24	C_SH	0.002	Not Tested	1
25	C_LM	0.089	Not Tested	1

* Not representative

** Not a very representative value

May not need a multiplier

Figure 9.3.12. Summary of layer-specific permeability multiplier and upscaled layer permeability input for simulation of Flower area.

	Well	Sim Name	Sim Start	Cum, mcf	SI date	Start SI, psi	End Prod
1	Zimmerman1	PZim	12/31/1937	12,811,895	12/31/1937	422	6/30/2003
2	Coxxon1	PCox	11/30/1949	12,481,346	11/30/1949	374	6/30/2003
3	Trotter1-25	PTrot25	12/31/1949	9,056,970	12/31/1949	385	6/30/2003
4	Vresland1	PVres	6/30/1949	16,244,041	12/31/1949	373	6/30/2003
5	Trotter1-24	PTrot24	6/30/1950	6,140,333	6/30/1950	395	6/30/2003
6	Musgrove1	PMusg	10/31/1950	12,519,815	10/31/1950	383	6/30/2003
7	Fulk1	PFulk	1/1/1951	12,880,765	1/01/1951	394	6/30/2003
8	Betts1	PBet	6/30/1951	10,271,314	6/30/1951	361	6/30/2003
9	Persinger1	PPer	10/1/1953	5,888,797	10/31/1955	372	6/30/2003

Avg Pr - Nov 1949 to Oct 1950, psi	**382.0**
Median Pr - Nov 1949 to Oct 1950, psi	**383**

Figure 9.3.13. Tabulation of start dates of and initial shut-in (SI) pressures recorded at Chase Parent wells in the Flower study area.

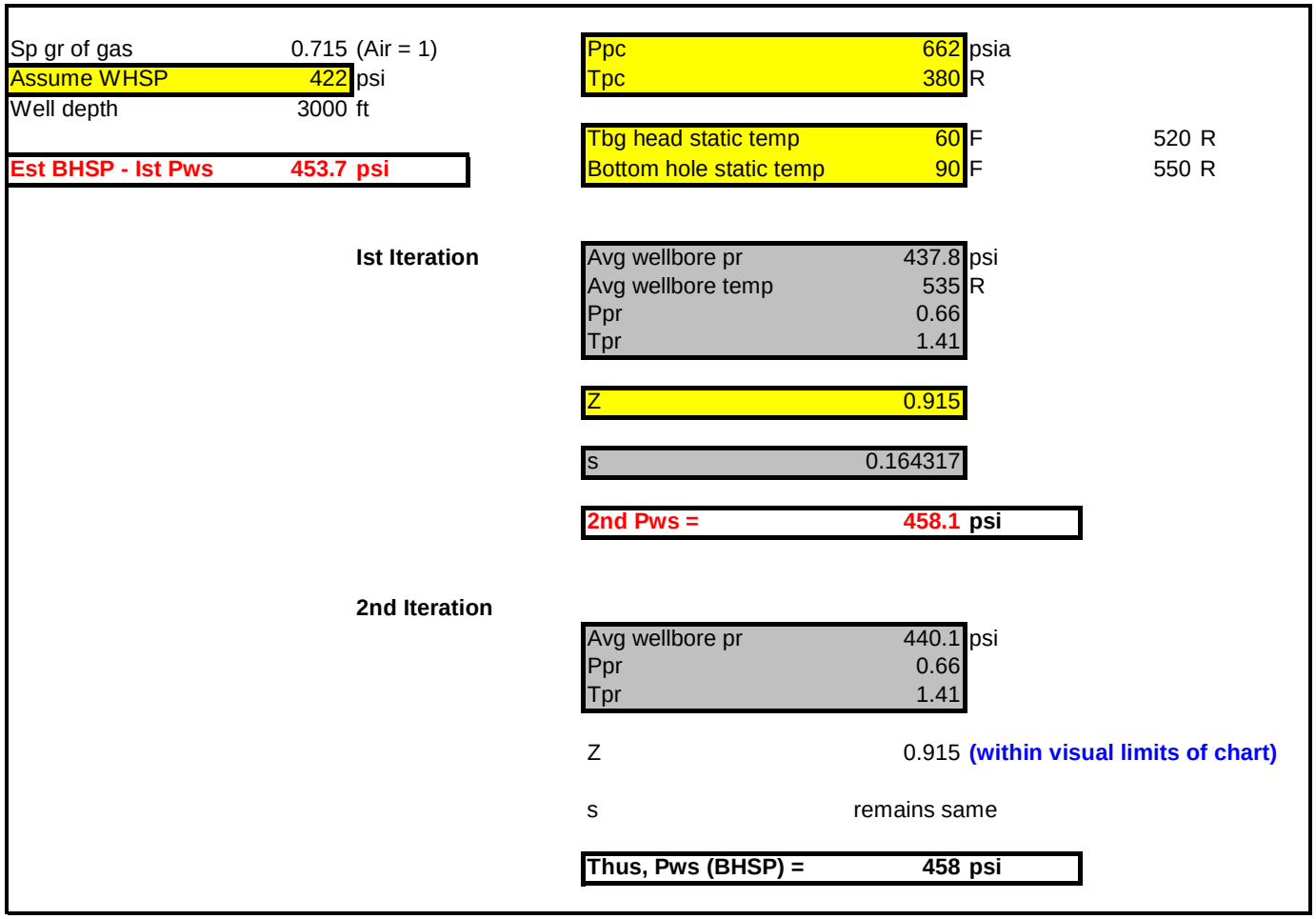

Figure 9.3.14A. Procedure to calculate bottom-hole shut-in pressure from well head shut-in pressure.

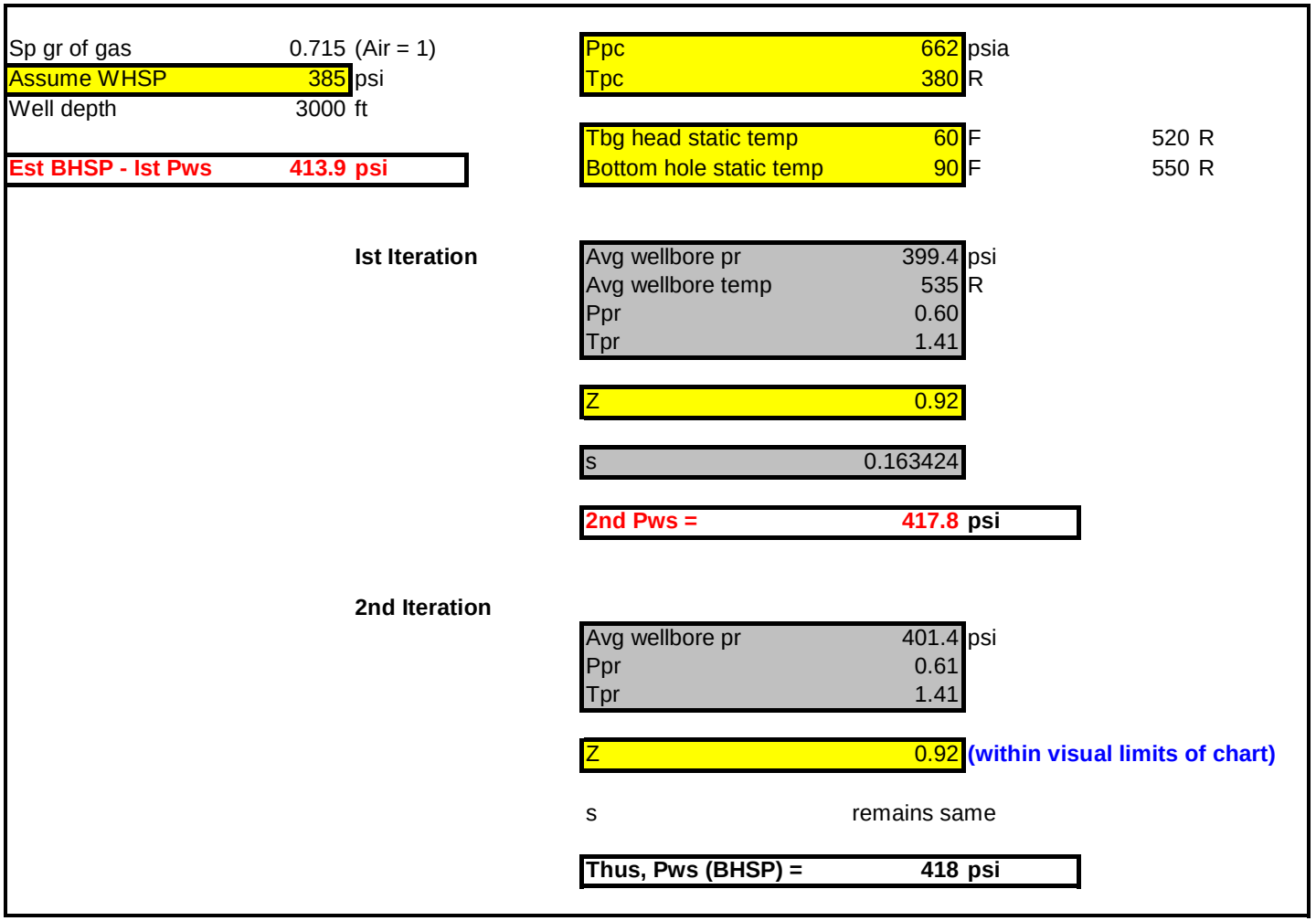

Figure 9.3.14B. Procedure to calculate bottom-hole shut-in pressure from well head shut-in pressure.

RUN 1 **– Pi = 460 psi., ff = 2 for PTrot24 & ff = 6 for all other Chase Parent wells.**
CH wells fractures constrained within Chase and CG wells in CG. CH fractures initiated – Jan 1, 1960.

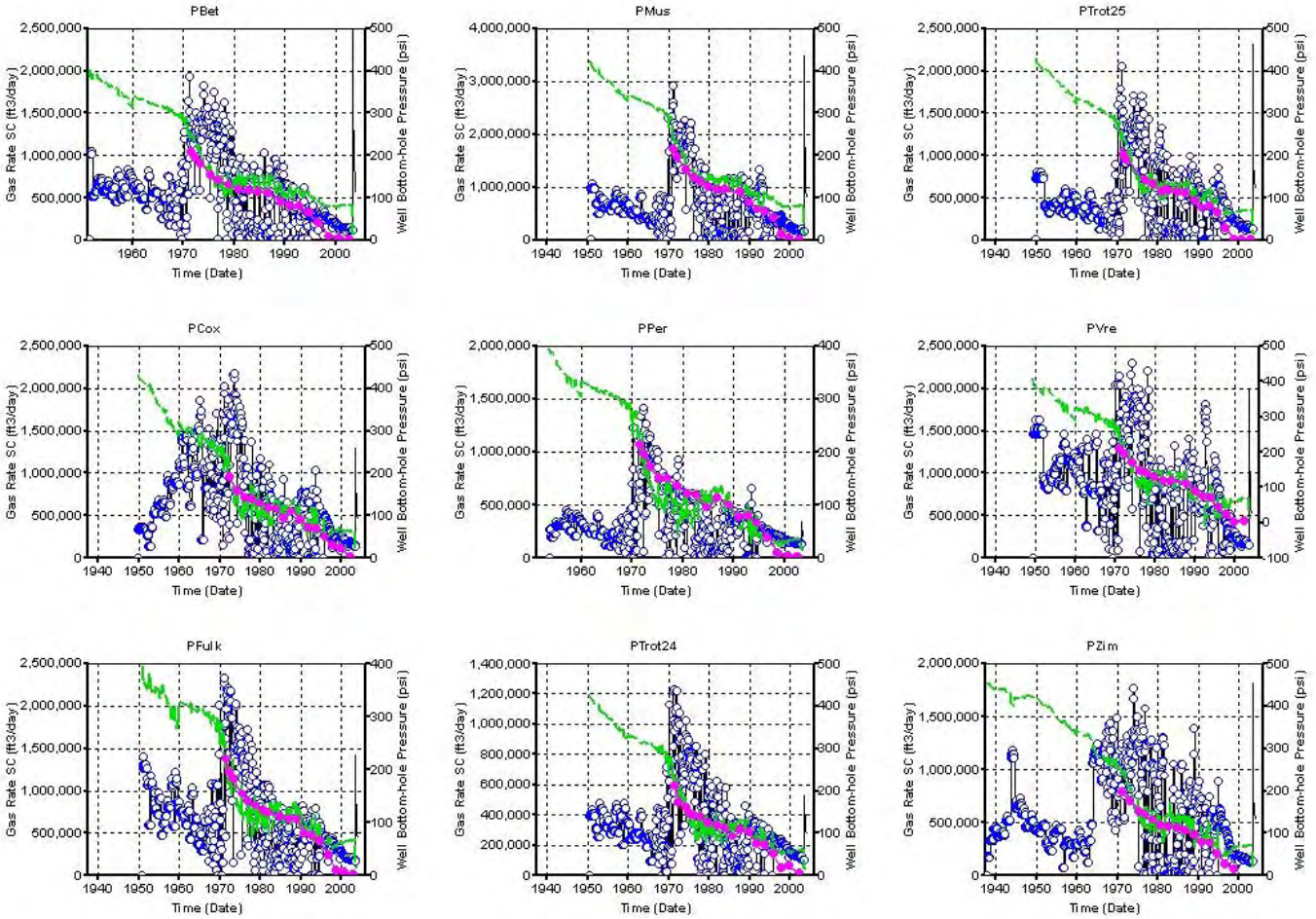

Black thin line – Simulator (Sim) calculated gas rate, Blue circles – historic gas production rate, Green broken line – Sim bottom hole pressure (BHP flowing), Magenta circles – Well head flowing pressure (WHFP).

Figure 9.3.15. RUN 1 Results – Comparison of simulator-calculated production rate and flowing bottom hole pressures with historic values at Chase Parent wells.

RUN 1 – Pi = 460 psi., ff = 6 for for all Chase Infill (CH I) wells

His Match of CH I wells

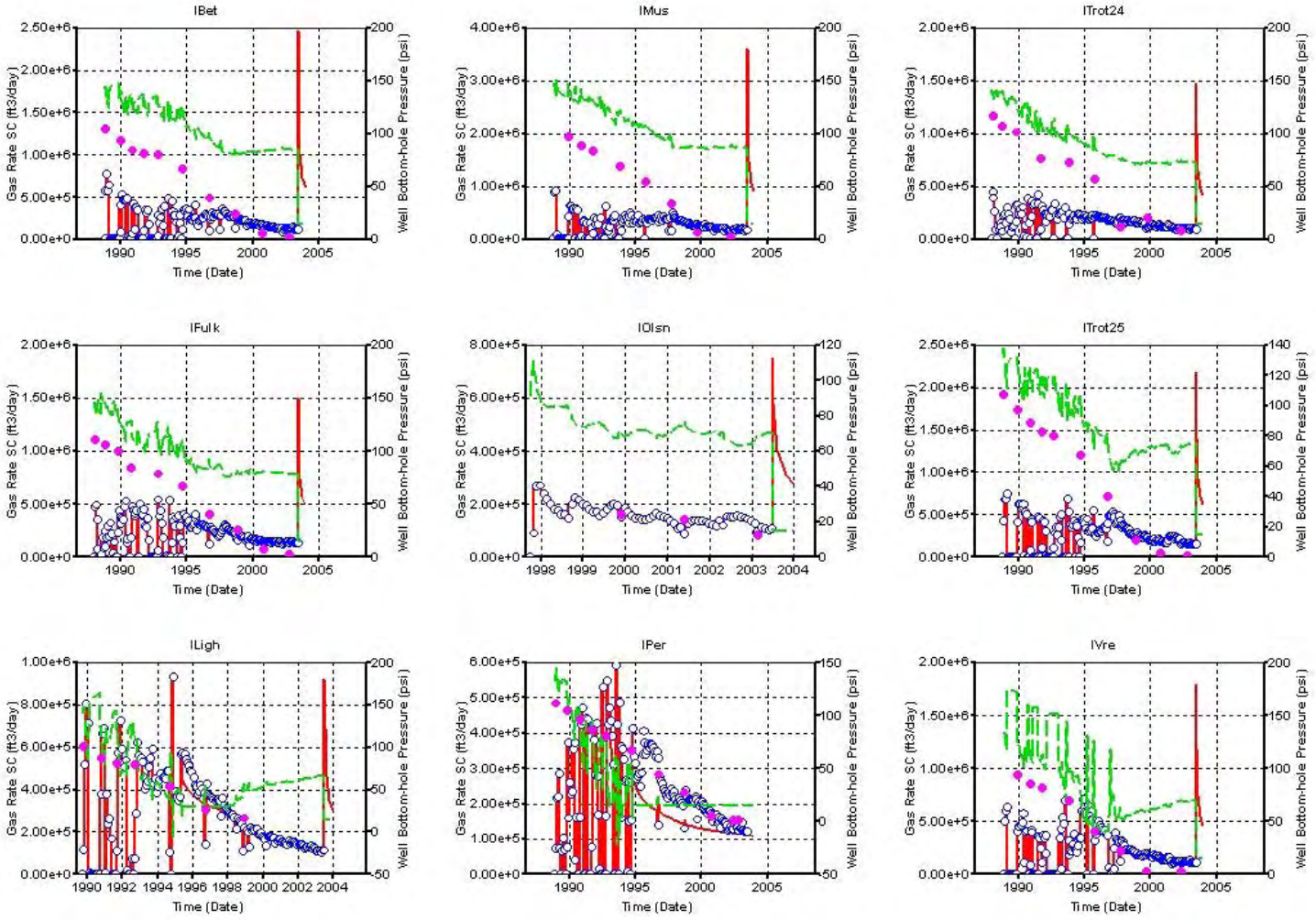

Red line – Simulator (Sim) calculated gas rate, Blue circles – historic gas production rate, Green broken line – Sim bottom hole pressure (BHP flowing), Magenta circles – Well head flowing pressure (WHFP).

Figure 9.3.16. RUN 1 Results – Comparison of simulator-calculated production rate and flowing bottom hole pressures with historic values at Chase Infill wells.

RUN 1 – Pi = 460 psi., ff = 6 for for all wells

His Match of CG wells

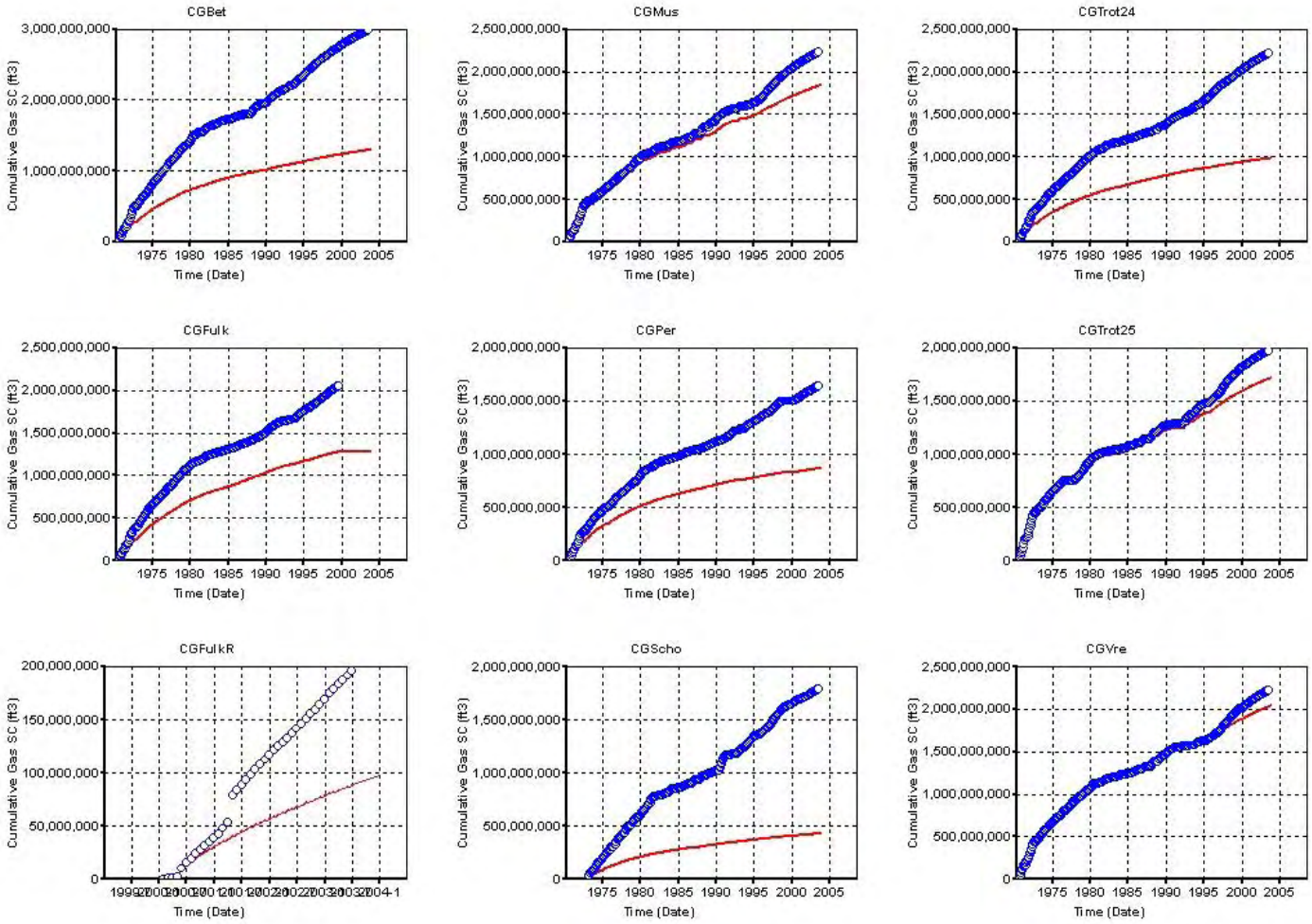

Red line – Simulator (Sim) calculated cumulative gas prod, Blue circles – historic cumulative gas production

Figure 9.3.17. RUN 1 Results – Comparison of simulator-calculated cumulative production with historic values at Council Grove wells.

Pr distribution as of Jan 1970 – just before CG wells came online

RUN 1 – K adj. Pi = 460 psi.

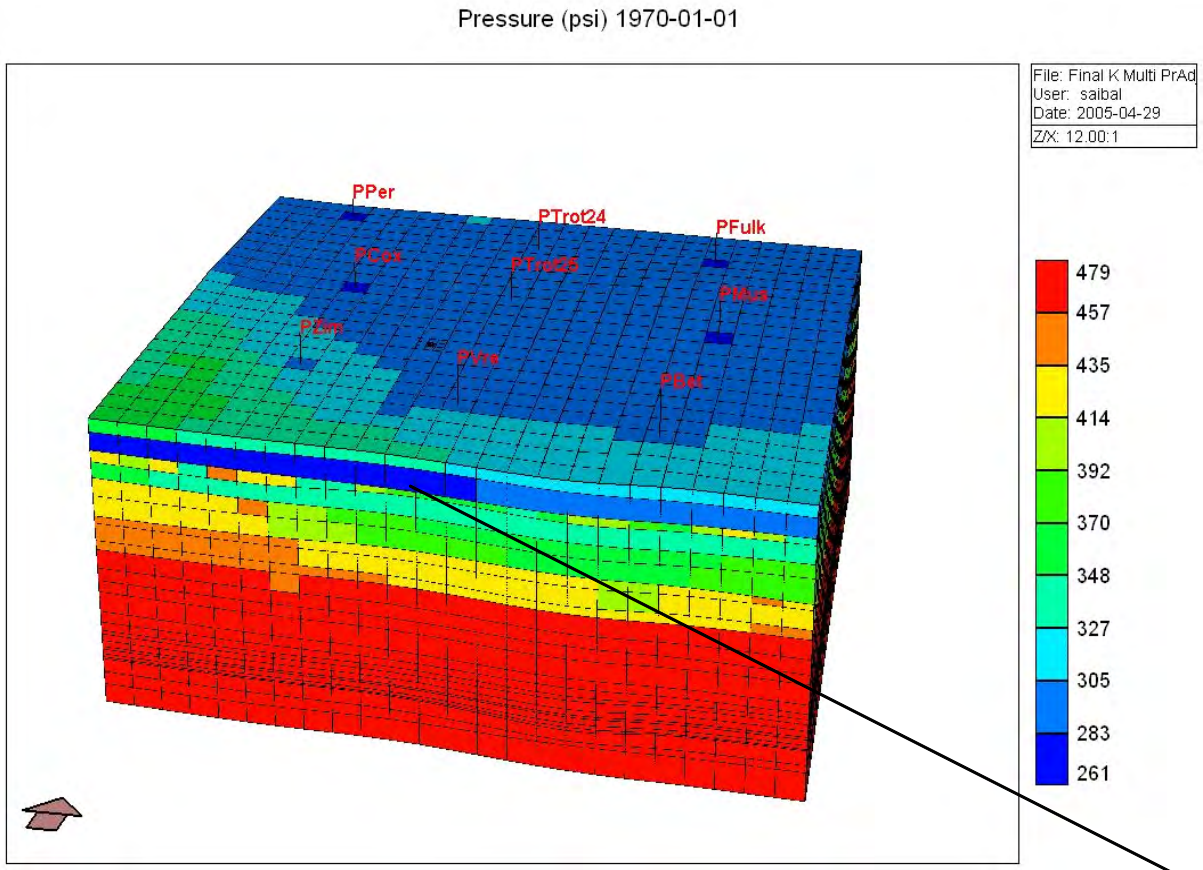

Figure 9.3.18. RUN 1 Results – Simulator-calculated reservoir pressure distribution as of January 1970.

2nd run – Pi = 460 psi.,
ff = 2 for PTrot24 & ff = 6 for all other CH P wells

CH P history matches (cum prod) when CG completions extended to L2

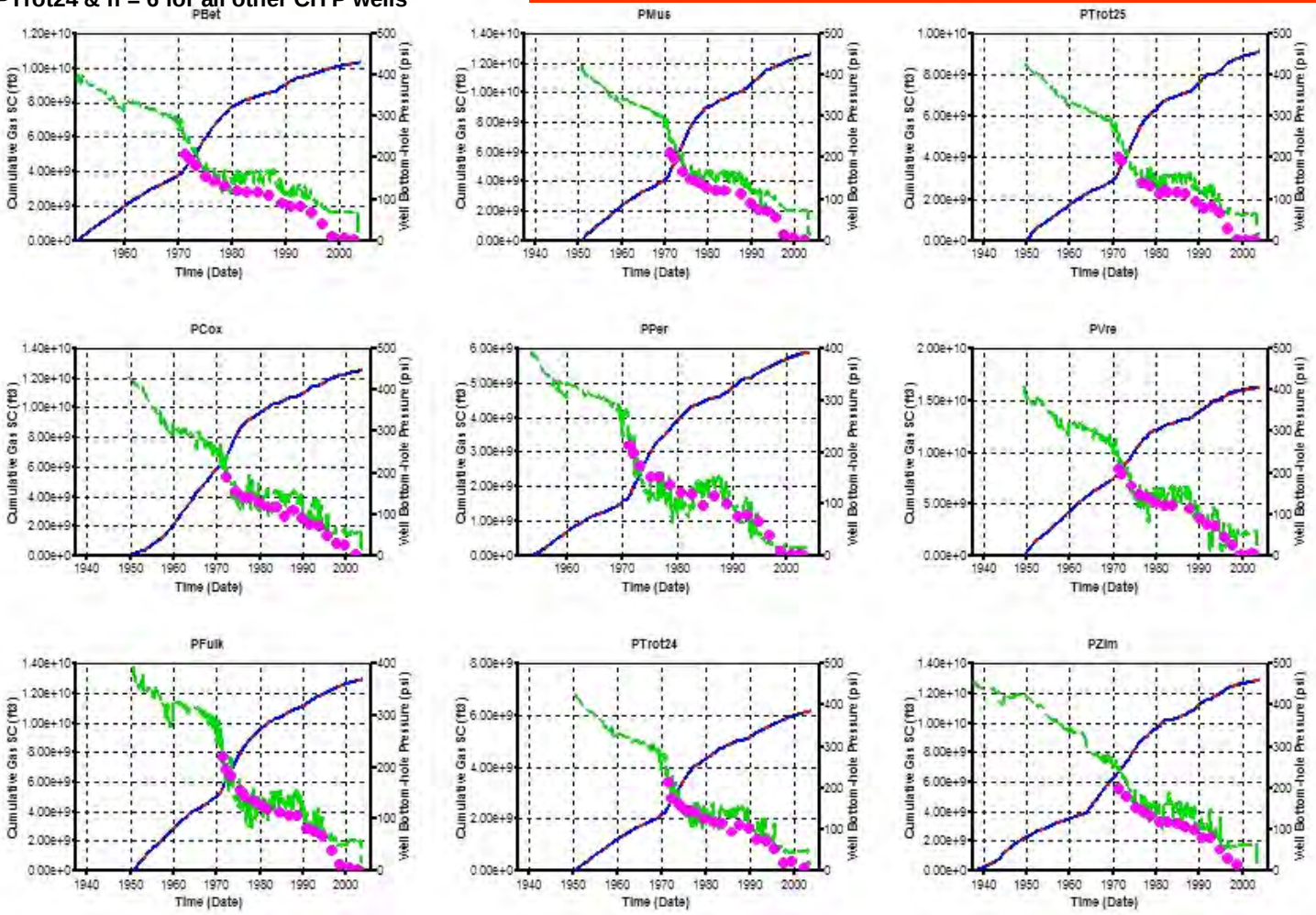

Red line – Simulator (Sim) calculated cumulative gas, Blue broken line – historic cumulative gas production, Green broken line – Sim bottom hole pressure (BHP flowing), Magenta circles – Well head flowing pressure (WHFP).

Figure 9.3.19. RUN 2 Results – Comparison of simulator-calculated cumulative production and flowing bottom hole pressures with historic values at Chase Parent wells when completions in Council Grove wells extended to Layer 2.

CH P history matches (prod rate) when CG completions extended to L2

2nd run – Pi = 460 psi.,
ff = 2 for PTrot24 & ff = 6 for all others CH P wells

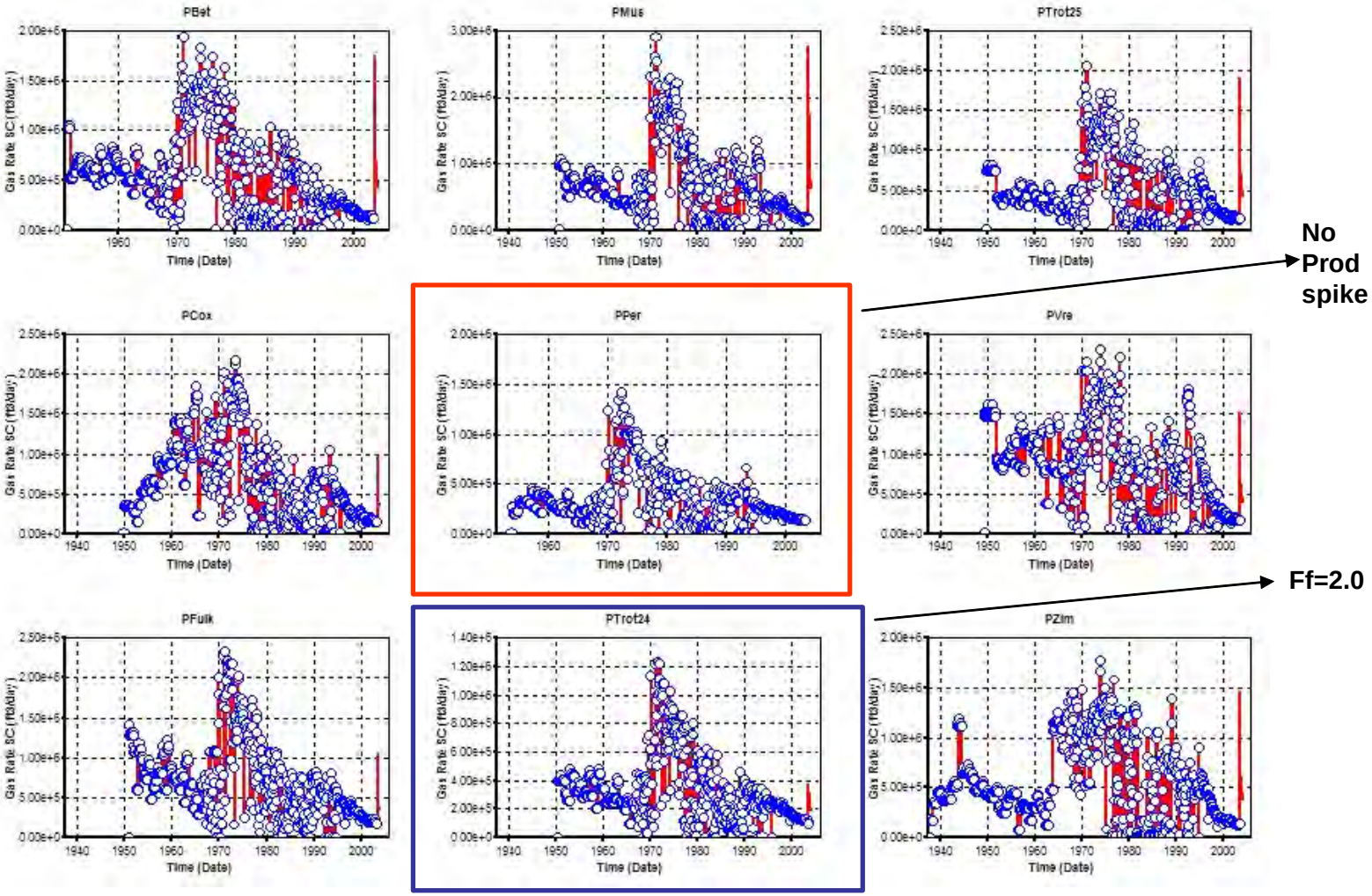

Red line – Simulator (Sim) calculated gas rate, Blue circles – historic gas production rate,

Figure 9.3.20. RUN 2 Results – Comparison of simulator-calculated production rate and flowing bottom hole pressures with historic values at Chase Parent wells when completions in Council Grove wells extended to Layer 2.

2nd run – Pi = 460 psi.,
ff = 6 for all CH I wells

CH I history matches (Cum prod) when CG completions extended to L2

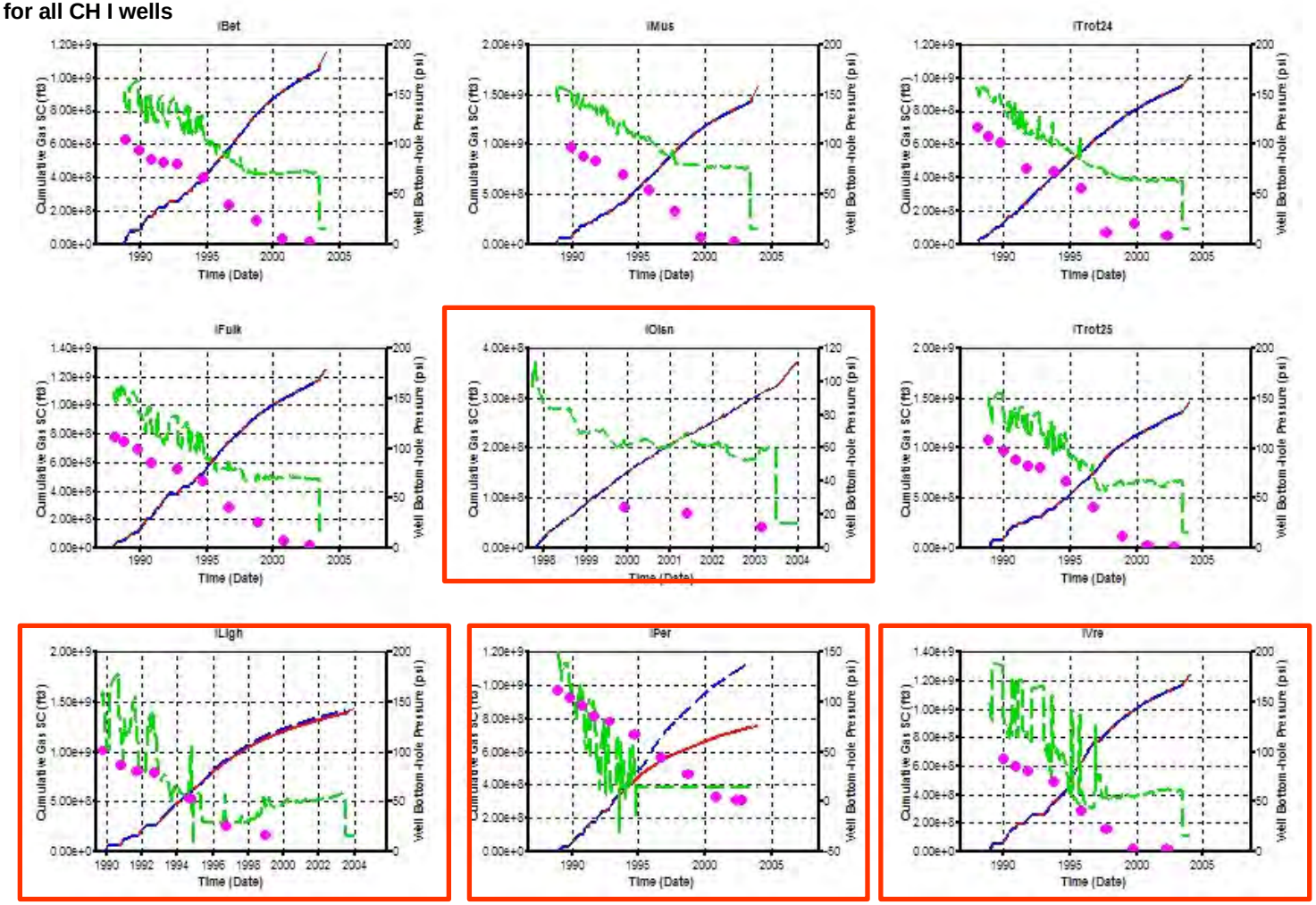

Red line – Simulator (Sim) calculated cum gas, Blue broken line – historic cum gas production, Green broken line – Sim bottom hole pressure (BHP flowing), Magenta circles – Well head flowing pressure (WHFP).

Figure 9.3.21. RUN 2 Results – Comparison of simulator-calculated cumulative production and flowing bottom hole pressures with historic values at Chase Infill wells when completions in Council Grove wells extended to Layer 2. Border wells boxed in red.

2nd run – K adj. Pi = 460 psi.
ff = 6 for all CG wells

CG history matches (Cum prod) when CG completions extended to L2

CGFulkR is a border well that is replacement of CGFulk.

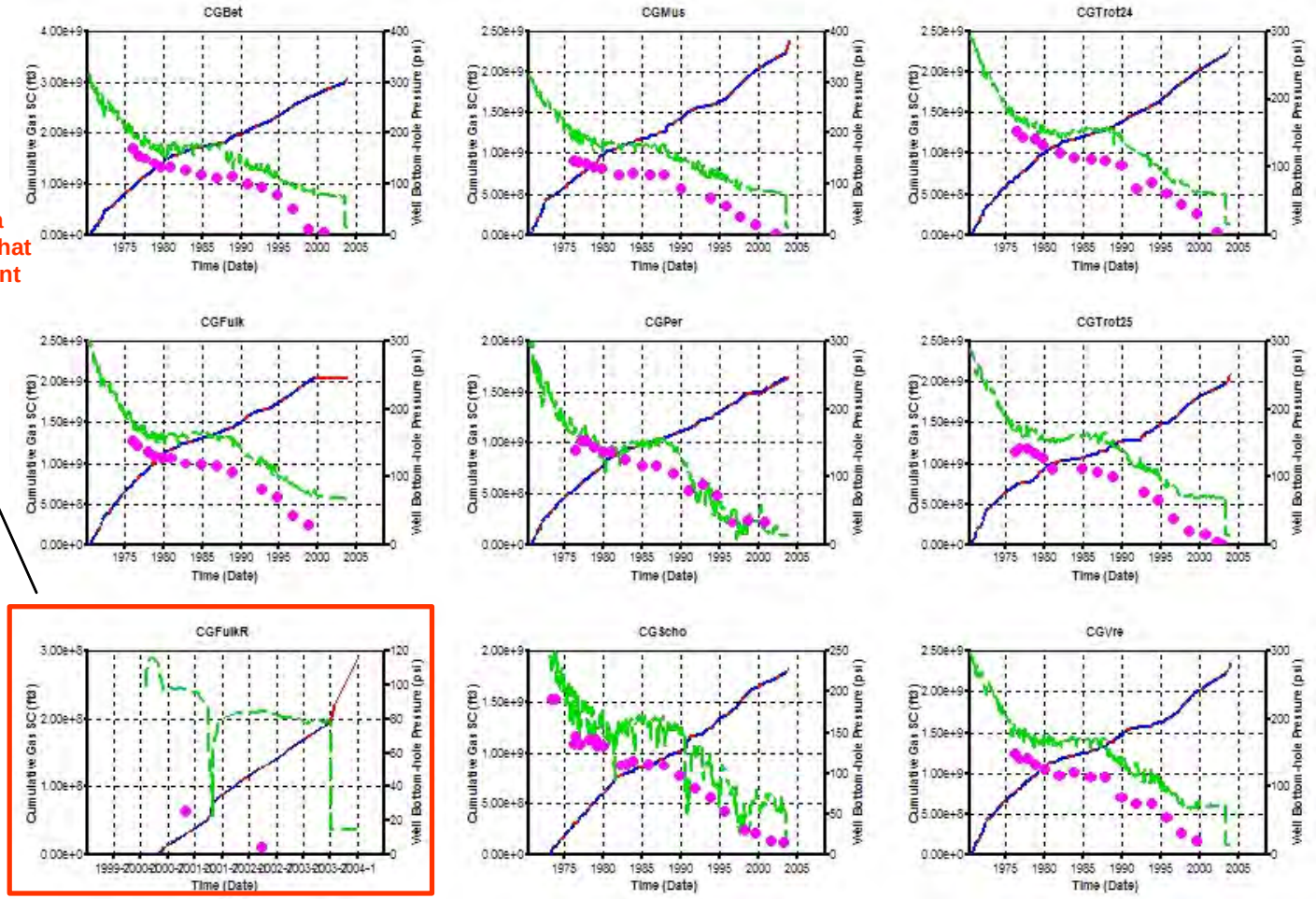

Red line – Simulator (Sim) calculated cum gas, Blue broken line – historic cum gas production, Green broken line – Sim bottom hole pressure (BHP flowing), Magenta circles – Well head flowing pressure (WHFP).

Figure 9.3.22A. RUN 2 Results – Comparison of simulator-calculated cumulative production and flowing bottom hole pressures with historic values at Council Grove wells when completions in Council Grove wells extended to Layer 2.

2nd run – K adj. Pi = 460 psi.
ff = 6 for all CG wells

CG history matches (Cum prod) when CG completions extended to L2

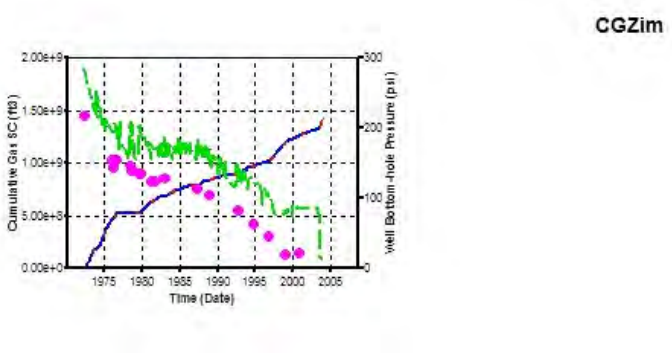

Red line – Simulator (Sim) calculated cum gas, Blue broken line – historic cum gas production, Green broken line – Sim bottom hole pressure (BHP flowing), Magenta circles – Well head flowing pressure (WHFP).

Figure 9.3.22B. RUN 2 Results – Comparison of simulator-calculated cumulative production and flowing bottom hole pressures with historic values at Council Grove wells when completions in Council Grove wells extended to Layer 2.

3rd Run – Pi = 435 psi, OGIP = 185 bcf.

Ff adjusted for CH P wells (ff between 5 and 9).

CH P history matches when CG completions extend to L2 & Pi = 435 psi

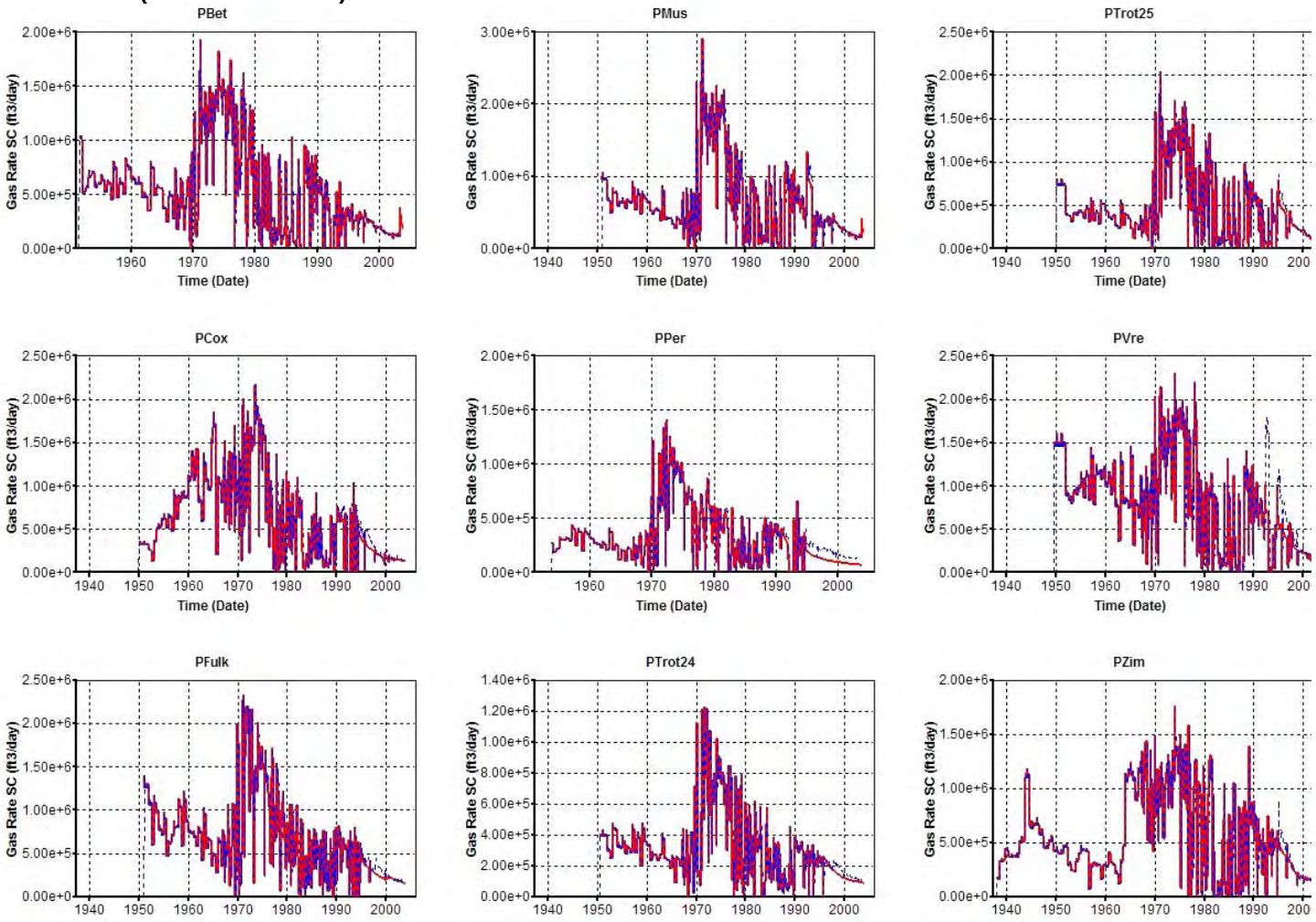

Red line – Simulator (Sim) calculated gas rate, Blue broken line – historic gas production rate

Figure 9.3.23. RUN 3 Results – Comparison of simulator-calculated production rate with historic values at Chase Parent wells when completions in Council Grove wells extended to Layer 2 and initial reservoir pressure is assumed to be 435 psi.

3rd Run – Pi = 435 psi, OGIP = 185 bcf.

Ff adjusted for CH P wells (ff between 5 and 9).

CH P flowing Pr matches when CG completions extend to L2 & Pi = 435 psi

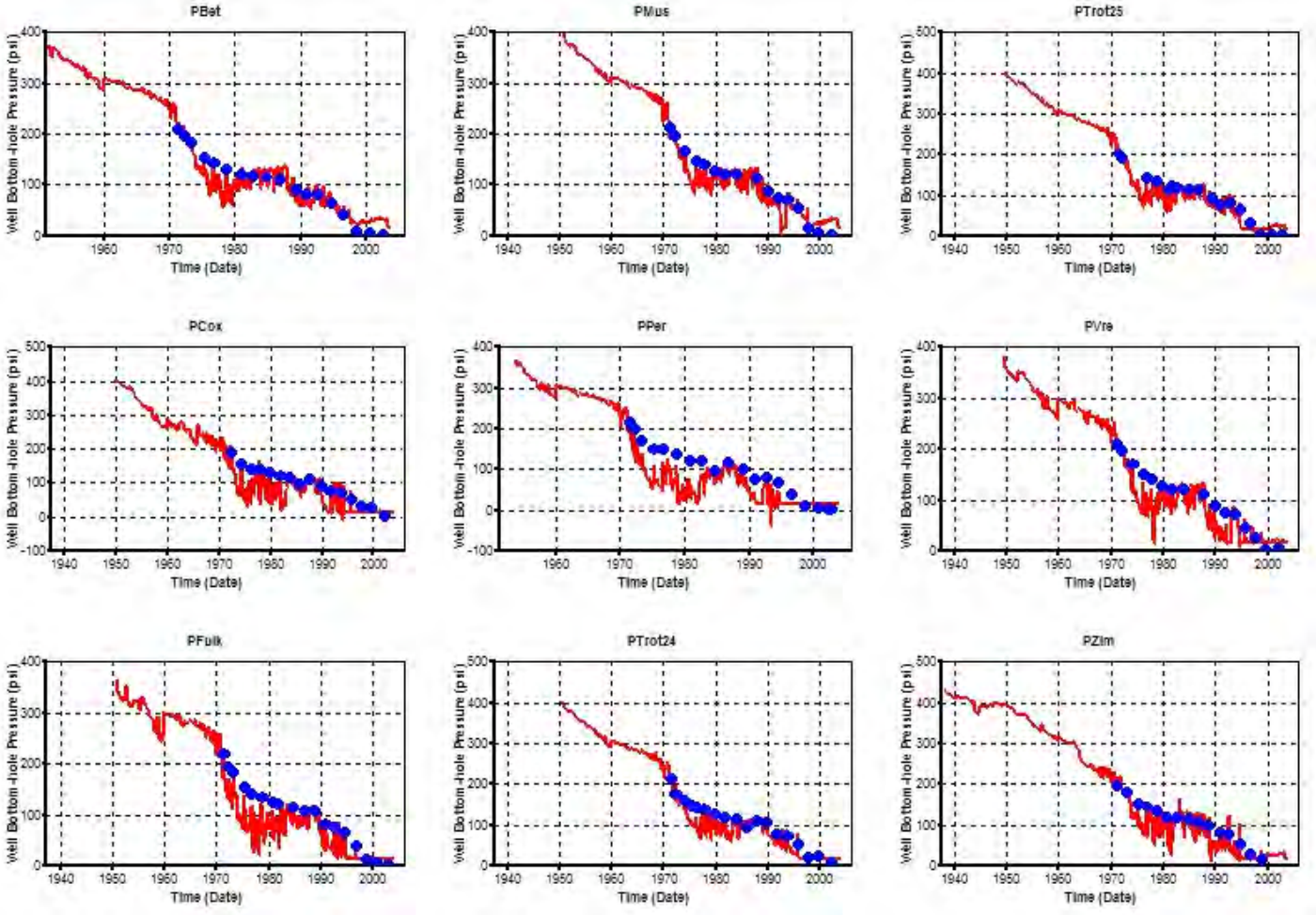

Red broken line – Sim bottom hole pressure (BHP flowing), Blue circles – Well head flowing pressure (WHFP).

Figure 9.3.24. RUN 3 Results – Comparison of simulator-calculated flowing pressure with historic values at Chase Parent wells when completions in Council Grove wells extended to Layer 2 and initial reservoir pressure is assumed to be 435 psi.

3rd Run – Pi = 435 psi, OGIP = 185 bcf.

Ff for CG wells set at 6.

CG history matches when CG completions extend to L2 & Pi = 435 psi

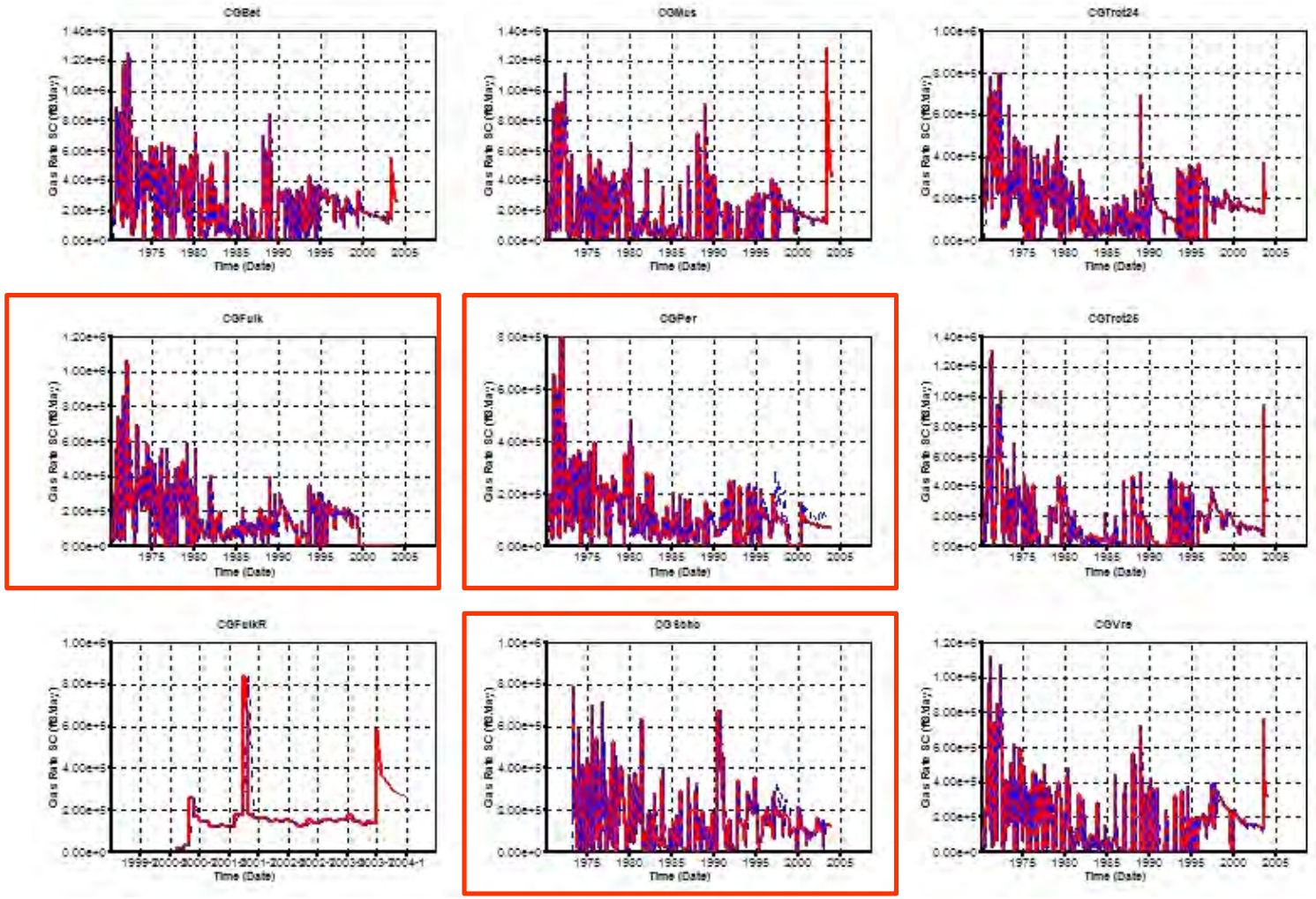

Red line – Simulator (Sim) calculated gas rate, Blue broken line – historic gas production rate

Figure 9.3.25A. RUN 3 Results – Comparison of simulator-calculated production rate with historic values at Council Grove wells when completions in Council Grove wells extended to Layer 2 and initial reservoir pressure is assumed to be 435 psi.

3rd Run – Pi = 435 psi, OGIP = 185 bcf.

Ff for CG wells set at 6.

CG history matches when CG completions extend to L2 & Pi = 435 psi

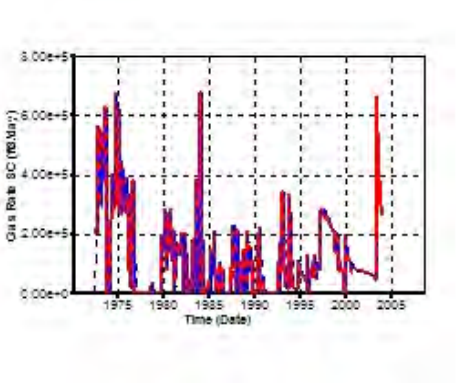

Figure 9.3.25B. RUN 3 Results – Comparison of simulator-calculated production rate with historic values at Council Grove wells when completions in Council Grove wells extended to Layer 2 and initial reservoir pressure is assumed to be 435 psi.

4th Run – Pi = 435 psi, OGIP = 185 bcf.

Ff for CG wells adjusted selectively.

CG history matches when CG completions extend to L2 & Pi = 435 psi

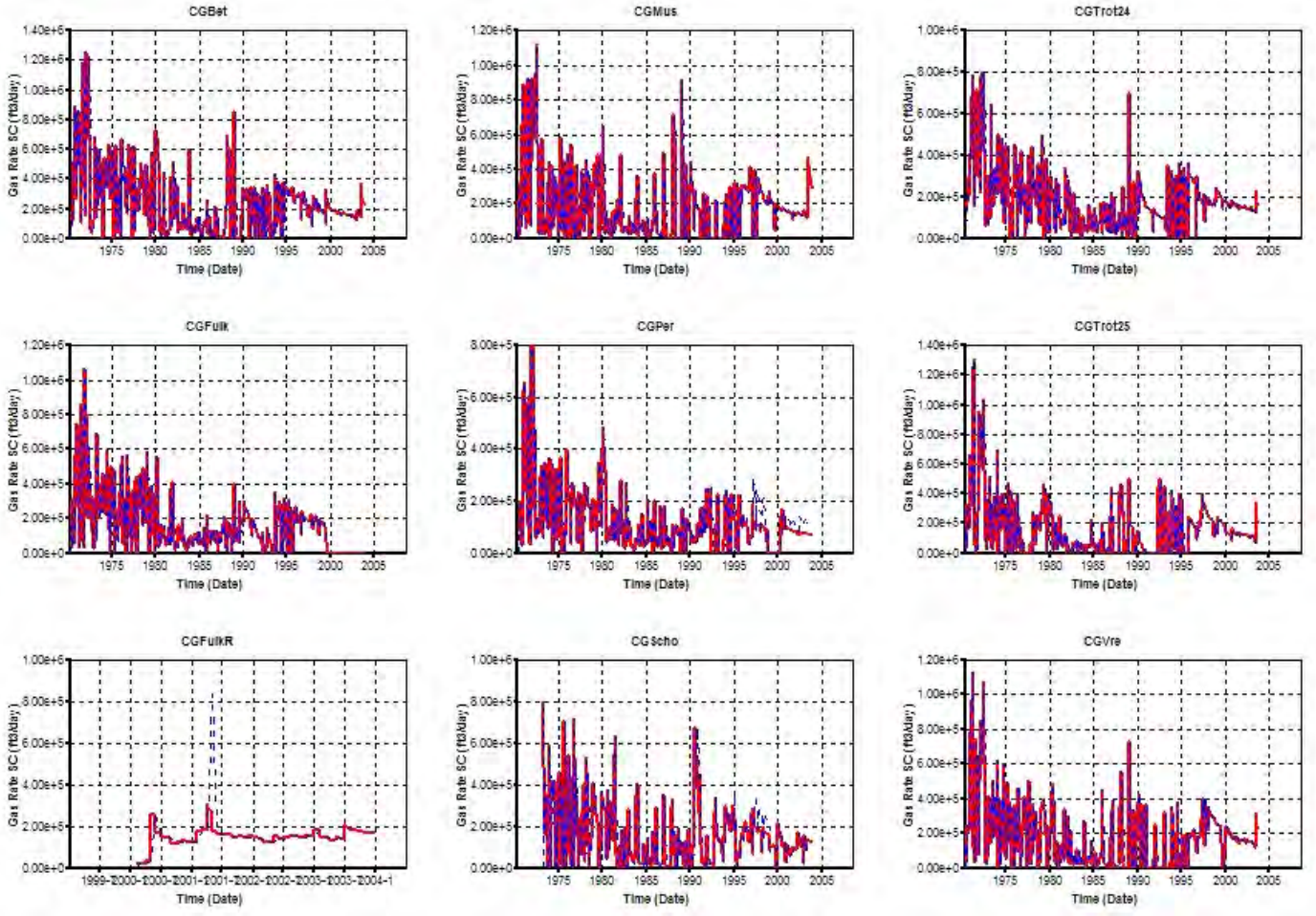

Red line – Simulator (Sim) calculated gas rate, Blue broken line – historic gas production rate

Figure 9.3.26A. RUN 4 Results – Comparison of simulator-calculated production rate with historic values at Council Grove wells when Council Grove completions extended to Layer 2, initial reservoir pressure is 435 psi, and ff adjusted selectively.

4th Run – Pi = 435 psi, OGIP = 185 bcf.

Ff for CG wells adjusted selectively.

CG history matches when CG completions extend to L2 & Pi = 435 psi

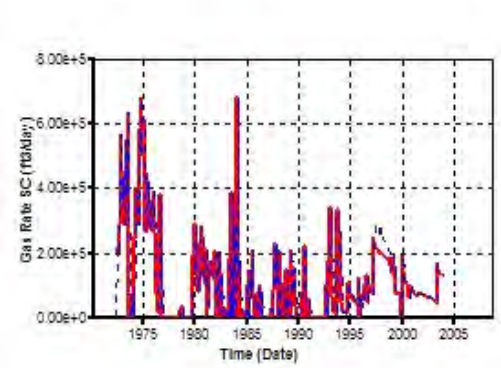

Red line – Simulator (Sim) calculated gas rate, Blue broken line – historic gas production rate

Figure 9.3.26B. RUN 4 Results – Comparison of simulator-calculated production rate with historic values at Council Grove wells when Council Grove completions extended to Layer 2, initial reservoir pressure is 435 psi, and ff adjusted selectively.

5th Run – Pi = 423 psi, OGIP = 179.5 bcf.

Ff for CH P wells set at 6.

CH P history matches when CG completions extend to L2 & Pi = 423 psi

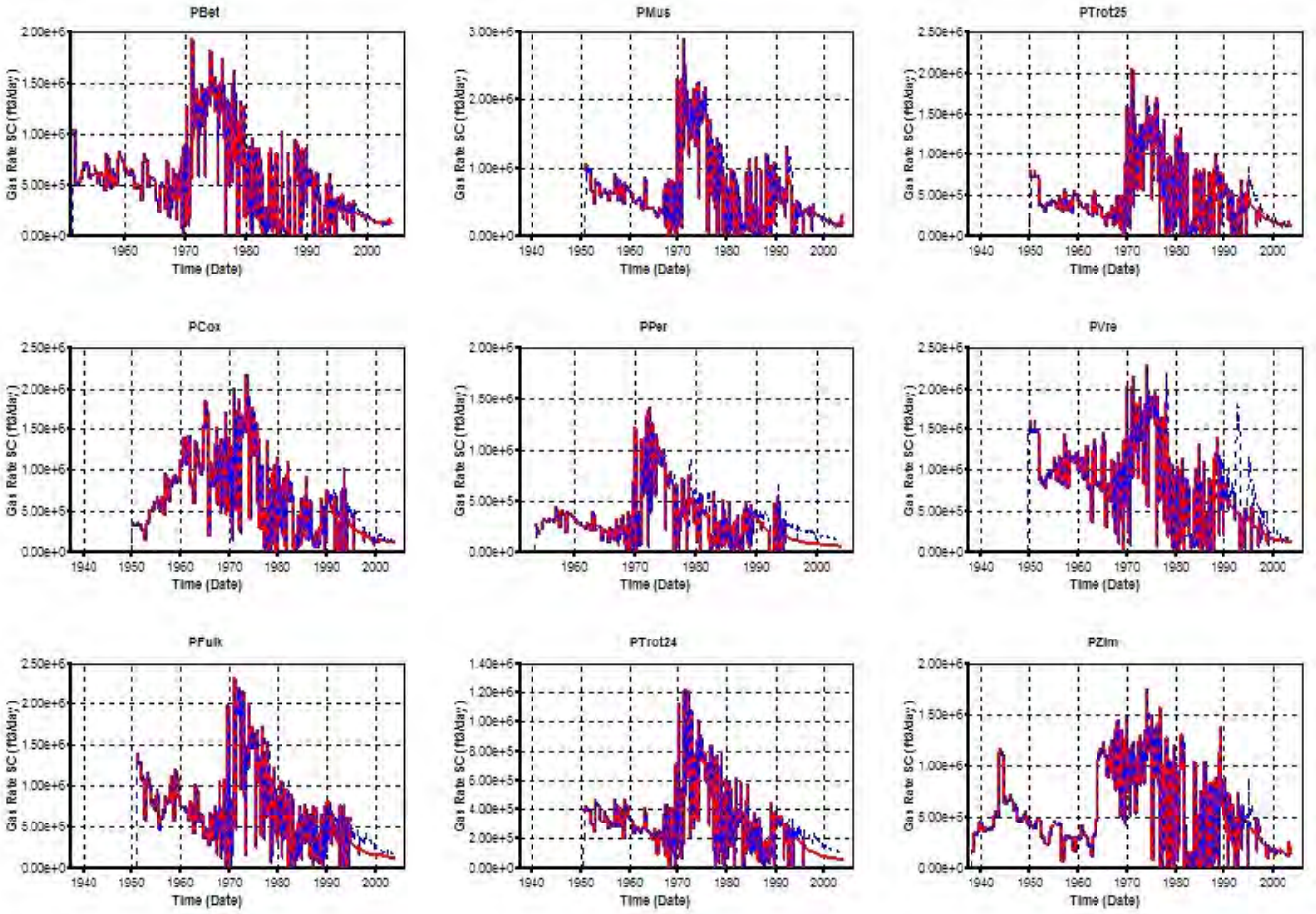

Figure 9.3.27. RUN 5 Results – Comparison of simulator-calculated production rate with historic values at Chase Parent wells when completions in Council Grove wells extended to Layer 2 and initial reservoir pressure is assumed to be 423 psi.

5th Run – Pi = 423 psi, OGIP = 179.5 bcf.

Ff for CG wells set at 6.

CG history matches when CG completions extend to L2 & Pi = 423 psi

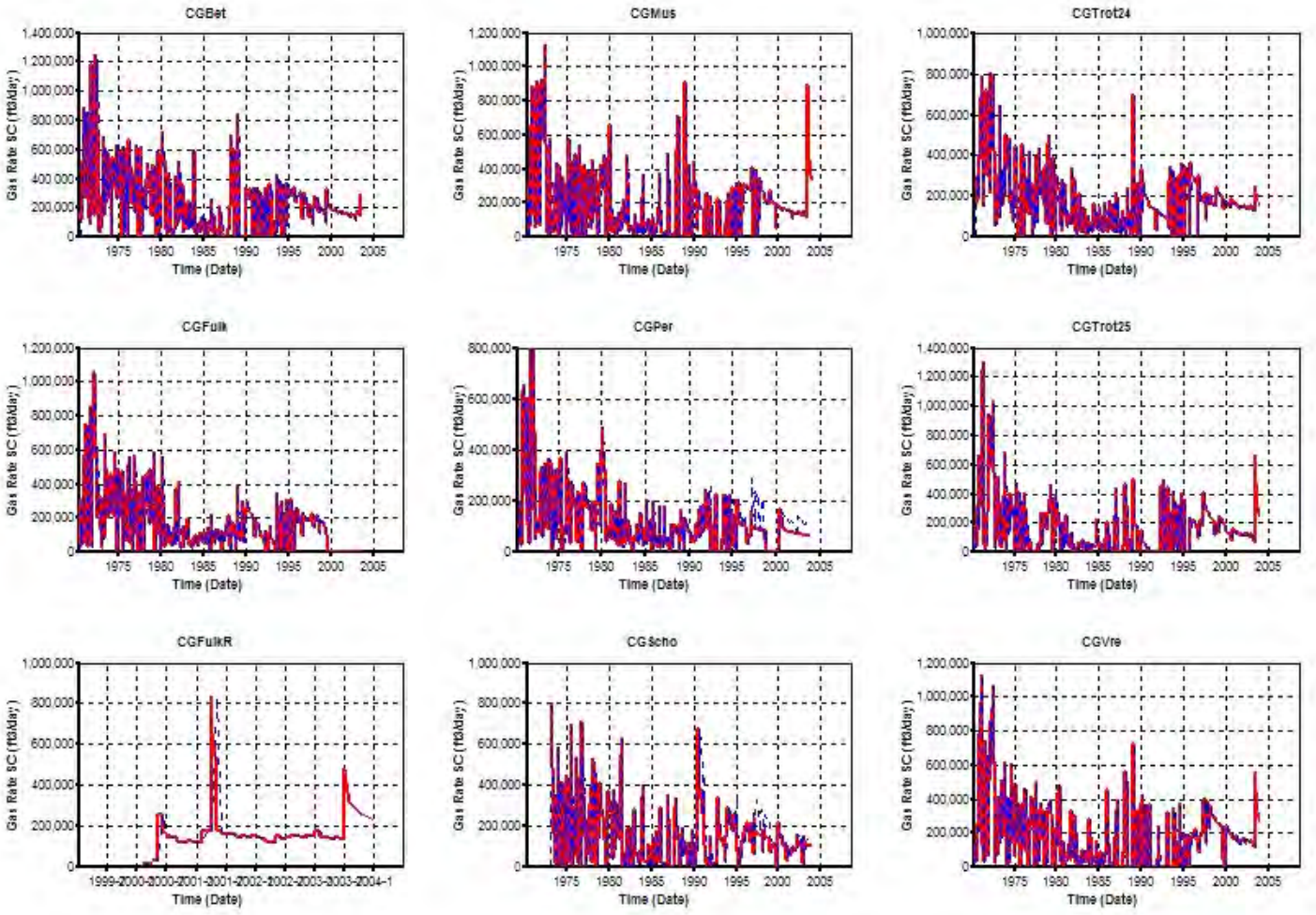

Figure 9.3.28A. RUN 5 Results – Comparison of simulator-calculated production rate with historic values at Council Grove wells when completions in Council Grove wells extended to Layer 2 and initial reservoir pressure is assumed to be 423 psi.

5th Run – Pi = 423 psi, OGIP = 179.5 bcf.

Ff for CG wells set at 6.

CG history matches when CG completions extend to L2 & Pi = 423 psi

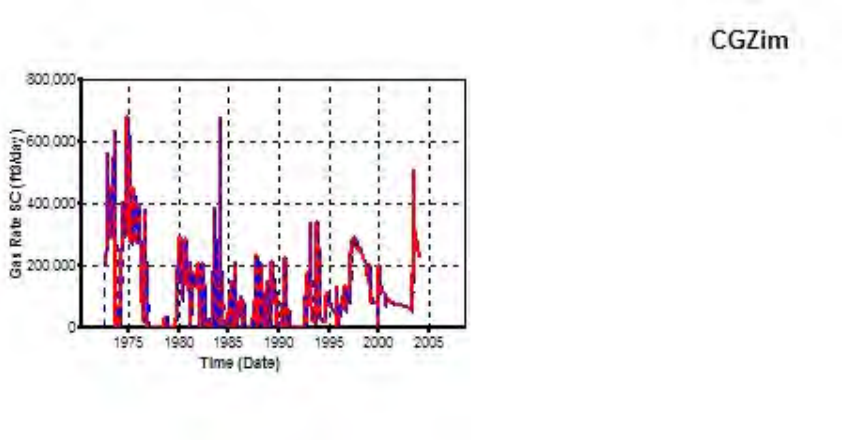

Red line – Simulator (Sim) calculated cum gas, Blue broken line – historic cum gas production

Figure 9.3.28B. RUN 5 Results – Comparison of simulator-calculated production rate with historic values at Council Grove wells when completions in Council Grove wells extended to Layer 2 and initial reservoir pressure is assumed to be 423 psi.

CH P history matches when CG completions extend to L2 & Pi = 423 psi

6th Run – Pi = 423 psi, OGIP = 179.5 bcf.

Ff for CH P wells adjusted around 6 (between 5 and 9).

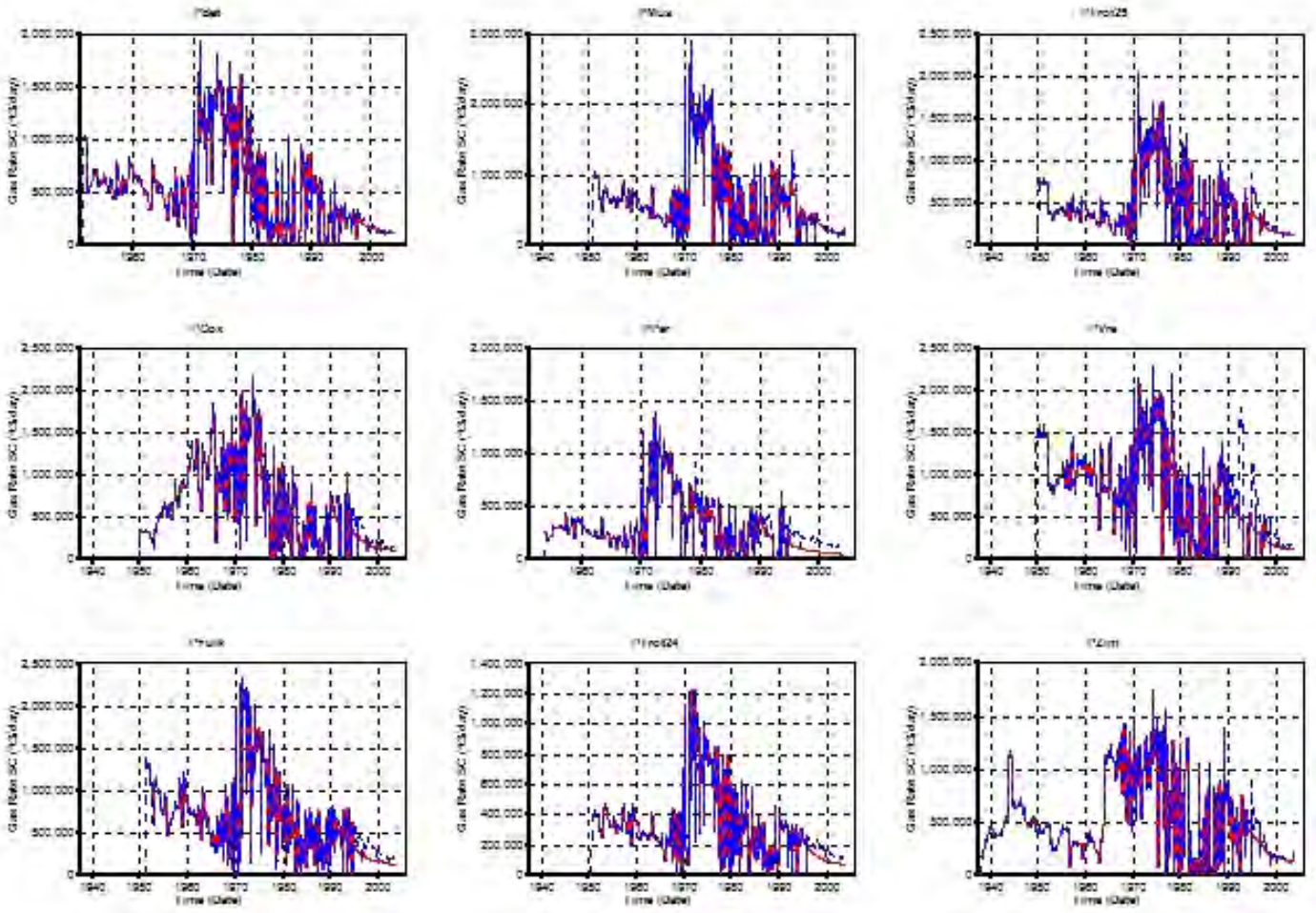

Red line – Simulator (Sim) calculated cum gas, Blue broken line – historic cum gas production

Figure 9.3.29. RUN 6 Results – Comparison of simulator-calculated production rate with historic values at Chase Parent wells when Council Grove completions extended to Layer 2, initial reservoir pressure set to 423 psi, and ff adjusted in CH P wells.

CH P flowing pr history matches when CG completions extend to L2 & Pi = 423 psi

6th Run – Pi = 423 psi, OGIP = 179.5 bcf.

Ff for CH P wells adjusted around 6 (between 5 and 9).

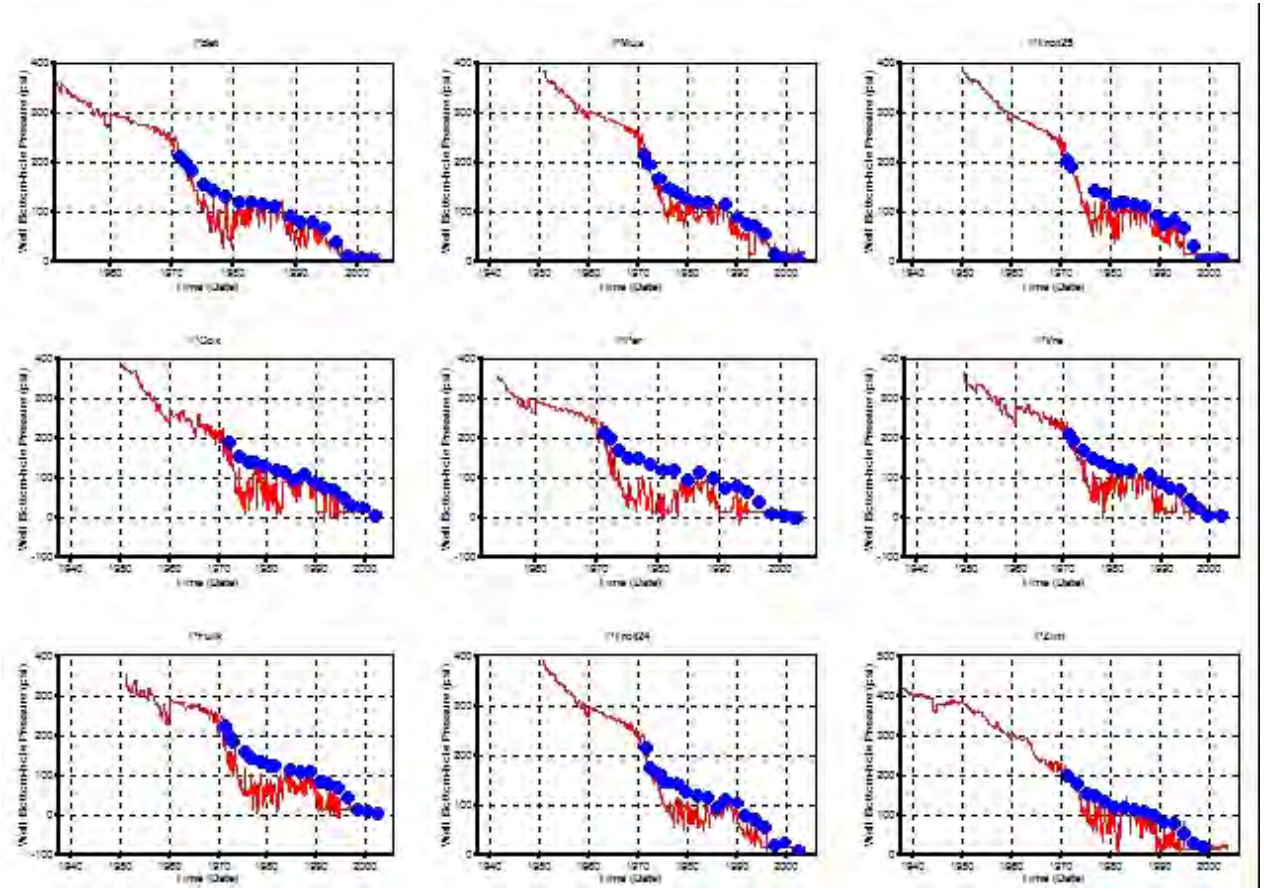

Red broken line – Sim bottom hole pressure (BHP flowing), Blue circles – Well head flowing pressure (WHFP).

Figure 9.3.30. RUN 6 Results – Comparison of simulator-calculated BHFP with WHFP at Chase Parent wells when Council Grove completions extended to Layer 2, initial reservoir pressure set to 423 psi, and ff adjusted in CH P wells.

6th Run – Pi = 423 psi, OGIP = 179.5 bcf.

Ff for CG wells adjusted around 6 (between 5 and 9).

CG history matches when CG completions extend to L2 & Pi = 423 psi

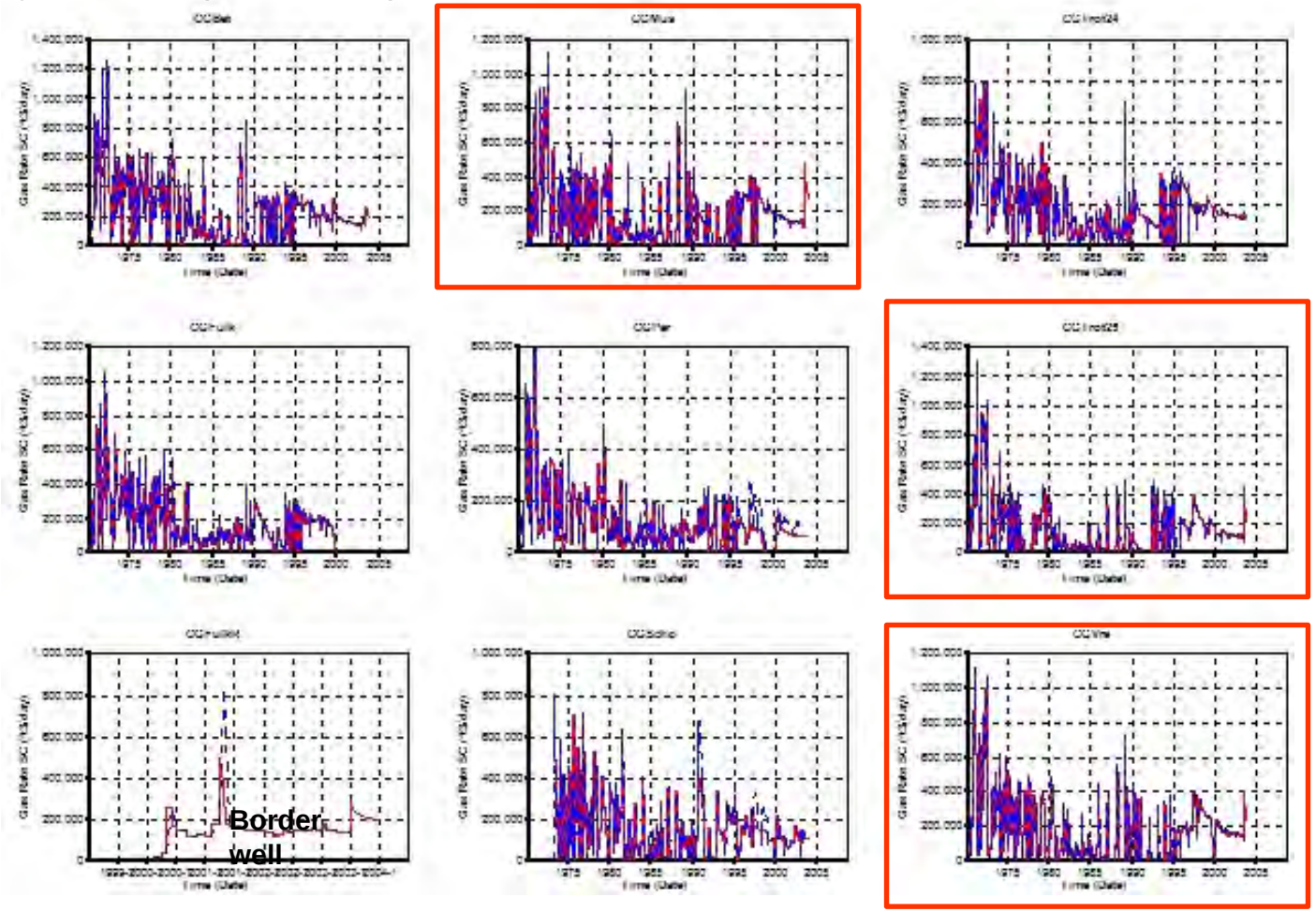

Figure 9.3.31A. RUN 6 Results – Comparison of simulator-calculated production rate with historic values at Council Grove wells when Council Grove completions extended to Layer 2, initial reservoir pressure set to 423 psi, and ff adjusted in CH P and CG wells.

CG history matches when CG completions extend to L2 & Pi = 423 psi

6th Run – Pi = 423 psi, OGIP = 179.5 bcf.

Ff for CG wells adjusted around 6 (between 5 and 9).

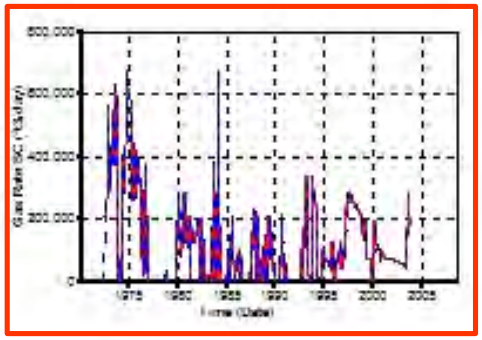

Figure 9.3.31B. RUN 6 Results – Comparison of simulator-calculated production rate with historic values at Council Grove wells when Council Grove completions extended to Layer 2, initial reservoir pressure set to 423 psi, and ff adjusted in CH P and CG wells.

CG flowing pr history matches when CG completions extend to L2 & Pi = 423 psi

6th Run – Pi = 423 psi, OGIP = 179.5 bcf.

Ff for CG wells adjusted around 6 (between 5 and 9).

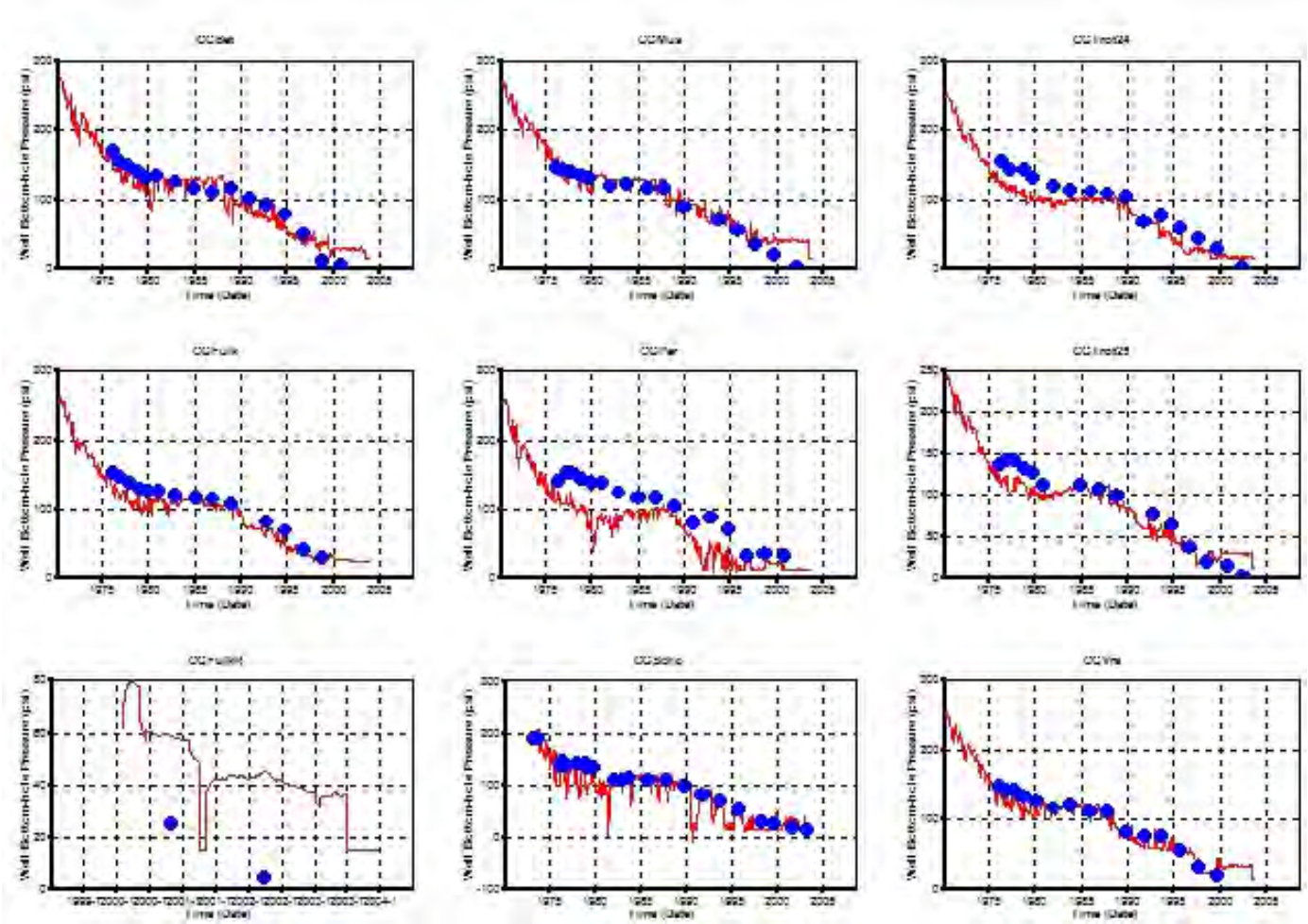

Red broken line – Sim bottom hole pressure (BHP flowing), Blue circles – Well head flowing pressure (WHFP).

Figure 9.3.32A. RUN 6 Results – Comparison of simulator-calculated BHFP with historic WHFP at Council Grove wells when Council Grove completions extended to Layer 2, initial reservoir pressure set to 423 psi, and ff adjusted in CH P and CG wells.

CG history matches when CG completions extend to L2 & Pi = 423 psi

6th Run – Pi = 423 psi, OGIP = 179.5 bcf.

Ff for CG wells adjusted around 6 (between 5 and 9).

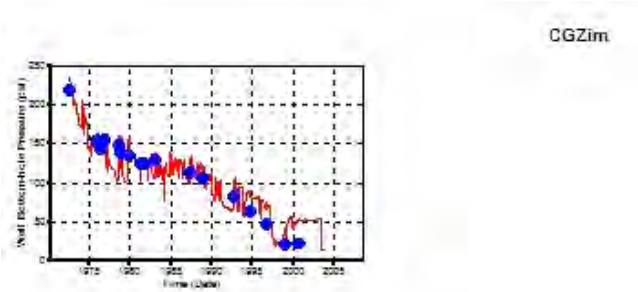

Red broken line – Sim bottom hole pressure (BHP flowing), Blue circles – Well head flowing pressure (WHFP).

Figure 9.3.32B. RUN 6 Results – Comparison of simulator-calculated BHFP with historic WHFP at Council Grove wells when Council Grove completions extended to Layer 2, initial reservoir pressure set to 423 psi, and ff adjusted in CH P and CG wells.

CH I history matches when CG completions extend to L2 & Pi = 423 psi

6th Run – Pi = 423 psi, OGIP = 179.5 bcf.

Ff for CH I wells adjusted around 6 (between 5 and 9).

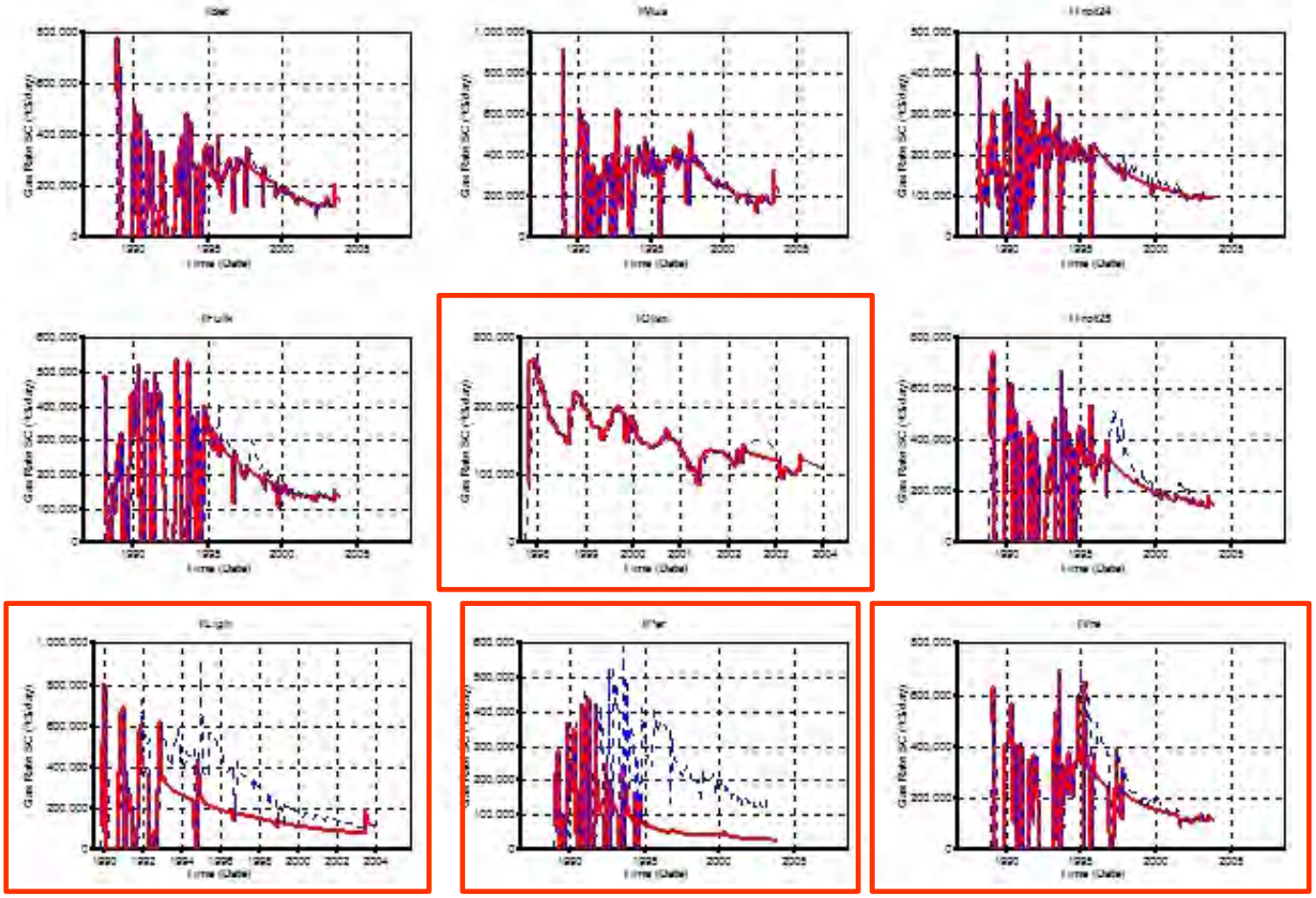

Figure 9.3.33. RUN 6 Results – Comparison of simulator-calculated production rate with historic values at Chase Infill wells when Council Grove completions extended to Layer 2, initial reservoir pressure set to 423 psi, and ff adjusted in all wells.

6th Run – Pi = 423 psi, OGIP = 179.5 bcf.

Ff for CH I wells adjusted around 6 (between 5 and 9).

CH I flowing pressure history matches when CG completions extend to L2 & Pi = 423 psi

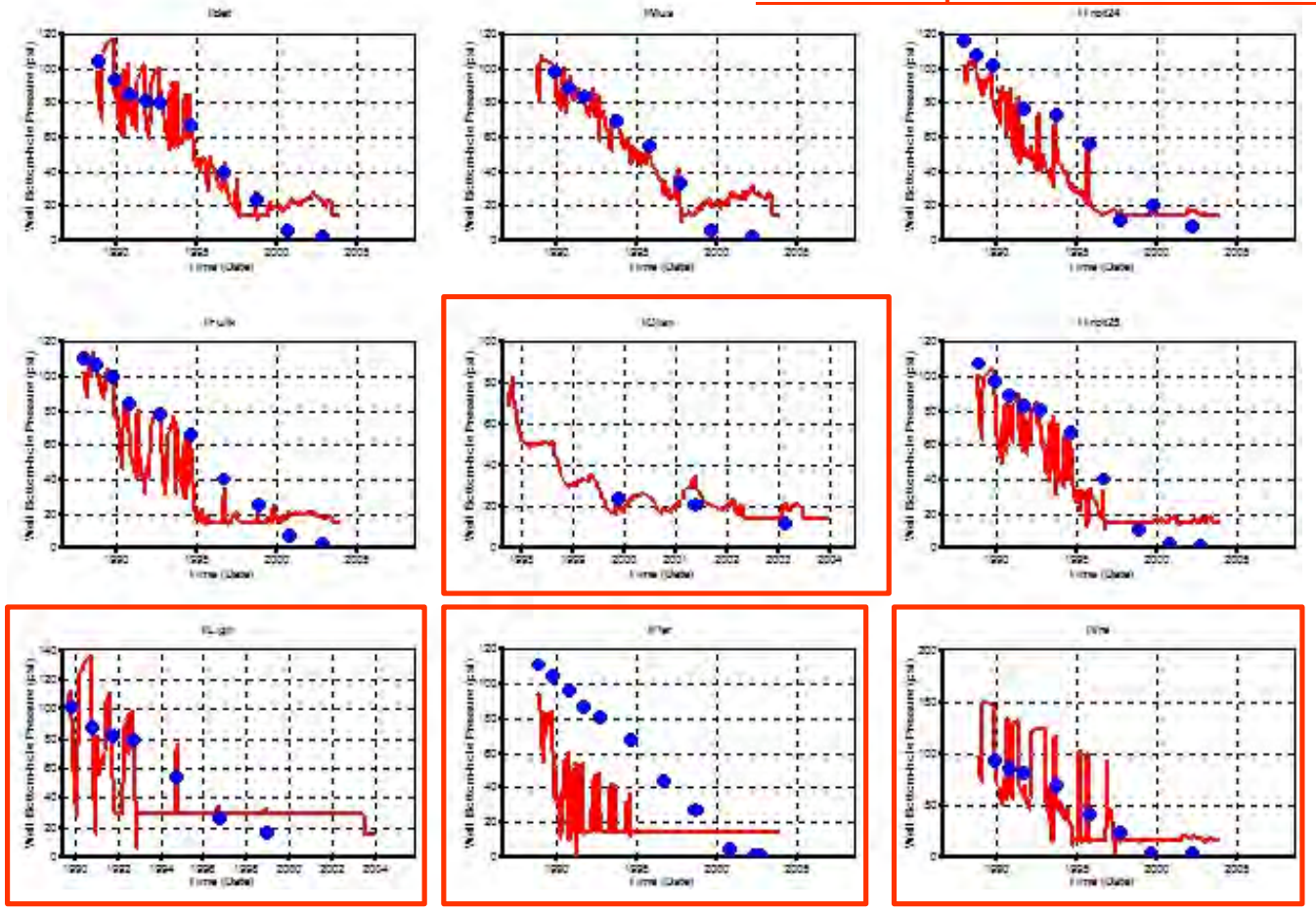

Red broken line – Sim bottom hole pressure (BHP flowing), Blue circles – Well head flowing pressure (WHFP). Border wells

Figure 9.3.34. RUN 6 Results – Comparison of simulator-calculated BHFP with historic WHFP at Chase Infill wells when Council Grove completions extended to Layer 2, initial reservoir pressure set to 423 psi, and ff adjusted in all wells.

6th Run – Pi = 423 psi, OGIP = 179.5 bcf.

Res Pr distribution as of Jan 1, 1970 – before CG wells

CG completions extend to L2 & Pi = 423 psi

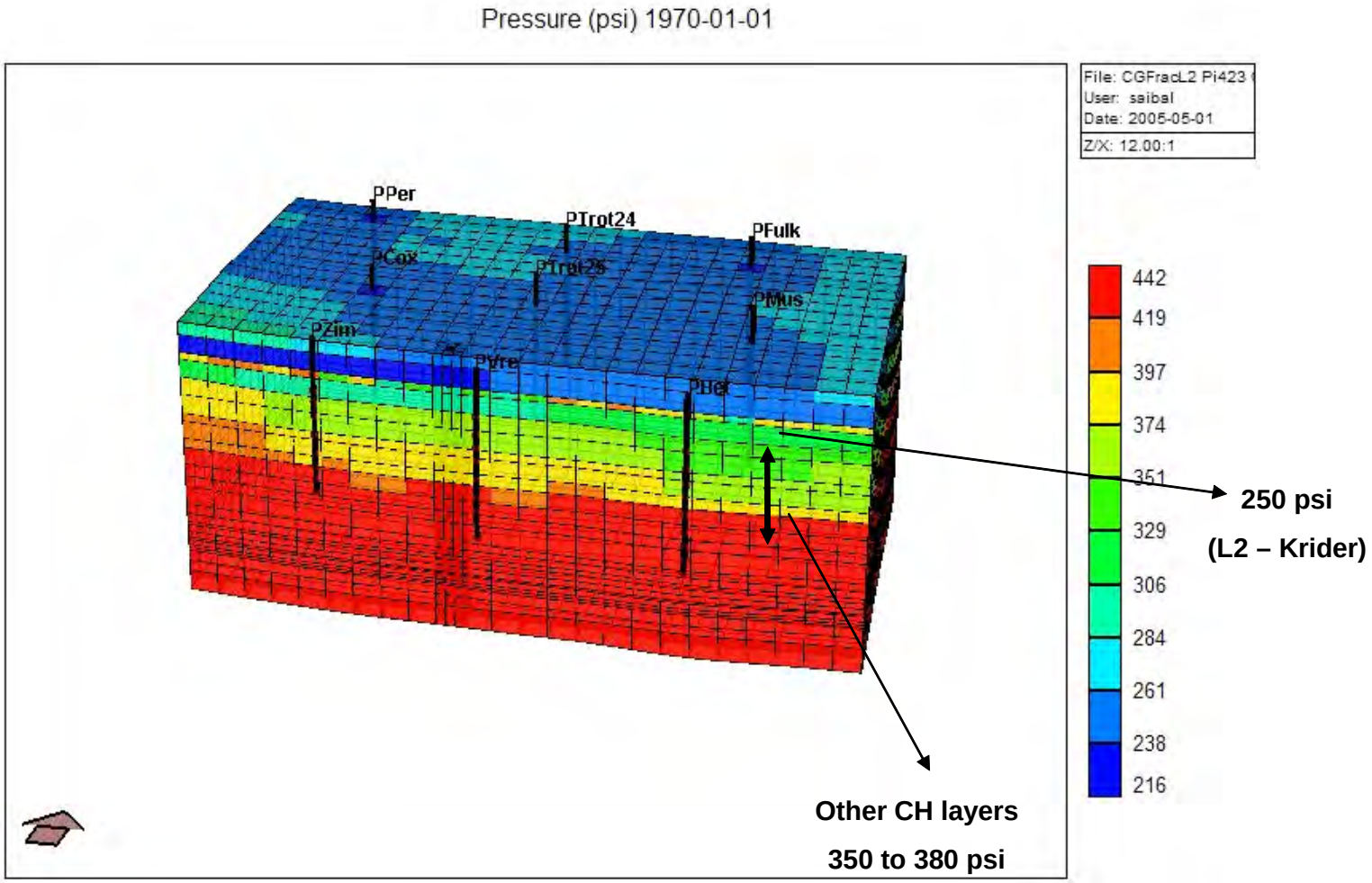

Figure 9.3.35. RUN 6 Results – Simulator-calculated reservoir pressure distribution as of January 1970.

6th Run – Pi = 423 psi, OGIP = 179.5 bcf.

A.

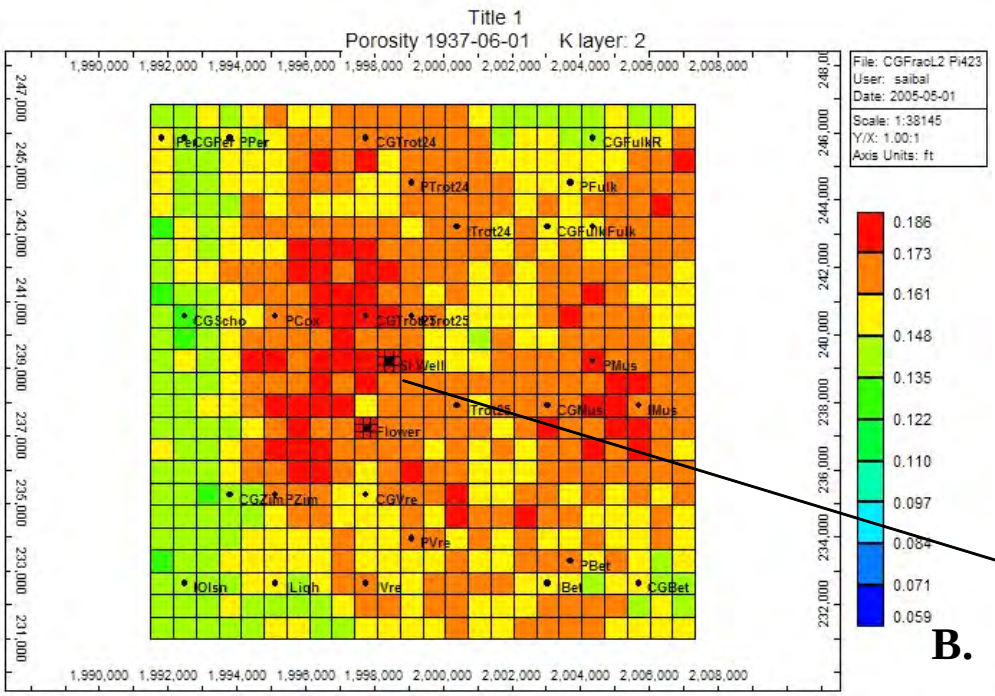

All CG wells in the model have ff ranging between 5 and 9.

Thus, to test what kind of shut in pressure could be obtained from a CG well before significant production, a hypothetical CG well ("SI Well") was located just north of the Flower well and shut-in tests were carried out on this well.

Located a Test well called "SI Well". Completed on Jan 1, 1970. Well located within a mesh of refined grids.

SI Well Completed from L2 to L23.

SI Well not fractured (ff=1).

SI Well flowed for 1 day.

Well shut in on Jan 2, 1970.

SI pressure stabilizes around 238 psi after 72 hrs. This is close to what has been typically recorded at CG wells upon completion in the study area.

B.

SI pr at a hypothetical CG well – Jan 1970

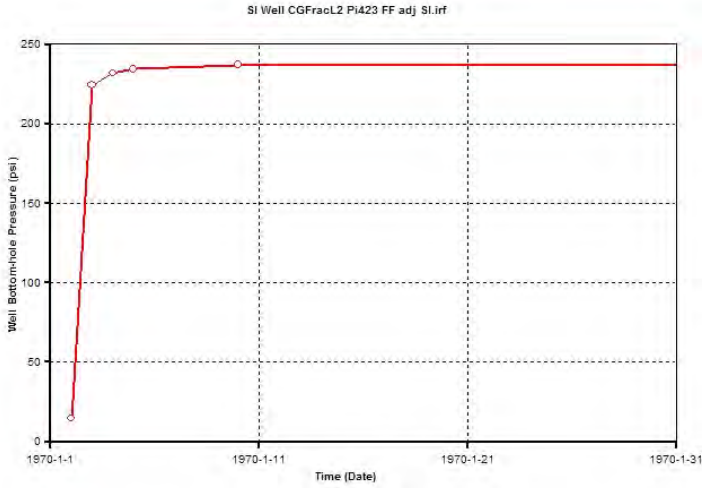

Figure 9.3.36. RUN 6 Results - A) Relative location of hypothetical Council Grove well in the Flower study area. B) Simulator-calculated shut-in pressure at the hypothetical Council Grove well as of January 1970.

6th Run – Pi = 423 psi, OGIP = 179.5 bcf.

Res Pr distribution as of Jan 1, 1995 – Flower test date

CG completions extend to L2 & Pi = 423 psi

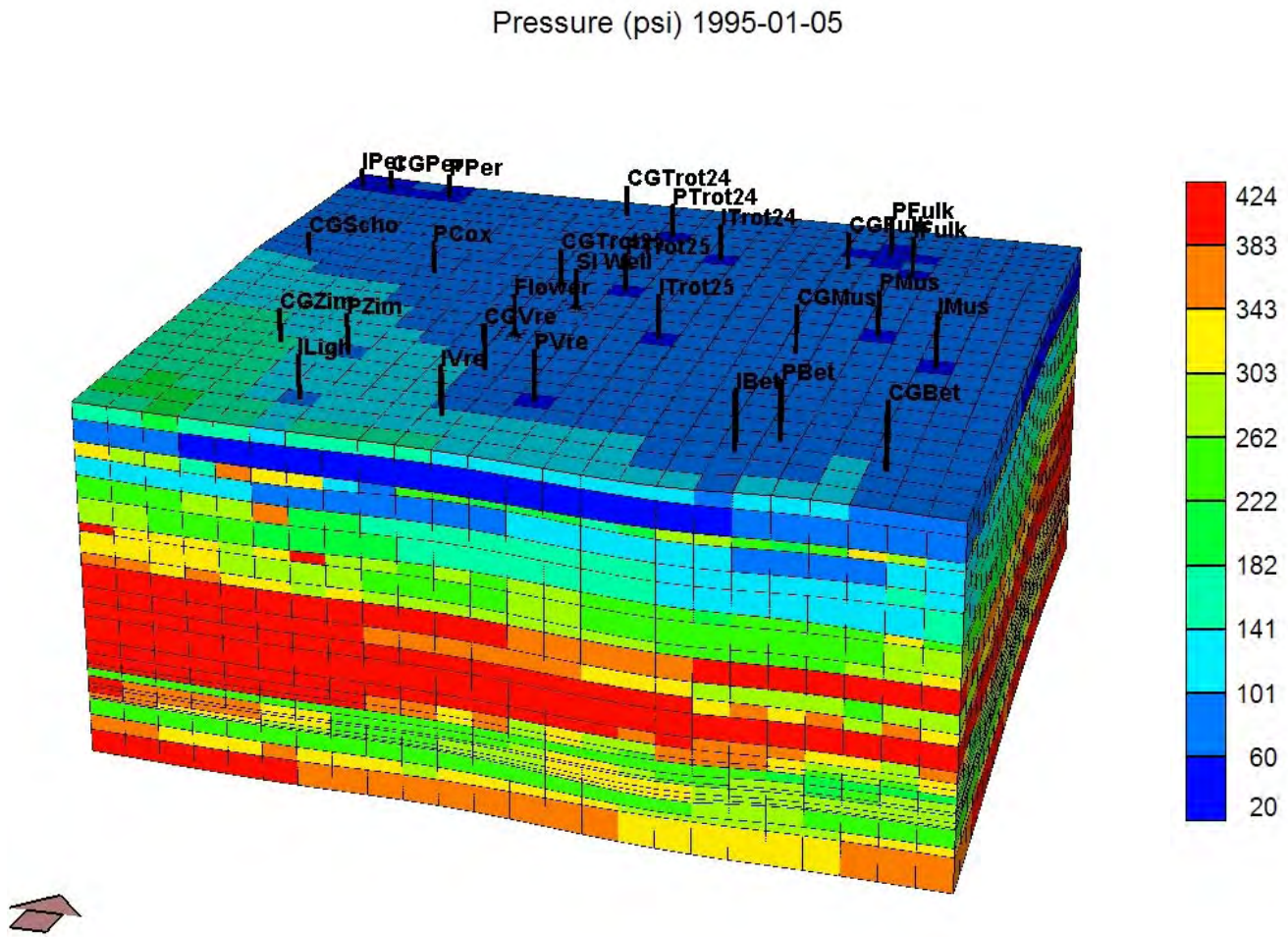

Figure 9.3.37. RUN 6 Results – Simulator-calculated pressure distribution in the Flower study area as of January 1995.

Compare Layer DST data at Flower on Jan 5, 1995

6th Run – Pi = 423 psi, OGIP = 179.5 bcf.

A.

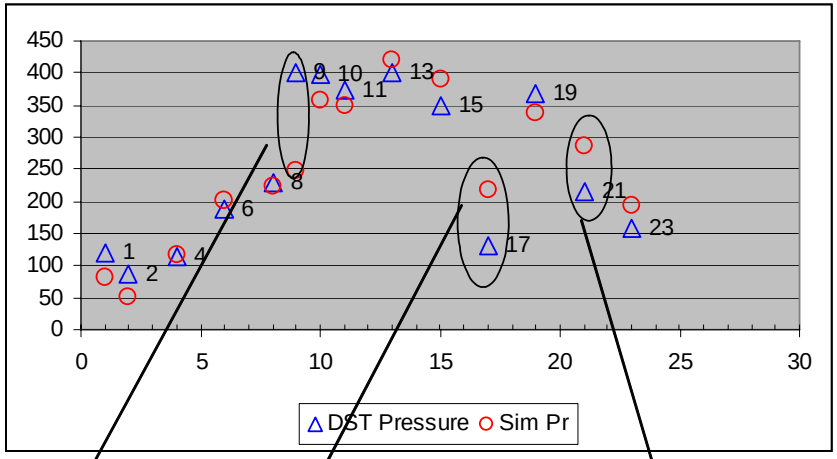

Layer 9 – L/FTRLY

Layer 17 – B2LM

Layer 21 – B4LM

Close matches obtained in most layers except L/FTRLY, B2LM and B4LM where the simulator calculated pressures are significantly higher than that recorded in Flower DSTs. It appears that despite matching CG production histories, layers such as B2LM and B4LM have not drained to the extent that the Flower DSTs indicate.

Is gas being drained from these layers by non-CG wells?

The only possible candidates are CH P and I wells.

May be hydraulic fractures in CH wells went into CG.

So next few simulator runs will have fractures in CH (P&I) wells extend to L23 along with CG fractures extending to L2 (as before).

B.

As of Jan 5, 1995
CG frac L2
All ff adj
Pi = 423 psi

	Layer	DST	Sim Pr
1 Hrngtn-Paddock	1	120.3	81
2 Krider	2	87.9	53
3 Odell Wnf SS	3		
4 Wnf LS	4	113.4	116
5 Gage	5		
6 Towanda	6	187.0	201
7 B/TWND	7		
8 FTRLY	8	229.9	224.4
9 L/FTRLY	9	400.0	249
10 B/FTRLY	10	398.4	356
11 WREFORD	11	372.4	350
12 A1_SH	12		
13 A1_LM	13	400.0	420
14 B1_SH	14		
15 B1_LM	15	350.0	389
16 B2_SH	16		
17 B2_LM	17	130.6	217
18 B3_SH	18		
19 B3_LM	19	368.0	339
20 B4_SH	20		
21 B4_LM	21	215.0	286
22 B5_SH	22		
23 B5_LM	23	159.5	194
24 C_SH	24		
25 C_LM	25		

Figure 9.3.38. RUN 6 Results – A) Simulator calculated layer pressure at Flower A1 compared with layer DST pressure. B) Tabulation of simulator-calculated layer pressure with that obtained from Flower well DSTs.

7th Run – Pi = 423 psi, OGIP = 179.5 bcf.

CH well (P&I) completions extended to L23 and CG fractures go to L2

FF factors unchanged from 6th Run

SI pr at a hypothetical CG well – Jan 1970

A.

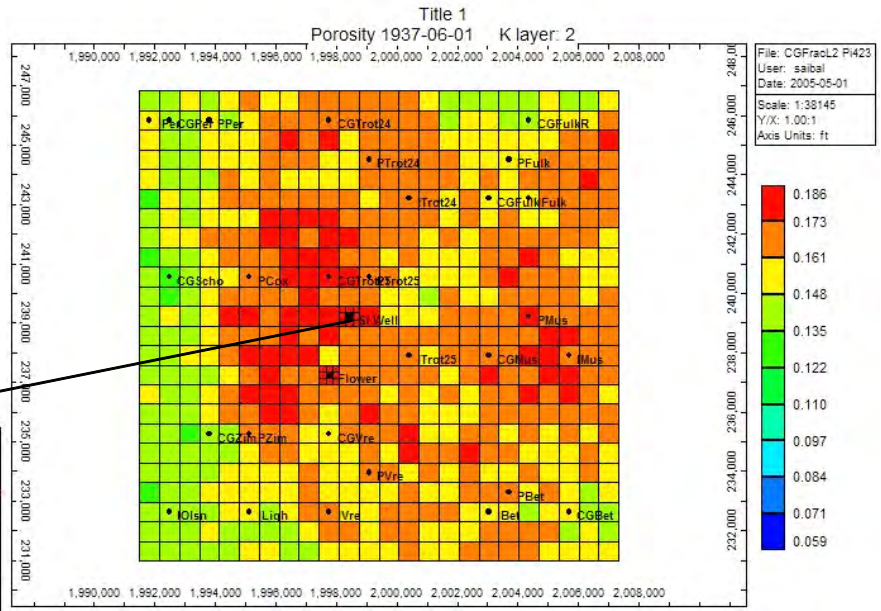

Production and pressure matches at CH wells (P&I) and CG wells remain largely unchanged.

B.

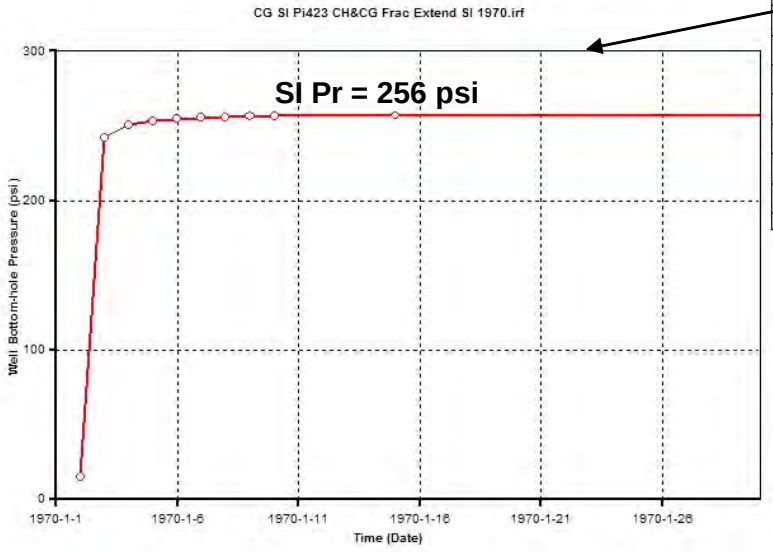

Extending CH fractures into CG enables getting slightly higher SI pressures at CG wells upon completion. This higher SI value is more closer to 265 psi – the pressure that has recorded at CG wells, than that obtained in 6th Run.

Figure 9.3.39. RUN 7 Results – Chase wells completions extended to Layer 23 while Council Grove completions extended to Layer 2. A) Relative location of hypothetical Council Grove well in the Flower study area. B) Simulator-calculated shut-in pressure at the hypothetical Council Grove well as of January 1970.

7th Run – Pi = 423 psi, OGIP = 179.5 bcf.

CH well (P&I) completions extended to L23 and CG fractures go to L2

FF factors unchanged from 6th Run

Compare Layer DST data at Flower on Jan 5, 1995

A.

	Layer	DST	Run 6 As of Jan 5, 1995 CG frac L2 All ff adj Pi = 423 psi Sim Pr	Run 7 FF same as before CH frac to CG CG ff to CH Pi = 423 psi Frac Ext
1 Hrngtn-Paddock	1	120.3	81	93.6
2 Krider	2	87.9	53	64
3 Odell	3			
Wnf SS				
4 Wnf LS	4	113.4	116	126.9
5 Gage	5			
6 Towanda	6	187.0	201	212.1
7 B/TWND	7			
8 FTRLY	8	229.9	224.4	232.2
9 L/FTRLY	9	400.0	249	255.2
10 B/FTRLY	10	398.4	356	347.7
11 WREFORD	11	372.4	350	320.3
12 A1_SH	12			
13 A1_LM	13	400.0	420	419.7
14 B1_SH	14			
15 B1_LM	15	350.0	389	371
16 B2_SH	16			
17 B2_LM	17	130.6	217	149
18 B3_SH	18			
19 B3_LM	19	368.0	339	308.4
20 B4_SH	20			
21 B4_LM	21	215.0	286	250.3
22 B5_SH	22			
23 B5_LM	23	159.5	194	131
24 C_SH	24			
25 C_LM	25			

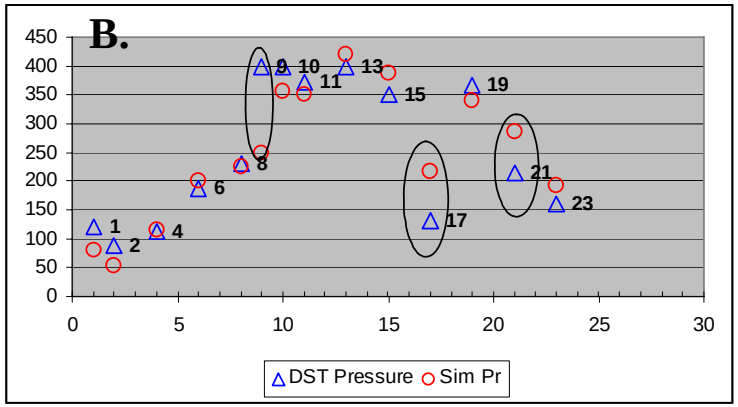

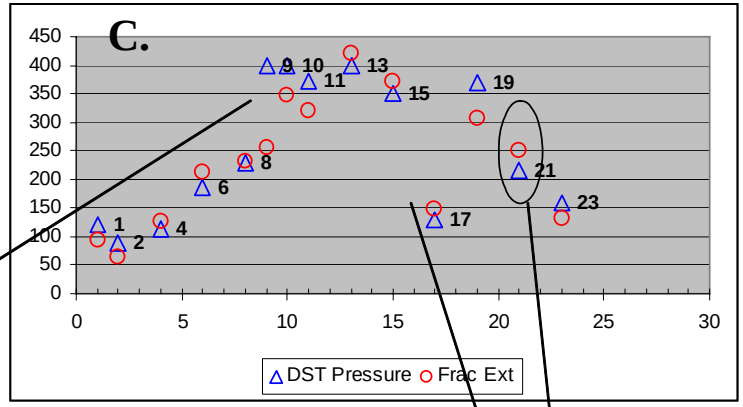

Layer 9 is L/FrtRly – simulator calculates a lower pressure at this zone

Pressure matches improve in Layers 17 and 21 when CH completions extended in CG

Figure 9.3.40. RUN 7 Results – A) Tabulation of simulator-calculated layer pressure from Runs 6 and 7 with that obtained from Flower well DSTs. B) & C) Simulator calculated layer pressure at Flower A1 from Runs 6 and 7 compared with layer DST pressure.

7th Run – Pi = 423 psi, OGIP = 179.5 bcf.

CH well (P&I) completions extended to L23 and CG fractures go to L2

FF factors unchanged from 6th Run

			Run 6		Run 7
			As of Jan 5, 1995	As of Jan 5, 1995	As of Jan 1, 2004
			CG frac L2	FF same as before	FF same as before
			All ff adj	CH frac to CG	CH frac to CG
			Pi = 423 psi	CG ff to CH	CG ff to CH
				Pi = 423 psi	Pi = 423 psi
	Layer	DST	Sim Pr	Sim Output	Sim Output
Hrngtn-Paddock	1	120.3	81	93.6	54.8
Krider	2	87.9	53	64	27.8
Odell	3		113	124	78.6
Wnf SS		105.4*			
Wnf LS	4	121.4	116	126.9	81.7
Gage	5	NO TEST	201	211.5	168.9
Towanda	6	187.0	201	212.1	165.1
B/TWND	7	NO TEST	219.5	227.4	180.8
FTRLY	8	229.9	224.4	232.2	185.2
L/FTRLY	9	>400.0	249	255.2	213.5
B/FTRLY	10	398.4	356	347.7	315.9
WREFORD	11	372.4	350	320.3	278.7
A1_SH	12	NO TEST	418	417	414.1
A1_LM	13	400.0	420	419.7	417.1
B1_SH	14	NO TEST	419.8	418.2	415.2
B1_LM	15	350.0	389	371	351.3
B2_SH	16	NO TEST	387	369	349.5
B2_LM	17	130.6	217	149	101.2
B3_SH	18	NO TEST	338	307	278.1
B3_LM	19	368.0	339	308.4	279.2
B4_SH	20	NO TEST	338	307.9	278.7
B4_LM	21	215.0	286	250.3	214.8
B5_SH	22	NO TEST	287	251	214.8
B5_LM	23	159.5	194	131	85.6
C_SH	24	NO TEST	342	321.2	302.1
C_LM	25	NO TEST	409	403	393.5

Figure 9.3.41. RUN 7 Results – Simulator-calculated layer pressures at the Flower A1 well as of January 1995 and January 2004 to identify layers that significantly contribute to production during this period of time.

7th Run – Pi = 423 psi, OGIP = 179.5 bcf.

Compare layer pressures at Flower – Jan 1995 and Jan 2004

CH well (P&I) completions extended to L23 and CG fractures go to L2

FF factors unchanged from 6th Run

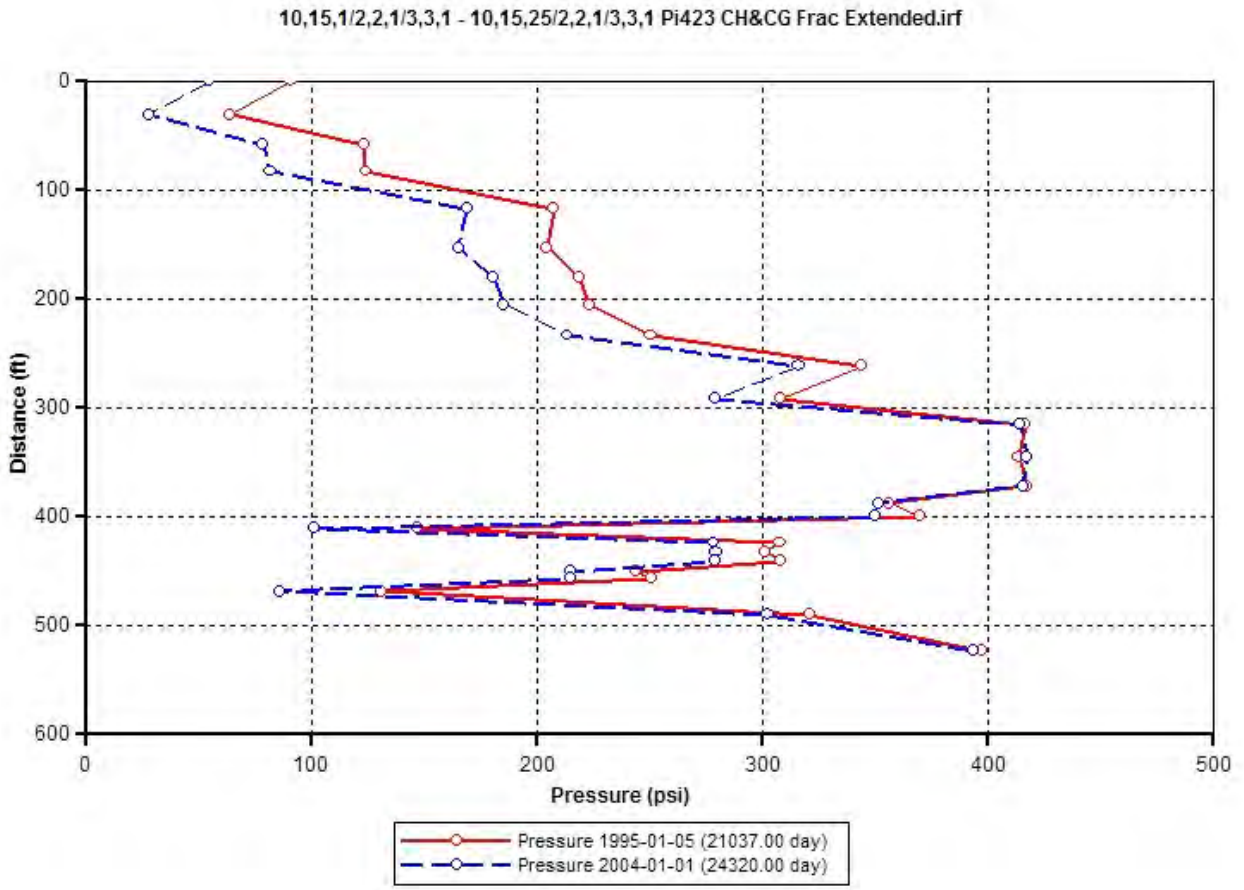

Figure 9.3.42. RUN 7 Results **-** Simulator-calculated layer pressure at Flower A1 in January 1995 and January 2004. Each circle represents a layer starting from the top (Layer 1) to the bottom (Layer 23).

7th Run – Pi = 423 psi, OGIP = 179.5 bcf.

CH well (P&I) completions extended to L23 and CG fractures go to L2

FF factors unchanged from 6th Run

Pressure distribution as of Jan 2004 – end of the simulation time period

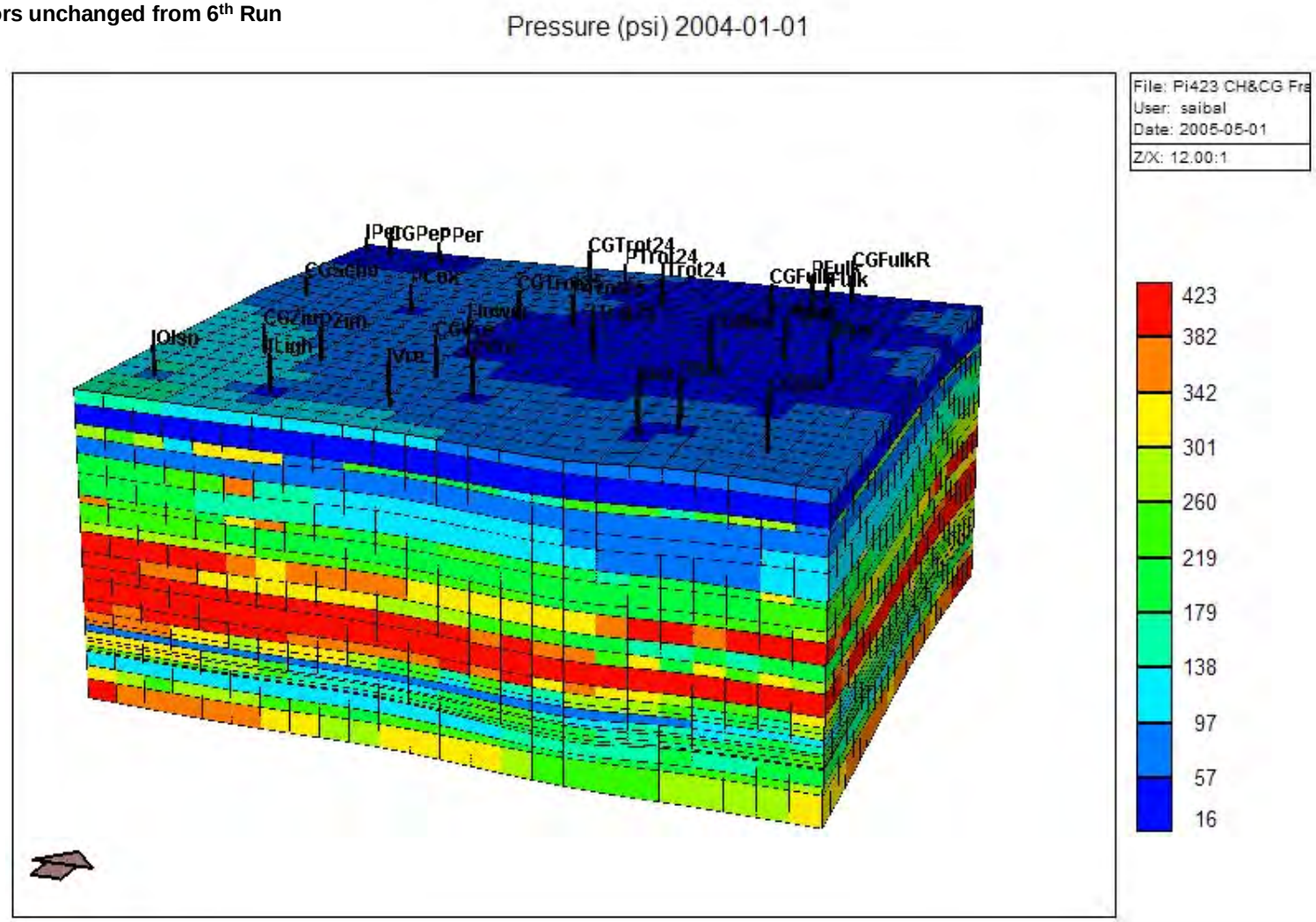

Figure 9.3.43. RUN 7 Results – Simulator-calculated reservoir pressure distribution as of January 2004.

7th Run – Pi = 423 psi, OGIP = 179.5 bcf.

CH well (P&I) completions extended to L23 and CG fractures go to L2

FF factors unchanged from 6th Run

Pressure distribution as of Jan 2004 – end of the simulation time period

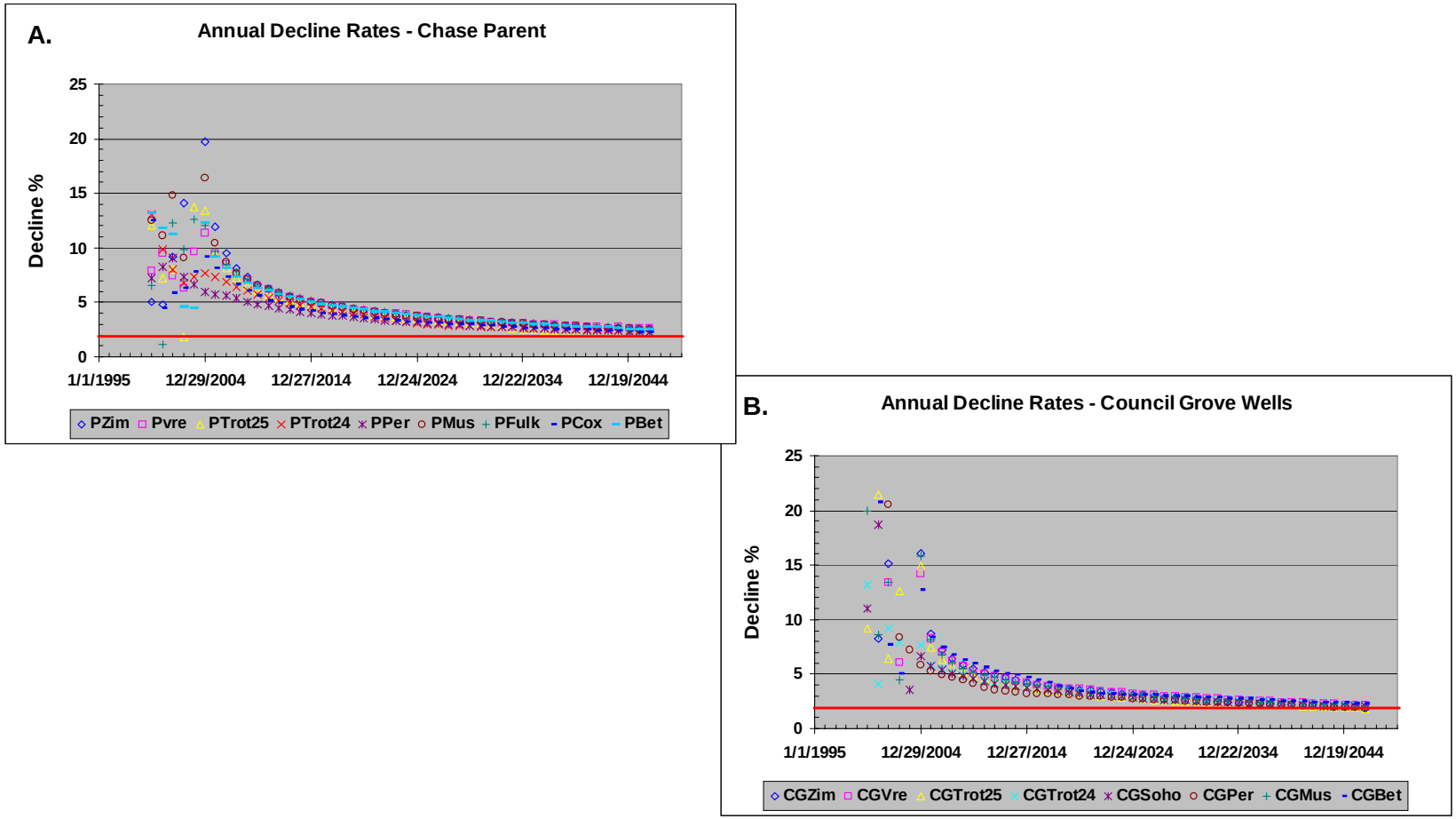

Figure 9.3.44. RUN 7 Results – Simulator-calculated annual production decline rates in Chase Parent and Council Grove wells till 2050.

8th Run – Pi = 423 psi, OGIP = 179.5 bcf.

CH well (P&I) completions extended through L17 and CG fractures go to L8

FF factors unchanged from 6th Run

A What happens if CH completions extended to B2LM and CG completions went up to Fort Rly?

CG Prod matches displayed

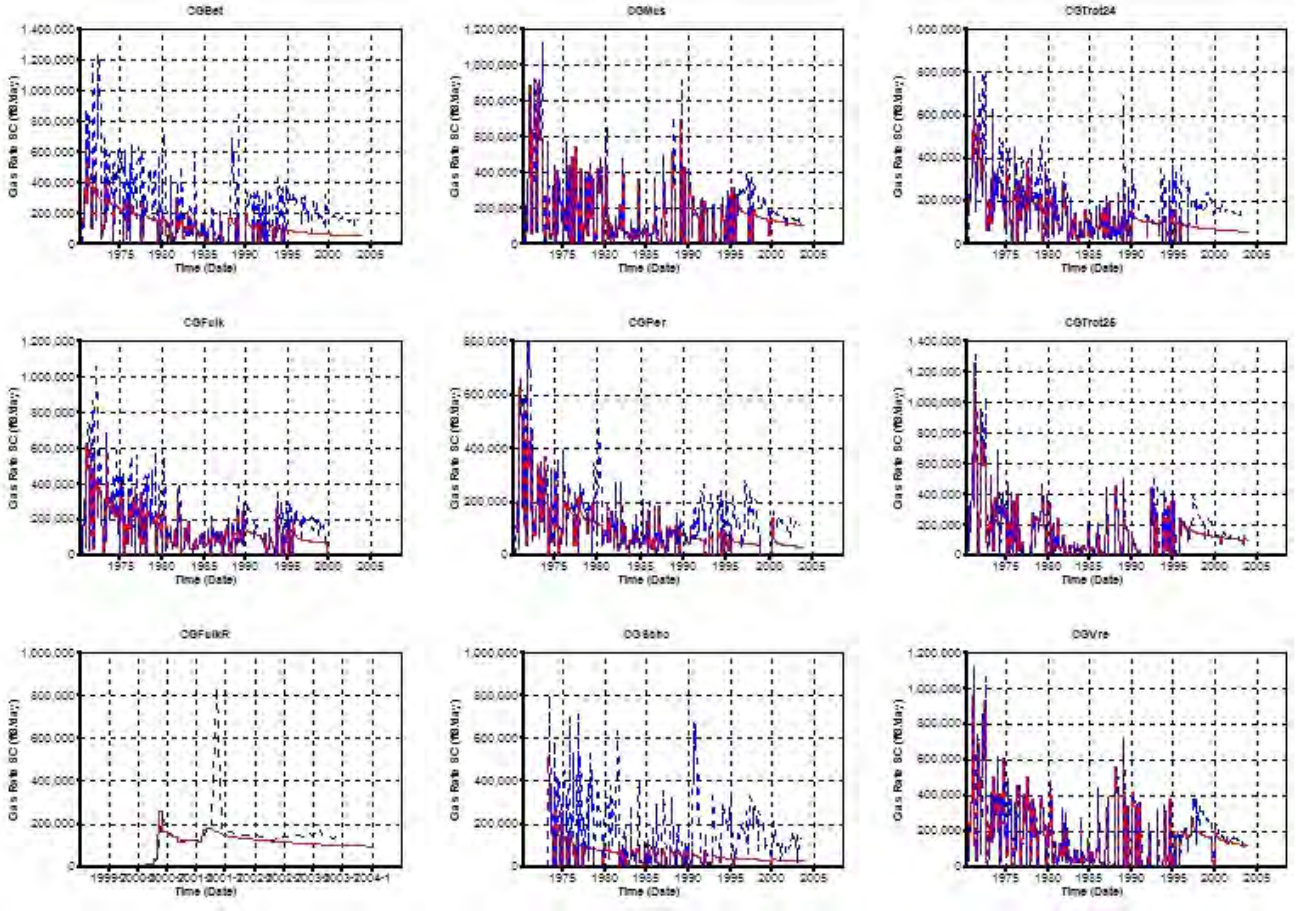

Red line – Simulator (Sim) calculated gas rate, Blue broken line – historic gas production

Figure 9.3.45. RUN 8 Results – Comparison of simulator-calculated production rate with historic values at Council Grove wells when completions in Chase wells extended to B2 Lime while those of Council Grove wells were extended to Fort Riley.

8th Run – Pi = 423 psi, OGIP = 179.5 bcf.

CH well (P&I) completions extended through L17 and CG fractures go to L8

FF factors unchanged from 6th Run

Compare layer pressures (1995) at Flower – Run 7 & Run 8

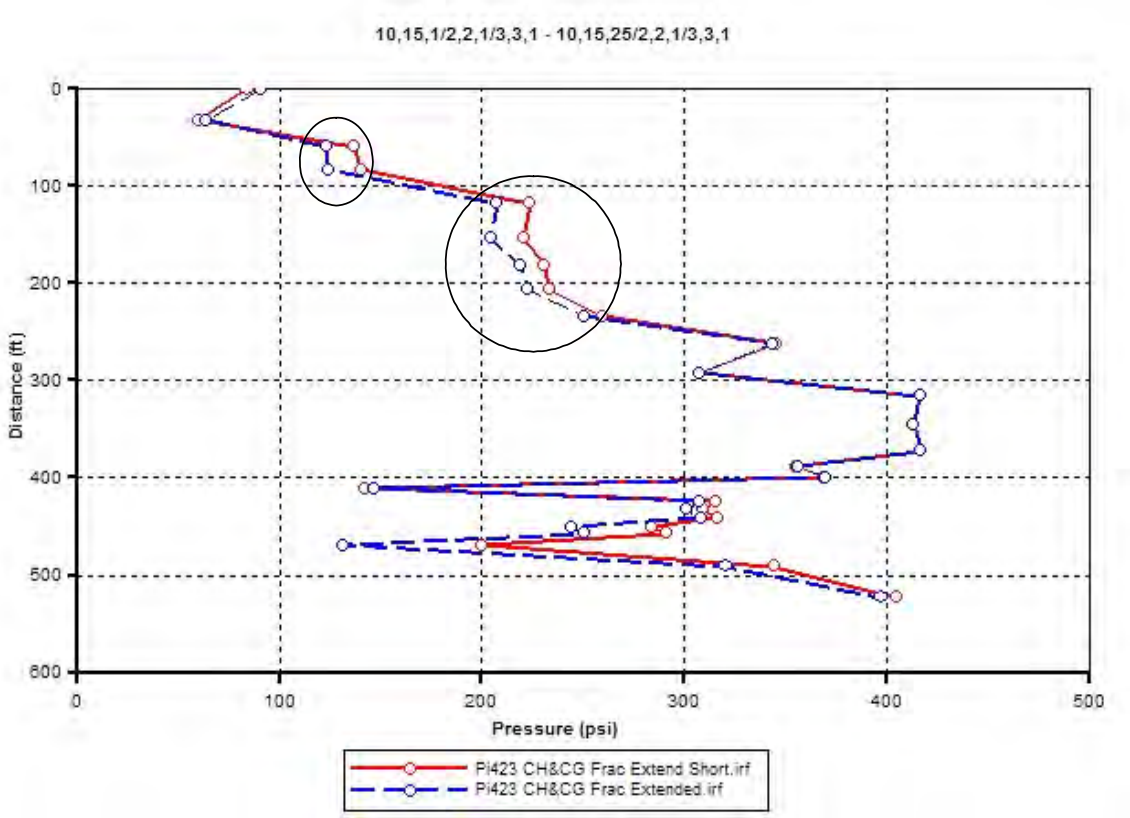

Blue line - represents Run 7. Red line - represents Run 8.

Figure 9.3.46. RUN 8 Results – Comparison of simulator-calculated layer pressure at Flower A1 well from RUN 8 with that from RUN 7. Each circle represents a layer starting from the top (Layer 1) to the bottom (Layer 23).

9.4 MULTI-SECTION SIMULATION – GRASKELL AREA

Saibal Bhattacharya, Martin K. Dubois and Alan P. Byrnes

Introduction

The Hugoton and Panoma gas fields (Figure 9.4.1), North America's largest, produce from 13 fourth-order marine-nonmarine sedimentary cycles of the Wolfcampian Chase and Council Grove Groups, respectively. A fine-layered cellular geomodel was constructed for these fields using a four-step workflow: 1) define lithofacies in core and correlate to wireline log curves and geologic variables (depositional environment and relative cycle-position), 2) train a neural network and predict lithofacies at non-cored wells, 3) populate a 3D-cellular model with lithofacies using stochastic methods, and 4) populate the model with petrophysical properties and fluid saturations using facies-specific equations based on core data. The fine-scale model was upscaled to 25 layers for simulation. A 12-section area, named Graskell in this report, was extracted from the field-wide model and used in simulation studies described below.

Objective

The objective of this study was to validate the above-mentioned geomodel by simulating the production/pressure performance of Hugoton Parent, Hugoton Infill, and Council Grove wells located in select multi-section areas, such as the Graskell, in the Hugoton field. The reservoir geomodel was developed using an automated facies-recognition technique and applying facies-specific capillary-pressure curves developed by integrating available core data. The intent of this exercise is, therefore, to evaluate the robustness of this geomodel by comparing how close the simulator-calculated pressure/production performances of individual wells match with respective histories with minimum modifications to the geomodel. The focus is not to obtain exact matches of pressure/production histories at individual wells with localized model modifications. Computer Modeling Group's (CMG's) IMEX simulator was used in this study.

The process of geomodel validation can be approached by answering the following set of questions:

a) Given the storage and permeability distribution in the model, can Chase Parent and Infill and Council Grove wells match their respective production histories and in the process undergo a pressure decline along historic trends?

b) Upon production and pressure history matching, what is the simulator-calculated shut-in pressure at a hypothetical Council Grove well as of January 1978?

c) How good a match is attained between simulator-calculated layer pressures with RFT layer pressures at Eliot A6 in the study area?

This report details the simulation studies carried out at Graskell area, which includes secs. 1, 2, 11, 12, 35, and 36, T 28 S., R 35 W., and secs 5, 6, 7, 8, 31, and 32 in

T 28 S., R 34 W. The location of the Graskell simulation area within the context of the Hugoton-Panoma fields is shown in Figure 9.4.1 while Figure 9.4.2 shows the study area bordered by a broken green line.

Graskell Area and Model

The Graskell area is situated in the east-central portion (Figure 9.4.1) of the Hugoton-Panoma field area directly inside the downdip margin of the Panoma field. The gas column is continuous from the top of the Chase to the uppermost zones in the Council Grove. However, only one well in the simulation area was completed in any zone below the A1_LM, the uppermost marine carbonate in the Council Grove, yet the cumulative gas produced per Council Grove (Panoma) is nearly 1 BCF gas. Zones with the most original gas in place are the Fort Riley, Towanda, lower Fort Riley, Wreford, Krider, and A1_LM in order of importance.

Static Model

The workflow used in building the static model for the Flower area simulation (Bhattacharya et al., 2005) was used for the Graskell study. A 70-square-mile, 806,000 cell fine scale model (bordered by pink broken line in Figure 9.4.2) was constructed in Petrel and populated with lithofacies, permeability X, Y, and Z, and water saturation for two free-water levels (FWL), 75 ft and 100 ft below the base of perforations in the Council Grove. The two lowest zones in the Council Grove were not modeled because they are well below the gas/water contact. Lithofacies at node wells were predicted at node wells using the Geomod 3 version of trained neural networks. A smaller 12-square-mile area (Figure 9.4.3) was extracted from the model and the 180-layer fine model was upscaled to 23 layers, one per zone for the Chase and Council Grove (through the B5_LM) using the same upscaling method as for the Flower model (Figure 9.4.4). For porosity and water saturation, the upscaling was volume-weighted arithmetic average, while Petrel's tensor upscaling using PSK solver was utilized for estimating X and Y direction permeability. Permeability Z was calculated using a function of lithofacies and permeability XY.

Free water level (Figure 9.4.5) is the most significant variable in determining water saturations in portions of the reservoir system that are low in the gas column such as in the Council Grove layers. As in the Flower model, the FWL was arbitrarily moved down 25 ft from the originally estimated FWL to allow the model to have higher gas saturations in the upper Council Grove. This provided for a better correspondence between original-gas-in-place (OGIP) volumes charging the model (Figure 9.4.6) and cumulative gas produced from Panoma wells, under the assumption that all Panoma Gas withdrawal is restricted to the Council Grove interval (Tables 9.4.1 and 9.4.2). However, this assumption is contrary with pressure data and simulation results that suggest that there is likely to have been communication in both directions.

Engineering Model

The 23-layer geomodel was exported to the reservoir simulator – Computer Modeling Group's IMEX. Each layer in this 23-layer model coincided with a formation- or member-level stratigraphic interval in the Chase and Council Grove system. Each layer represents a half-cycle of marine/non-marine sedimentary cycle. In most cases, the model layer closely approximates the RFT intervals at wells in and around the study area. Grid-cell dimensions were set at 660 ft by 660 ft for all layers.

Figure 9.4.7 lists the basic PVT properties input for simulation.

Permeability Modeling

One Council Grove core (Alexander D2 in sec 29, T 27 S., R 35 W., Grant County, Kansas) was available in the vicinity of the study area. No cores representing the Chase formations were available. Log-porosity and permeability estimated using facies-specific correlations were compared with corresponding values obtained from whole cores in all CG layers and Wreford to obtain layer-specific permeability multiplier (Figure 9.4.8). A multiplier of 1.0 was used for shale layers. Most permeability multipliers in the non-shale layers were in the vicinity of 3.0. Thus, without Chase core data, a permeability multiplier of 3.0 was assumed for all non-shale Chase layers.

Reservoir Pressure

The first recorded surface shut-in (SI) pressures (soon after completion) at the Chase Parent wells in the area studied varied between 400 to 432 psi (Figure 9.4.9) with the pressure at the two earliest wells being 406 psi and 432 psi. Surface shut-in pressures were converted to bottom-hole shut-in pressures. The bottom-hole shut-in pressures corresponding to the average and median surface shut-in pressures were 445 and 448 psi. Given the variation in the recorded shut-in pressures at the initial wells, a starting reservoir pressure of 440 psi was assumed in this study. Thus, the reservoir model in the simulator was initialized using a starting pressure of 440 psi resulting in a charge of 170.61 bcf gas (Figure 9.4.10) as OGIP with Fort Riley and Towanda being the major gas storage units with OGIPs of 43.9 and 29.9 bcf, respectively.

Hydraulic Fractures

Most of the wells in the study area were drilled before 1950. Current records indicate that all wells were hydraulically fractured some time during their production life. However, the exact date on which each well was fractured is not available. Fracturing technology came into use in the study area in the 1960's. In this study, it was assumed that wells were fractured as of January 1, 1960. Later infill/replacement wells drilled in the 1980's or later were assumed to be fractured upon completion.

However, no information or test data are available which would enable one to estimate the physical characterization of these fractures. The intent of the fracturing was

to enhance the well productivity. Lacking physical descriptions of hydraulic fractures, the enhanced well productivities were modeled in this study using the well productivity (ff) factor greater than 1 with the ff set to 1.0 for an unfractured well. The ff value was modified at each well to match the post-1960 production.

Flow Constraints

Annual production data for individual wells were available for initial completion to 1966. From 1967 onwards, monthly production data were available for all the Chase wells in the study area. Regular tubing-head flow and shut-in pressure data were available for all wells from 1967 onwards. Between 1952 and 1966, six-month cumulative production data were available for all Chase Parent wells. Only total cumulative production until 1951 was available for each Chase Parent well. Complete monthly production histories were available for Chase Infill and Council Grove wells.

In the simulator, all wells were flowed under rate constraints until May 2004. Thereafter, all wells were flowed under a constant bottom-hole pressure (BHP) of 14.7 psi until December 2006. The intent of changing from rate constraint to pressure constraints was to see if the simulator-calculated production rates from May 2004 to December 2006 followed the already established decline trends without showing production spikes (or signs of excess flow capacity). The well names and their abbreviated names used in the simulator model along with their starting dates, cumulative production, and initial perforation intervals are listed in Figures 9.4.11 and 9.4.12.

Reservoir Simulation Studies

Well operators confirm that each of these wells was hydraulically fractured during some point in its production life. However, the exact date when each well was fractured is unavailable. In the model, it was assumed that each well was fractured as of January 1, 1960 – the approximate time frame when fracturing came in vogue in the study area.

Because the wells were not fractured pre-1960, flow in this period was dominated by matrix. Also during this period, the well completions could not extend beyond the layers recorded in completion reports. Thus, the strategy employed in designing the following set of simulation runs was to first try to match pre-1960 field production by adjusting matrix permeability through the application of different multipliers. It was only after obtaining a match with the historic production volumes prior to January 1, 1960, that other factors such as layers drained by the fractures and productivity gains from hydraulic fracturing were modified on a well-by-well basis to improve both the production and flowing-pressure matches at each well.

The model used in this study was an 11-layer model with grid-cell sizes of 660 feet by 660 feet. A consistent set of legends was used to analyze the simulation results. The simulator-calculated production and bottom-hole flowing pressure are displayed in red and green lines while the historic production and well-head-flowing pressures (WHFPs) are displayed in blue and magenta. Hence, through this report, Chase

Parent wells will be referred as P, while Chase Infill wells will be referred as I, and Council Grove wells will be referred as G.

RUN 1

All P, I, and G wells were completed in the perforated intervals obtained from completion records. Hydraulic fractures were modeled using ff = 6.0 at all P wells as of January 1, 1960. The initial reservoir pressure was set at 440 psi and initial permeability multipliers (as described in Figure 9.4.8) were applied to each of the pay (gas) layers. Figures 9.4.13 and 9.4.14 compare the simulator-calculated cumulative gas production with the historic volumes at the P wells. It appears that the simulator-calculated gas production matched or came close to matching the well history only at those P wells where completions (and therefore fractures) extended to L8 (Fort Riley). Simulator-calculated gas production fell short in every other Chase Parent (P) well. Figures 9.4.15 and 9.4.16 showed that simulator-calculated gas production fell significantly short at every Council Grove (G) well.

Simulation results from the initial run indicate that the current model is unable to deliver the recorded gas production from both P and G wells. Therefore, the next series of simulator runs (from Run 2 to Run 5) details model modifications necessary to match production histories at the P wells while Runs 6 to 8 revolve around model adjustments required to match G well production histories.

RUN 2

The well productivity as a result of hydraulic fracturing (as of January 1, 1960) was increased at all P wells using ff = 10.0, compared to ff = 6.0 in Run 1, while all other model parameters were left unchanged. Figures 9.4.17 and 9.4.18 show that the simulator-calculated gas production for P wells increased (slightly) over that obtained in Run 1 with the cumulative gas production at P wells not completed to L8 (Fort Riley) still falling short of historic volumes.

RUN 3

Hydraulic-fracture completions were extended to L8 (Fort Riley) at all P wells where recorded perforations stopped short of L8. All other model parameters were left unchanged from Run 1 (such as ff = 6.0 for all P wells). Figures 9.4.19 and 9.4.20 showed that the simulator-calculated gas production increased at P wells that had previously not been perforated in L8. However, simulator-calculated cumulative gas production still fell short in some of these P wells where fracture completions were extended to L8.

RUN 4

As noted before, no Chase core was available from or near the Graskell study area, nor was layer-specific DST carried out at any of the wells in or around the study area to calculate layer-specific permeability at the test well. Thus, permeability

multipliers applied on permeability estimated by facies-specific equations at each of the Chase gas zones was arbitrary. No core- or DST-based permeability data were available to compare the permeability estimated by facies-specific equations for each Chase gas zone and to develop appropriate multipliers. Thus, an arbitrary multiplier of 3.0 was used for each Chase gas zone in the previous simulation models. Given the inability of the simulator-calculated gas production to match historic volumes at some of the P wells, an additional permeability multiplier of 2.0 (over the original multiplier of 3.0) was employed on two of the most productive Chase zones, i.e. L6 (Towanda) and L8 (Fort Riley) in this run. All other model parameters were left unchanged from Run 3.

Figures 9.4.21 and 9.4.22 summarize the results of Run 4. Simulator-calculated gas production matched or almost matched at all P wells except those located in the southwest (SW) corner of the simulation area. For example, Higgenbotham (PHigB1) is located in the SW corner of the Graskell study area. This well is the second-highest gas producer in the study area having produced 10 bcf of gas. However as per the current model, the OGIP (Figure 9.4.23A) and permeability (Figure 9.4.23B) distributions in the driver layers, such as L8 (Fort Riley) and L6 (Towanda), in the SW corner of the study area including the drainage area of PHigB1 (Figure 9.4.23) are low compared to other regions of the Graskell study area. Figure 9.4.23C shows that within the study area no wells with qualified logs are located in the southwestern corner. Wells with qualified logs are located outside the study and at a considerable distance from the SW corner of the study area, resulting perhaps in non-representative OGIP and permeability distributions being mapped in this section of the study area.

RUN 5

Permeability was adjusted (Kxy*6 over the initial multiplier, Figure 9.4.8) in L1 (Herington) to match the estimated RFT layer pressure data. All other inputs were kept the same as in Run 4. Figures 9.4.24 and 9.4.25 display the simulator-calculated cumulative production and bottom-hole flowing pressure matched against historic production and well-head flowing pressures. Simulator-calculated gas production matched historic volumes at all but five wells namely, PHogB1, PMor1, PStan1 (all located at the SW corner of the study area), and PGoer1 and PEub1 located in the southeast (SE) corner of the study area. Wells where a good production match was obtained also showed close matches between FTHP (historic flowing surface pressure) and FBHP (simulator-calculated bottom-hole flowing pressures) except in PDev where despite a production match the simulator-calculated FBHP fails to match the recorded FTHP match and shows flow-capacity limitations in the well's drainage area. It may be noted that PDev is also located in the SW corner of the study area. Thus, reasonable matches of production and pressure were obtained at seven out of 12 Chase Parent wells in the study area using the current geomodel.

Layer pressures from RFT tests were available from five wells in and around the study area. One of wells, Eliot A-6 (PEliot), was located within the study area. However, available RFT data show significant variation (Figure 9.4.26) in recorded shut-in pressures within each of the pay layers in and around the study area. Figure 9.4.27

compares the RFT layer-pressure data recorded at Eliot A6 (as of December 2004) with the simulator-calculated grid-block pressure at the location of this well in the model and also shows the degree of variation (in the "Comments" column) in recorded RFT layer pressures within a layer at different wells in and around the study area. RFT layer pressure data were recorded in L1 (Herington), L4 (Winfield), L6 (Towanda), L8 (Fort Riley), L10 (Florence), and L11 (Wreford). The goodness of fit (or lack of it) between simulator-calculated layer pressures and RFT layer pressures should be considered in the context of discrepancies existing in reported RFT layer-pressure data and the fact that production and pressure histories have been matched in only seven out of 12 Chase Parent wells using the current geomodel.

The permeability and OGIP distributions in L1 (Herington) are poorer than that in L6 (Towanda) in the current geomodel input to the simulator. However, RFT layer-pressure data indicate that L1 (Herington) has produced an equal fraction of its storage as L6 (Towanda) despite having significantly lesser storage and flow capabilities because both L1 and L6 are assumed to have an initial pressure of 440 psi and have declined to 78 and 74 psi, respectively, as of December 2004. Discrepancies, such as these, exist in the RFT data and need to be resolved in order to match against simulator-calculated layer pressures.

RUN 6 and 7

Runs 6 to 8 were designed to identify modifications required on the geomodel in order to obtain history matches at the Council Grove (G) wells in the study area. The Kxy distribution in the Chase layers were kept the same as in Run 3 while a multiplier of 10 (over the initial multiplier, Figure 9.4.8) was used for the CG pay layers in Run 6. The ff denoting the productivity enhancement by hydraulic fracturing was set at 6.0 for all the G wells. Also, the fractures in the G wells were constrained to the perforated intervals. In Run 7, the Kxy in the Chase and the Council Grove pay layers were kept the same as Run 3 while the productivity enhanced due to hydraulic fracturing in G wells was increased by using ff = 10.0. Figures 9.4.28 and 9.4.29 compare the simulator-calculated cumulative production from the G wells. It is apparent from these figures that the simulator-calculated gas production matches or is close to historic volumes at G wells in Run 6, while it remained significantly short of historic volumes in Run 7.

RUN 8

The Kxy in the Council Grove pay layers were the same as that obtained after the use of the original multipliers (Figure 9.4.8). However, the completions in the G wells were extended to L8 (Fort Riley) using ff = 6.0. Figures 9.4.30 and 9.4.31 compare the simulator-calculated cumulative production from the G wells with historic volumes and that obtained from Run 6. It is apparent from the above-mentioned figures that the simulator-calculated cumulative production at the G wells matches or is close to matching historic volumes at all but four wells, namely Stanley 3C (GStan3C), Eubank 4C (GEub4C), Davatz Gas Unit 2 (GDav2), and Higgenbotham 2A (GHigB2A). Of the above-mentioned wells, GEub4C, GDav2, and GHigB2A are located along the southern

boundary of the study area which in the current model (Figure 9.4.25) has lower OGIP and tighter permeability distribution than other areas of the study area. GStan3C is located in the northeast corner of the study area.

RUN 9

Fracture completions in the P wells were extended to L8 (Fort Riley) using ff = 6.0. Permeability multiplier of 2 (over the initial multiplier) was applied to L6 (Towanda) and L8 (Fort Riley) while that of 6 (over the initial multiplier) was applied to L1 (Herington). A permeability multiplier of 10 (over the initial multiplier) was applied to all Council Grove pay layers. Simulator-calculated cumulative production matched historic volumes at the majority of the P and G wells. Figure 9.4.32 shows the simulator-calculated pressure distributions as of January 1978, i.e., the time after which most of the G wells were drilled in the modeled area. Figure 9.4.33 shows the simulator-calculated shut-in pressure stabilized to 400 psi, after 4 days of shut-in followed by a day of flow in January 1978, at a hypothetical G well (named CG SI) located at the center of the study area when its completions (ff = 6.0) were restricted to the Council Grove pay layers. Figure 9.4.34 plots the first recorded surface shut-in pressures at all the G wells drilled in the study area. This plot clearly shows that the initial shut-in pressures recorded at newly drilled G wells in the late 1970's ranged between 150 psi to 210 psi, and thus the simulator-calculated shut-in pressure of 400 psi for a hypothetical G well is significantly higher than pressures characteristically recorded at G wells in the study area.

RUN 10

The input parameters for the P wells were left unchanged from Run 9. For the G wells, the fracture completions were extended to L8 (Fort Riley) using ff = 6.0 while the permeability distribution was the same as obtained after using the initial multipliers. Figures 9.4.35 and 9.4.36 show the production and pressure history matches obtained at the P wells. Simulator-calculated production matched historic volumes at all P wells except PHigB1. Good pressure matches were obtained at some of the P wells while for others the simulator-calculated BHFP followed the trend set by recorded THFPs. Presence of spikes in the simulator-calculated BHFP profiles at P wells where the simulator-calculated BHFP pressures did not match history may be indicative of low permeability prevailing in the driver pay zones in the current model. Also, production spikes are evident in some of the P wells when they are released from flow constraints after May 2004. Figures 9.4.37 and 9.4.38 compare the simulator-calculated production and bottom-hole flowing pressures with historic production volumes and recorded surface-flowing pressures for the G wells. The simulator-calculated production matches the historic rates at all G wells. However, in most G wells, the simulator-calculated BHFPs are, despite showing spikes, close to and follow the trend of the recorded THFPs. Also, production spikes become visible in many G wells when released of flow constraints. Figure 9.4.39 and 9.4.40 show the history matches for cumulative production and flowing pressures for the Chase Infill (I) wells in the study area. The above figures show that the simulator-calculated production matches or is close to matching the historic volumes at most I wells except those located in the tight border areas along the south and

south western border of the study area. Also, many of I wells show spikes in the simulator-calculated flowing pressure profiles, which may indicate tight permeability present in the drainage areas of the affected wells in the current model. Production spikes are also evident (Figures 9.4.41 and 9.4.42) at most of the Chase Infill wells when released of flow constraints in the simulator and this may indicate excess flow capacity. Figure 9.4.43 shows the location of the Chase Infill wells where the simulator-calculated production failed to match the historic volumes. Each of these I wells is located along the southern and southwestern border of the study area where the OGIP and permeability distribution in the driver layers (such as L6 and L8) are relatively lower than other areas within the same layers.

Figure 9.4.44A plots the shut-in pressure at a hypothetical Council Grove well (CG SI) that was completed in the simulator in January 1978. The CG SI well was flowed for one day before shut-in and recorded a stabilized shut-in pressure of 200 psi after four days. This simulator-calculated shut-in pressure is within the range of shut-in pressures recorded at G wells in the study area upon their completion in and around 1978.

Figure 9.4.45 tabulates the simulator-calculated layer pressures as of December 2004 at the location of the Eliot A6 (IElli5) well and compares them with corresponding layer pressures recorded by RFT tests. The simulator-calculated layer pressure is close to that recorded by RFTs for L6 (Towanda) and L8 (Fort Riley) – the two driver zones in terms of storage and flow capacity in the study area. The approximate nature of these pressure matches has to be put in the context of the current geomodel which shows relatively low OGIP and tighter permeability distribution along the southern and southwestern borders of the study area, and therefore is inadequate for obtaining production/pressure history matches at P, G, and I wells located in these above-mentioned border areas. It is only after reasonable history matches have been obtained at all the wells in the study area that the exercise of matching simulator-calculated layer pressures at a specific location with RFT layer pressures can be carried out in order to validate the underlying geomodel. Also, operator feedback and presence of significant variations in pressures within a layer in and around the study area as evident from RFT data raises questions about how representative the RFT data are for comparison with simulator-calculated pressures.

RUN 11

The input permeability distribution for Chase and Council Grove layers is the same as Run 10. However, hydraulic fractures at the P wells were extended to L14 (B1 Shale) using ff = 6.0 while the G wells were completed to L8 (Fort Riley) using ff = 6.0. The production and pressure history matches for the P wells remained unchanged from Run 10. However, more prominent production spikes became visible when P wells were released of flow constraints. For the G wells, the simulator-calculated well production rates were similar to Run 10 with a slight reduction in production spikes at some of the wells when released from flow constraints. At the I wells, production spikes increased when wells released from flow constraints. The shut-in pressure at a hypothetical Council Grove well (located at the center of the study area) stabilized to 225 psi (Figure 9.4.46) upon completion after a 4 day shut-in followed by 1 day of flow. The simulator-

calculated layer pressures from this run, at the location of Eliot A6, were compared with the RFT layer pressures in Figure 9.4.47 and were found to be close to those obtained from Run 10.

Conclusions

a) The current geomodel for the Graskell study area has insufficient OGIP and permeability distribution along the southern and southwestern border areas to enable production history matches at Chase Parent, Chase Infill, and Council Grove wells located therein.

b) It is imperative that the underlying geomodel be modified to enable successful history matching (of production and pressure) at all wells within the study area.

c) For wells located in the study area and away from the southern or southwestern borders, the simulator-calculated production matches or is close to matching the historic volumes. The simulator-calculated (bottom-hole) flowing pressures are close to and follow the trends set by recorded (surface) flowing pressures particularly at wells where good production matches have been obtained.

d) Production spikes are visible at most wells when released of flow constraints despite production and pressure history matches indicating presence of excess flow capacity in the current model in the drainage areas of the corresponding wells.

e) Significant intra-layer variation in RFT pressures recorded in and around the study area has been observed leading to doubts about the accuracy and representativeness of RFT recordings.

f) Using the current geomodel, production and pressure history matches were obtained at majority of the wells outside the southern and southwestern border. Despite lack of history matches at border wells, the simulator-calculated layer pressure at the Eliot A6 well is close (within 30 psi) to that recorded by RFT measurements for the two major driver zones in the study area, i.e. L6 (Towanda) and L8 (Fort Riley).

It is hoped that further refinement of the geomodel, particularly along the southern and southwestern borders, will help to attain history matches at these border wells and thereby lead to better layer-pressure matches.

Reference:

Bhattacharya, S., Dubois, M. K., and Byrnes, A. P., 2005, Reservoir simulation of 9-section area around Flower A1 well – Chase/Council Grove reservoir systems, Kansas Geological Survey Open File Report 2005-54.

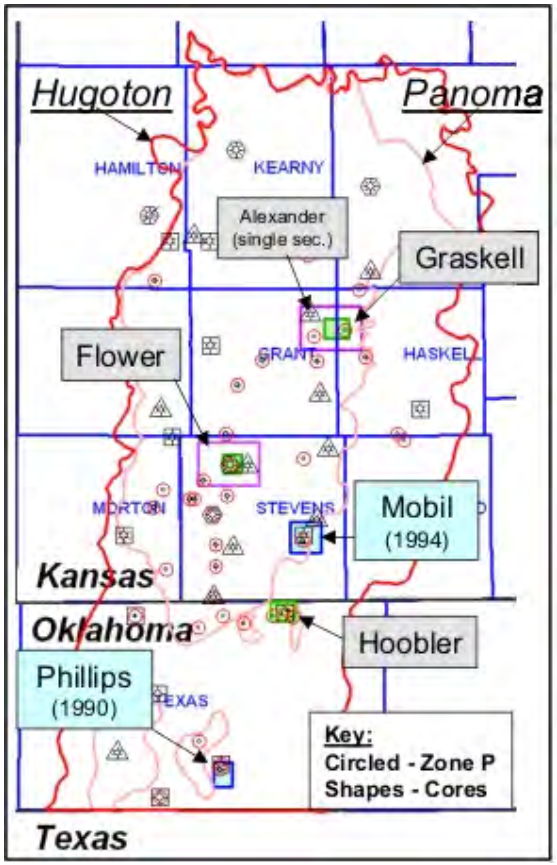

Figure 9.4.1. Map showing location of Graskell study area in the Hugoton and Panoma fields.

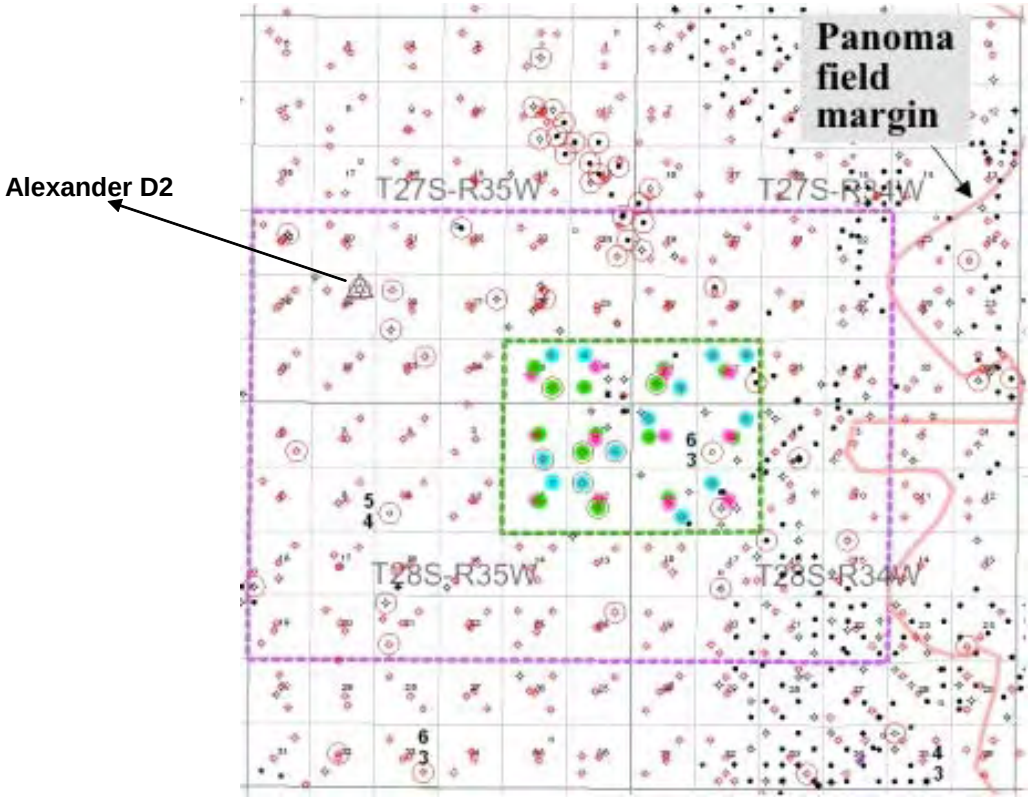

Figure 9.4.2. Map showing the 12-square-mile Graskell study area bordered by the green broken line and the location of the Alexander D2 well. The Graskell geomodel was built from a fine-scale geomodel covering 70-square-miles and is shown bordered by the pink broken line.

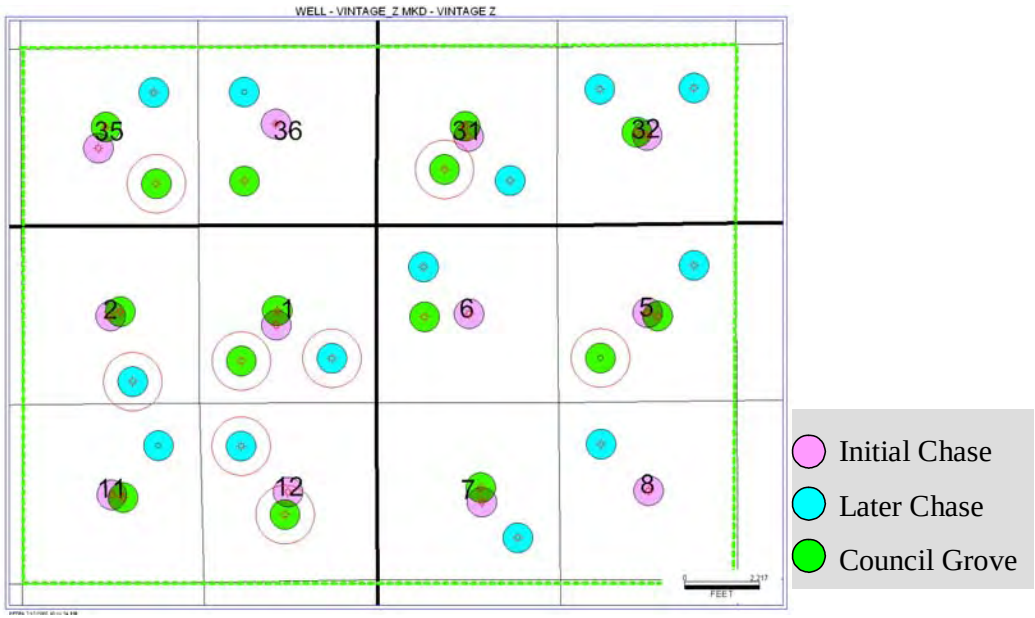

Circled wells have qualified logs.

Figure 9.4.3. Map showing the 12-square-mile Graskell study area along with the Chase Parent, Chase Infill, and Council Grove wells.

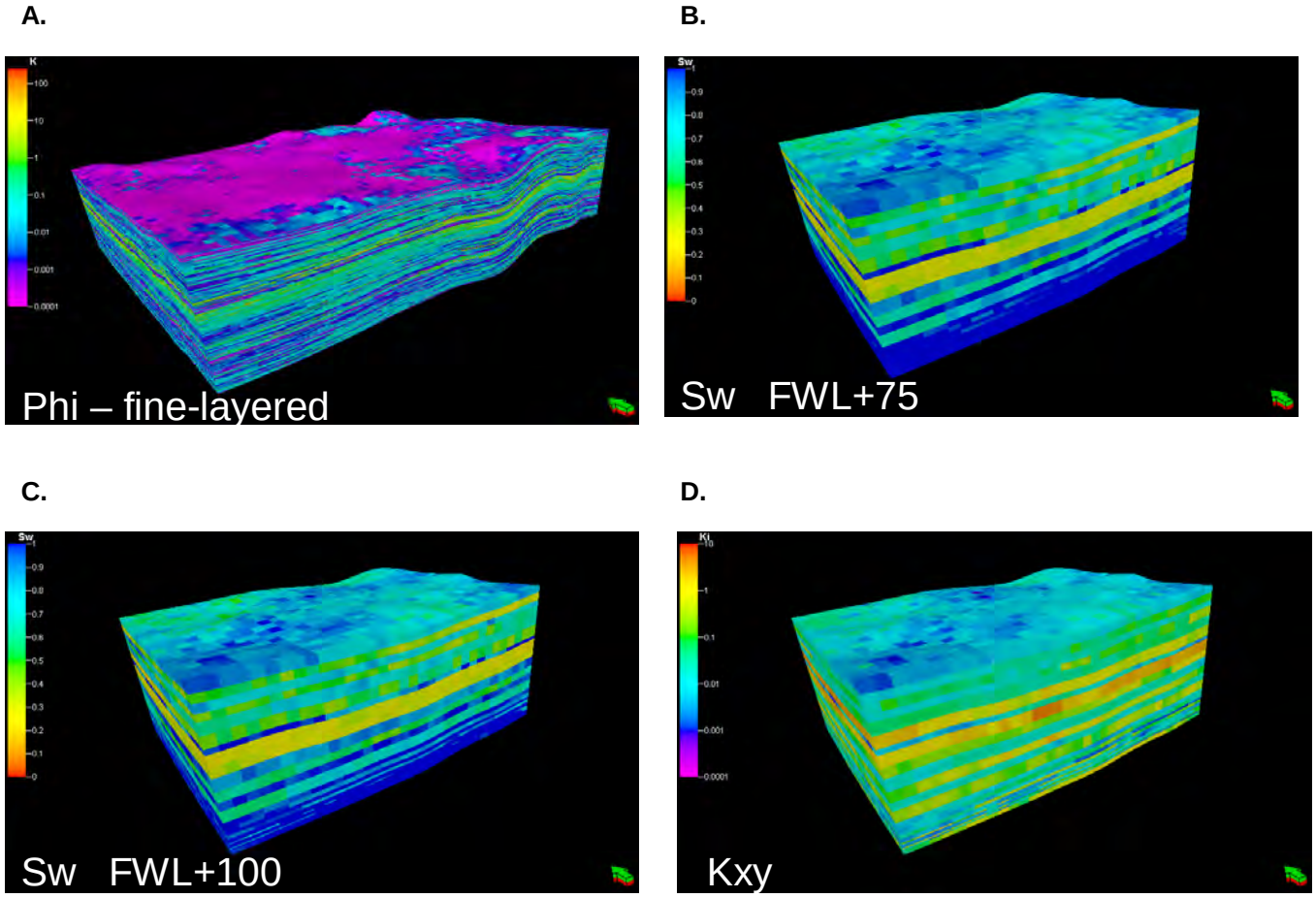

Figure 9.4.4. A) Fine-scale porosity model of the 120 square-mile area around the Graskell study area. B and C) Upscaled Sw model for the Graskell area using different free-water levels (FWLs). D) Upscaled permeability model for Graskell area.

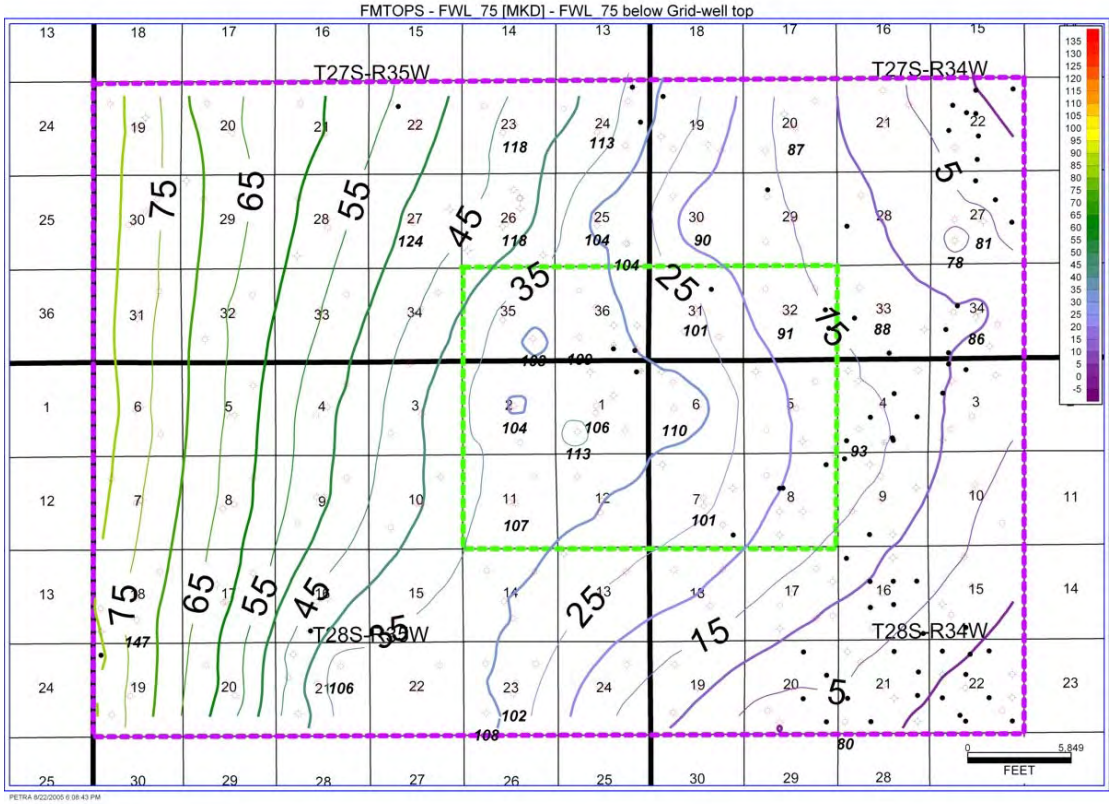

Figure 9.4.5. Structure on the free-water-level (FWL) surface, datum is sea level. Elevation of lowest perforation in Council Grove is posted by well spots where available. Elevation of FWL surface = (Elevation of lowest Council Grove perforations – 75 ft).

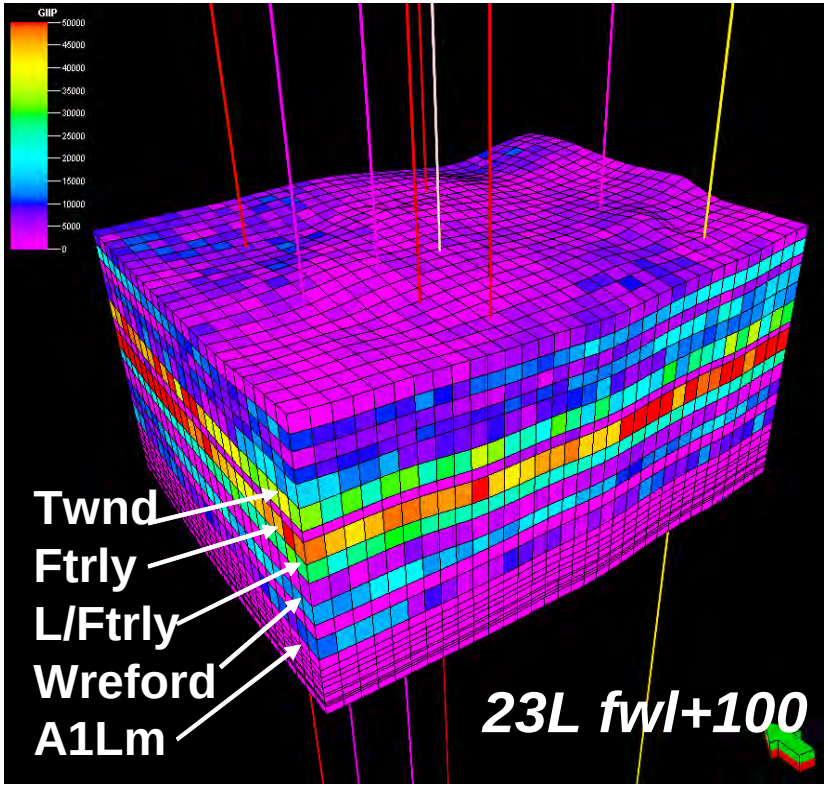

Figure 9.4.6. Original-gas-in-place (OGIP) charging the Graskell model that served as the basis for reservoir simulation studies.

Assumed PVT properties:		
Reference pressure	465	psi
Rock compressibility	0.000002	1/psi (assumed)
Reservoir temp	90	F
Gas gravity (Air = 1.0)	0.715	
Water salinity	110,000	ppm

Figure 9.4.7. PVT properties used in simulation studies on Graskell study area.

Permeability Multiplier Applied to Layers

	Sample #	Log Phi	K md (trans)	Core Phi	Core K, md	Multi	Layer	Multiplier Used
HRNGTN							1	3.0
KRIDER							2	3.0
ODELL							3	1
WINF							4	3.0
GAGE							5	1
TWND							6	3.0
B/TWND							7	1
FTRLY							8	3.0
LFTRLY							9	3.0
B/FTRLY							10	1
WREFORD	7	0.10	0.11	0.09	0.15	1.38	11	1.4
A1_SH	3						12	1
A1_LM	23	0.11	0.18	0.08	0.71	3.93	13	3.9
B1_SH	2						14	1
B1_LM	10	0.07	0.04	0.06	0.17	4.29	15	4.3
B2_SH	0						16	1
B2_LM	8	0.09	0.14	0.08	0.40	2.87	17	2.9
B3_SH	1						18	1
B3_LM	0						19	3.0
B4_SH	4						20	1
B4_LM	3						21	3.0
B5_SH	0						22	1
B5_LM	13	0.12	3.20	0.10	4.65	1.45	23	1.5

Layers in Red – Chase, Layers in Blue - CG

Figure 9.4.8. Layer-specific permeability multipliers used to convert permeability estimated from facies-specific permeability-porosity correlations to that obtained from cores. A multiplier of 1.0 was used for shale layers.

Well	IP Date	Initial SIP, psi
1 Biggs	Dec-47	411
1 Cromer	Feb-47	412
1 DaVatz	Sep-51	400
1 Elliot	Oct-47	411
1 Fee	Dec-47	409
1 Goering	Dec-48	418
1 Higgenbotham	Nov-47	417
1 McMorran	Nov-47	413
1 Stanley	Dec-46	432
1 Stanley	Oct-47	411
1 Taton	Sep-51	411
C-1 Eubank	Dec-45	406

Avg SI pr, psi
413
Median pr, psi
411

Figure 9.4.9. Date of initial production (IP) and the first recorded surface shut-in pressures at the Chase Parent wells.

Simulator OGIP and Production

Layer OGIP in Simulator Model

OGIP (bcf) in Sim at 440 psi = 170.61

Layer	bcf
1	3.6
2	12.1
3	3.6
4	9.2
5	9.3
6	29.9
7	2.9
8	43.9
9	17.8
10	2.6
11	17.6
12	1.5
13	12.9
14	0.2
15	1.3
16	0.03
17	0.9
18	0.07
19	0.4
20	0.5
21	0.07
22	0.04
23	0.2

Initial reservoir pressure = 440 psi
Simulator calculated OGIP = 170.7 bcf

Cumulative Production from Chase Parent, CG, and Chase Infill wells vs. Simulator-calculated total production

Production as of May 2004

	bcf
Chase Parent	89.82
Chase Infill	8.38
Council G	10.91
Total Prod	109.11
Sim Prod	104.7

L6 and L8 are the driver zones in this study area

Figure 9.4.10. Layer-specific gas-in-place charged in the input geomodel when initial reservoir pressure is assumed to be 440 psi.

Chase Parent and Council Grove (CG) Wells in Study Area

Production, Perforation Intervals, and Cumulative Production

Chase Parent wells

	Well	Sim name	Prod Start	Perf Top	Perf Base	Cum Gas, mcf
1	Taton1	PTat1	1/1/1951	1	6	8,958,461
2	Stanley1	PStan1	1/1/1947	1	8	7,997,756
3	Stanley1 Oxy	PStanO	1/1/1948	1	8	7,049,501
4	McMoran1	PMor1	1/1/1948	1	8	10,786,642
5	Higginbotham 1	PHigB1	1/1/1948	1	8	10,188,790
6	Goering1	PGoer1	1/1/1949	1	7	8,117,999
7	Fee1	PFee1	1/1/1948	1	8	5,686,279
8	Eubanks1	PEub1	1/1/1946	1	6	7,744,731
9	Elliot1	PEliot	1/1/1948	1	6	4,696,387
10	DaVatz1	PDav	1/1/1951	1	6	5,722,071
11	Cromer1	PCrom	1/1/1947	1	8	5,924,928
12	BiggsA1	PBigs	1/1/1948	1	8	6,946,830

89,820,375

CG wells

	Well	Sim Name	Prod Start	Perf Top	Perf Base	Cum Gas, mcf
1	2 TATON GAS UNIT	GTat2	10/1/1980	8	13	1,144,835
2	3 C STANLEY	GStan3C	9/1/1985	8	14	863,418
3	2 STANLEY C	GStan2C	5/1/1978	8	14	288,828
4	2 STANLEY A	GStan2A	7/1/1978	8	14	889,403
5	2 MC MORRAN A	GMor2A	6/1/1978	8	14	986,529
6	2 HIGGENBOTHAM A	GHigB2A	5/1/1978	8	13	908,559
7	4 EUBANK C	GEub4C	10/1/1978	8	14	1,357,899
8	4 ELLIOTT	GElot4	10/1/1978	8	15	573,261
9	2 DAVATZ GAS UNIT	GDav2	8/1/1986	8	13	667,730
10	3 A CROMER	GCrom3A	4/1/1985	8	14	1,034,950
11	2 CROMER A	GCrom2A	5/1/1978	8	14	214,258
12	2 BIGGS A TWIN	GBigs2A	8/1/1978	8	14	176,747
13	BIGGS A 4	GBigs4A	6/1/1991	8	13	573,312
14	2 APPLEMAN-JACKSON-F	GApplJ2	3/1/1980	8	13	1,228,034

10,907,763

Figure 9.4.11. Production-start date, completion intervals, and cumulative production from Chase Parent and Council Grove wells in the Graskell study area.

Chase Infill Wells in Study Area

Production, Perforation Intervals, and Cumulative Production

Chase Infill wells

	Well	Sim Name	Prod Start	Perf Top	Perf Base	Cum Gas
1	3-HI TATON GU	ITatn3	10/1/1993	1	10	774,838
2	Stanlee 4	IStan4	9/1/1990	1	10	970,395
3	3 STANLEY A	IStan3A	12/1/1992	1	8	644,102
4	3 MCMORRAN A	IMor3A	9/1/1988	1	8	733,055
5	A-3 HIGGENBOTHAM	IHig3A	5/1/1994	1	11	632,961
6	Goering 2	IGor2	4/1/1995	1	8	687,707
7	Fee 1-2	IFee	5/1/1994	1	8	421,043
8	Eubank 5	IEub5	11/1/1993	1	10	540,658
9	Elliot 5A	IElli5	11/1/1990	1	10	685,113
10	3 HI DAVATZ G.U.	IDav3	12/1/1988	1	8	672,062
11	Crommer 4A	ICrom4A	9/1/1990	1	11	870,452
12	BiggsA3	IBig3A	9/1/1990	1	11	747,619
						8,380,005

Figure 9.4.12. Production-start date, completion intervals, and cumulative production from Chase Parent and Council Grove wells in the Graskell study area.

RUN 1: P, I, G - fractures constrained to perforated intervals

Initial K multipliers applied to gas zones, ff= 6, Pi = 440 psi

Match Chase Parent wells

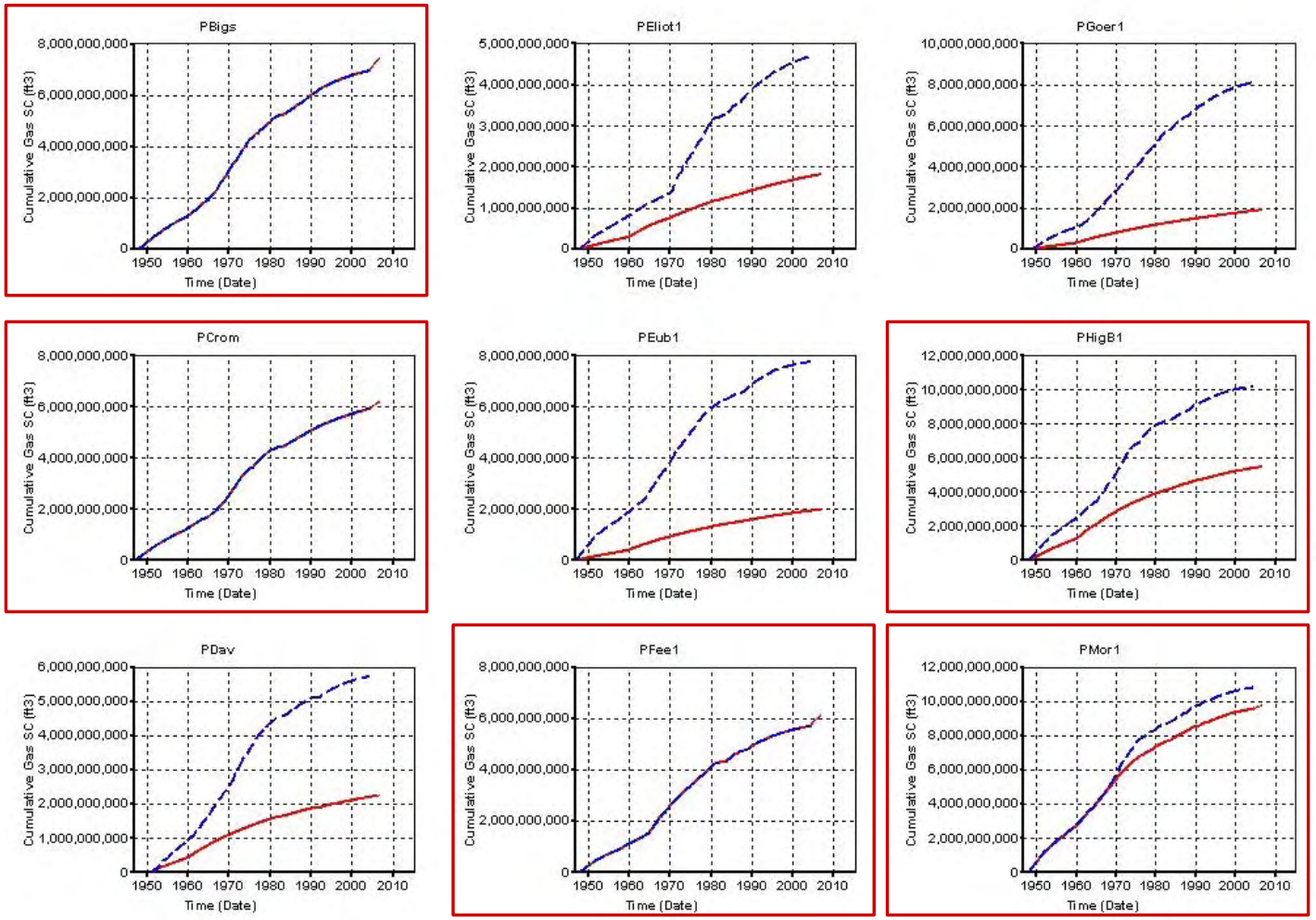

Broken blue – Historic gas prod **Red – Simulator-calculated gas prod**

Figure 9.4.13. RUN 1 Results – Simulator-calculated cumulative gas production compared with historic production for Chase Parent wells.

RUN 1: P, I, G - fractures constrained to perforated intervals

Initial K multipliers applied to gas zones, ff= 6, Pi = 440 psi

Match Chase Parent wells (Continued)

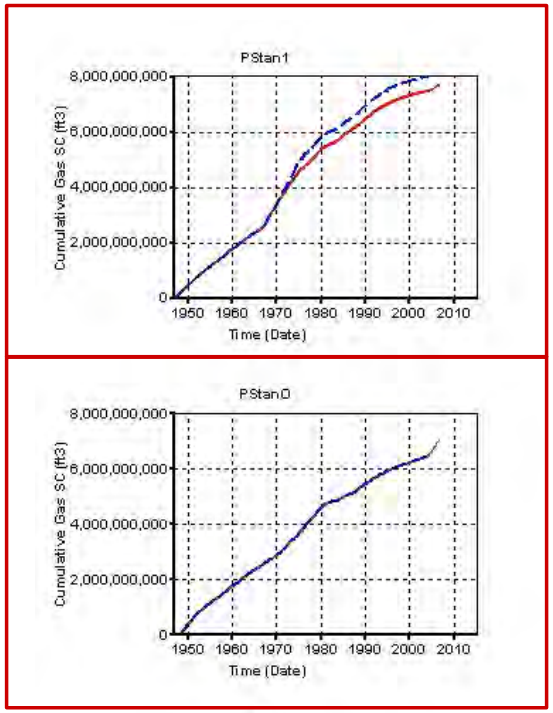

Gas production matched or come close to matching in Chase Parent wells where perforations (and hence the fractures) extend to Layer 8 (L8)

Well Completed in L8

Broken blue – Historic gas prod

Red – Simulator calculated gas prod

Figure 9.4.14. RUN 1 Results – Simulator-calculated cumulative gas production compared with historic production for Chase Parent wells.

RUN 1: P, I, G - fractures constrained to perforated intervals

Initial K multipliers applied to gas zones, ff= 6, Pi = 440 psi

Match Council Grove wells

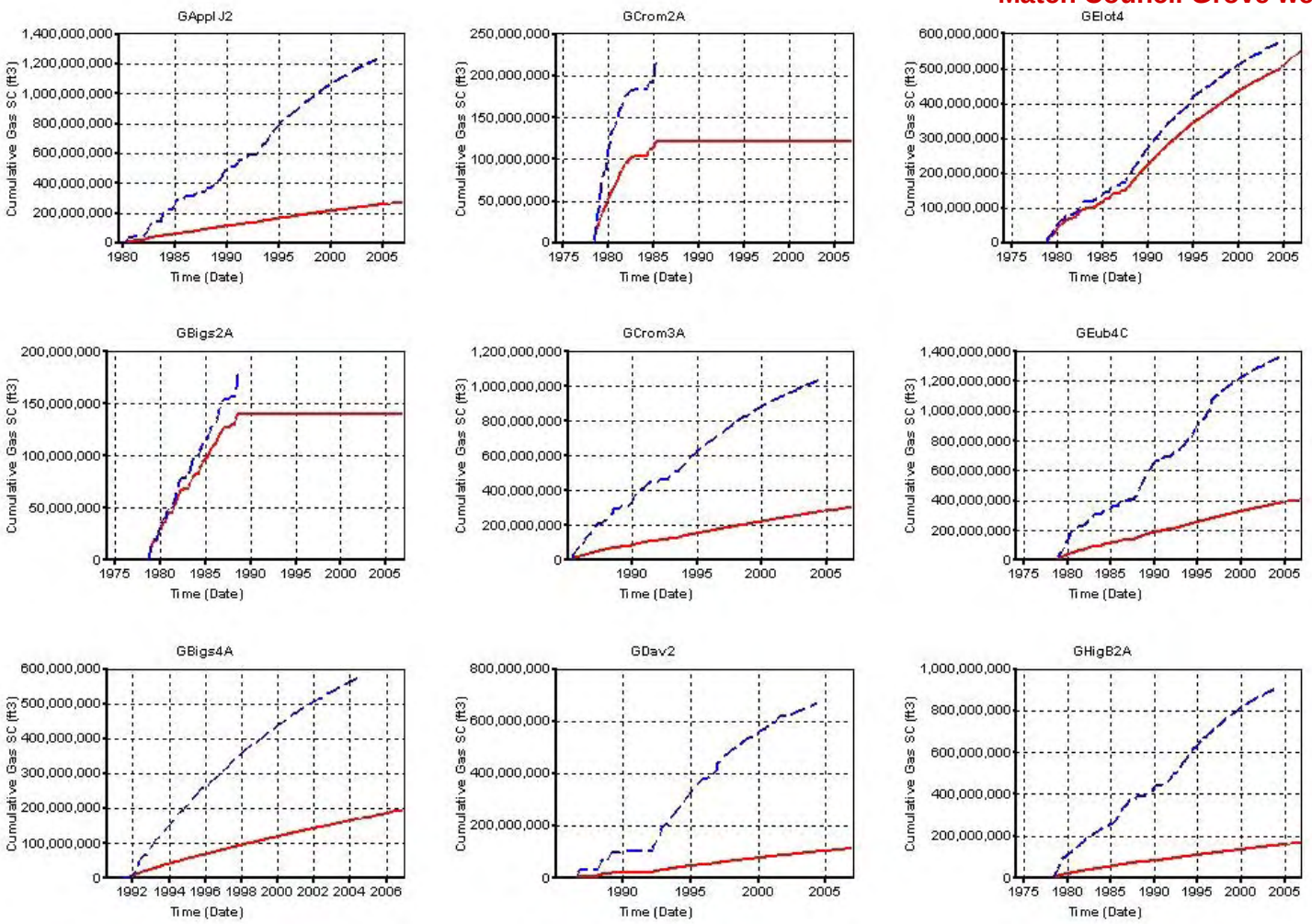

Broken blue – Historic gas prod **Red – Simulator-calculated gas prod**

Figure 9.4.15. RUN 1 Results – Simulator-calculated cumulative gas production compared with historic production for Council Grove wells.

RUN 1: P, I, G - fractures constrained to perforated intervals

Initial K multipliers applied to gas zones, ff= 6, Pi = 440 psi

Match Council Grove wells

(Continued)

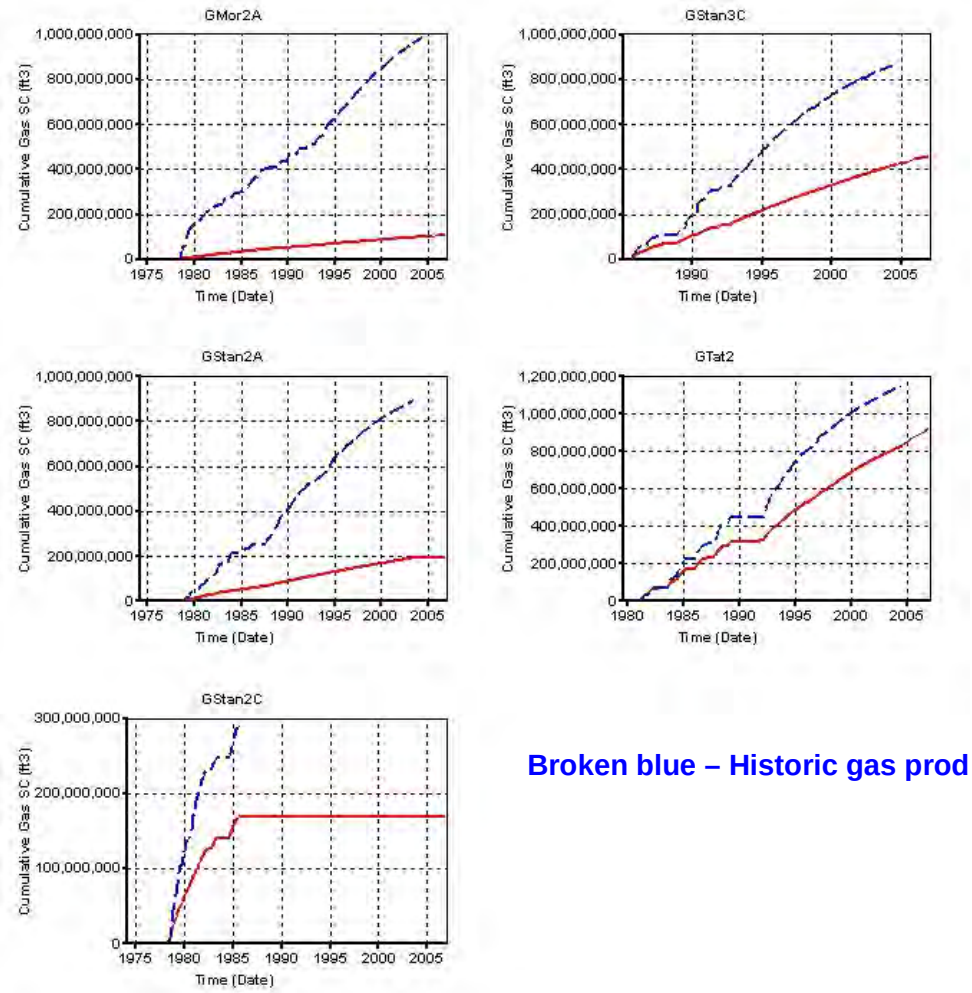

Simulator-calculated gas production fell significantly short of historic production in every Council Grove well.

Broken blue – Historic gas prod **Red – Simulator-calculated gas prod**

Figure 9.4.16. RUN 1 Results – Simulator-calculated cumulative gas production compared with historic production for Council Grove wells.

RUN 2: P, I, G - fractures constrained to perforated intervals

Initial K multipliers applied to gas zones, ff = 10, Pi = 440 psi

Match Chase Parent wells

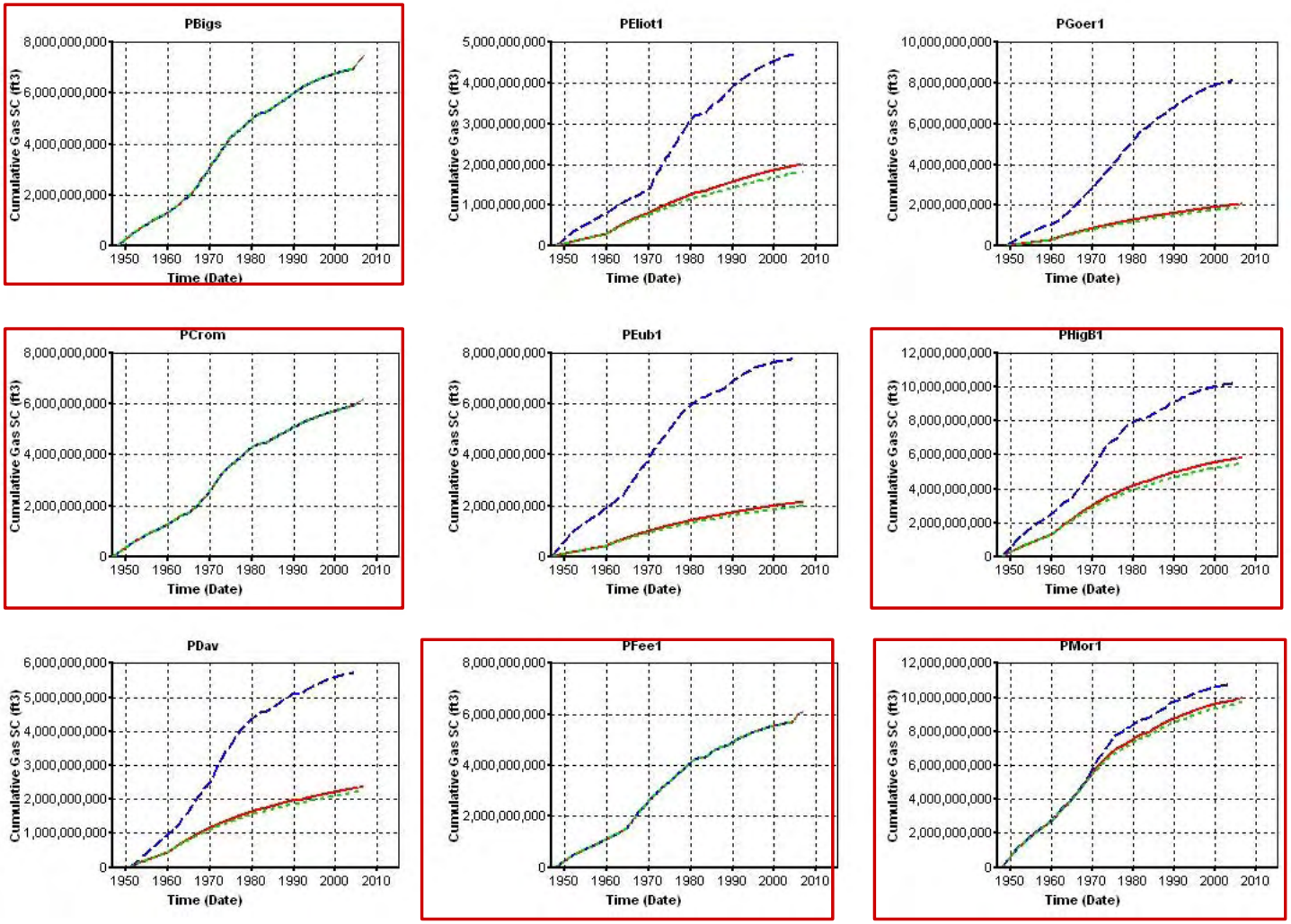

Broken blue – Historic gas prod, Red – Simulator-calculated gas prod, Green – Results from Run 1

Figure 9.4.17. RUN 2 Results – Simulator-calculated cumulative gas production compared with historic production for Chase Parent wells.

RUN 2: P, I, G - fractures constrained to perforated intervals

Initial K multipliers applied to gas zones, ff= 10, Pi = 440 psi

Match Chase Parent wells (Continued)

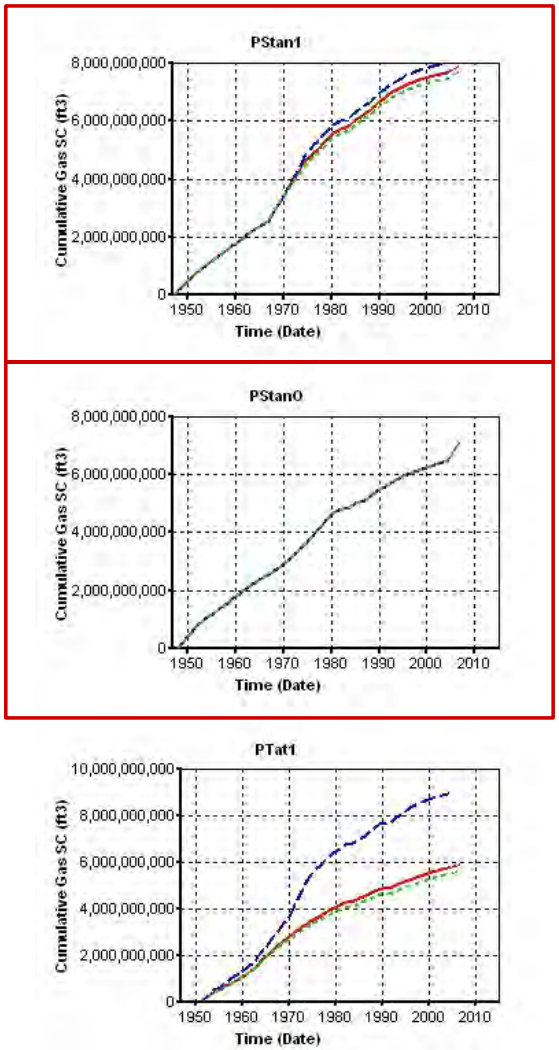

Gas production increased only slightly as compared to Run 1. Simulator-calculated cumulative production rates in Chase parent wells not completed in L8 are significantly short of historic volumes.

Broken blue – Historic gas production

Red – Simulator-calculated gas production

Green – Results from Run 1

Completed in L8

Figure 9.4.18. RUN 2 Results **–** Simulator-calculated cumulative gas production compared with historic production for Chase Parent wells.

RUN 3: P&I - fractures extended to L8

Initial K multipliers applied to gas zones, ff= 6, Pi = 440 psi

Match Chase Parent wells

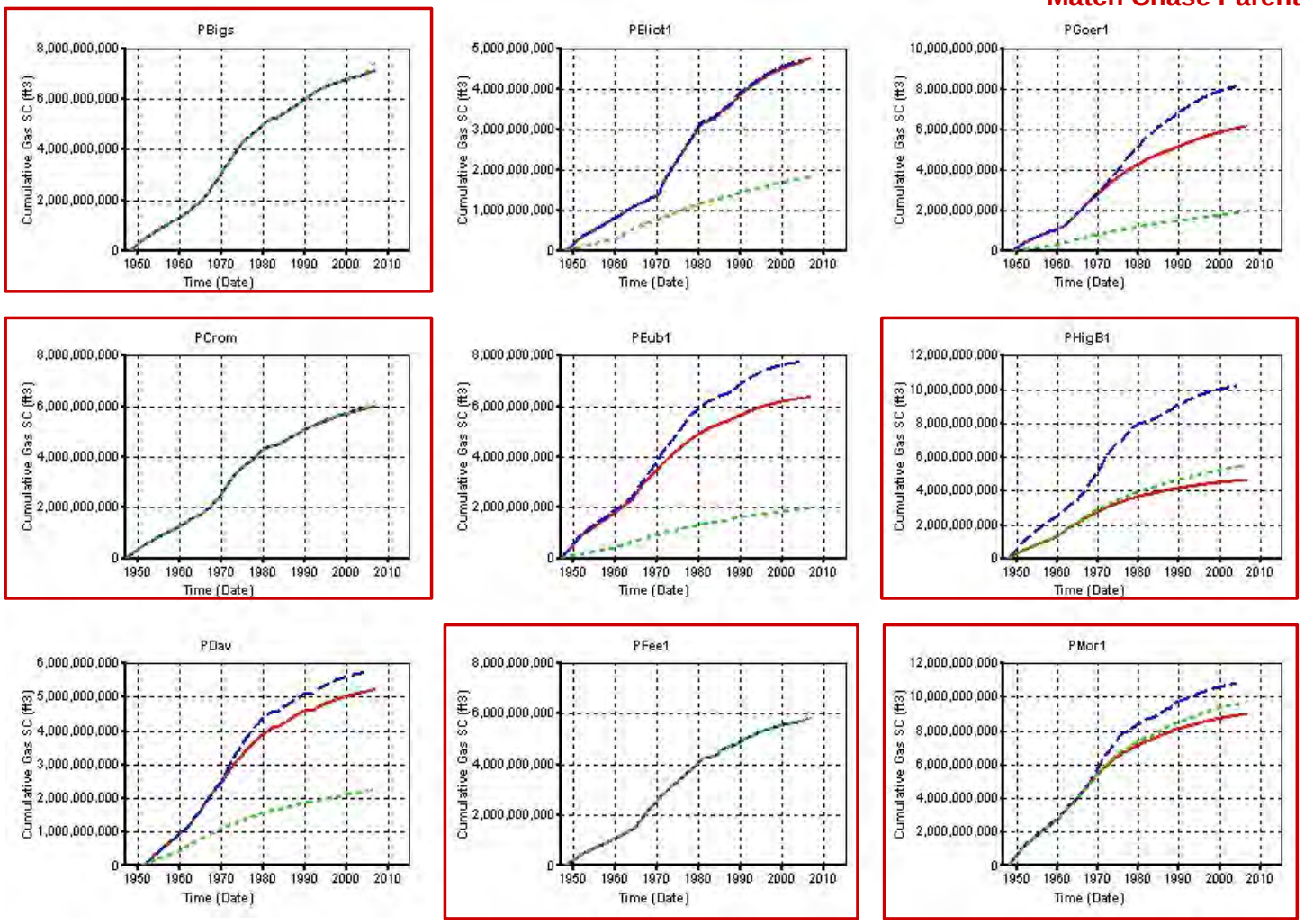

Broken blue – Historic gas prod, **Red – Simulator-calculated gas prod**, **Green – Results from Run 1**

Figure 9.4.19. RUN 3 Results – Simulator-calculated cumulative gas production compared with historic production for Chase Parent wells.

RUN 3: P&I - fractures extended to L8

Initial K multipliers applied to gas zones, ff = 6, Pi = 440 psi

Match Chase Parent wells

(Continued)

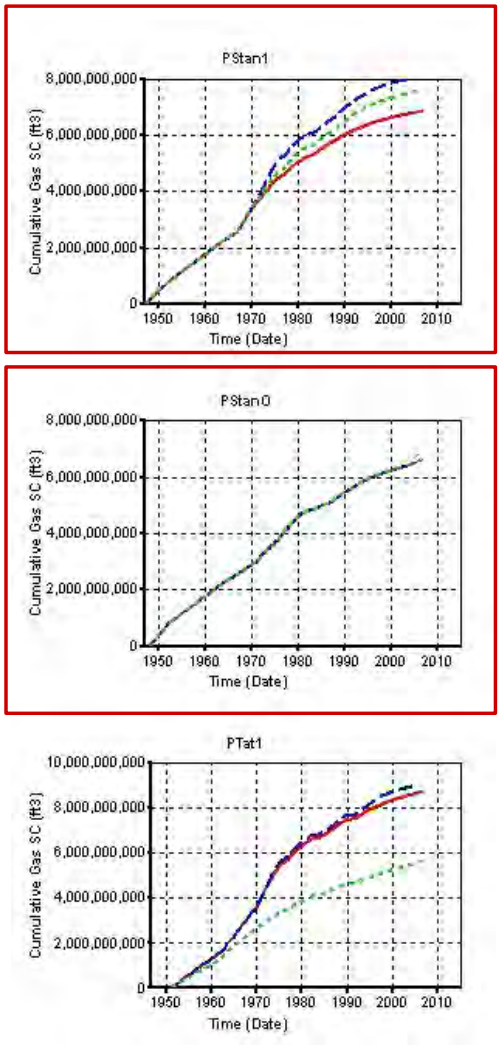

Gas production improved in wells that had not been perforated in L8. However, cumulative production is still short in some of these wells.

Completed in L8

Broken blue – Historic gas production

Red – Simulator-calculated gas production

Green – Results from Run 1

Figure 9.4.20. RUN 3 Results – Simulator-calculated cumulative gas production compared with historic production for Chase Parent wells.

RUN 4: P&I - fractures extended to L8. K*2 in driver Chase zones are L6 and L8 (OGIP and K)

K multiplier applied over and above initial multiplier of 3, ff = 6, Pi = 440 psi

Match Chase Parent wells

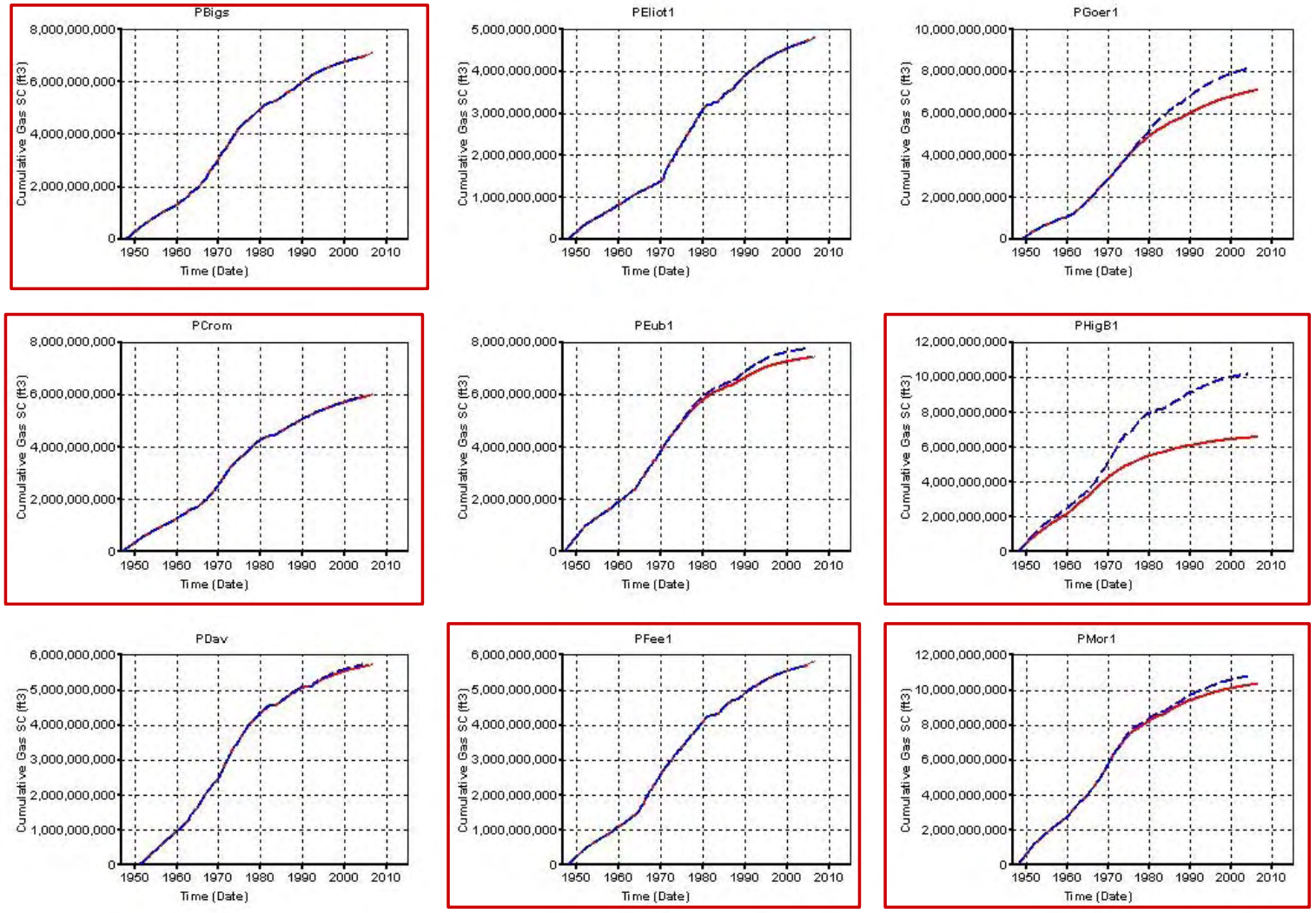

Broken blue – Historic gas prod **Red – Simulator-calculated gas prod**

Figure 9.4.21. RUN 4 Results – Simulator-calculated cumulative gas production compared with historic production for Chase Parent wells.

RUN 4: P&I - fractures extended to L8. K*2 in driver Chase zones are L6 and L8 (OGIP and K)

K multiplier applied over and above initial multiplier of 3, ff = 6, Pi = 440 psi

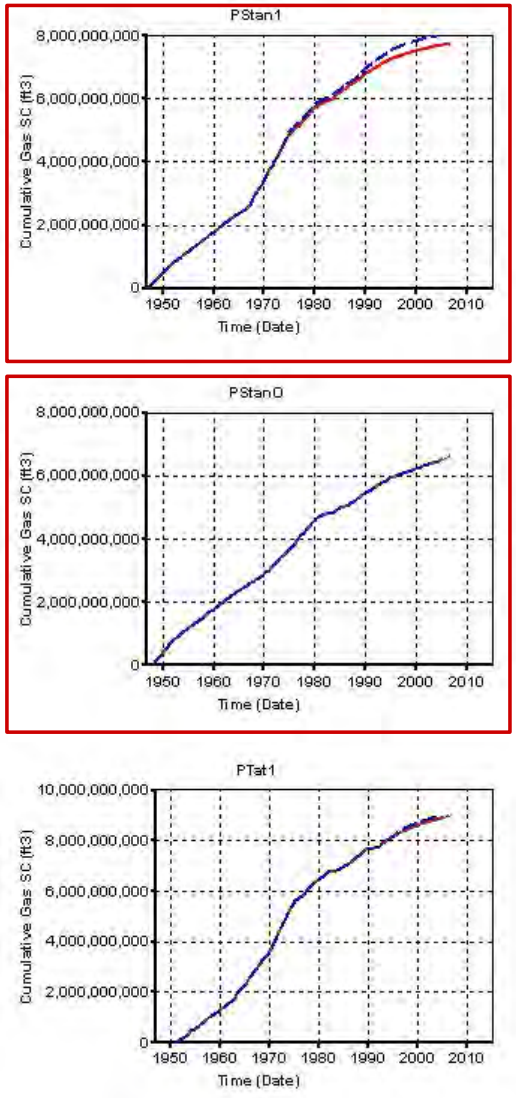

Match Chase Parent wells

(Continued)

Gas production matched or almost matched in all wells except those located in the SW corner of the simulation area.

Example: PHiggenbotham – located in the SW corner. This well is the second-highest gas producer in the study area and has produced 10 bcf. However, the OGIP and K mapped in the drainage area of this well is low in the geomodel input to the simulator.

Within the study area no wells with qualified logs are located in the southwestern corner. Wells with qualified logs are located outside the study and at a considerable distance from the SW corner of the study area, resulting perhaps in non-representative OGIP and permeability distribution in this section of the study area.

Well completed in L8

Broken blue – Historic gas prod

Red – Simulator-calculated gas prod

Figure 9.4.22. RUN 4 Results **–** Simulator-calculated cumulative gas production compared with historic production for Chase Parent wells.

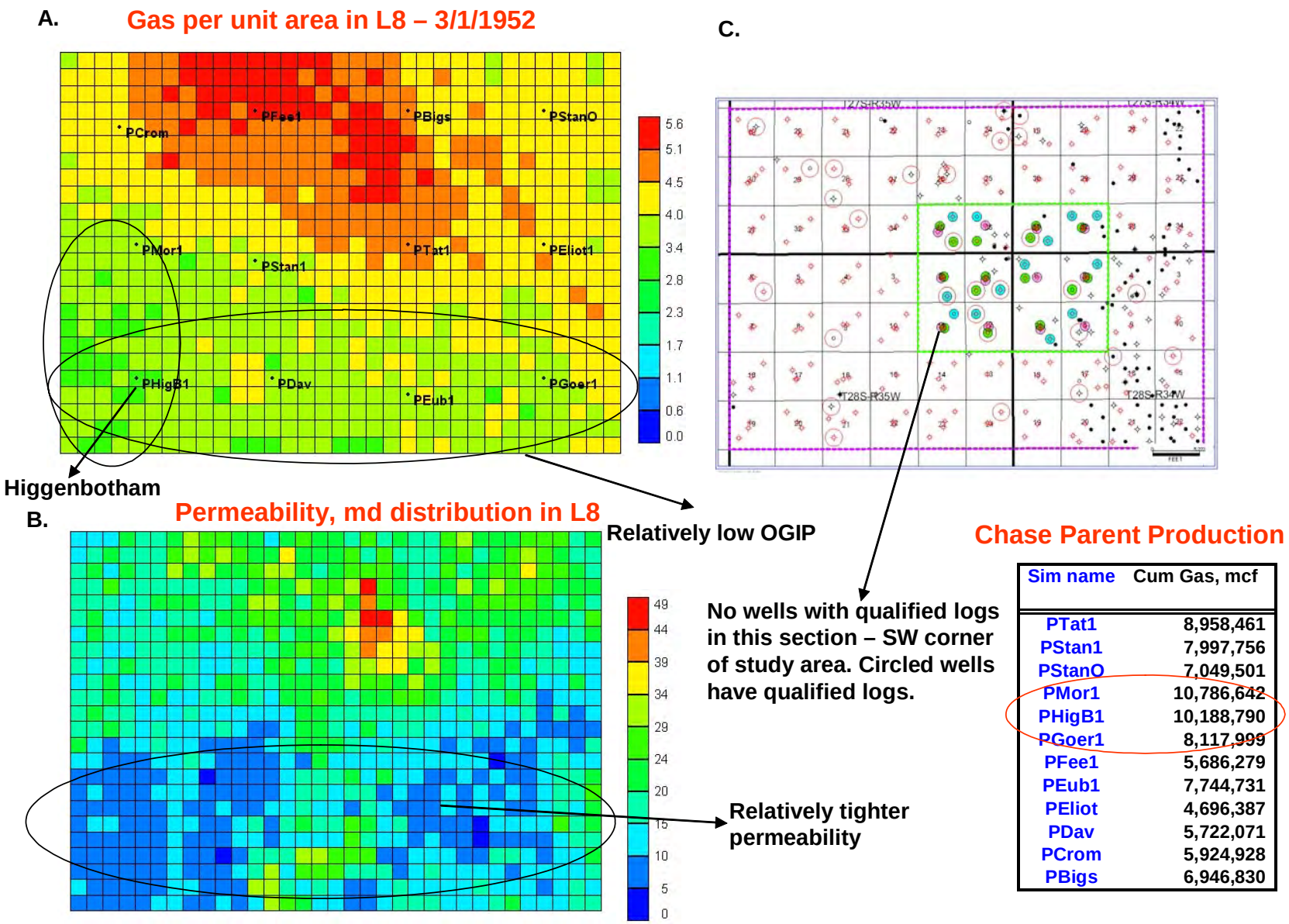

Figure 9.4.23. A) Original-gas-in-place distribution in Layer 8. B) Permeability distribution in Layer 8. C) Map showing absence of wells with qualified logs in the southwestern corner of the study area.

RUN 5: P&I - fractures extended to L8. K*2 in driver (in terms of OGIP and K) Chase zones, i.e., L6 and L8 Permeability adjusted in Chase zones (Kxy*6 in L1) to better match RFT layer pressures. Also, ff = 6, Pi = 440 psi

Match Chase Parent wells

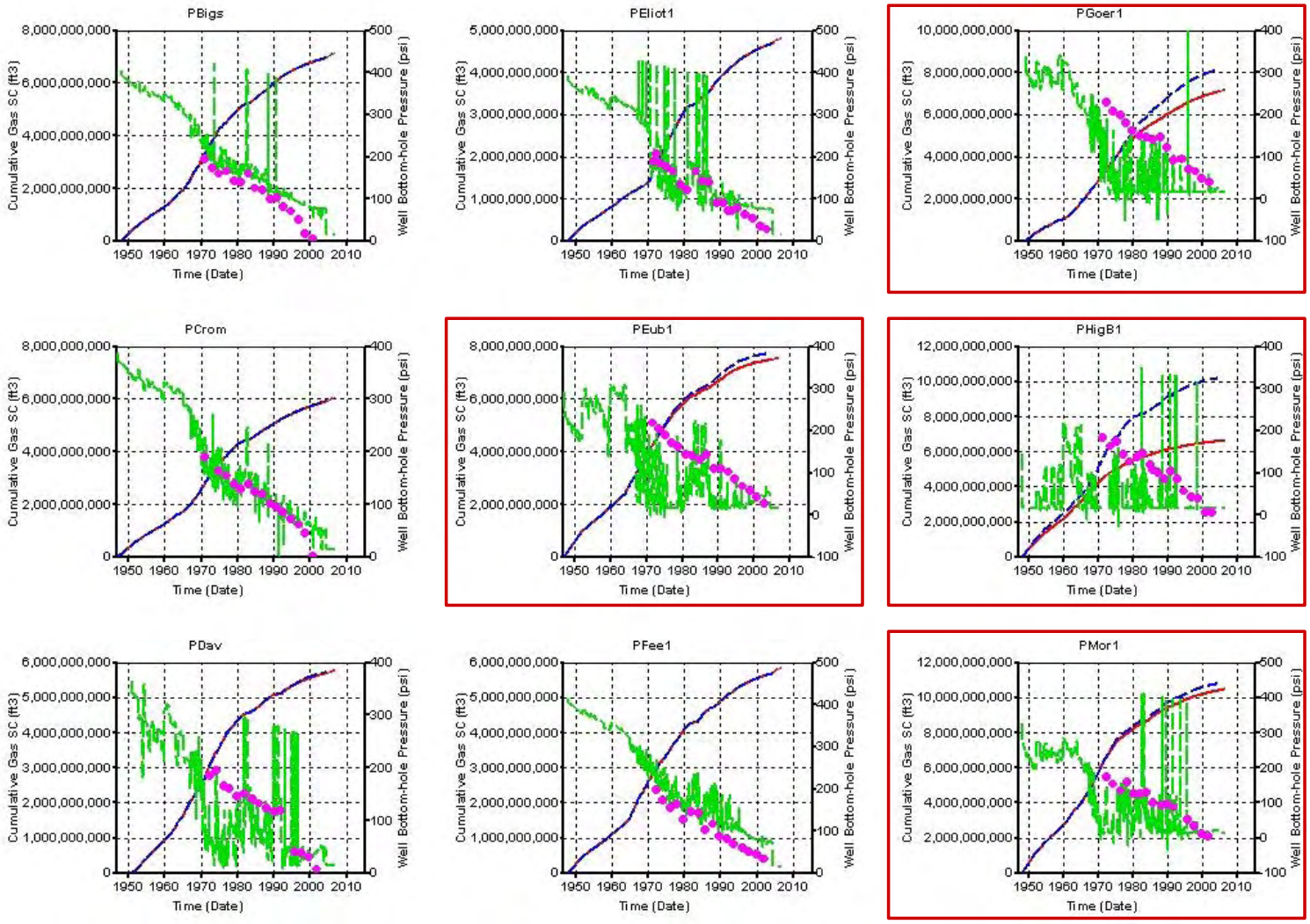

Broken blue – Historic gas prod **Red – Simulator-calculated gas prod** **Green – Sim BHFP** **Magenta – Historic FTHP**

Figure 9.4.24. RUN 5 Results - Simulator-calculated cumulative gas production and flowing pressures compared to historic values at Chase Parent wells.

RUN 5: P&I - fractures extended to L8. K*2 in driver (in terms of OGIP and K) Chase zones, i.e., L6 and L8 Permeability adjusted in Chase zones (Kxy*6 in L1) to better match RFT layer pressures. Also, ff = 6, Pi = 440 psi

Match Chase Parent wells

(Continued)

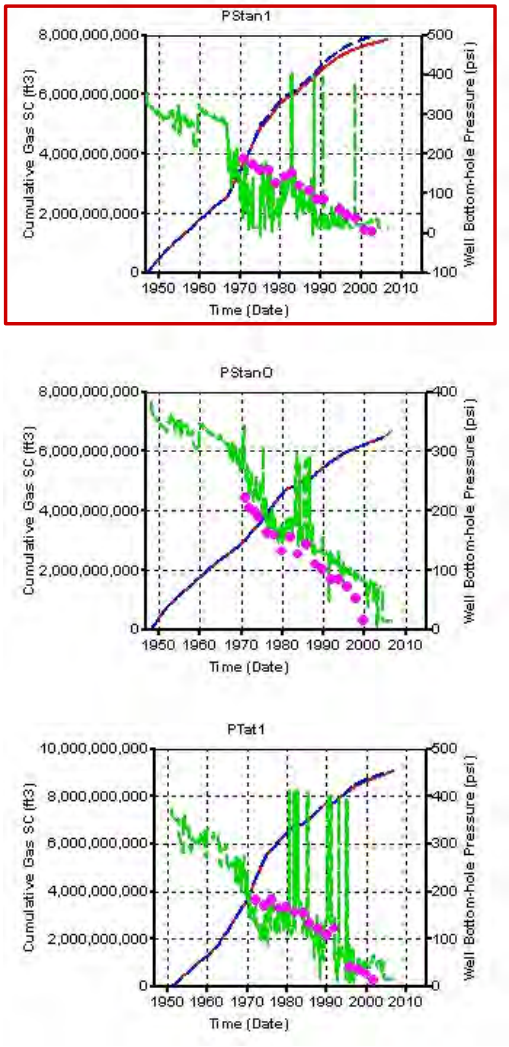

Gas production matched at all wells except those in the tight border areas.

Wells with good production matches also show close match between FTHP (historic flowing surface pressure) and FBHP (simulator-calculated bottom-hole flowing pressures).

Broken blue – Historic gas production

Red – Simulator-calculated gas production

Green – Sim BHFP

Magenta – Historic FTHP

Figure 9.4.25. RUN 5 Results - Simulator-calculated cumulative gas production and flowing pressures compared to historic values at Chase Parent wells.

Graskell Layer RFT Data

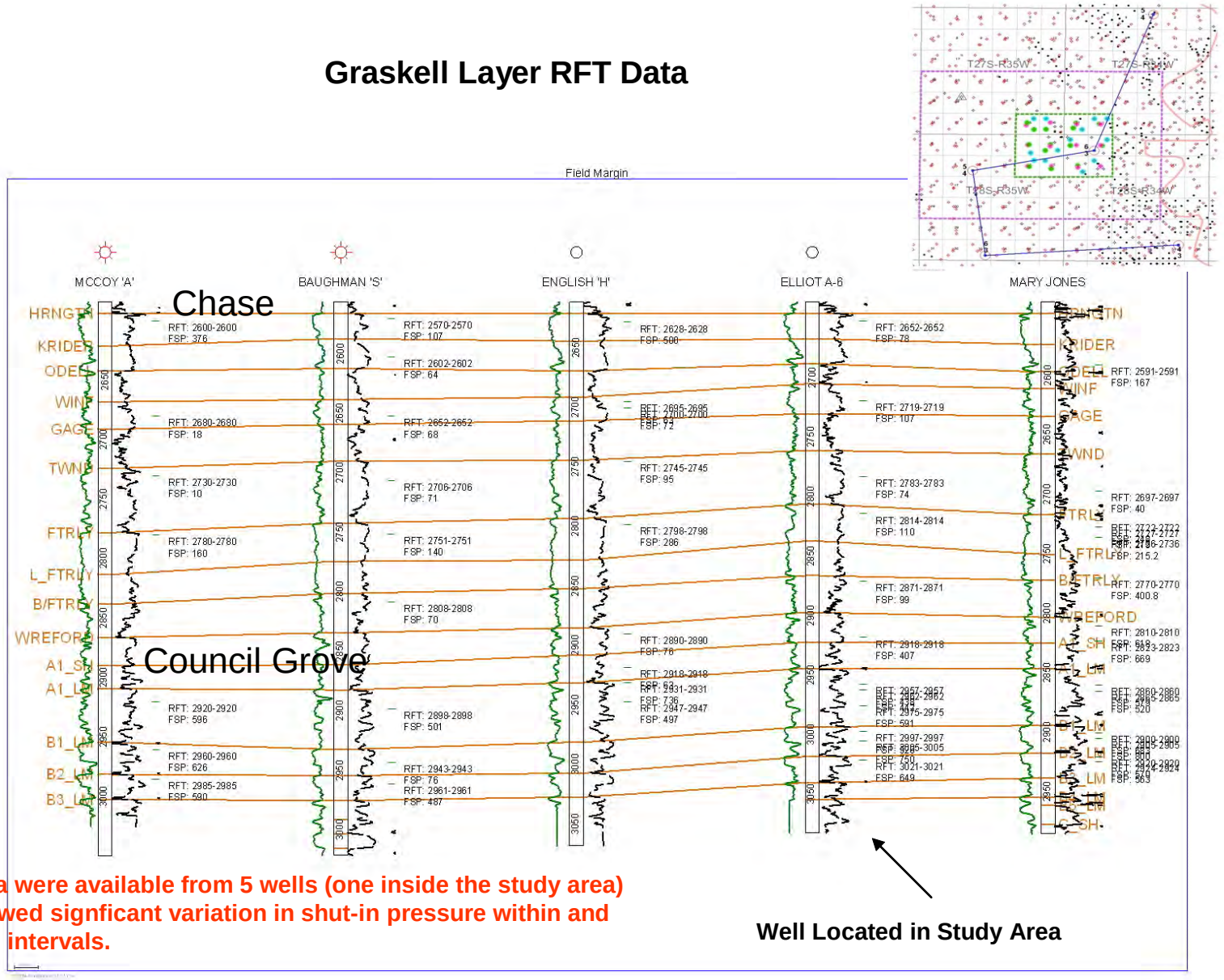

Figure 9.4.26. Cross section and map showing location of wells with RFT data in and around the Graskell study area.

Simulator-calculated Pressure (Run 5) vs. Chase RFT Data

Location Eliot A6 well - Dec 2004

Formation	Layer	Simulator, psi	RFT, psi	Best Guess, psi	*COMMENTS*
HRNGTN	1	420	78	**78**	**may be low**; 107, 379, 500 in other wells
KRIDER	2	384	na	**300**	not tested; low k in area; 64, 167 in other wells
ODELL	3	383	na	400	Silt-shale; should be high
WINF	4	251	107	107	may be high; 18,68,72 in other wells
GAGE	5	181	na	400	Silt-shale; should be high
TWND	6	127	74	74	okay; 10, 40, 71, 95, in other wells
B/TWND	7	117	na	400	Silt-shale; should be high
FTRLY	8	89	110	110-200	may be low; 140, 160, 215, 286 in other wells
L/FTRLY	9	90	na	200-300	
FLRNC	10	300	99	99	70 in one other well, **mostly shale**
WREFORD	11	303	407	200	too high; 76 in one other well
A1_SH	12	362	na	400	Silt-shale; should be high

Appearance of discrepancy in the RFT layer-pressure data

Figure 9.4.27. Simulator-calculated layer pressure (as of December 2004) at the location of Eliot A6 well with corresponding RFT pressure data recorded at this well.

RUNS 6 and 7: Initial Kxy in Chase (as Run 3). Fractures constrained to perfs in CG. Pi = 440 psi

Run 6 – K*10 (over initial multiplier) in CG pay and ff = 6

Run 7 – Original K multiplier in CG pay & ff = 10

Match CG wells

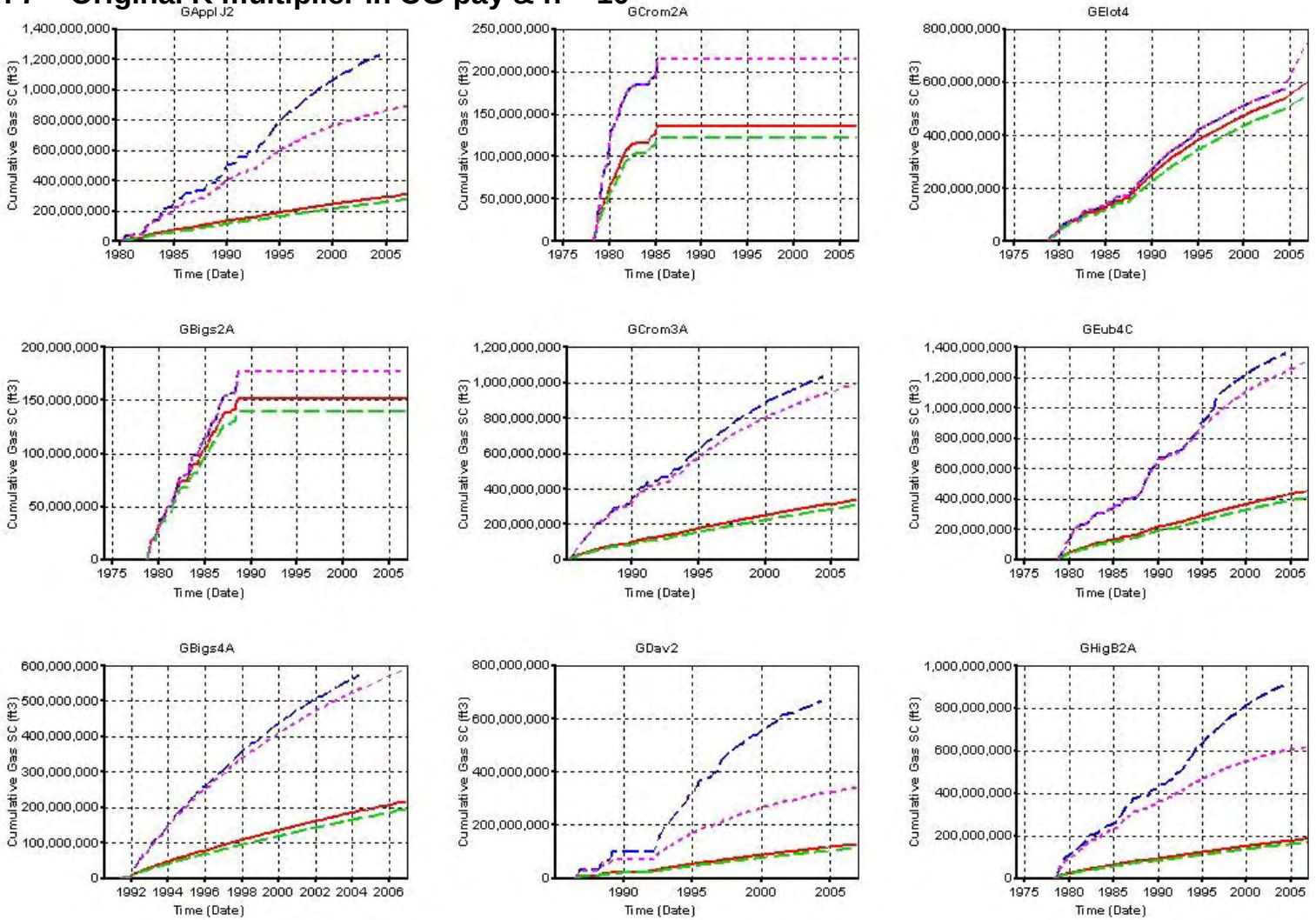

Broken blue – Historic gas prod **Red – Run 7** **Green – Run 1 results** **Magenta – Run 6 results**

Figure 9.4.28. RUN 6 and 7 Results – Simulator-calculated cumulative production at Council Grove wells compared with historic values.

RUNS 6 and 7: Initial Kxy in Chase (as Run 3). Fractures constrained to perfs in CG. Pi = 440 psi

Run 6 – K*10 (over initial multiplier) in CG pay and ff = 6

Run 7 – Original K multiplier in CG pay and ff = 10

Match CG wells

(Continued)

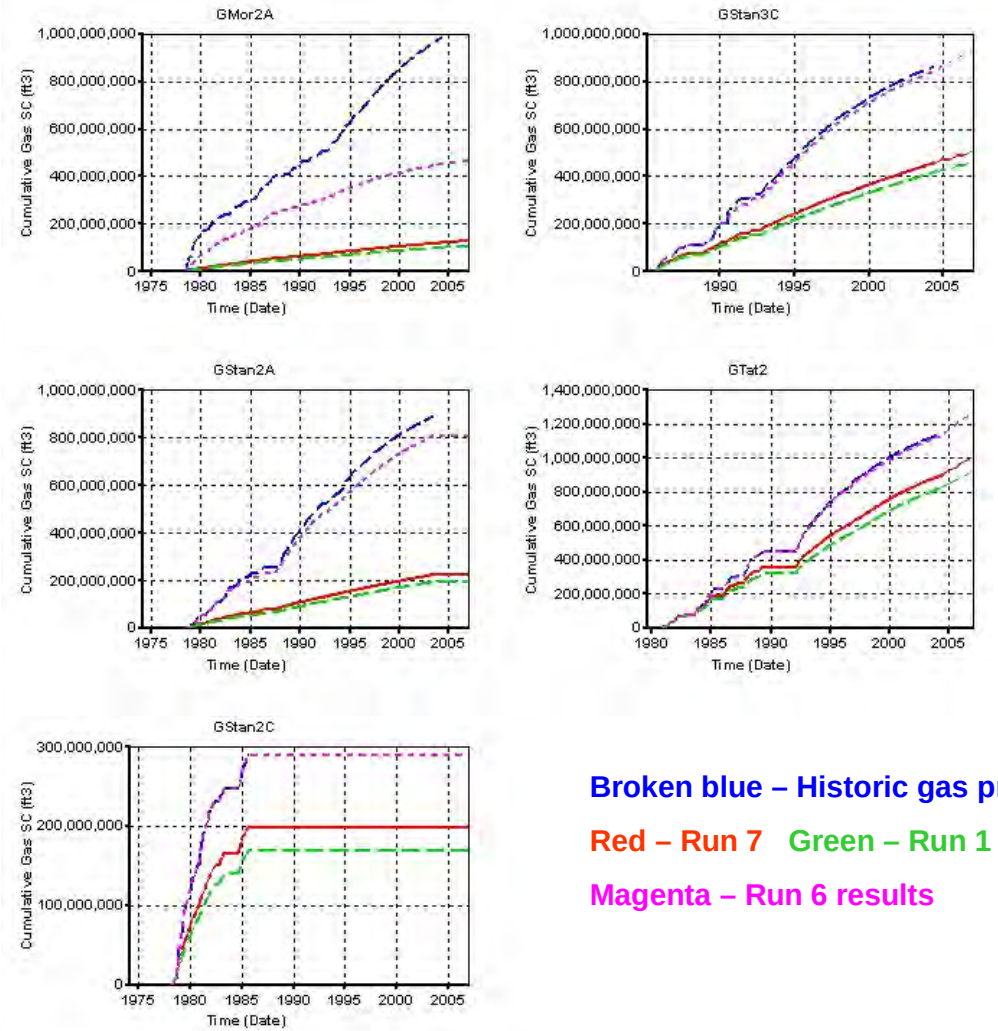

Run 6 - Gas production matched or comes close to matching history in most Council Grove wells

Run 7 - Gas production increased slightly over base case (Run 1) but remained significantly short of history

Broken blue – Historic gas production

Red – Run 7 Green – Run 1 results

Magenta – Run 6 results

Figure 9.4.29. RUN 6 and 7 Results – Simulator-calculated cumulative production at Council Grove wells compared with historic values.

RUN 8: CG fractures extended to L8, ff = 6. Original K multiplier in CG. Pi = 440 psi

Run 6 – K*10 (over initial multiplier) in CG pay and ff = 6

Match Council Grove wells

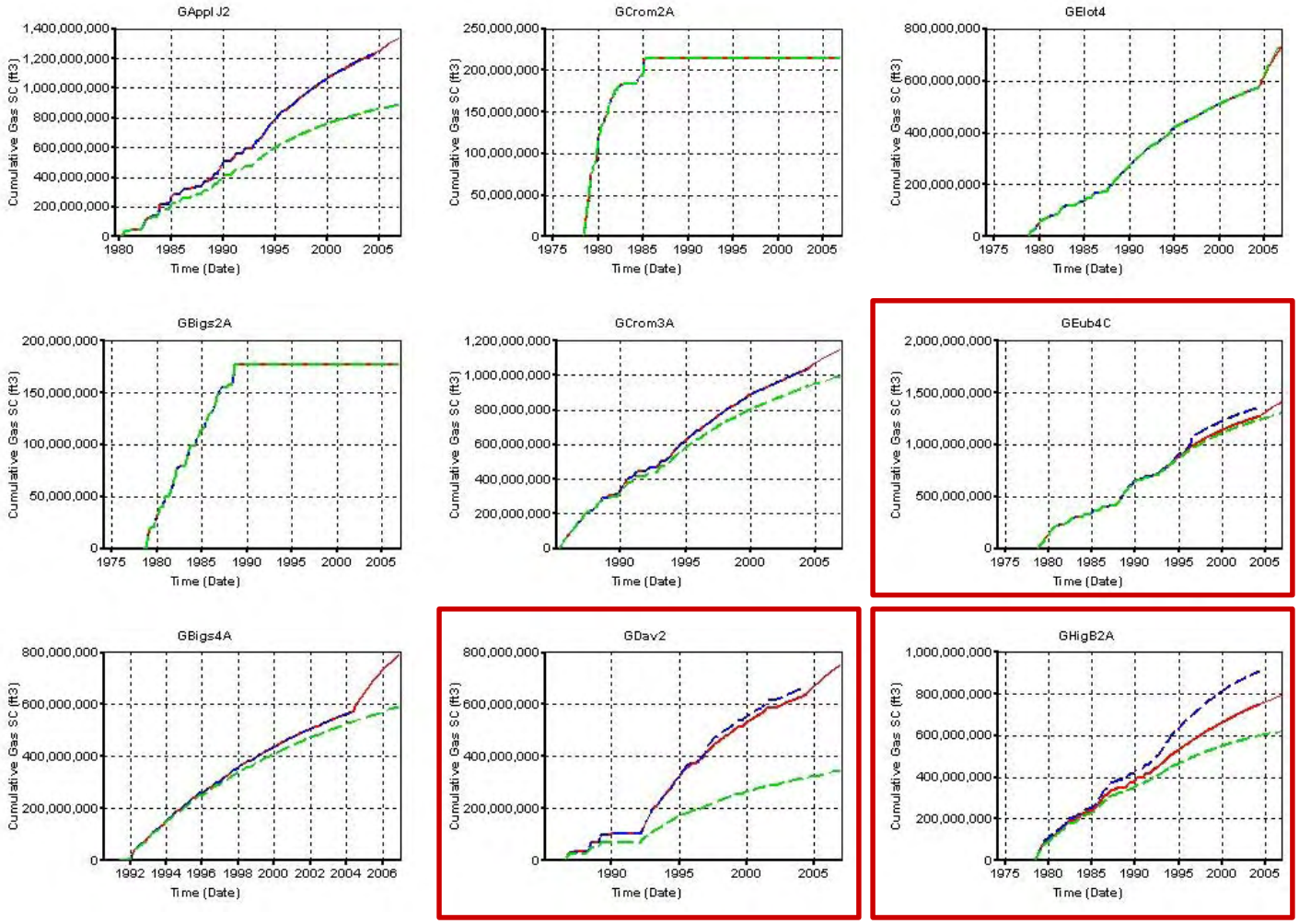

Broken blue – Historic gas prod **Red – Run 8 results** **Green – Run 6 results**

Figure 9.4.30. RUN 8 Results – Simulator-calculated cumulative production at Council Grove wells compared with historic values.

RUN 8: CG fractures extended to L8, ff = 6. Original K multiplier in CG. Pi = 440 psi

Run 6 – K*10 (over initial multiplier) in CG pay and ff = 6

Match Council Grove wells

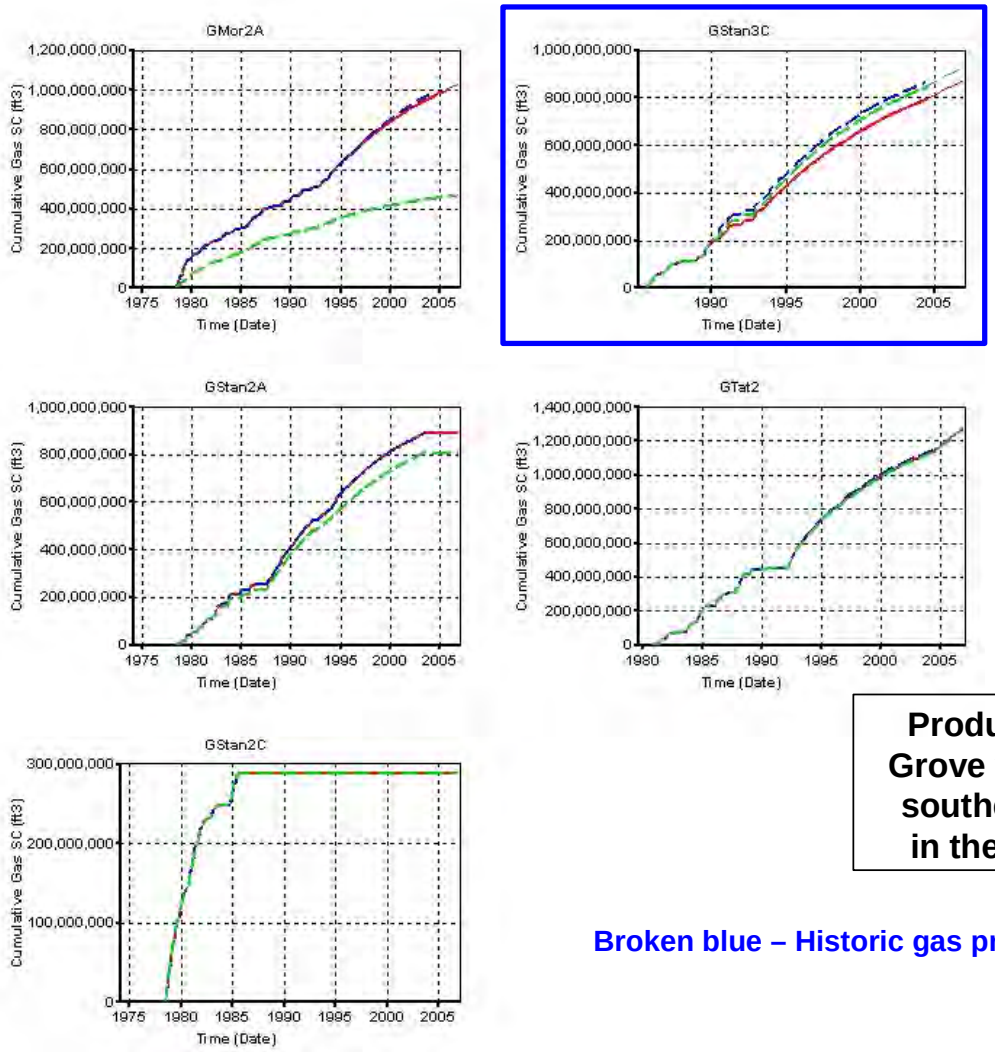

Wells in tight border areas

Well in NE corner of study area

Production matched at all Council Grove wells except 3 wells along the southern border and 1 well located in the NE corner of the study area

Broken blue – Historic gas prod **Red – Run 8** **Green – Run 6**

Figure 9.4.31. RUN 8 Results – Simulator-calculated cumulative production at Council Grove wells compared with historic values.

RUN 9: Chase Parent wells - Frac to L8 and ff = 6.0, K*2 in L6 and 8. Permeability modifications in other Chase layers (K*6 in L1). Council Grove wells - K*10 in pay layers (over initial K multiplier) and ff =6

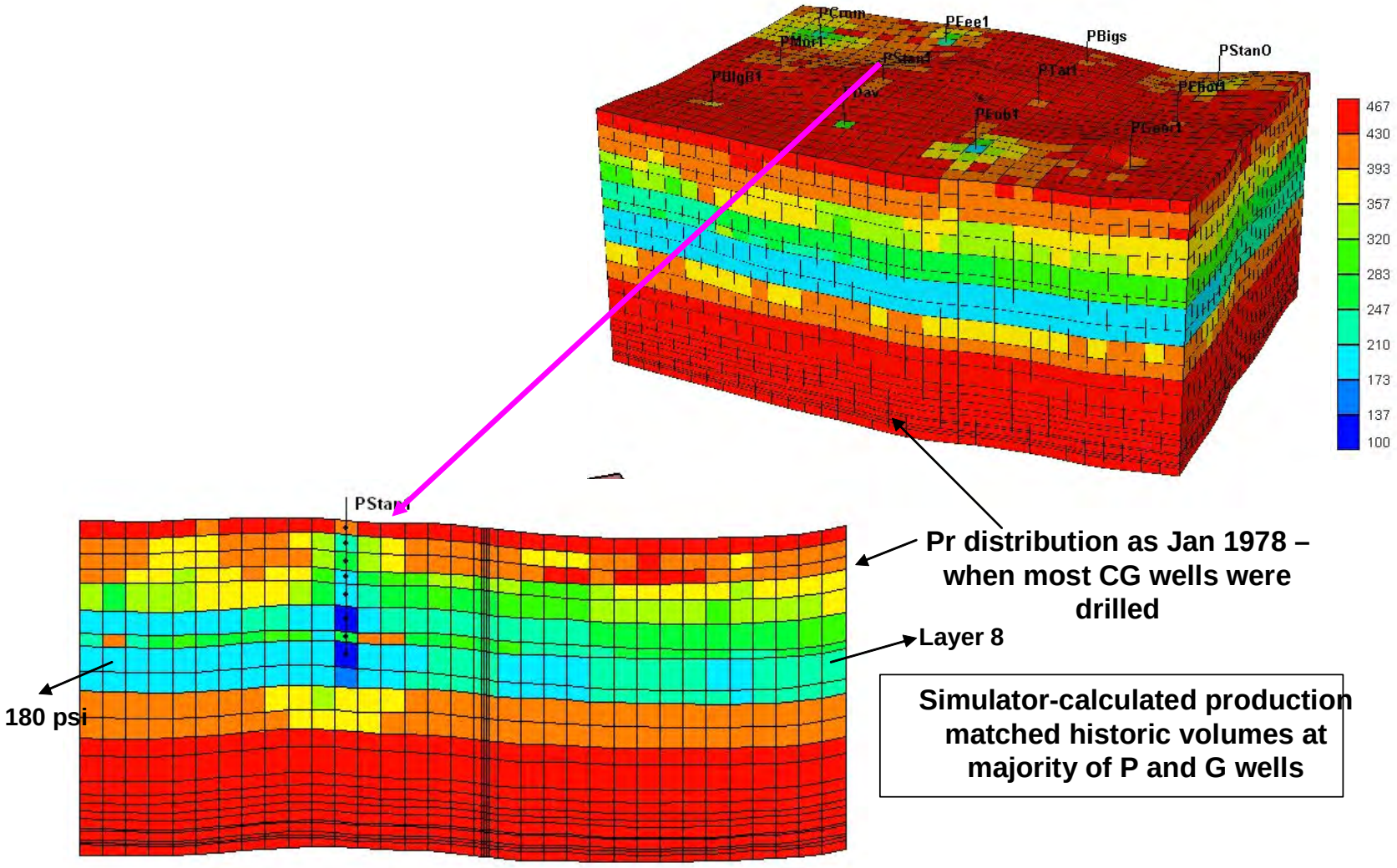

Figure 9.4.32. RUN 9 Results – Simulator-calculated pressure distribution as of January 1978 after which majority of Council Grove wells came online.

RUN 9: Chase Parent wells - Frac to L8 and ff = 6.0, K*2 in L6&8. Perm modifications in other Chase layers (K*6 in L1). Council Grove wells - K*10 in pay layers (over initial K multiplier) and ff =6

Bottom-hole SI pressure at a hypothetical CG well as of January 2, 1978

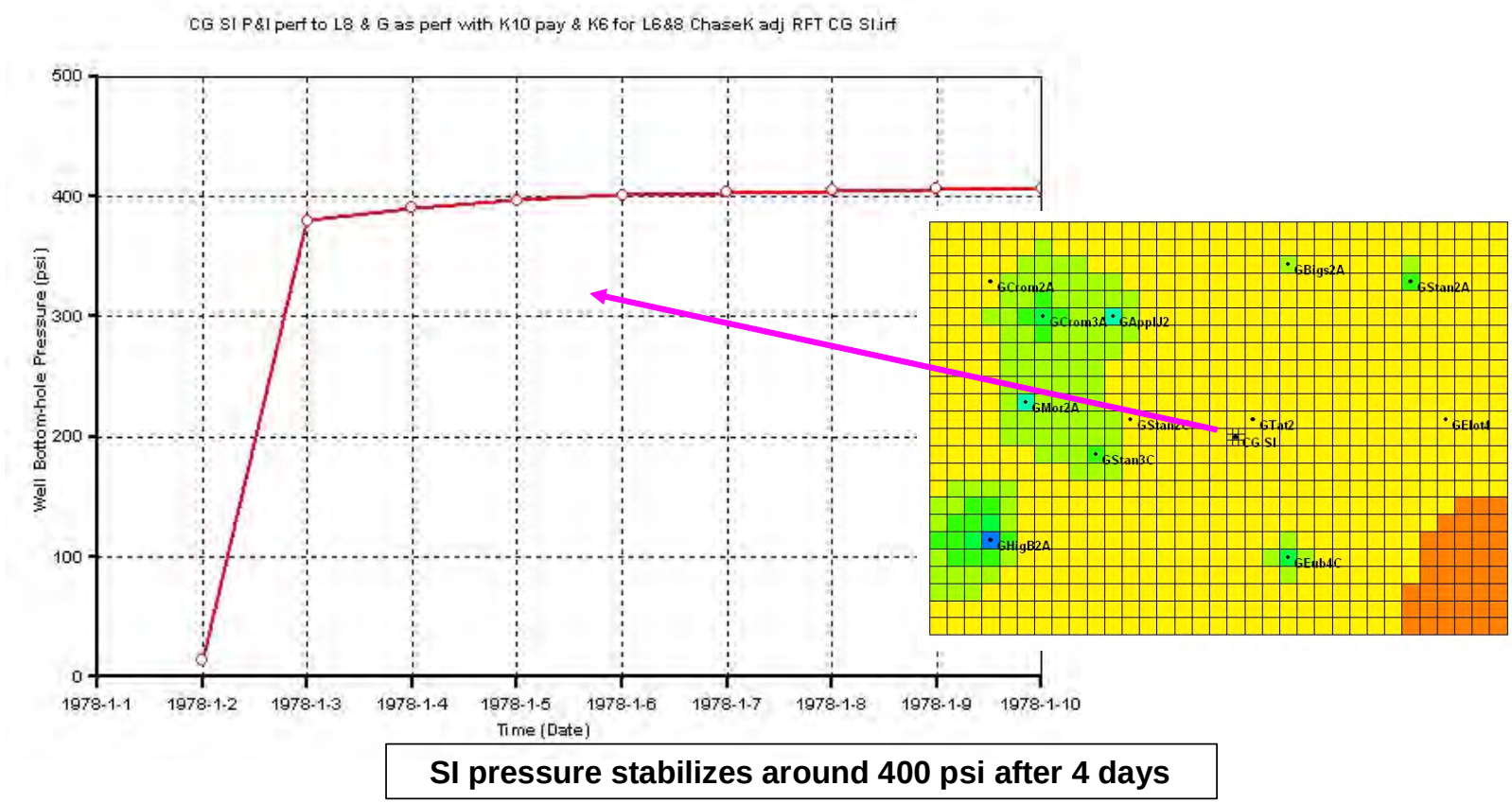

SI pressure stabilizes around 400 psi after 4 days

Figure 9.4.33. RUN 9 Results – Simulator-calculated shut-in pressure at a hypothetical Council Grove well completed in January 1978.

Historically recorded initial surface shut-in pressures at Council Grove wells

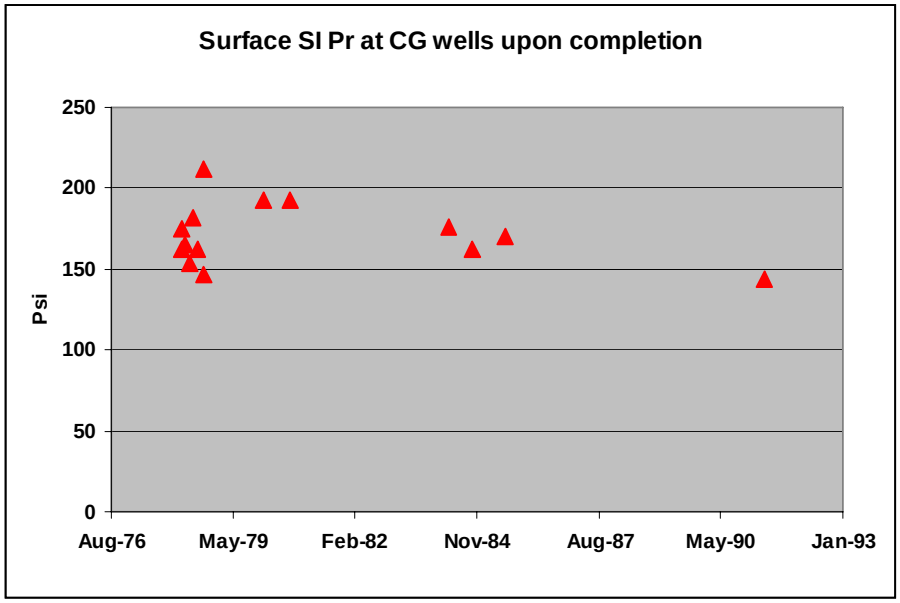

Simulator-calculated SI pr at CG well as of January 1978 = 400 psi

Figure 9.4.34. First recorded shut-in pressures at Council Grove wells drilled in the Graskell study area.

RUN 10: Chase Parent wells - Frac to L8, ff = 6.0, K*2 in L6 and 8. Permeability modifications in other Chase layers (K*6 in L1) Council Grove wells – Frac extended to L8, ff = 6.0 and original K multipliers

Chase Parent well matches

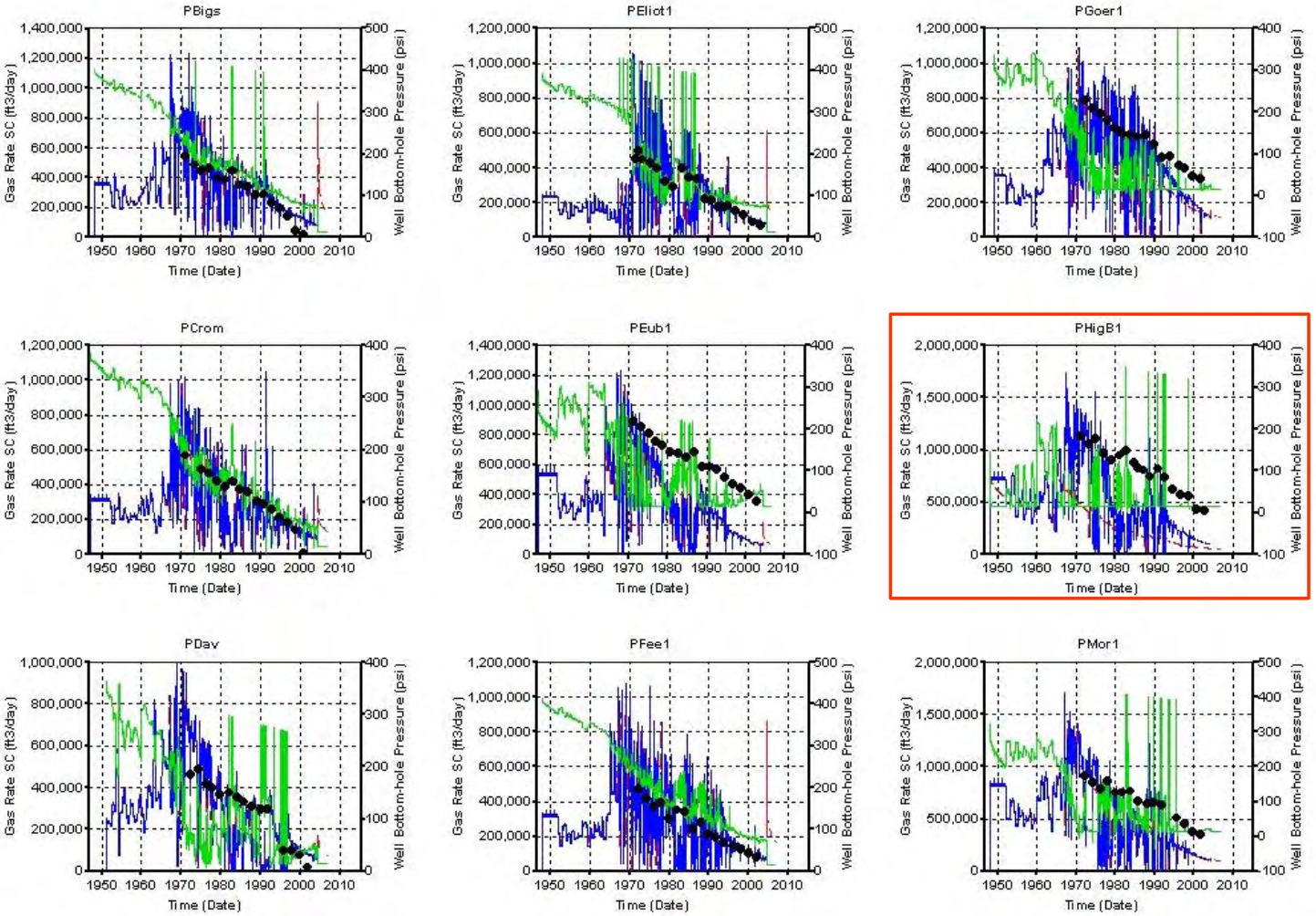

Figure 9.4.35. RUN 10 Results – Production and pressure history matches at the Chase Parent wells.

RUN 10: Chase Parent wells - Frac to L8, ff = 6.0, K*2 in L6 and 8. Permeability modifications in other Chase layers (K*6 in L1) Council Grove wells – Frac extended to L8, ff = 6.0, and original K multipliers

Chase Parent well matches

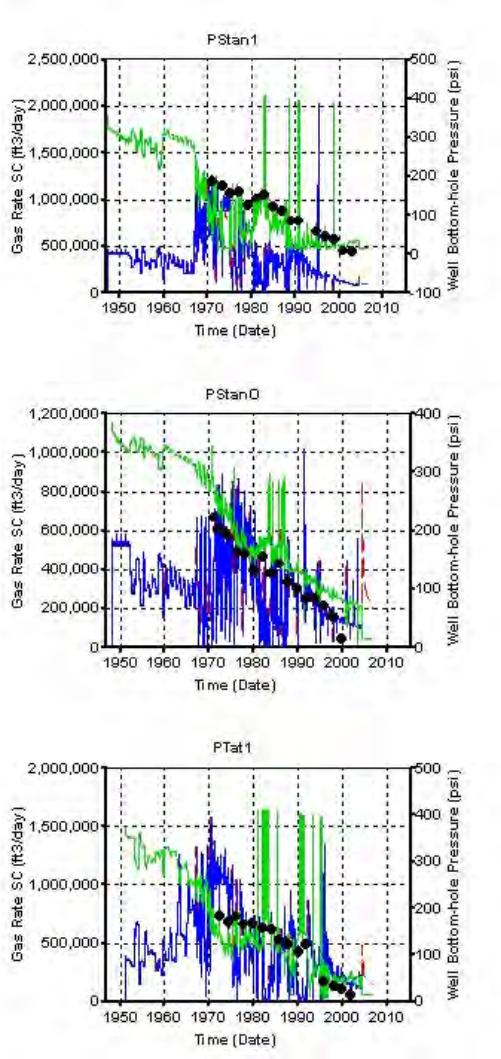

Final history matches – CH P wells

Production matched at all but PHigB1

Pressure matched at few wells

Pressure spikes indicate tight K

Production spikes when released of flow constraints

Blue – Historic gas production
Red – Simulator-calculated gas production
Green – Simulator-calculated BHFP
Black – Historic FTHP

Figure 9.4.36. RUN 10 Results – Production and pressure history matches at the Chase Parent wells.

RUN 10: Chase Parent wells - Frac to L8, ff = 6.0, K*2 in L6 and 8. Permeability modifications in other Chase layers (K*6 in L1) Council Grove wells – Frac extended to L8, ff = 6.0, and original K multipliers

Council Grove well matches

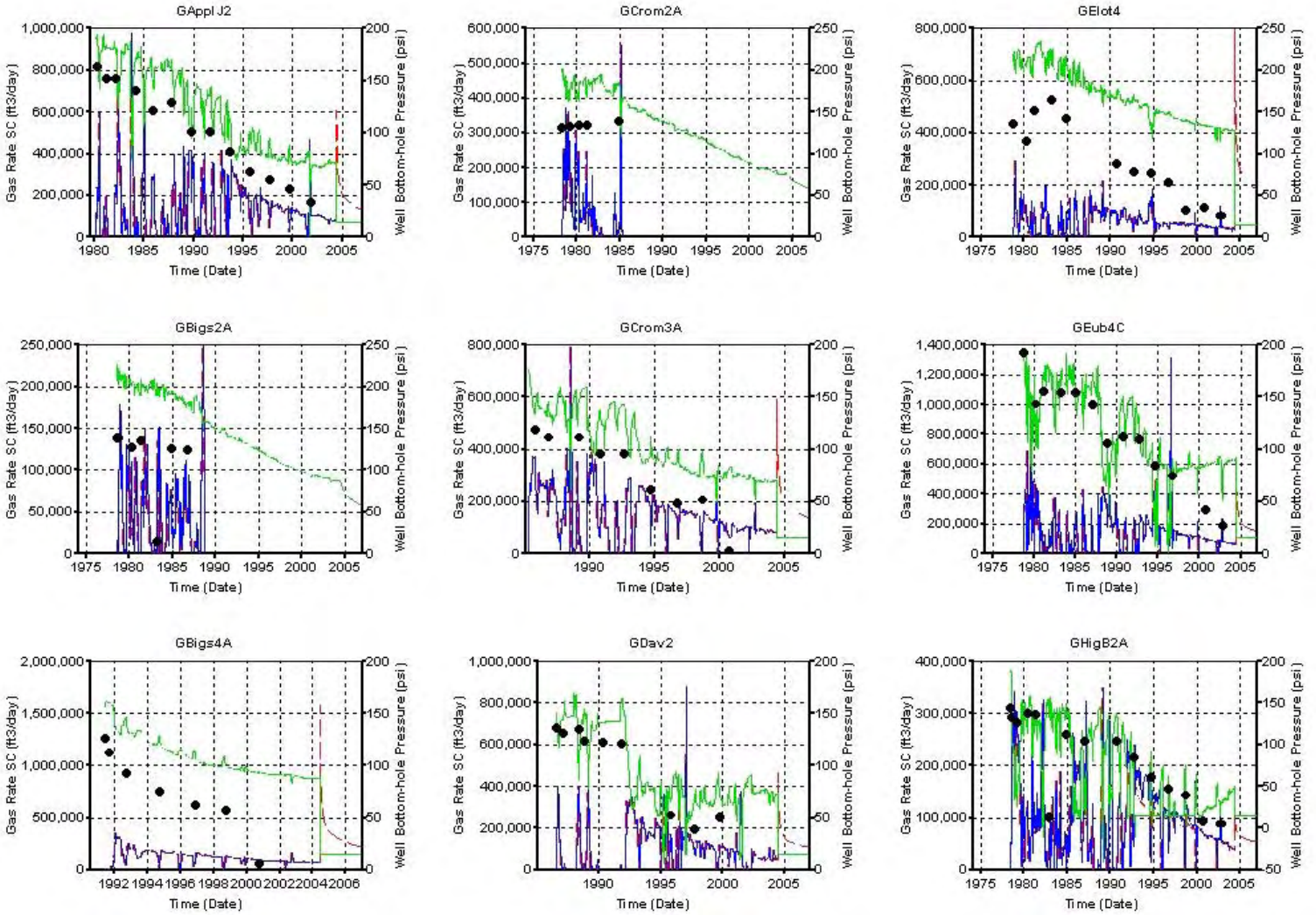

Blue – Historic gas prod **Red – Simulator-calculated gas prod** **Green – Sim BHFP** **Black – Historic FTHP**

Figure 9.4.37. RUN 10 Results – Production and pressure history matches at the Council Grove wells.

RUN 10: Chase Parent wells - Frac to L8, ff = 6.0, K*2 in L6 and 8. Permeability modifications in other Chase layers (K*6 in L1) Council Grove wells – Frac extended to L8, ff = 6.0, and original K multipliers

Council Grove well matches

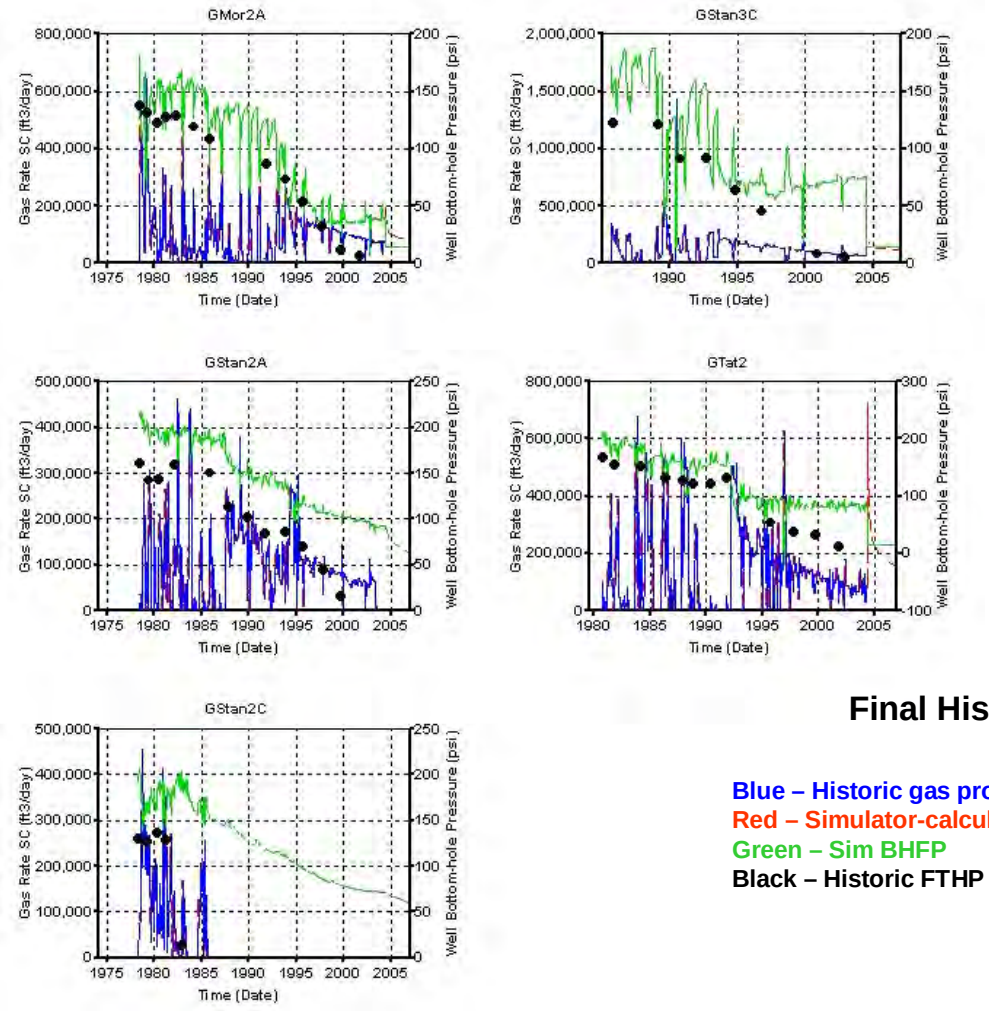

Final History matches – CG wells

Blue – Historic gas production
Red – Simulator-calculated gas production
Green – Sim BHFP
Black – Historic FTHP

Figure 9.4.38. RUN 10 Results – Production and pressure history matches at the Council Grove wells.

RUN 10: Chase Parent wells - Frac to L8, ff = 6.0, K*2 in L6 and 8. Permeability modifications in other Chase layers (K*6 in L1) Council Grove wells – Frac extended to L8, ff = 6.0, and original K multipliers

Chase Infill well matches

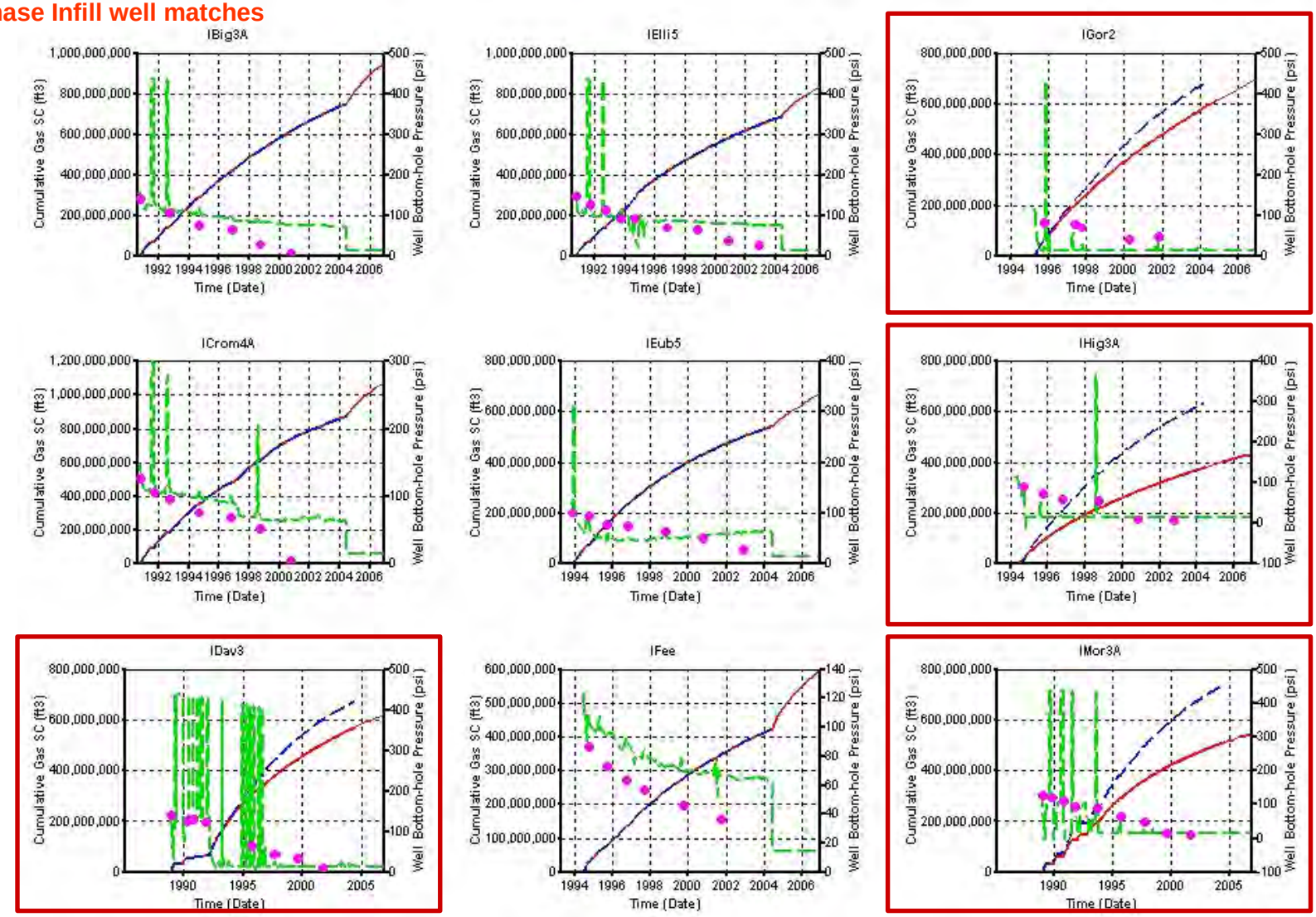

Red – Simulator-calculated gas prod

Figure 9.4.39. RUN 10 Results – Cumulative production and pressure history matches at the Chase Infill wells.

RUN 10: Chase Parent wells - Frac to L8, ff = 6.0, K*2 in L6 and 8. Permeability modifications in other Chase layers (K*6 in L1) Council Grove wells – Frac extended to L8, ff = 6.0, and original K multipliers

Chase Infill well matches (Continued)

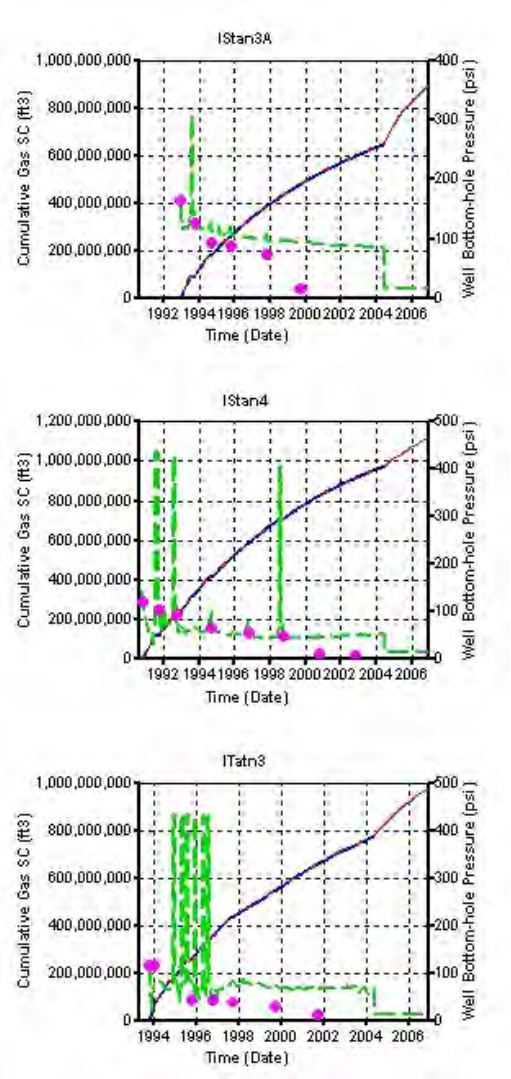

Chase Infill wells

Production matched or close to matching in most wells except those in tight border areas.

Bottom-hole flowing pressure (spikes) indicative of perhaps tight permeability.

Blue – Historic gas production

Red – Simulator-calculated gas production

Green – Simulator-calculated BHFP

Black – Historic FTHP

Figure 9.4.40. RUN 10 Results – Cumulative production and pressure history matches at the Chase Infill wells.

RUN 10: Chase Parent wells - Frac to L8, ff = 6.0, K*2 in L6 and 8. Permeability modifications in other Chase layers (K*6 in L1) Council Grove wells – Frac extended to L8, ff = 6.0, and original K multipliers

Chase Infill well matches

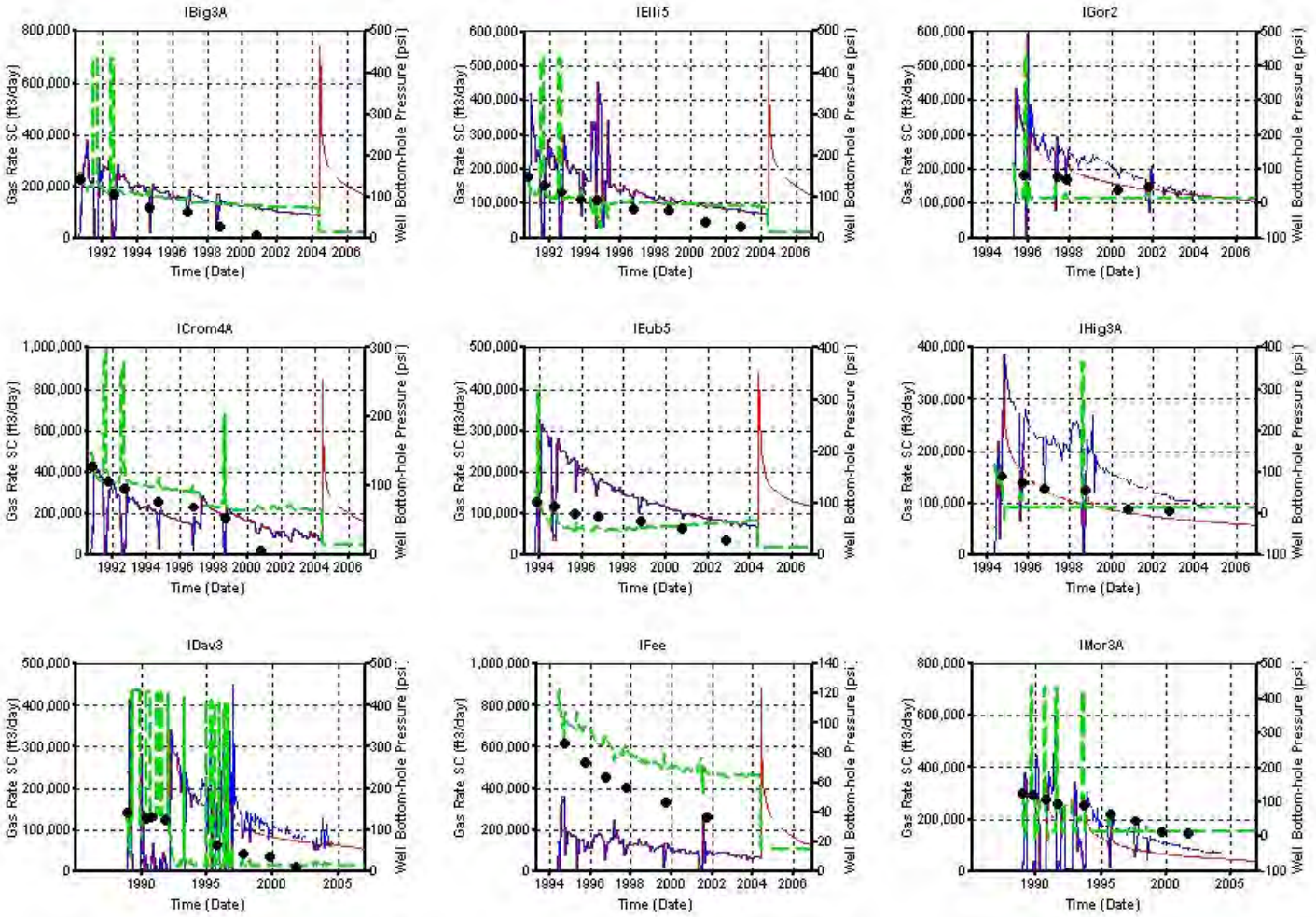

Production matched in most wells. However, production spikes visible in some wells.

Blue – Historic gas prod **Red – Simulator-calculated gas prod** **Green – Sim BHFP** **Black – Historic FTHP**

Figure 9.4.41. RUN 10 Results – Production rate and pressure history matches at the Chase Infill wells.

RUN 10: Chase Parent wells - Frac to L8, ff = 6.0, K*2 in L6 and 8. Permeability modifications in other Chase layers (K*6 in L1) Council Grove wells – Frac extended to L8, ff = 6.0, and original K multipliers

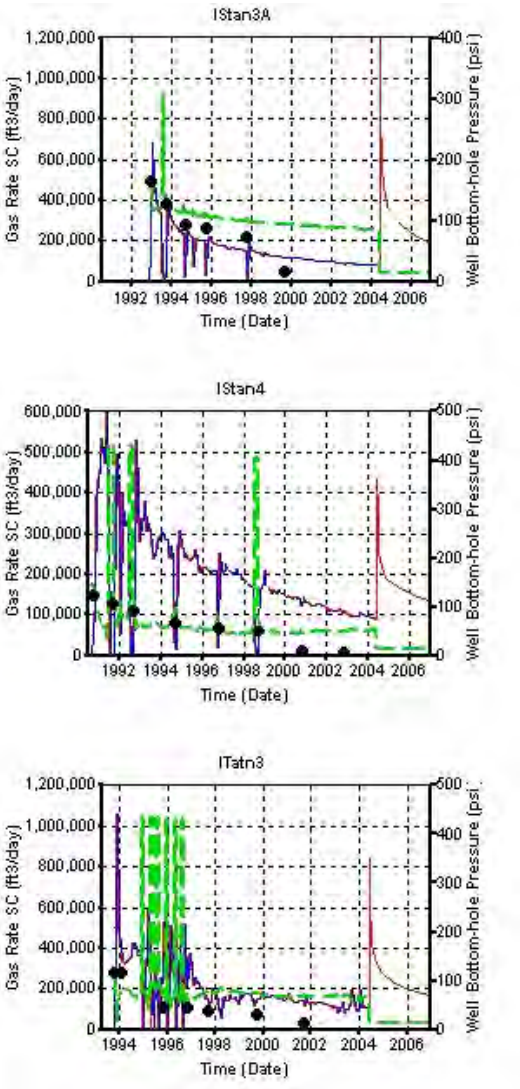

Chase Infill well matches

Production matched in most wells. Many wells do show a production spike when released from rate constraints indicating presence of excess flow capacity.

Blue – Historic gas production

Red – Simulator-calculated gas production

Green – Simulator-calculated BHFP

Black – Historic FTHP

Figure 9.4.42. RUN 10 Results – Production rate and pressure history matches at the Chase Infill wells.

RUN 10: Chase Parent wells - Frac to L8, ff = 6.0, K*2 in L6 and 8. Permeability modifications in other Chase layers (K*6 in L1 and K*100 in L5 & L7 (shale)) Council Grove wells – Frac extended to L8, ff = 6.0, and original K multipliers

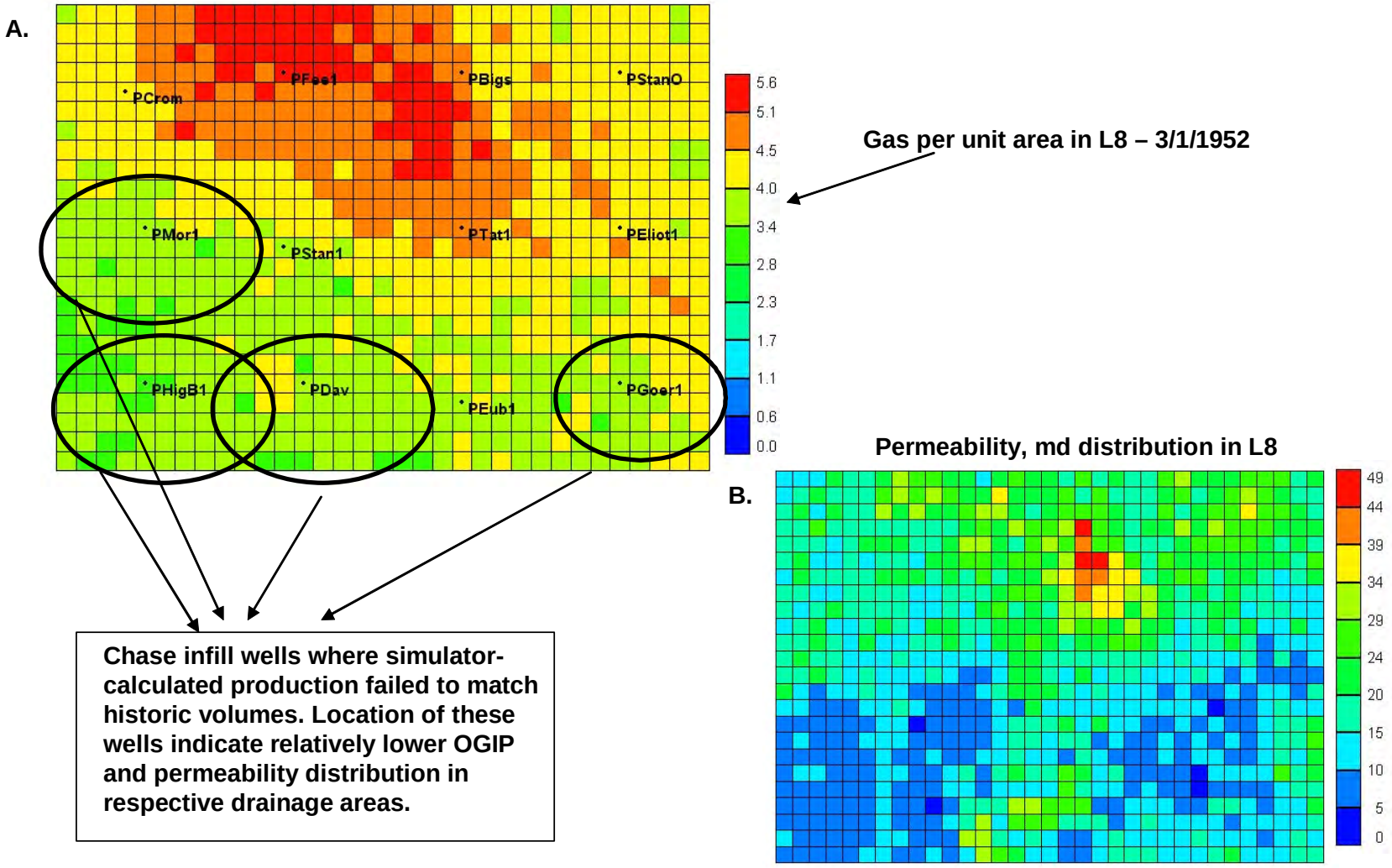

Figure 9.4.43. A) Location of Chase Infill wells where simulator-calculated production failed to match historic volumes. B) Permeability distribution in Layer 8 (one of the main driver zones) shows tight permeability along the southern part of the study area.

RUN 10: Chase Parent wells - Frac to L8, ff = 6.0, K*2 in L6 and 8. Permeability modifications in other Chase layers (K*6 in L1) Council Grove wells – Frac extended to L8, ff = 6.0, and original K multipliers

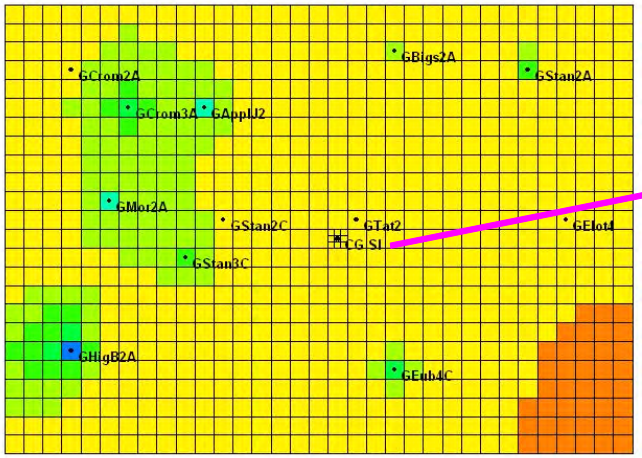

A.

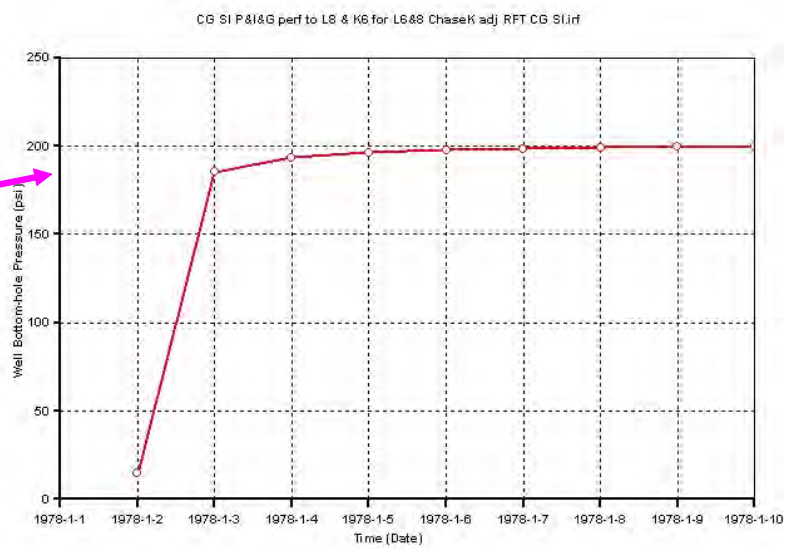

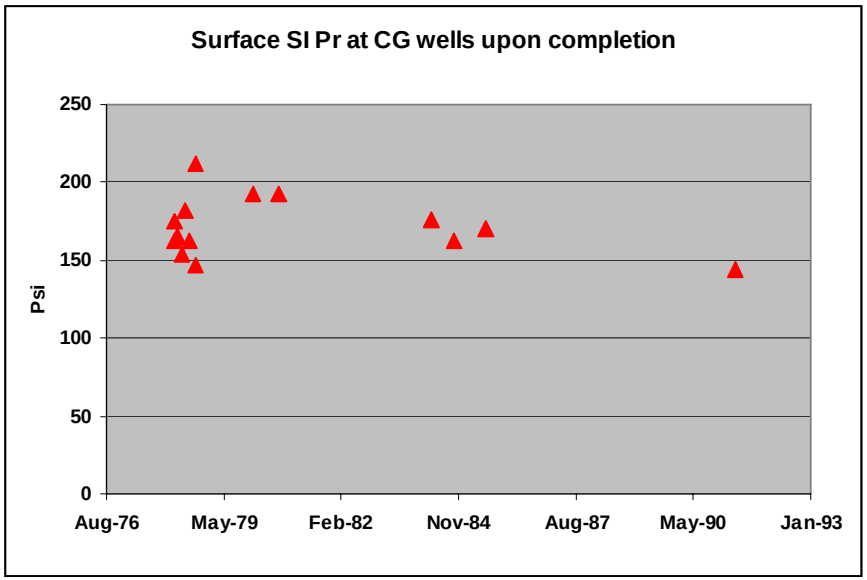

Chase Parent wells - Gas production matched at all wells except those in tight border areas.

Council Grove wells - Production matched at all wells except those in tight border areas.

SI pr at hypothetical CG well in 1978 = 200 psi.

Figure 9.4.44. RUN 10 Results – A) Simulator-calculated shut-in pressure at a hypothetical Council Grove well completed in January 1978.

RUN 10: Chase Parent wells - Frac to L8, ff = 6.0, K*2 in L6 and 8. Permeability modifications in other Chase layers (K*6 in L1 and K*100 in L5 & L7 (shale)) Council Grove wells – Frac extended to L8, ff = 6.0, and original K multipliers

		Dec-04			
Formation	Layer #	Run 10 - PV Avg Pr	RFT, psi	Best Guess	*COMMENTS*
HRNGTN	1	397	78	78	**May be low**; 107, 379, 500 in other wells
KRIDER	2	326		300	Not tested; low k in area; 64, 167 in other wells
ODELL	3	339		400	Silt-shale; should be high
WINF	4	250	107	107	May be high; 18,68,72 in other wells
GAGE	5	225		400	Silt-shale; should be high
TWND	6	115	74	74	Okay; 10, 40, 71, 95, in other wells
B/TWND	7	149		400	Silt-shale; should be high
FTRLY	8	79	110	110-200	May be low; 140, 160, 215, 286 in other wells
L/FTRLY	9			200-300	
FLRNC	10	281	99	99	70 in one other well, **mostly shale**
WREFORD	11	285	407	200	Too high; 76 in one other well
A1_SH	12	314		400	Silt-shale; should be high
A1_LM	13	259	438	<100	Too high; tight test?
A1_LM	13		442	<100	Too high; tight test?
A1_LM	13		591	<100	Too high; tight test?
B1_SH	14			400	Silt-shale; should be high
B1_LM	15	410	526	Not perfd	Too high; tight test?
B1_LM	15		750	Not perfd	Too high; tight test?
	16			Not perfd	Silt-shale; should be high
B2_LM	17	434	649	Not perfd	Too high; tight test?

It is difficult to make a best estimate of layer pressure from RFT data because the data from the available 5 wells (1 within the study area and 4 from around the study area) show significant variation within each layer.

Figure 9.4.45. RUN 10 Results – Simulator-calculated layer pressures at the location of Eliot A6 as of December 2004 compared with layer pressures from available RFT data in and around the study area.

RUN 11: Chase parent wells - Frac to L14 and ff = 6.0, K*2 in L6 and 8. Perm modifications in other Chase layers (K*6 in L1). Council Grove wells – Frac extended to L8, ff = 6, and original K multipliers in pay

Shut-in pressure at hypothetical Council Grove well – Jan 1978

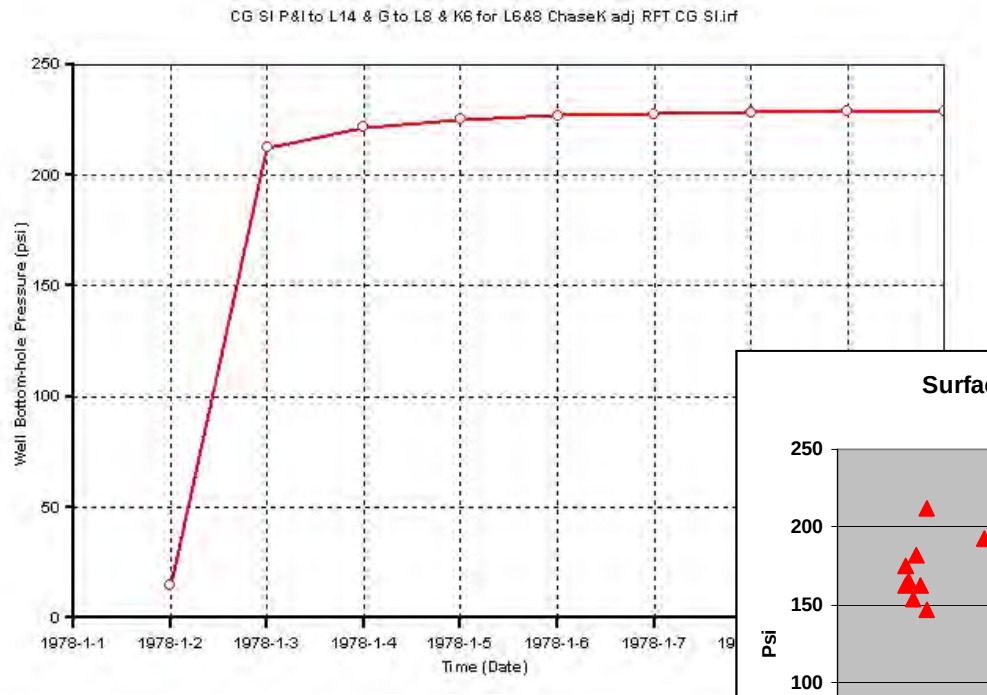

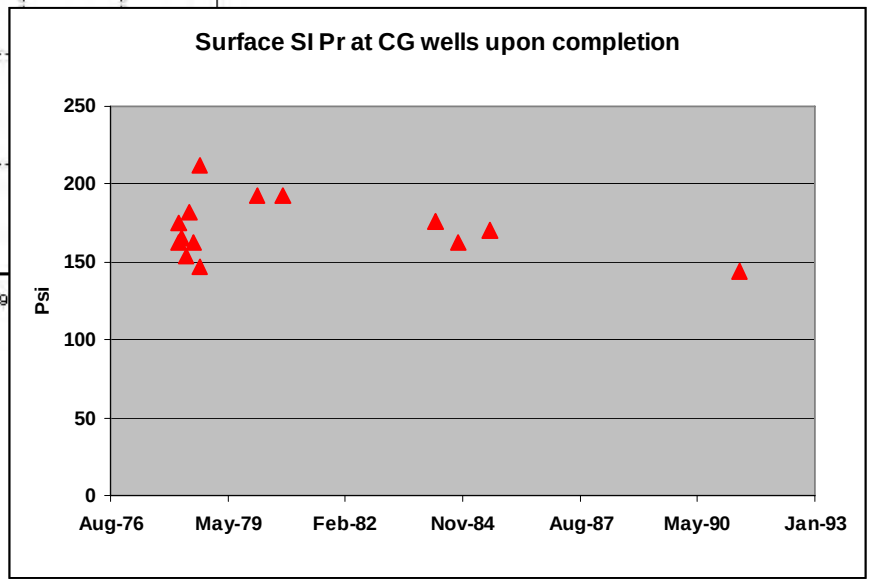

Shut in pressure stabilizes around 225 psi and is close to that historically recorded at the surface when Council Grove wells came online in the study area

Figure 9.4.46. RUN 11 Results – Simulator-calculated shut-in pressure at a hypothetical Council Grove well as of January 1978.

RUN 11: Chase parent wells - Frac to L14 and ff = 6.0, K*2 in L6 and 8. Permeability modifications in other Chase layers (K*6 in L1). Council Grove wells – Frac extended to L8, ff = 6, and original K multipliers in pay.

Comparison of Layer Pressures – Run 10 and 11 vs. RFT (best estimates)

		Dec-04	Dec-04			
Formation	Layer #	Run 10 - PV Avg Pr	Run 11 - PV Avg Pr	RFT, psi	Best Guess	*COMMENTS*
HRNGTN	1	397	400	78	78	**May be low**; 107, 379, 500 in other wells
KRIDER	2	326			300	Not tested; low k in area; 64, 167 in other wells
ODELL	3	339			400	Silt-shale; should be high
WINF	4	250	261	107	107	May be high; 18,68,72 in other wells
GAGE	5	225			400	Silt-shale; should be high
TWND	6	115	131	74	74	Okay; 10, 40, 71, 95, in other wells
B/TWND	7	149			400	Silt-shale; should be high
FTRLY	8	79	89	110	110-200	May be low; 140, 160, 215, 286 in other wells
L/FTRLY	9				200-300	
FLRNC	10	281	234	99	99	70 in one other well, **mostly shale**
WREFORD	11	285	225	407	200	Too high; 76 in one other well
A1_SH	12	314			400	Silt-shale; should be high
A1_LM	13	259	149	438	<100	Too high; tight test?
A1_LM	13			442	<100	Too high; tight test?
A1_LM	13			591	<100	Too high; tight test?
B1_SH	14				400	Silt-shale; should be high
B1_LM	15	410		526	Not perfd	Too high; tight test?
B1_LM	15			750	Not perfd	Too high; tight test?
	16				Not perfd	Silt-shale; should be high
B2_LM	17	434		649	Not perfd	Too high; tight test?

Figure 9.4.47. Simulator-calculated layer pressures at the location of Eliot A6 as of December 2004 from Run 10 and 11 compared with layer pressures from available RFT data in and around the study area.

9.5 MULTI-SECTION SIMULATION – HOOBLER AREA

Saibal Bhattacharya, Martin K. Dubois and Alan P. Byrnes

Introduction

The Hugoton and Panoma gas fields (Figure 9.5.1), North America's largest, produce from 13 fourth-order marine-nonmarine sedimentary cycles of the Wolfcampian Chase and Council Grove Groups, respectively. A fine-layered cellular geomodel was constructed for these fields using a four-step workflow: 1) define lithofacies in core and correlate to wireline log curves and geologic variables (depositional environment and relative cycle-position), 2) train a neural network and predict lithofacies at non-cored wells, 3) populate a 3D-cellular model with lithofacies using stochastic methods, and 4) populate the model with petrophysical properties and fluid saturations using facies-specific equations based on core data. The fine-scale model was upscaled to 25 layers for simulation.

Objective

The objective of this study was to validate the above-mentioned geomodel by simulating the production/pressure performance of wells located in select multi-section areas in the Hugoton field. The reservoir geomodel was developed using an automated facies-recognition technique and specific capillary-pressure curves developed by integrating available core data. The intent of this exercise is, therefore, to evaluate the robustness of this geomodel by comparing how close the simulator-calculated pressure/production performances of individual wells match with respective histories with minimum modifications to the geomodel. The focus is not to obtain exact matches of pressure/production histories at individual wells with localized model modifications. Computer Modeling Group's (CMG's) IMEX simulator was used in this study.

This report details the simulation studies carried out at one such area – 12 sections around the Hoobler Estate Unit well (sec 20, T. 6 N., R. 17 E.). The location of the Hoobler simulation area within the context of the Hugoton-Panoma fields is shown in Figure 9.5.1 while Figure 9.5.2 shows the locations of the wells within this study area.

Some of the reasons behind selection of this study area include: a) location outside the Panoma field and on the edge of the "other" Council Grove production area, b) presence of relatively thick Chase gas column, c) availability of Chase core from within the study area and nearby Council Grove cores, and d) presence of limited layer pressure data from 1995 and 2005. Figure 9.5.3 shows that 6 node wells with modern log suite and three wells with zone pressure data are present within the Hoobler study area. Figure 9.5.4 shows the position of wells in and around the study area where RFT layer pressures were available.

Hoobler Area Geologic Model

The Hoobler area is located in the east-central portion of the Hugoton field on the Oklahoma side of the Kansas-Oklahoma border. The model is situated immediately

shelfward of an area of steepened dip on the Wolfcamp ramp (or gently dipping shelf, that has been interpreted as a shelf margin (Dubois et al., in press). The Hoobler study area is outside the Panoma field and the Council Grove production on the east side of the study area is from a closed structural feature that is downdip from and unrelated to the Panoma gas field accumulation. Here the Chase and Council Grove reservoirs behave as separate gas reservoirs and the Council Grove was not simulated.

The nine-section Hoobler static model was extracted from the field-wide geomodel version Geomod (Figure 9.5.5) and upscaled from 269 layers to 24 layers for the simulation model (Figure 9.5.6). Figure 9.5.5 shows the area extracted from the larger model. The XY-grid dimensions are 660 ft by 660 ft (200 m by 200 m). Because the model is outside the Panoma and layers within the model below layer 11 are 100% water saturated, the model was reduced to the top 11 zones, the Chase through the Council Grove A1_SH. In reality the Council Grove does not have 100% water saturation in the closed structure on the east side of the model. Our current geomodel is focused only on the Hugoton that has a much higher (structurally) free-water level (FWL). Figure 9.5.7 shows the distribution of GIP for the 11-layer model with a FWL at +65 ft above sea level and Figure 9.5.8 illustrates the other critical properties. Corrected porosities at the node wells were estimated using algorithms developed from core- to log-porosity regression analysis (Figure 9.5.9).

Engineering Model

The 11-layer geomodel was exported to the reservoir simulator – Computer Modeling Group's IMEX. Each layer in this 11-layer model coincided with a formation- or member-level stratigraphic interval in the Chase system. Each layer represents a half-cycle of marine/non-marine sedimentary cycle. In most cases, the model layer closely approximates the RFT intervals at wells in and around the study area. The area simulated extends over 12 sections around the Hoobler Estate Unit well. Grid-cell dimensions were set at 660 ft by 660 ft for all layers.

Porosity was upscaled using an arithmetic average, conditioned on lithofacies, water saturation was upscaled using a porosity-weighted arithmetic average, and permeability was upscaled utilizing flow-based tensor upscaling using PSK-solver.

Figure 9.5.10 lists the basic PVT properties input for simulation.

Permeability Modeling

Porosity-permeability measurements taken on whole cores on a foot-by-foot basis were available from the Chase interval at Hoobler Estate Unit (EU) well. Permeability recordings from Krider, Winfield, and Towanda zones at the above mentioned wells are shown in Figure 9.5.11. Permeability was not measured on core plugs from the available core. The whole-core-derived (horizontal) permeability values were arithmetically averaged (upscaled) to derive the layer horizontal permeability. Absent layer-DST permeability values, the upscaled layer permeability derived from

whole cores was assumed to be representative of effective permeabilities in each layer within the drainage area of the Hoobler EU well.

The geomodel built in Petrel® consisted of 269 layers. Facies-specific permeability-porosity co-relationships were used to estimate of grid permeabilities from grid porosities. The tensor-upscaling algorithm in Petrel® was used to upscale vertical and horizontal permeability to 11 layers before exporting the model to CMG. For each layer at the place of location of the Hoobler EU well, the upscaled permeability (from Petrel®) was compared with that calculated by upscaling the whole-core-based permeability values (Figure 9.5.12). For layers where the upscaled permeability differed from whole-core permeability, an appropriate multiplier was applied so that the layer permeability matched that calculated by upscaling whole-core measurements. For each layer, Figure 9.5.12 tabulates the multiplier applied so that the grid-cell permeability at the location of the Hoobler EU well in the CMG model matched the corresponding whole-core-based upscaled layer permeability. As discussed in the previous section, whole-core K values are higher than plug K below 0.5 md because micro-fractures present in whole cores result in measured K values to exceed 0.5 md. Also, plugs are biased to represent matrix rock and possibly are minimally affected by micro-fractures especially in tight rocks. Thus, multipliers close to 1.0 were found applicable for pay layers where average whole-core K values are higher than 0.5 md.

Reservoir Pressure

The first recorded surface shut-in (SI) pressures (soon after completion) at the Chase Parent wells in the area studied varied between 390 to 423 psi (Figure 9.5.13). Surface shut-in pressures were converted to bottom-hole shut-in pressures. Figure 9.5.14 shows the estimation of initial reservoir pressure from recorded surface shut-in pressures following the average temperature and z-factor method. The estimated initial reservoir pressure was about 450 psi assuming a WHSP of 420 psi. Thus, the reservoir model in the simulator was initialized using a starting pressure of 450 psi and resulted in charging the input geomodel (for the area studied) with an original-gas-in-place (OGIP) of 131.1 bcf (as compared to 128 bcf in the Petrel® geomodel, Figure 9.5.15).

Hydraulic Fractures

Most of the wells in the study area were drilled before 1950. Current records indicate that all wells were hydraulically fractured some time during their production life. However, the exact date on which each well was fractured is not available. Fracturing technology came in use in the study area some time in the early 1970’s. In this study, it was assumed that wells were fractured as of January 1, 1970. Later infill/replacement wells drilled in the 1980’s or later were assumed to be fractured upon completion.

However, no information or test data are available which would enable one to estimate the physical characterization of these fractures. The intent of the fracturing was to enhance the well productivity. Lacking physical descriptions of hydraulic fractures, the enhanced well productivities were modeled in this study using the well-productivity (ff)

factor greater than 1 with the ff set to 1.0 for an unfractured well. The ff value was modified at each well to match the post-1970 production.

Flow Constraints

Annual production data for individual wells were available for initial completion to 1966. From 1967 onwards, monthly production data were available for all the Chase wells in the study area. Regular tubing-head flowing and shut-in pressure data were available for all wells from 1967 onwards.

In the simulator, all wells were flowed under rate constraints until April 2005. Thereafter, all wells were flowed under a constant bottom-hole pressure (BHP) of 14.7 psi until May 2006. The intent of changing from rate constraint to pressure constraints was to see if the simulator-calculated production rates from May 2005 to May 2006 followed the already established decline trends without showing production spikes (or signs of excess flow capacity). The well names and their abbreviated names used in the simulator model along with their starting dates, cumulative production, and initial perforation intervals are listed in Figure 9.5.16.

Reservoir Simulation Studies

The completion records (Figure 9.5.17A) indicate that the Chase wells were initially perforated in the upper four layers, i.e., Herington, Krider, Odell, and Winfield. Well operators confirm that each of these wells was hydraulically fractured during some point in its production life. However, the exact date when each well was fractured is unavailable. In the model, it was assumed that each well was fractured as of January 1, 1970 – the approximate time frame when fracturing came in vogue in the study area. Figure 9.5.16 reveals that the Chase wells in the study area produced around 70.13 bcf while the OGIP charged in the first 4 layers totals 58 bcf (Figure 9.5.17B). Thus to obtain a match with production history, gas from lower layers such as the Towanda and the Fort Riley has to be produced. If the completion is assumed to be restrained to L4 (Winfield), then the gas from the lower layers has to flow across the intervening shale zones taking advantage of vertical permeabilities.

The model used in this study was an 11-layer model with grid-cell sizes of 660 ft by 660 ft. A consistent set of legends was used to analyze the simulation results. The simulator-calculated production and bottom-hole flowing pressure are displayed in red and green lines while the historic production and well-head flowing pressures (WHFPs) are displayed in blue and magenta.

Because the wells were not fractured pre-1970, flow in this period was dominated by matrix. Also during this period, the well completions did not extend beyond the perforated layers. Thus, the strategy employed in the designing of the following set of simulation runs was to first try to match pre-1970 field production by adjusting matrix permeability through the application of different multipliers. After obtaining a match with the historic production volumes prior to January 1, 1970, other factors such as layers

drained by the fractures and productivity gains from hydraulic fracturing were modified on a well-by-well basis to improve both the production and flowing pressure matches at each well.

RUN 1

All wells were initially completed as per available information from well records (Figure 9.5.17). Wells without any initial completion records were assumed to be completed in the upper four layers. As of January 1, 1970, all wells were fractured in the simulator using an ff = 6.0. However, the fractures were constrained to the initial completion interval at each well. Also, (horizontal) permeability multipliers (Figure 9.5.12) were applied to layers 1, 2, and 4 only, i.e. L1, L2, and L4. As a result of the application of these multipliers, the layer permeability in each of the above-mentioned layers around the Hoobler EU well in the simulator model corresponds closely to the whole-core-based upscaled permeability. Permeability multipliers were not applied to the shale layers such as L3 (Odell). Results from this run are shown in Figure 9.5.18. The simulator-calculated production falls short by about 8 bcf before 1970 and by about 20 bcf in 2005.

Figures 9.5.19 and 9.5.20 display the production and pressure matches obtained at individual wells. The simulator-calculated production (red line) falls short of history (blue line) for many wells even before 1970. Thus, matrix K appears insufficient to match pre-1970 production at most wells. However, simulator-calculated production matched history at Wilson (named Wils in simulation results) and Blackmer 28 (named Blk28 in simulation results). Figure 9.5.21 shows that there is a bull's eye in the horizontal-permeability distribution in Winfield (Layer 4) around Blk28 as it is significantly higher than in other parts of the study area. It appears that the automated facies-prediction model must have incorrectly assigned facies in this area and, therefore, resulted in non-representative permeability estimations. Also, the simulator-calculated bottom-hole flowing pressure (BHFP, in green line) is consistently higher than the historically recorded WHFP (in magenta) indicating excess gas and/or flow capacity in the drainage area of Blk28. As for Wilson (named Wils in simulation results), the simulator-calculated BHFP is close to the historic WHFP. However, the simulator-calculated production falls short of the historic production near the year 2000.

RFT records from wells in and around the study area were available. Despite variations between readings from within a layer, reservoir pressures in Krider (L2) and Winfield (L4), as of 2005, were estimated to be between 40 to 60 psi respectively. Figure 9.5.22 lists the best estimates of layer pressures in the study area as of 2005. Figure 9.5.23 shows the pressure distribution through an east-west cross section across the Hoobler EU well as of May 2006. These simulator-calculated results indicate that the pressure in Krider (L2) varies between 50 to 130 psi while that in Winfield (L4) varies between 90 to 300 psi.

RUN 2

The horizontal-permeability (Kxy) distribution in L2 (Krider) was multiplied by 2 (over the starting multiplier) in order to increase simulator-calculated gas production in the pre-1970 period. Figure 9.5.24 compares the simulator-calculated field production with historic volumes, and it becomes evident that as of 1970, the simulator-calculated cumulative production falls short by 5 bcf as opposed to 8 bcf in Run 1. Thus, additional gas needs to be mobilized in the pre-1970 period in the simulator model. A display of pressure distribution (Figure 9.5.25) in an east-west cross section through the Hoobler EU (HobEU) wells shows that the pressure in the Krider (L2) layer is less than 85 psi while that at HobEU is 39 psi. Thus, L2 appears to have drained close to best estimates from RFT data, i.e., layer pressure varying between 40-60 psi.

RUN 3

The horizontal-permeability (Kxy) distribution in L4 (Krider) was multiplied by 2 (over the starting multiplier) in order to increase simulator-calculated gas production in the pre-1970 period. Thus, both L2 and L4 have a multiplier of 2 applied on the permeability distribution present in Run 1. Figure 9.5.26 compares the simulator-calculated field production with historic volumes, and it becomes evident that as of 1970, the simulator-calculated cumulative production falls short by 2 bcf as opposed to 5 bcf in Run 2. Hence, additional gas still needs to be mobilized in the pre-1970 period in the simulator model. A display of pressure distribution (Figure 9.5.27) in an east-west cross section through the Hoobler EU (HobEU) wells shows that the pressure in Winfield (L4) layer is less than 260 psi while that at HobEU is 72 psi. Thus, L4 in the vicinity of the HobEU appears to have drained close to best estimates from RFT data, i.e., layer pressure varying between 40-60 psi.

RUN 4

To increase production from the simulator model, the Kxy distribution in L2 and L4 was multiplied by 3 over the initial multiplier, i.e., the permeability distribution in these layers in Run 1. Figure 9.5.28 compares the simulator-calculated field production with historic volumes. As of 1970, the simulator-calculated cumulative production still falls short of historic volumes by 0.92 bcf. Figure 9.5.29 shows the gas in place in Herington (L1). As of 1970, there is about 3.25 bcf of gas in L1. Figure 9.5.30 shows the layer pressure distribution across a cross section through the HobEU well. The pressure at HobEU is 70 psi while higher pressures prevail in L1 away from the well. As a comparison, the pressure at HobEU in L2 (Krider) is 33 psi while pressures away from the well in L2 never exceed 85 psi. Similarly, the pressure at HobEU in L4 (Winfield) is 62 psi while pressures away from the well in L4 never exceed 230 psi.

RUN 5

Figure 9.5.11 and Figure 9.5.31 tabulate the whole-core-measured permeability distributions at HobEU well for Krider (L2), Winfield (L4), Towanda (L6), and

Herington (L1), respectively. The whole-core-based permeability values were upscaled in each of these layers and compared with that estimated from facies-specific permeability-porosity equations. Differences were reconciled using appropriate multipliers (Figure 9.5.12). These multipliers were used in the initial simulation run (Run 1) for L1, L2, and L4. A closer look at the whole-core data from these 3 layers reveals that there are streaks of high permeability in each of these layers. These high-permeability zones are the drivers for gas production and yet get smoothed in the process of permeability upscaling (of the whole-core data). Permeability calculated from reservoir-pressure testing is considered most representative to simulate well performance as it is the effective permeability prevalent in the drainage area of the well(s). Thus without permeability calculated from well tests, layer-permeability multipliers were calculated using the upscaled whole-core-based permeability data, which under-represents the high-permeability streaks. For example in Krider (Figure 9.5.11), the upscaled whole-core-based permeability is 2.24 md while the whole-core data reveal high streaks ranging between 3 to 6 md. It is impossible to estimate the effective-permeability prevalent L2 (Krider) in the drainage area of HobEU well without a well test but critical examination of whole-core data indicates that application of permeability multipliers between 2 to 4 times the upscaled whole-core data is not unreasonable, especially when lower permeability distributions are unable to produce historically recorded gas volumes. Similar high permeability streaks are visible in the whole-core data in Herington and Winfield.

Figure 9.5.32 shows the simulator-calculated production when the permeability distributions in L1, L2, and L4 were multiplied by 3 (over the initial distribution in Run 1). It appears that the simulator-calculated pre-1970 production is very close to historic volumes but still less by 0.92 bcf (as of 1970).

RUN 6

Figure 9.5.33 compares the simulator-calculated production with field history when the permeability distribution in L1, L2, and L4 were multiplied by 3 and that of L6 by 2 over the initial respective values in Run 1. The simulator-calculated production almost matches historic volumes as of 1970. Thus, even increasing permeability in L6 (Towanda) did not enable production history matching as of 1970.

RUN 7

Figure 9.5.34 compares the simulator-calculated production with field history when the permeability distribution in L1, L2, and L4 were multiplied by 4 over the initial respective values in Run 1. It is evident from Figure 4.7 that the simulator-calculated production almost matched historic production volumes as of 1970. Thus given the geomodel (with its distribution of gas saturation), the matrix-permeability distribution in L1, L2, and L4 had to be increased 4 times over that obtained by upscaling whole-core permeabilities at HobEU well in order to match historic pre-1970 production. Figures 9.5.35 and 9.5.36 display the production/pressure matches obtained at individual wells. It appears that the simulator-calculated production matched pre-1970 historic production in

all wells except Muller (Mull) - a well located close to the southern border of the study area. The simulator-calculated BHFP was higher than the recorded WHFP in wells such as the Blk25, Blk25U, Blk28, EberF, and EberU suggesting presence of excess gas and/or flow capacity. However in remaining wells, the BHFP was less than the WHFP, often hovering at 14.7 psi, suggesting that these wells are running out of gas in the post-1970 period under the current completion framework, i.e., fractures constrained to L4 in the post-1970 period.

Figure 9.5.37 displays the pressure distribution as of May 2006 along an east-west cross section across the HobEU well. The maximum pressure in L2 is 80 psi while the well grid is at 30 psi. The maximum pressure in L4 is 200 psi (away from the well) while the well grid is at 57 psi. Figure 9.5.38 plots the gas in place over time in the top 6 layers of the reservoir model in the simulator. It shows that, as expected, the gas in place decreases over time in L1, L2, and L4. However, the gas in place in L3 and L5 increased over time indicating the movement of gas from adjacent layers into shale layers and the flow of gas and water out of shale layers into adjacent layers, leaving residual gas in L3 and L5. This plot also shows that gas in place in L6 declines over time despite completions restrained to L4 in the post-1970 period. Thus, gas from L6 is able to travel through L5 and into the wells completed in L4 at vertical permeabilities set in the model in Run 7.

RUN 8

Given the shortfall in simulator-calculated production in the wells Daniels (Dan), Hampston, and Towner (Town), post-1970 fractures in these wells were extended to L6 (Towanda) using ff = 1.0. Using ff = 1.0 across fractured intervals means that the fracturing resulted in establishing communication with L5 and L6 layers but did not lead to productivity gains beyond a normal completion (such as perforation) in these layers. Also, many of the wells (stated in the section above) showed signs of excess gas in their drainage and thus a permeability multiplier of 0.8 was used on the initial permeability distribution (as in Run 1) in L6 (Towanda) and L8 (Fort Riley). The permeability multiplier selected for L6 and L8 is based on the estimates made by comparing upscaled whole-core data and that predicted using facies-specific permeability correlations (Figure 9.5.12). Figures 9.5.39 and 9.5.40 shows the production/pressure matches at individual wells. The simulator-calculated production matched historic volumes at Hampston and Towner. Also, the match between the simulator-calculated FBHPs and the historic WHFPs improved at these 2 wells. However, simulator-calculated production at Daniels still is short of historic volumes though higher than that calculated in Run 7. Also, simulator-calculated cumulative production fell short of historic volumes in Schmelzel (Schml), Wilson (Wils), Muller (Mull), and Williams (Wilm).

RUN 9

It is evident from Figure 4.1d that the permeability distribution around Blackmer 28 (Blk28) in L4 (Winfield) is significantly higher than prevalent values elsewhere. These high permeability values cause the simulator-calculated gas production to match

historic production volumes from this well in Run 1 and other subsequent runs while the simulator-calculated BHFPs remain greater than the WHFPs. Thus the permeability distribution in the drainage area around Blk28 was multiplied by 0.06 to reduce it to the same level as permeability at other wells in Winfield. Figure 9.5.41 shows that this localized permeability adjustment resulted in a production history match and a reduction in the calculated BHFPs bringing it closer, though still higher, to the historic WHFPs.

Well matches still show excess gas in many of the wells (Figures 9.5.39 and 9.5.40). Figure 9.5.42A shows that the upscaled vertical-permeability (Kz) values (at HobEU) in the simulator model for L5 and L7 are an order higher or greater than those of L1, L3, and L9. The initial estimates for Kxy in the fine-layer model were upscaled using Petrel's® tensor-upscaling routine and then facies-specific correlations related to the horizontal permeability (Kxy) were used to estimate the Kz in each of the layers input to the simulator. It is evident from various simulation runs that relatively high Kz allows migration of gas from zones below the completed (fractured) layers into the well. Figure 9.5.42B shows that significant volumes (about 8 bcf) of gas were produced out of L8 (Fort Riley).

RUN 10

To reduce the availability of gas around most wells in the study area, the vertical permeability in L7 (B/Towanda) was reduced by multiplying the original permeability distribution by 0.1. Also, to increase production at Daniels (Dan) and Schmelzel (Schml) wells, ff factor (post 1970) was increased to 4.0 at Dan while the hydraulic fracturing in Schml was extended to L6 (post-1970) using ff = 1.0. Figures 9.5.43 and 9.5.44 show the resultant cumulative production and flowing pressure matches at individual wells. The production and pressure matches are close to historic values at most wells. However, wells such as EberF, EberU, Blackmer 25U, Blackmer 28, and Hoobler EU still show excess flow capacity as their BHFPs are higher than historic WHFPs. Muller (Mull) and Williams (Willm) are adjacent wells located at the southern border of the study area and both appear to run out of producible gas. The simulator-calculated production rates at the Mull well matches the post-1970 history though falling short during the pre-1970 production period.

RUN 11

In order to address excess production capacity in the above-mentioned wells, adjustments were made in the effectiveness of hydraulic fracturing on production at select wells. At Blackmer 28 (Blk28), the matrix permeability in the drainage area was reduced by multiplying the permeability distribution (in Run 9) by 0.67 in order to bring the permeability values closer to its neighboring wells. Also, the ff was reduced to 3.0 (from 6.0) in the post-1970 period for hydraulic fracturing at this well constrained already to L4 (Winfield). For the wells Blackmer 25 (Blk25) and Blackmer 25U (Blk25U), the ff was reduced to 1.0 in the post-1970 period. Also, ff values in the post-1970 period were reduced to 2.0 at Ebersole, to 1.0 at Ebersole F and Ebersole U, and to 3.0 at Hoobler EU. The results of individual well production and pressure matches are shown in Figures 9.5.45 and 9.5.46. Figure 9.5.47 summarizes the quality of matches obtained against

production and pressure histories at each well and also the presence or absence of production spikes when wells were flowed free of rate constraints. Close production and pressure history matches have been obtained at majority of the wells. However, most wells still show a production spike when released of flow constraints. Simulator-calculated production fell short of historic rates at two wells, namely Muller (Mull) and Williams (Willm), which are located at the southern border of the study area.

Figure 9.5.48A shows the average pore-volume weighted pressures at L1, L2, L4, L6, and L8 over the production life of the field. Figure 9.5.48B compares the simulator-calculated average pore-volume weighted reservoir pressure as of May 2006 with corresponding estimates of layer pressures from RFT tests carried out in and around the study area. Figure 9.5.49 shows that despite no wells being completed in L8 (Fort Riley), about 6.4 bcf of gas has moved out of Fort Riley to layers above and to wells completed in L6 (Towanda) and L4 (Winfield). The volume of gas flowing across shale layers is dictated by the vertical permeability assigned to the shale layers.

Conclusions

The intent of the simulation study was to evaluate robustness of a geomodel developed using an automated facies-recognition technique anchored to a limited number of node wells in the study area, in this case only three in a 12-section area, and available facies-specific petrophysical data. The above-mentioned geomodel served as the basis for this reservoir simulation study. The goal for this study was to see how closely the simulator could match the production and pressure histories of wells located in the geomodel with minimum modifications to the geomodel. Most geomodel modifications were applied all over the study area, such as using layer specific permeability multipliers. The only well-specific modifications made included varying productivity and reach of the hydraulic fractures.

1. Out of 16 wells, good matches with production histories were obtained at 13 wells.
2. Close to good matches were obtained with flowing-pressure histories at 12 out of the 16 wells in the study area.
3. Small to high production spikes were visible at seven out of 12 producing wells. Production spikes were not visible at the three wells where the simulator-calculated production fell short of historic volumes.
4. The pore-volume weighted average layer pressures in L1 (Herington), L2 (Krider), L4 (Winfield), L6 (Towanda), and L8 (Fort Riley) matched closely with corresponding estimated pressures from available RFT data.
5. It appears that the reservoir is more complex than the model input to the simulator because some of the wells show presence of excess flow capacity while others remain short of gas. The complexity of the reservoir is further revealed by a closer look at individual well performances such as Blackmer 28 (Blk28), where the simulator-calculated bottom-hole flowing pressures exceed historic surface-flowing pressures indicating excess flow capacity and yet the same well fails to meet the historically recorded gas volumes after the year 2000. Also, the

simulator is unable to match production history at Muller (Mull) even in the pre-1970 period. Thus, any field-wide increase in layer permeability or layer OGIP to obtain production match will result in excess flow capacity at wells where production history matches have already been achieved.

6. None of the wells has been completed in Fort Riley (L8), and yet 6.4 bcf of gas flowed out of this layer to layers above and to the wells completed in Winfield (L4) and Towanda (L6). Based on the layer-specific gas-in-place plots, it appears that fluid movement is taking place across the shale layers with vertical permeability playing a critical role in determining the amount of fluid flow in shale.

Reference:

Dubois, M. K., Byrnes, A. P., Carr, T. R., Bohling, G. C., and Doveton, J. H., in press, Multiscale geologic and petrophysical modeling of the giant Hugoton gas field (Permian), Kansas and Oklahoma, *in* P. M. Harris and L. J. Weber eds., Giant reservoirs of the world: From rocks to reservoir characterization and modeling, AAPG Memoir 88.

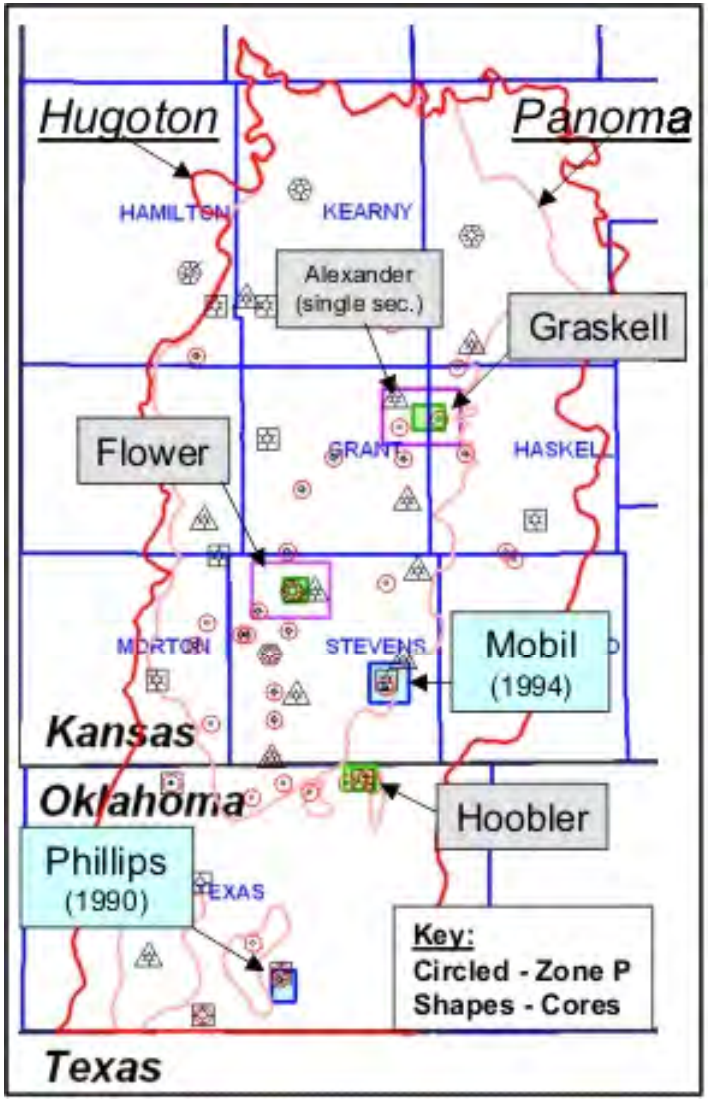

Figure 9.5.1. Map showing location of the Hoobler study area in the Hugoton and Panoma fields.

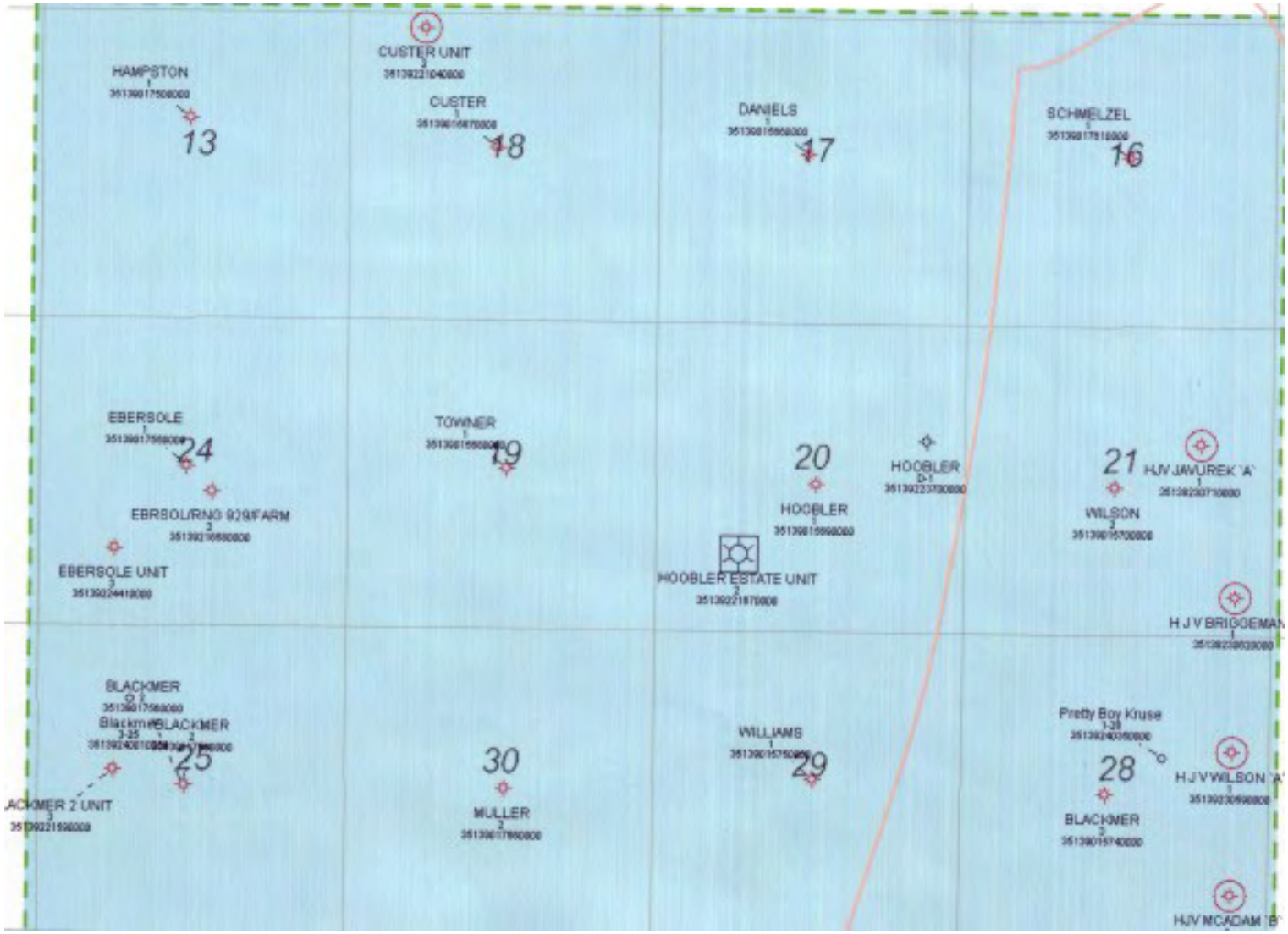

Figure 9.5.2. Map showing the locations of the Chase wells in the Hoobler study area.

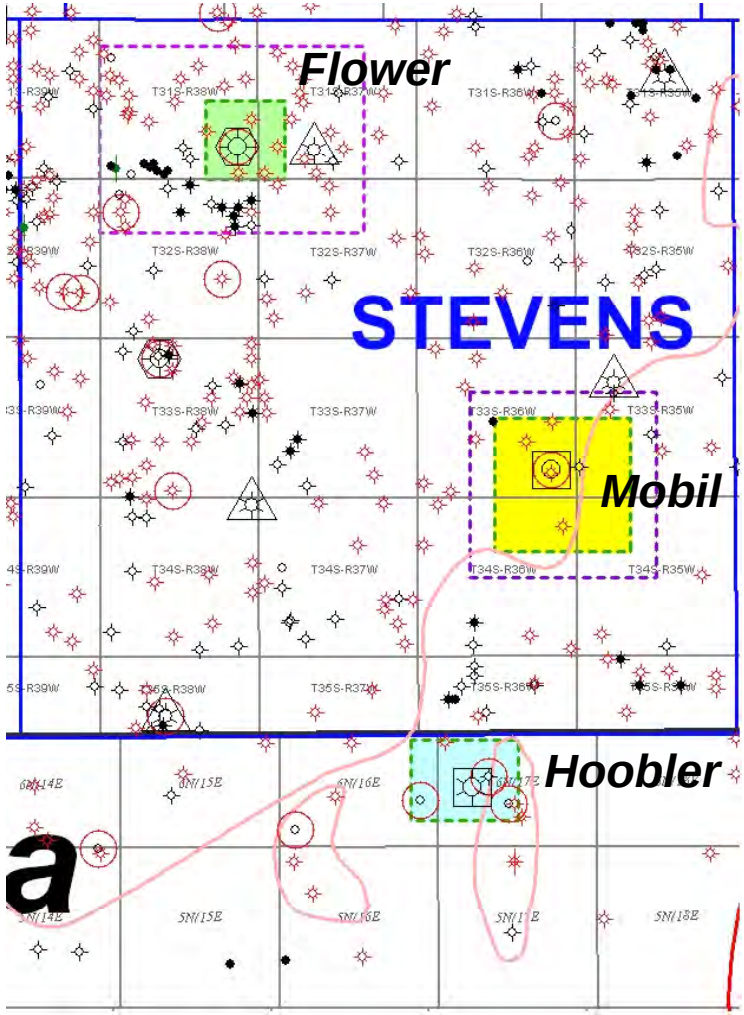

Figure 9.5.3. Map showing node wells in and around the Hoobler study area that were used in Geomod 4 to build a full-field model. Wells with pressure data are shown circled.

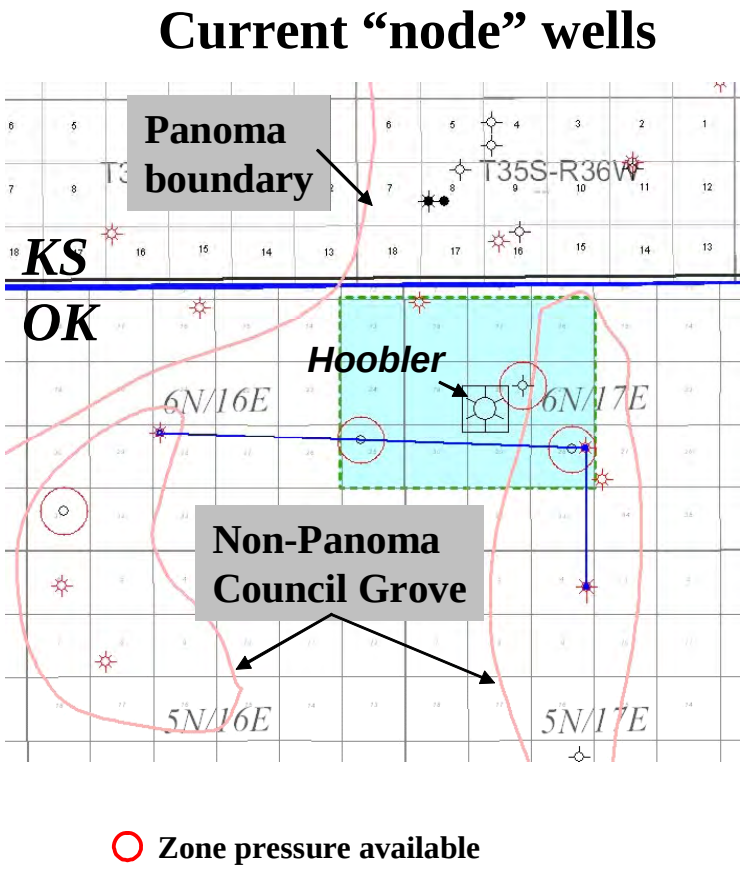

Figure 9.5.4. Map showing location of wells with available RFT data in and around the Hoobler study area.

Hoobler model extraction

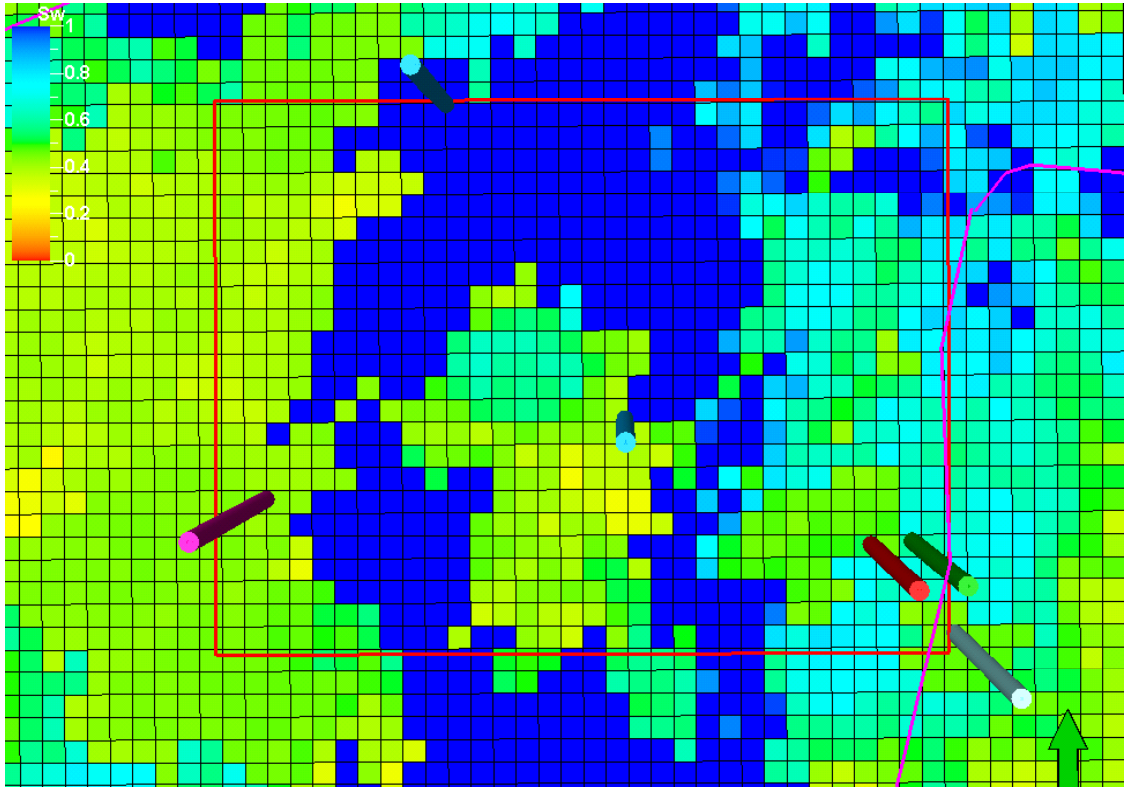

Figure 9.5.5. Map view of water saturation for top layer in the Herington in Geomod4. Outline of Hoobler area is marked in red. Wells shown are the model “node” wells with qualified log data.

Upscaling petrophysical properties

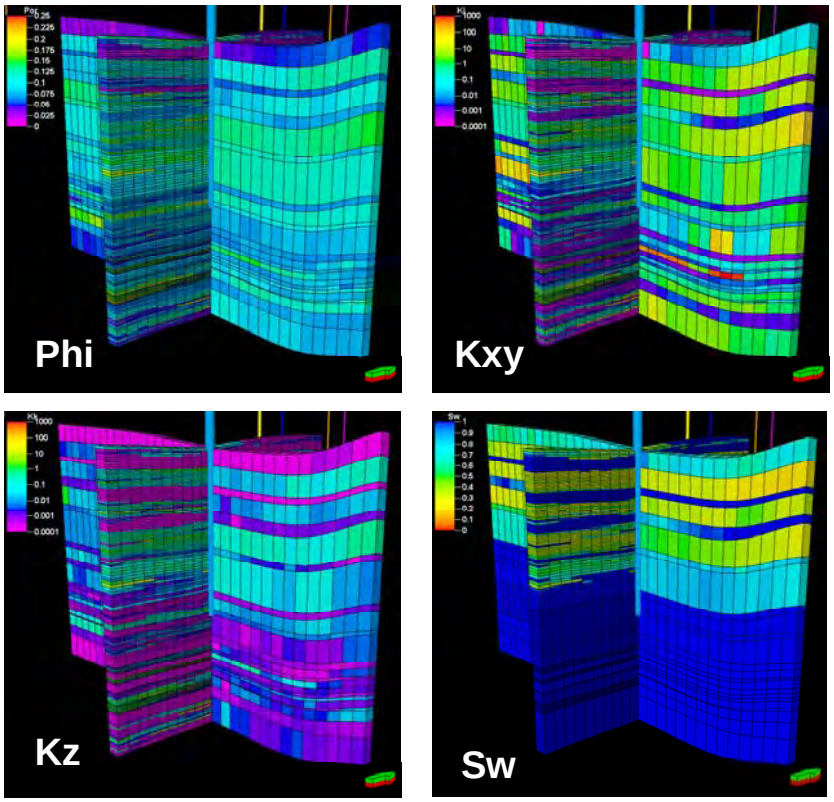

Figure 9.5.6. Porosity, permeability, and water saturation upscaled from 269 layers to 24 layers, one layer per zone in the Chase and Council Grove.

Hoobler 11-layer model -OGIP

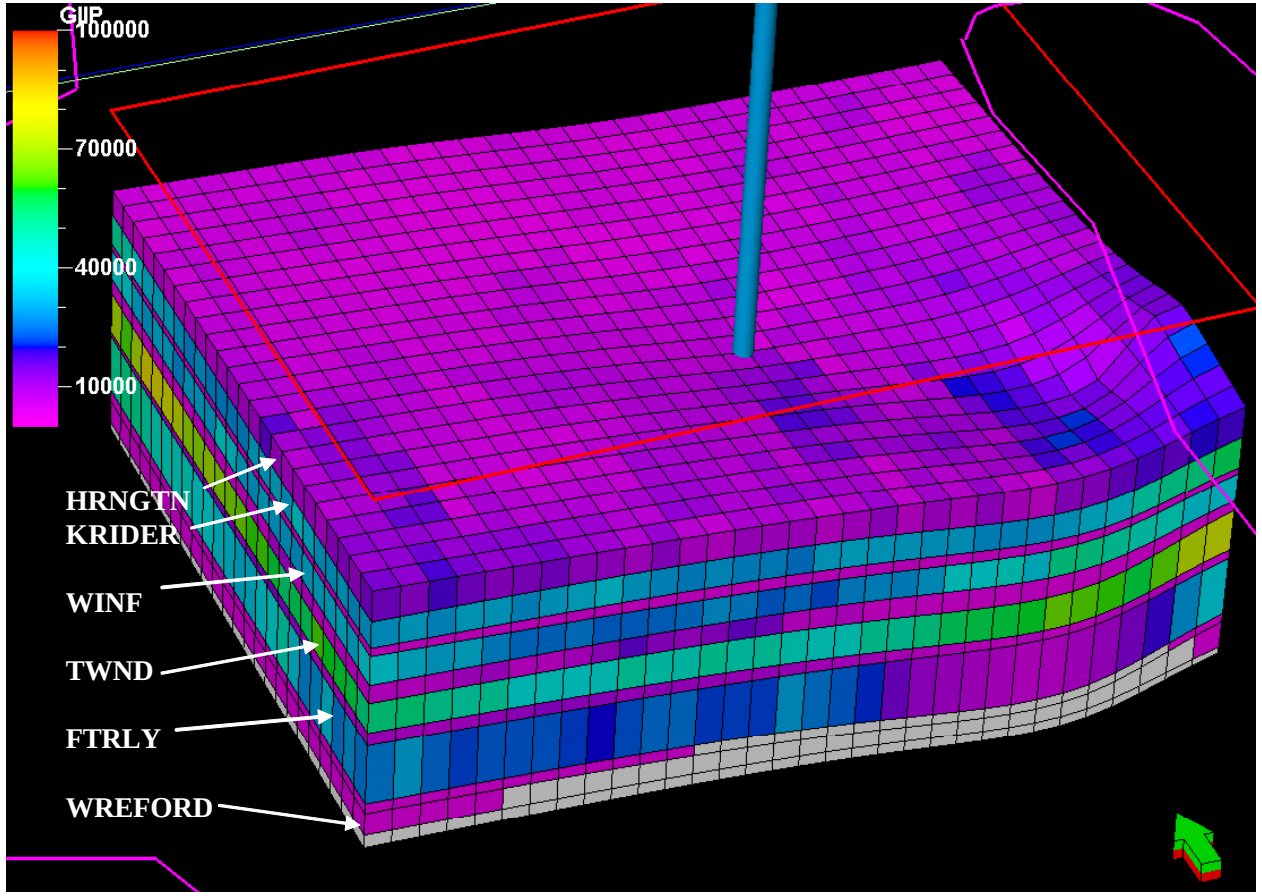

Figure 9.5.7. Distribution of gas-in-place (GIP) for the 11-layer model with a FWL at +65 ft above sea level. Hoobler well bore is shown located in the middle of the study area.

Hoobler 11-layer model – other properties

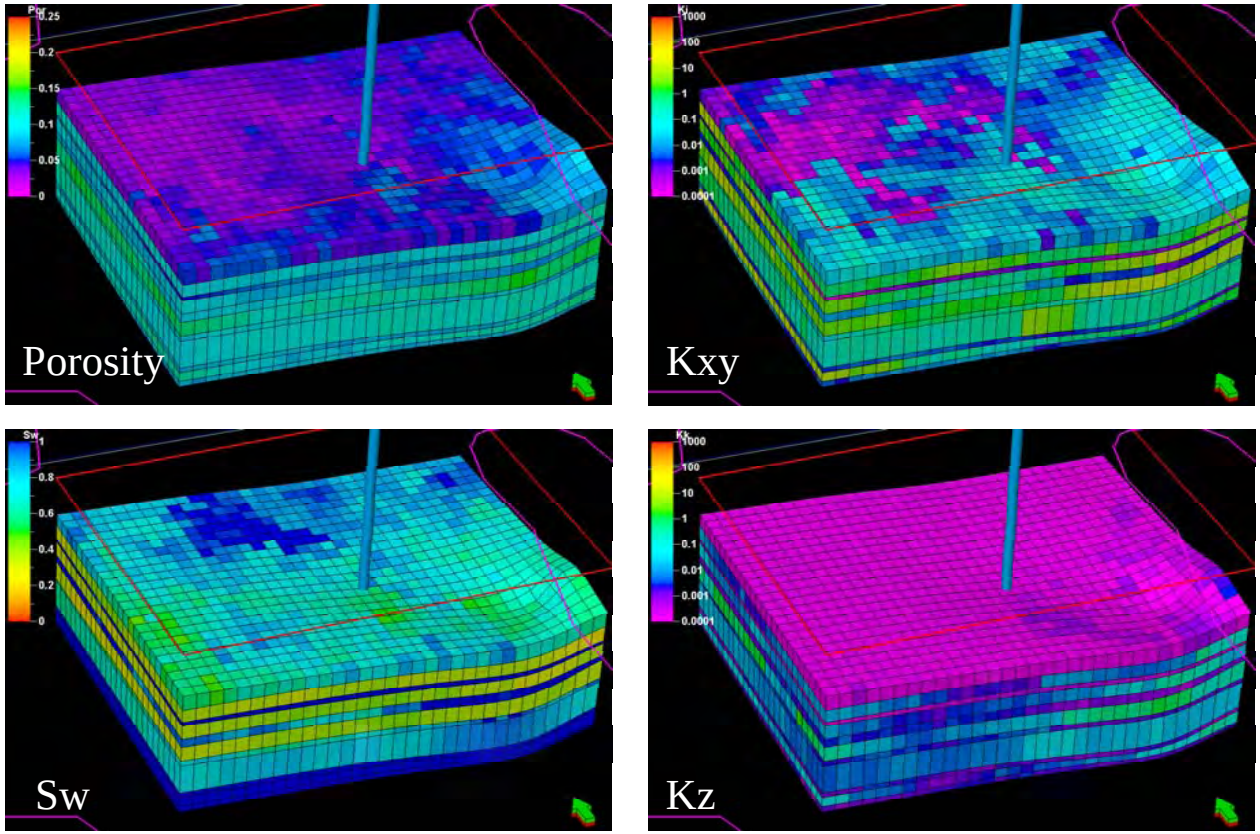

Figure 9.5.8. Distribution of upscaled petrophysical properties in the Hoobler 11-layer model. Hoobler well bore is shown located in the middle of the study area.

$$PHI\_CORR = A + B*DPHI + C*NPHI$$

	Intercept A	PHID B	PHIN C
Facies 1 & 2	0.018	0.843	0.000
Facies 3 & 4	0.019	0.662	0.000
Facies 5 & 7 & 8	4.278	0.400	0.209
Facies 6	0.000	0.500	0.500
Facies 9	8.918	0.447	0.131
Facies 10	4.484	0.524	0.135

Figure 9.5.9. Equation and set of constants by lithofacies developed from regression analysis of core-to-log porosity data.

Assumed PVT properties:			
Reference pressure	465	psi	
Rock compressibility	0.000002	1/psi	(assumed)
Reservoir temp	90	F	
Gas gravity (Air = 1.0)	0.715		
Water salinity	110,000	ppm	

Figure 9.5.10. PVT properties input to the simulator.

Layer	Depth	WC Phi	WC K, md
Krider	2753	7.7	0.18
Krider	2754	7.9	0.15
Krider	2755	8.3	0.11
Krider	2756	10.8	0.2
Krider	2757	11.8	2.08
Krider	2758	12.5	3.14
Krider	2759	14.4	3.67
Krider	2760	14.7	4.23
Krider	2761	14.4	4.23
Krider	2762	14.6	4.23
Krider	2763	14.4	4.23
Krider	2764	13.3	1.56
Krider	2765	11.1	0.36
Krider	2766	12.1	1.46
Krider	2767	12.7	4.5
Krider	2768	12.1	1.45
Krider	2769	11.8	0.9
Krider	2770	13.1	1.85
Krider	2771	13.6	1.76
Krider	2772	10.1	0.59
Krider	2773	10.8	0.83
Krider	2774	11.4	1.29
Krider	2775	10.7	0.82
Krider	2776	12.4	1.65
Krider	2777	11.5	1.76
Krider	2778	11.3	1.98
Krider	2779	12.1	5.78
Krider	2780	13	3.73
Krider	2781	12.2	3.29
Krider	2782	12.6	3.43
Krider	2783	10.2	1.8
Krider	2784	10.9	1.46
Krider	2785	9.8	1.21
Krider	2786	12.8	2.92
Krider	2788	11	5.1
Krider	2789	9.9	4.5
Krider	2790	10.1	3.09
Krider	2791	9.6	1.71
Krider	2792	8	0.35

L2 (Krider) Mean K = 2.24 md

Added multiplier of 2 can be used

Layer	Depth	WC Phi	WC K, md
Winfield	2811	4.5	0.02
Winfield	2812	6.7	0.22
Winfield	2813	3.1	0.06
Winfield	2814	3.3	0.88
Winfield	2815	4.2	0.35
Winfield	2816	4.3	37.86
Winfield	2817	6	0.81
Winfield	2818	7.7	0.36
Winfield	2822	12.9	0.73
Winfield	2823	13.2	1.84
Winfield	2824	9.1	0.73
Winfield	2825	6.9	0.1
Winfield	2826	7.4	0.03
Winfield	2827	7.5	0.12
Winfield	2828	10	1.37
Winfield	2829	8.7	0.44
Winfield	2830	7	0.14
Winfield	2831	5.7	0.06
Winfield	2832	11.4	0.92
Winfield	2833	16.8	8.35
Winfield	2834	13.9	13.94
Winfield	2835	17.3	13.95
Winfield	2836	14.3	4.12
Winfield	2837	12.5	2.89
Winfield	2838	12.1	3.5
Winfield	2839	10.7	2.26
Winfield	2840	8.4	0.94
Winfield	2841	5.5	0.09
Winfield	2842	6.9	0.02

Avg with 37.86	3.34
Avg without 37.86	2.11

Added multiplier of 2 can be used

(Except drainage of Blk28)

Mean K = 0.93 md

Layer	Depth	WC Phi	WC K, md
Towanda	2868	15.2	0.37
Towanda	2869	15.7	0.57
Towanda	2870	16.3	0.57
Towanda	2871	17	0.57
Towanda	2872	17.4	0.65
Towanda	2873	17.4	1
Towanda	2874	17.5	1.75
Towanda	2875	17.5	1.75
Towanda	2876	17.1	1.07
Towanda	2877	15	0.53
Towanda	2878	12.8	0.42
Towanda	2879	13.1	0.21
Towanda	2880	13	0.2
Towanda	2881	13	0.16
Towanda	2882	11.2	0.07
Towanda	2883	10.8	0.04
Towanda	2884	11.5	0.04
Towanda	2885	12.3	0.08
Towanda	2886	12.3	0.14
Towanda	2887	12.6	0.28
Towanda	2888	13.5	0.53
Towanda	2889	14.3	1.21
Towanda	2890	14.1	1.76
Towanda	2891	14.5	1.76
Towanda	2892	15.4	1.99
Towanda	2893	16	3.97
Towanda	2894	15.5	0.83
Towanda	2895	12.7	0.53
Towanda	2896	13.2	0.53
Towanda	2897	14.5	0.56
Towanda	2898	14.4	1.1
Towanda	2899	14.2	1.87
Towanda	2900	14.1	1.99
Towanda	2901	14	1.99
Towanda	2902	13.9	1.99
Towanda	2903	13.8	1.87
Towanda	2904	13.7	1.27
Towanda	2905	13.6	0.89
Towanda	2906	13.1	0.39
Towanda	2907	12.6	0.39
Towanda	2908	13.7	0.6
Towanda	2909	13.5	0.82
Towanda	2910	13.5	0.44
Towanda	2912	15.4	0.39
Towanda	2913	16.5	0.78
Towanda	2914	15.7	1.87
Towanda	2915	14	0.83

Figure 9.5.11. Whole-core porosity and permeability measurements from different Chase intervals measured on core taken at the Hoobler EU well.

Model	Formation	Core Kxy (mean)	Model Kxy	Model Kz	Multiplier
1	Herrington	0.286	0.0274	0.000005	10.4
2	Krider	2.246	1.7833	0.036	1.3
3	Odell	0.067	0.0005	0.000007	134.0
4	Winfield	3.348	2.2702	0.00138	1.5
5	Gage	0.359	0.0077	0.0016	46.6
6	Towanda	0.928	1.126	0.0586	0.8
7	B/TWND	0.3	0.0385	0.00323	7.8
8	Ft. Riley	0.215	0.2929	0.0273	0.7
9	Matfield	1.518	0.0032	0.00068	474.4
10	Wreford	0.315	1.21	0.027	0.3
11	A1-SH		0.0029	0.0011	

A multiplier significantly greater than 1.0, i.e., 10.4, is calculated for this layer where the core Kxy is less than 0.5 md, i.e., 0.286 md.

Exception: A multiplier close to 1.0, i.e., 0.7, is calculated for this layer where the core Kxy is less than 0.5 md (i.e., 0.215).

Figure 9.5.12. Multiplier applied to each layer to convert permeability estimated from facies-specific porosity-permeability correlations to the corresponding upscaled permeability from whole-core measurements taken from the corresponding layer.

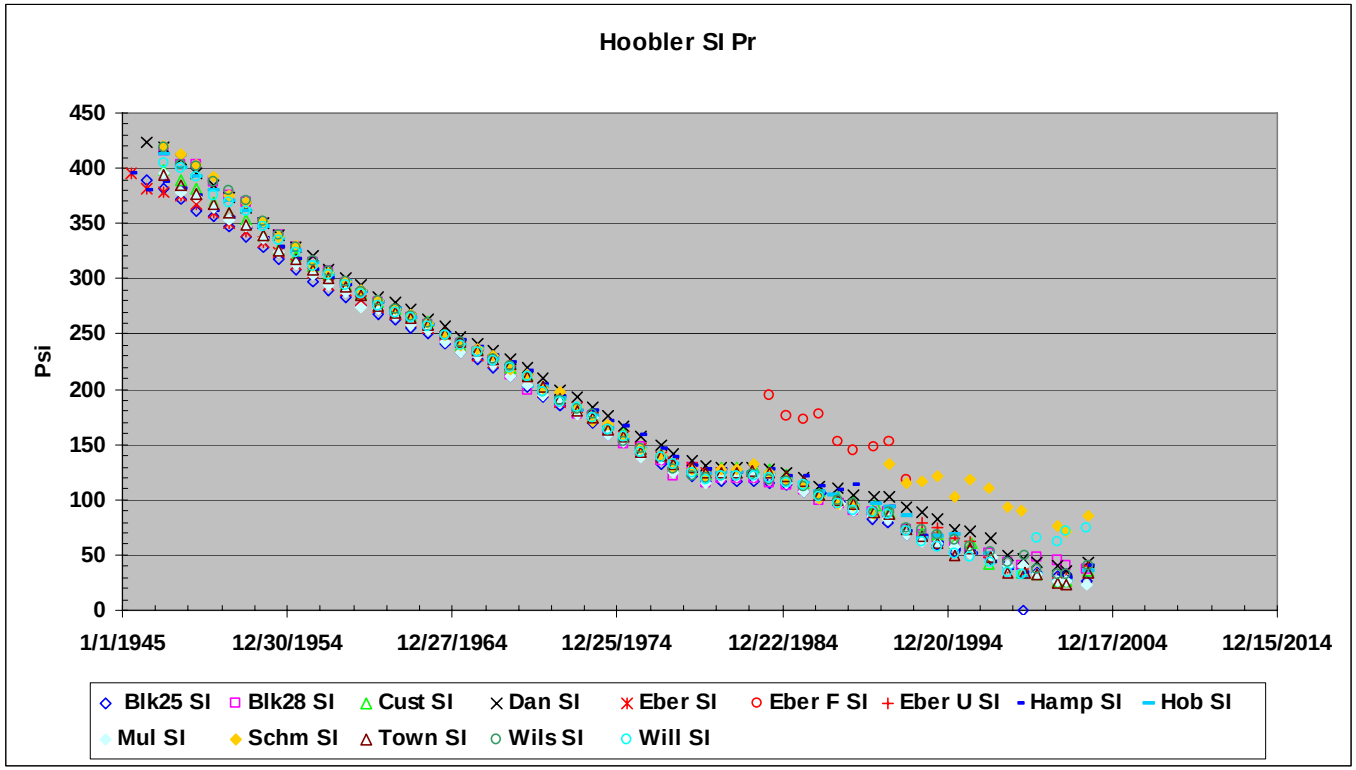

Figure 9.5.13. Plot of surface shut-in pressures at Chase wells in the Hoobler area over time.

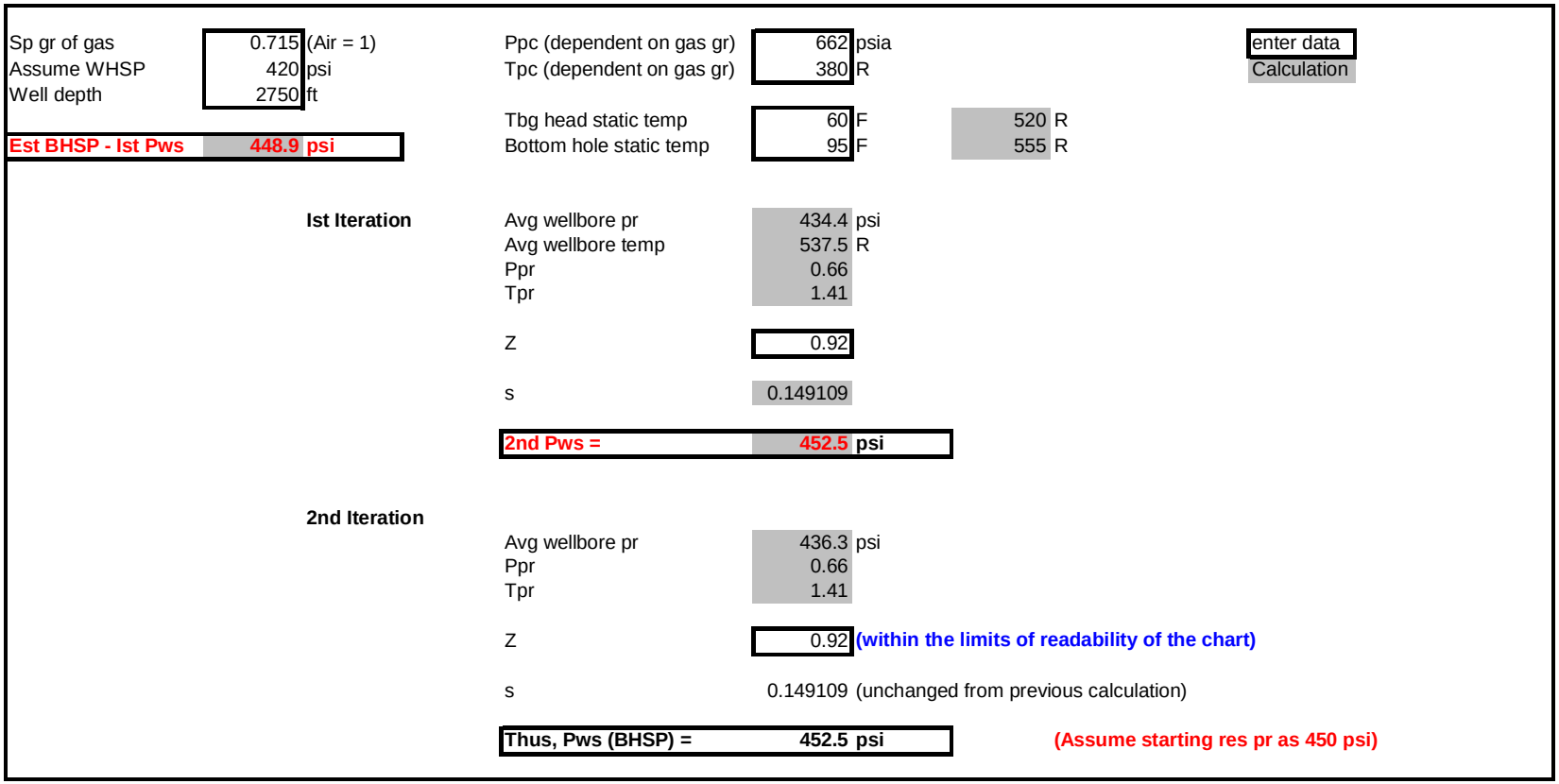

Figure 9.5.14. Calculation flow chart to convert surface shut-in pressures to sub surface shut-in pressures.

Layer	Name	Petrel OGIP, bcf	Sim OGIP, bcf
1	Hrngtn	4	4.2
2	Krider	31	30.8
3	Odell	0	0.0123
4	Winf	23	23.1
5	Gage	2	1.89
6	Twnd	42	42.85
7	B/Twnd	3	3.04
8	Ftrly	23	25.19
9	Matfield	0	0
10	Wreford	0	0.0097
11	A1_ SH	0	0
At 450 psi, bcf OGIP		**128**	**131.1**

Figure 9.5.15. Layer-specific gas-in-place (GIP) in the geomodel input to the simulator assuming initial-reservoir pressure of 450 psi.

						Total Prod, bcf	70.13
	Well	Sim Name	Start Prod	X address	Y address	Perf Layers	Cum, mcf
1	Blackmer 25	Blk25	9/1/1946	3	20	1-2-3-4	6,321,500
2	Blackmer 25U	Blk25U	4/1/1987	1	19	1-2-3-4	
3	Blackmer 28	Blk28	2/1/1947	27	20		3,731,024
4	Custer	Cust	2/1/1947	12	3		6,020,519
5	Daniels	Dan	7/1/1946	20	4		8,356,932
6	Ebersole	Eber	7/1/1941	4	11	2-3-4	5,278,760
7	Ebersole F	EberF	11/1/1982	4	12	1-2-3-4	271,689
8	Ebersole U	EberU	12/1/1992	2	13	2-3-4	903,085
9	Hampston	Hamp	5/1/1941	4	2	1-2-3-4	9,230,934
10	Hobbler	Hob	1/1/1947	20	12		4,436,418
11	HobbE	HobEU	6/1/1987	18	14	1-2-3-4	
12	Muller	Mull	10/1/1946	12	20	1-2-3-4	5,539,541
13	Schmelzel	Schml	12/1/1946	28	4	1-2-3-4	7,345,449
14	Towner	Town	9/1/1946	12	12		4,532,704
15	Willams	Willm	2/1/1947	20	20		4,021,503
16	Wilson	Wils	2/1/1947	28	12		4,137,886

Figure 9.5.16. Production-start dates, initial-completion intervals, and cumulative production at the Chase wells in the Hoobler study area.

A.

							Total Prod, bcf	70.13
	Well	Sim Name	Start Prod	X address	Y address	Perf Layers	Spud date	Cum, mcf
1	Blk25	Blk25	9/1/1946	3	20	1-2-3-4	7/25/1946	6,321,500
2	Blk25U	Blk25U	4/1/1987	1	19	1-2-3-4	1/27/1987	
3	Blk28	Blk28	2/1/1947	27	20		1/1/1947	3,731,024
4	Custer	Cust	2/1/1947	12	3		1/1/1947	6,020,519
5	Daniels	Dan	7/1/1946	20	4		1/1/1946	8,356,932
6	Ebersole	Eber	7/1/1941	4	11	2-3-4	5/21/1940	5,278,760
7	Ebersole F	EberF	11/1/1982	4	12	1-2-3-4	5/29/1982	271,689
8	Ebersole U	EberU	12/1/1992	2	13	2-3-4	9/11/1992	903,085
9	Hampston	Hamp	5/1/1941	4	2	1-2-3-4	3/19/1940	9,230,934
10	Hobbler	Hob	1/1/1947	20	12		1/1/1947	4,436,418
11	HobbE	HobEU	6/1/1987	18	14	1-2-3-4	5/8/1987	
12	Muller	Mull	10/1/1946	12	20	1-2-3-4	8/22/1946	5,539,541
13	Schmelzel	Schml	12/1/1946	28	4	1-2-3-4	10/26/1946	7,345,449
14	Towner	Town	9/1/1946	12	12		1/1/1946	4,532,704
15	Willams	Willm	2/1/1947	20	20		1/1/1947	4,021,503
16	Wilson	Wils	2/1/1947	28	12		1/1/1946	4,137,886

B.

		OGIP in top 4 layers, bcf	58.1	
Layer	Name	Marty's OGIP	Sim OGIP	Comments
1	Hrngtn	4	4.2	
2	Krider	31	30.8	
3	Odell	0	0.0123	Increasing OGIP with trime
4	Winf	23	23.1	

Figure 9.5.17. A) Initial-completion records indicate Chase wells completions to be restricted to the top four layers (L1 to L4). B) Gas-in-place in the first 4 layers of the geomodel input to the simulation.

Sim 6 – 11-layer model, ff = 6, K multi on pay

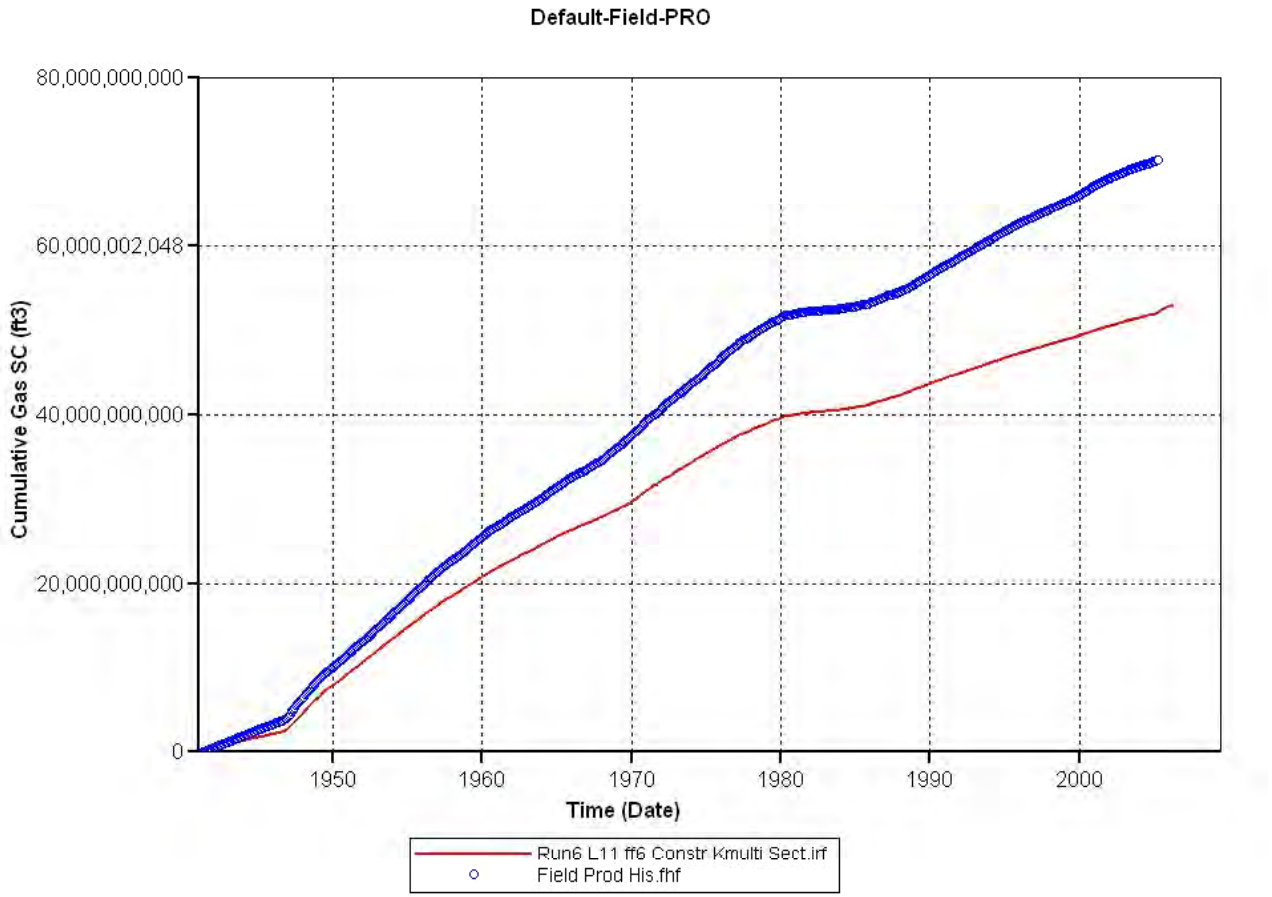

Figure 9.5.18. RUN 1 Results – Simulator-calculated cumulative production from Chase wells compared to historic volumes.

Sim 6 – 11-layer model, ff = 6, K multi on pay

Blue – Prod his, Red – Sim Prod, Green – Sim FBHP, Magenta – Pr His

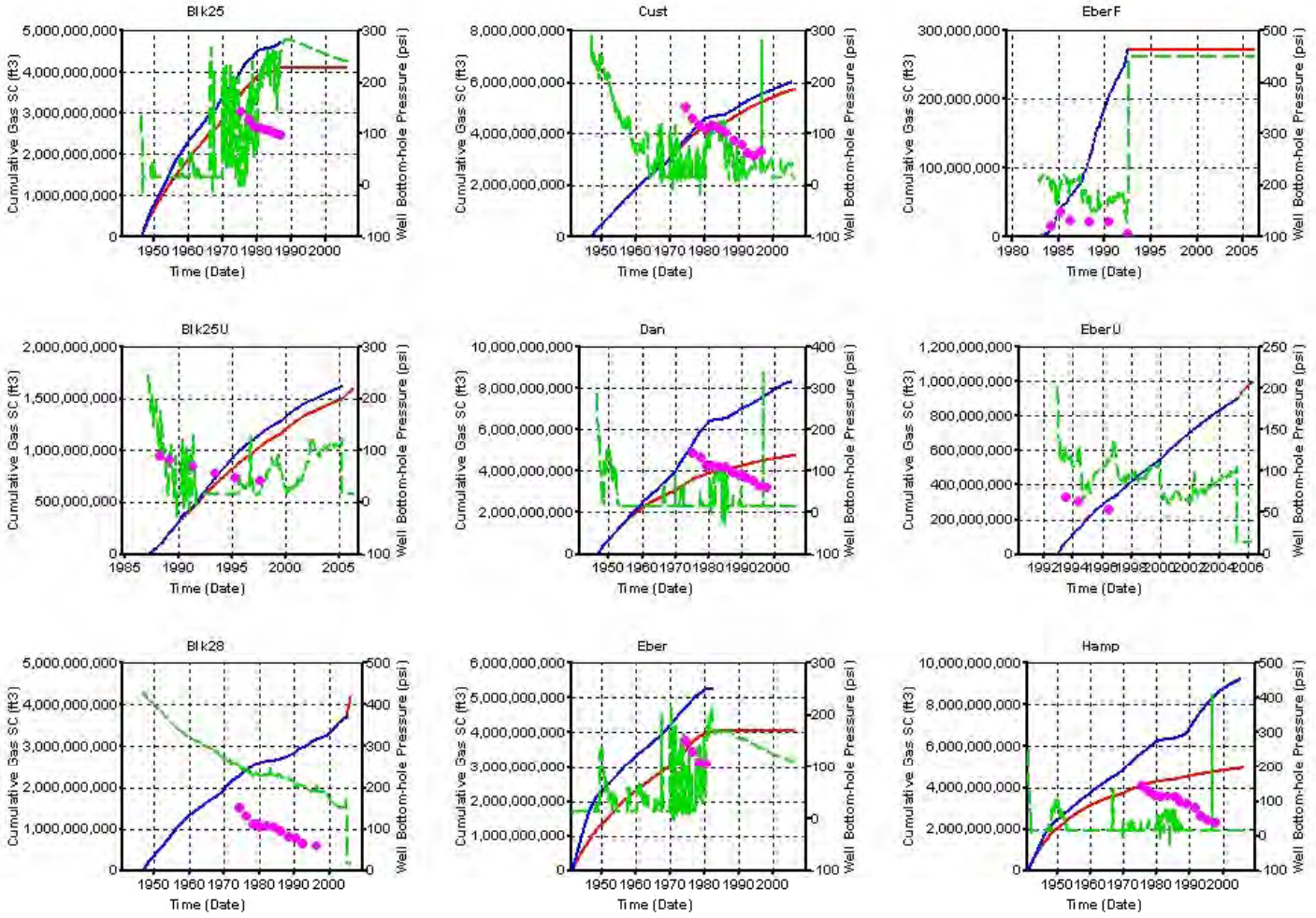

Figure 9.5.19. RUN 1 Results – Cumulative production- and pressure-history matches obtained at the Chase wells.

Sim 6 – L11, ff = 6, K multi on pay

Blue – Prod his, Red – Sim Prod, Green – Sim FBHP, Magenta – Pr His

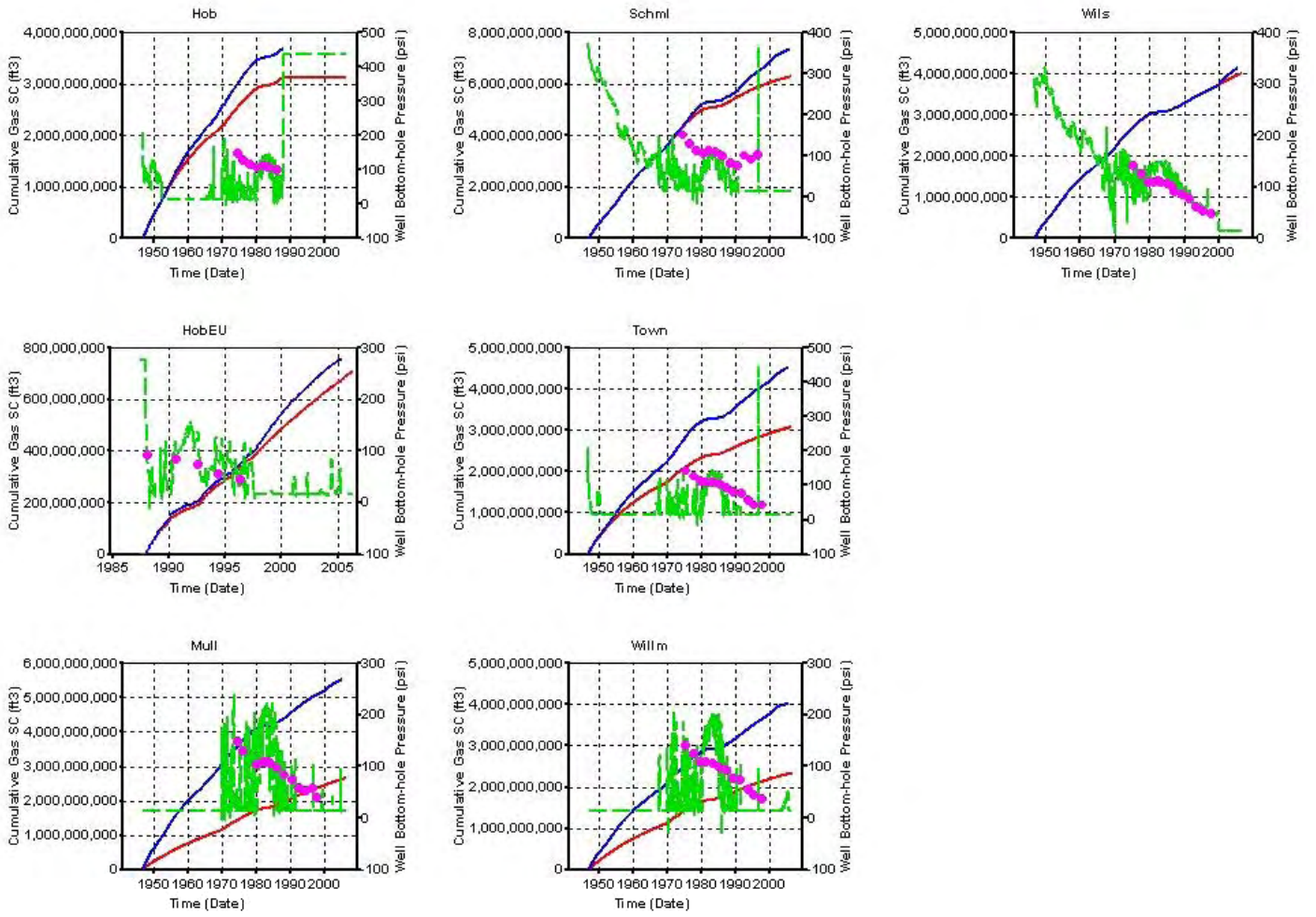

Figure 9.5.20. RUN 1 Results – Cumulative production- and pressure-history matches obtained at the Chase wells.

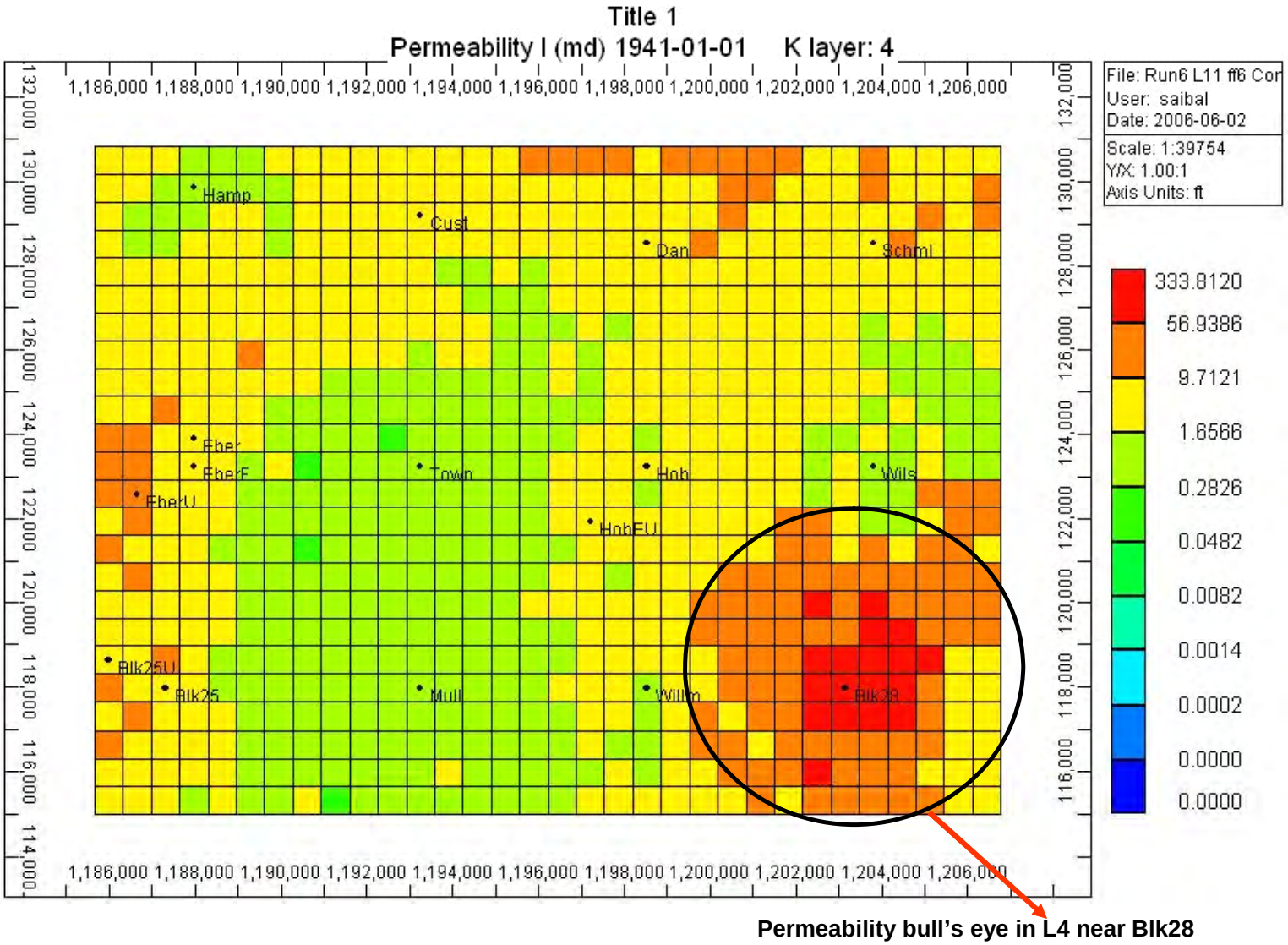

Figure 9.5.21. Bull's eye in the estimated permeability distribution for Winfield (Layer 4) input to the simulator.

RFT Pressures - Hoobler

If we assume the following:

1. **WHSIP adjusted to BHP is the likely lowest-pressure, highest-permeability zone**
2. **RFT's are likely to be too high by a considerable margin**
3. **Towanda was not regularly completed**
4. **Krider and Winfield have approximately equal permeability and depletion**
5. **Initial BHP = 450 psig (adjusted from IWHSIP)**

The following pressures may be expected at individual layers as of 2005:

Herrington	**200+ psi**	**Probably poorly drained. No test info**
Krider	**40-60 psi**	
Winfield	**40-60 psi**	
Towanda	**150-300 psi**	**Variable. Dependent on communication**
Ft Riley	**450 psi**	**Not drained; too far below completed intervals**

(above are best guesses and should be considered a starting point)

Figure 9.5.22. List of best-estimated layer pressure as of 2005 based on available RFT data from wells in and around the Hoobler study area.

Sim 6 – L11, ff = 6, K multi on pay

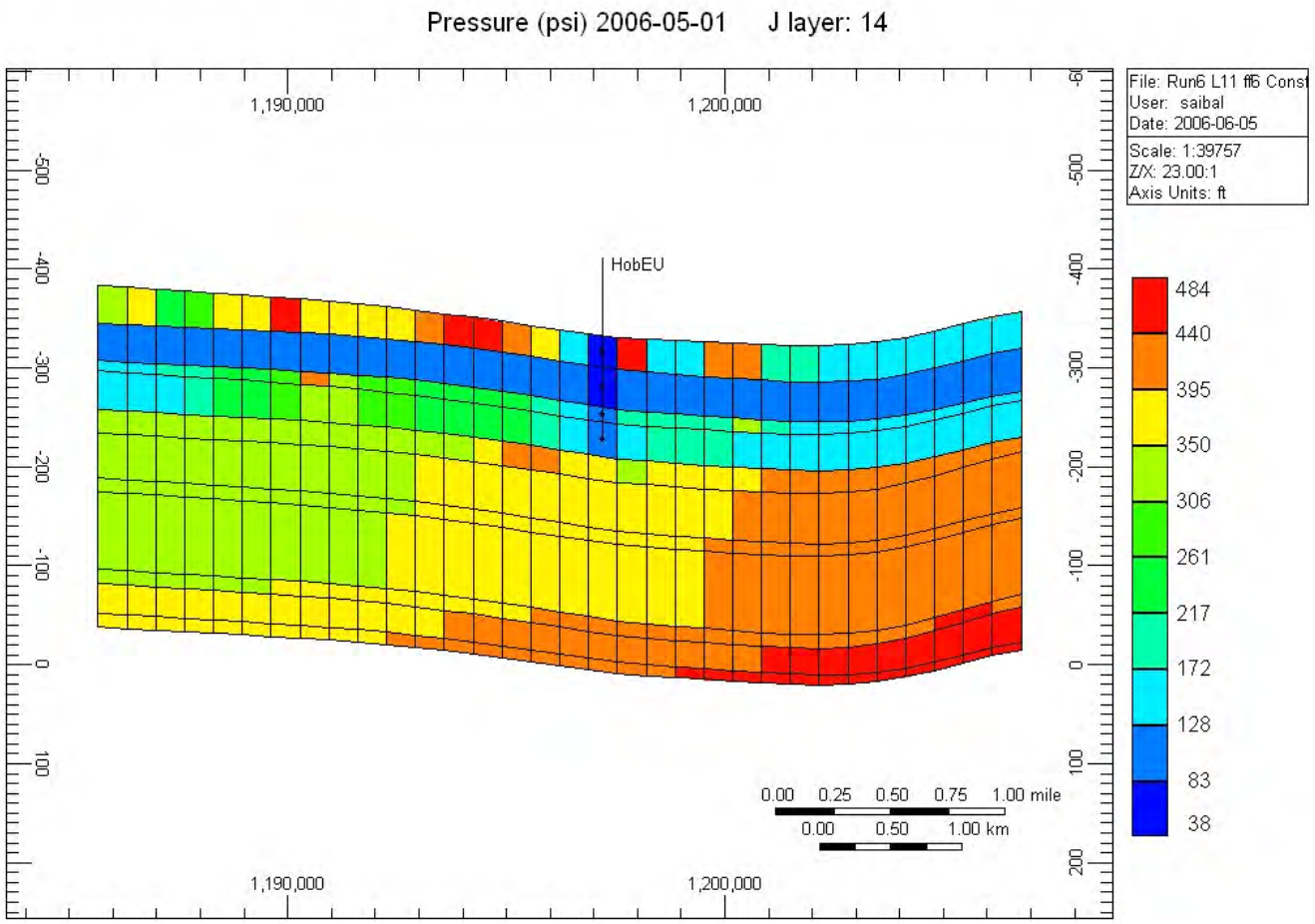

Figure 9.5.23. RUN 1 Results – Simulator-calculated pressure distribution along an east-west cross section through the Hoobler EU well as of May 2006.

Sim 7: L2 (Krider) Kxy*2 (on starting multiplier)

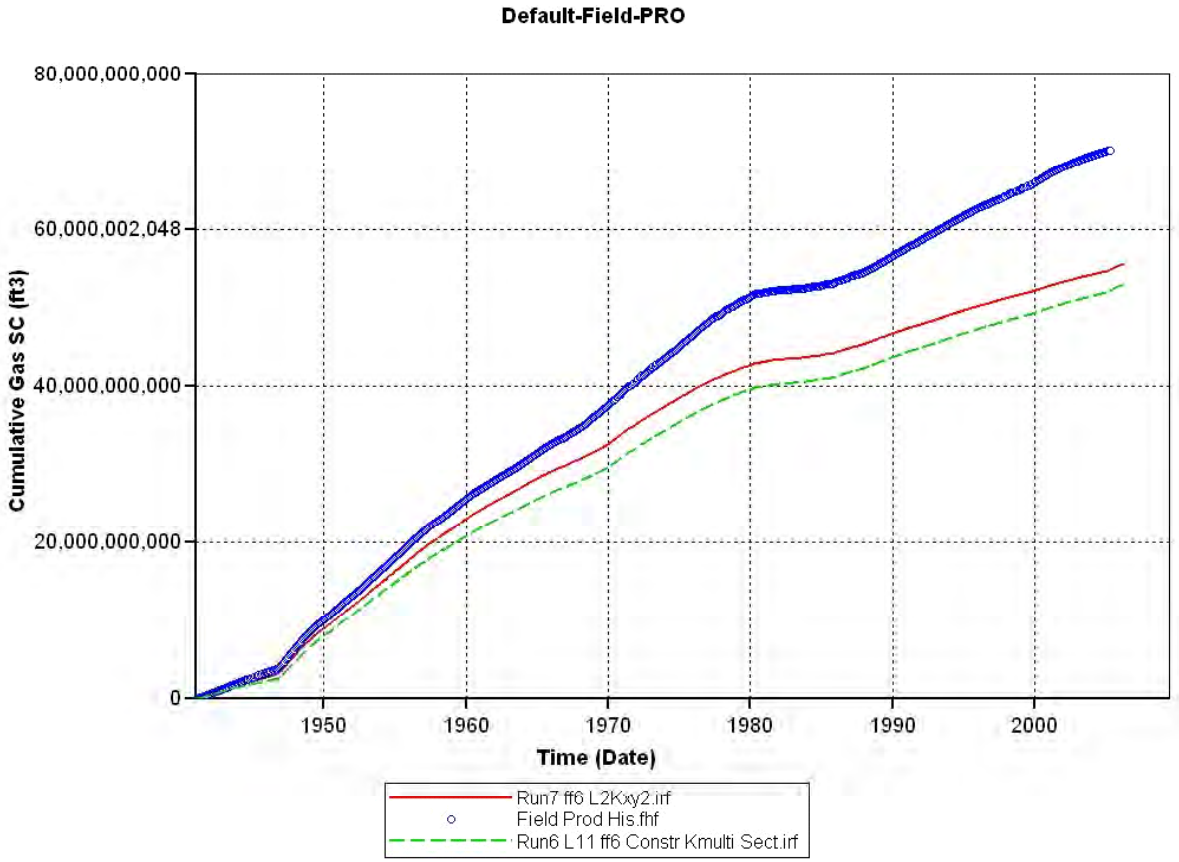

Figure 9.5.24. RUN 2 Results – Simulator-calculated field production from Hoobler area compared to historic volumes.

Sim 7: L2 (Krider) Kxy*2 (additional)

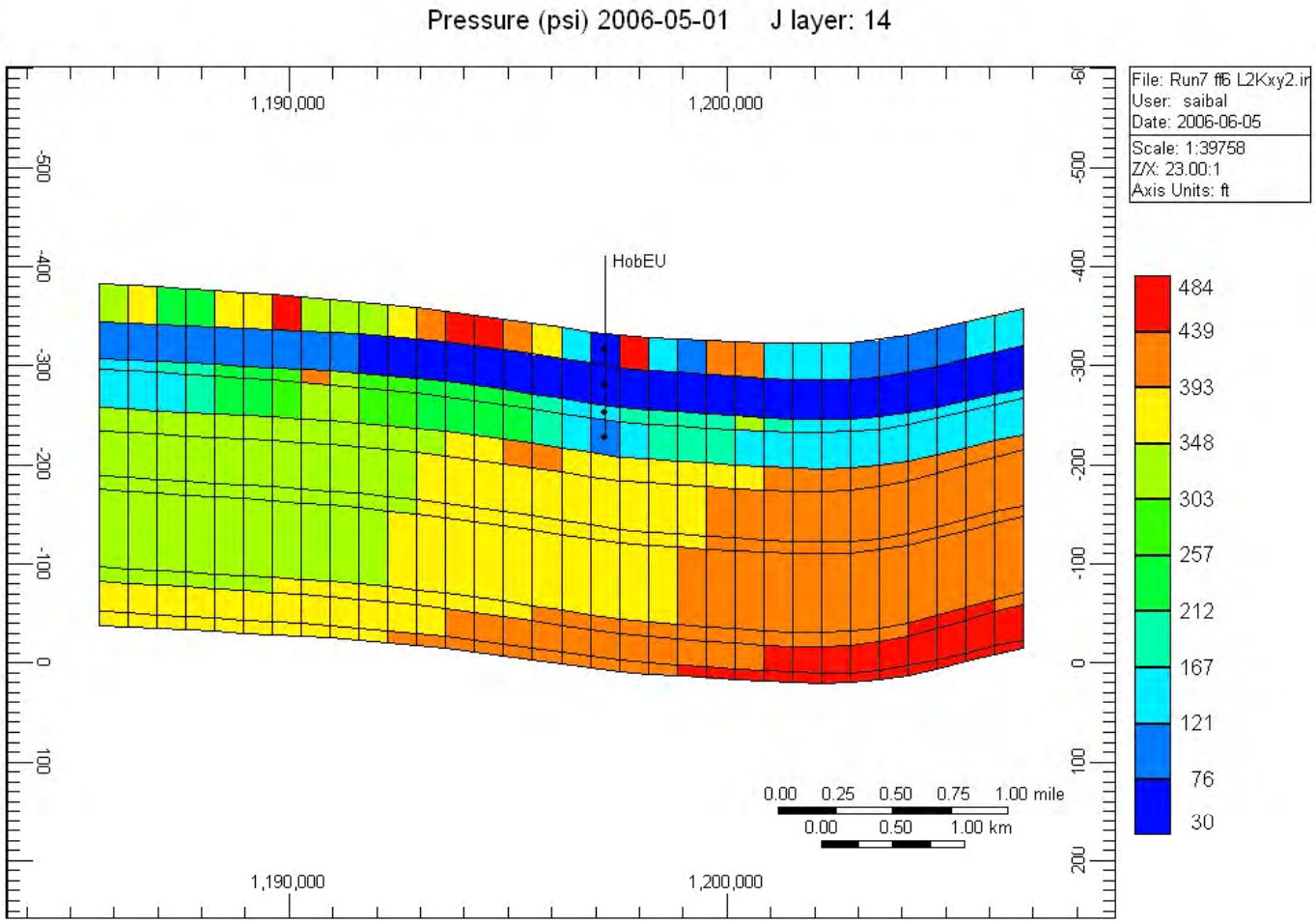

Figure 9.5.25. RUN 2 Results – Simulator-calculated pressure distribution along an east-west cross section through the Hoobler EU well as of May 2006.

Sim 8: L2 (Krider) and L4 (Winfield) Kxy*2 (on starting multiplier)

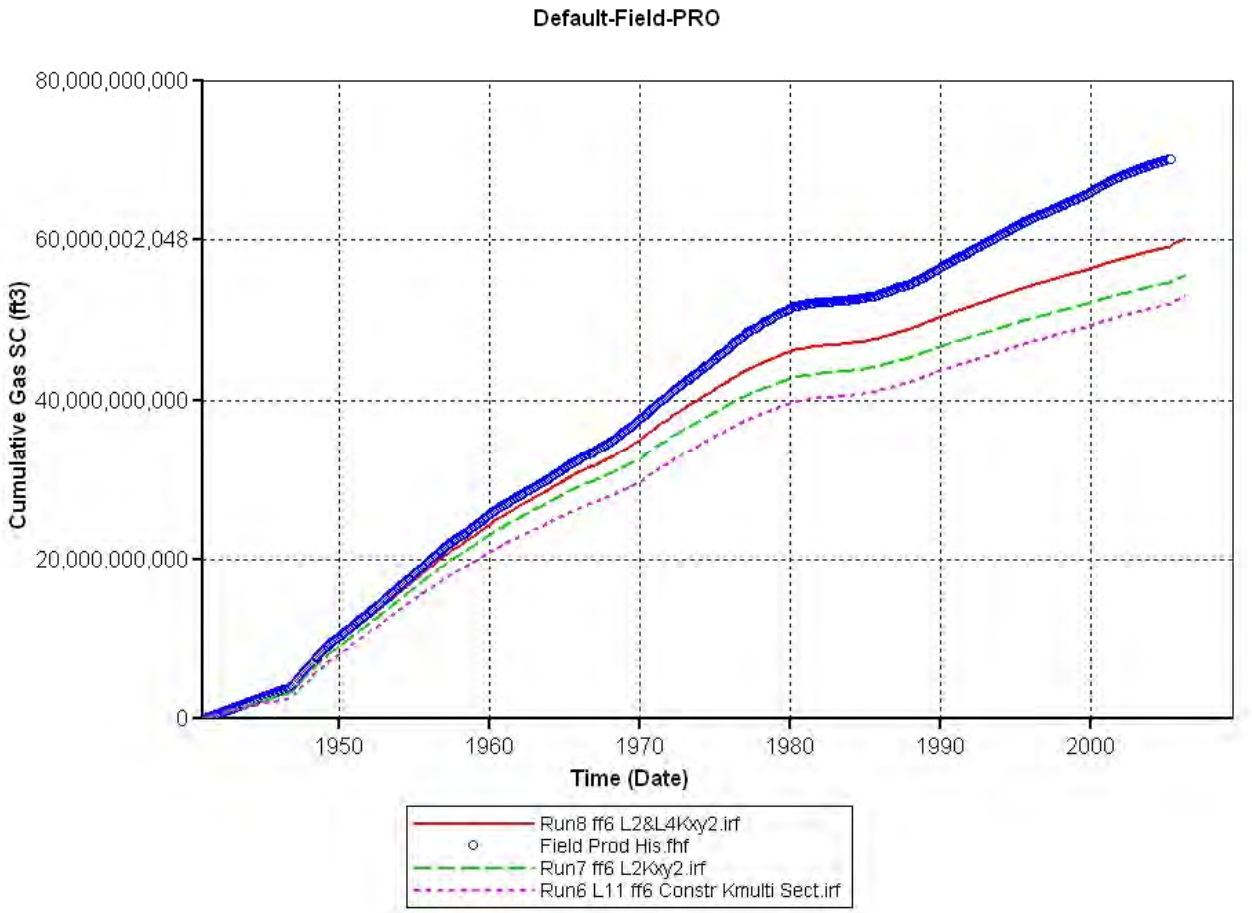

Figure 9.5.26. RUN 3 Results – Simulator-calculated field production from Hoobler area compared to historic volumes and those obtained from RUN 2 and 1.

Sim 8: L2 (Krider) and L4(Winfield) Kxy*2 (on starting multiplier)

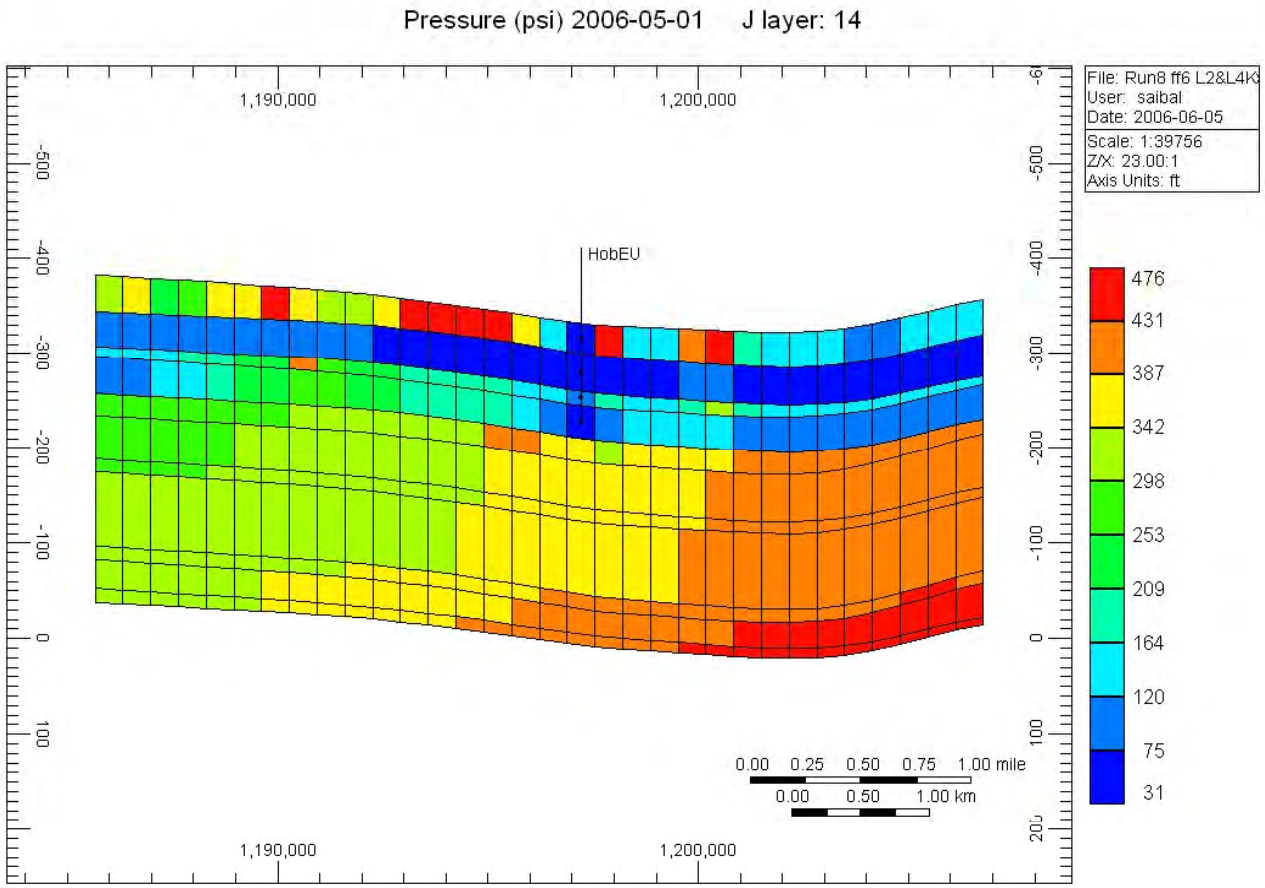

Figure 9.5.27. RUN 3 Results – Simulator-calculated pressure distribution along an east-west cross section through the Hoobler EU well as of May 2006.

Sim 9: L2 (Krider) and L4 (Winfield) Kxy*3 (on starting multiplier)

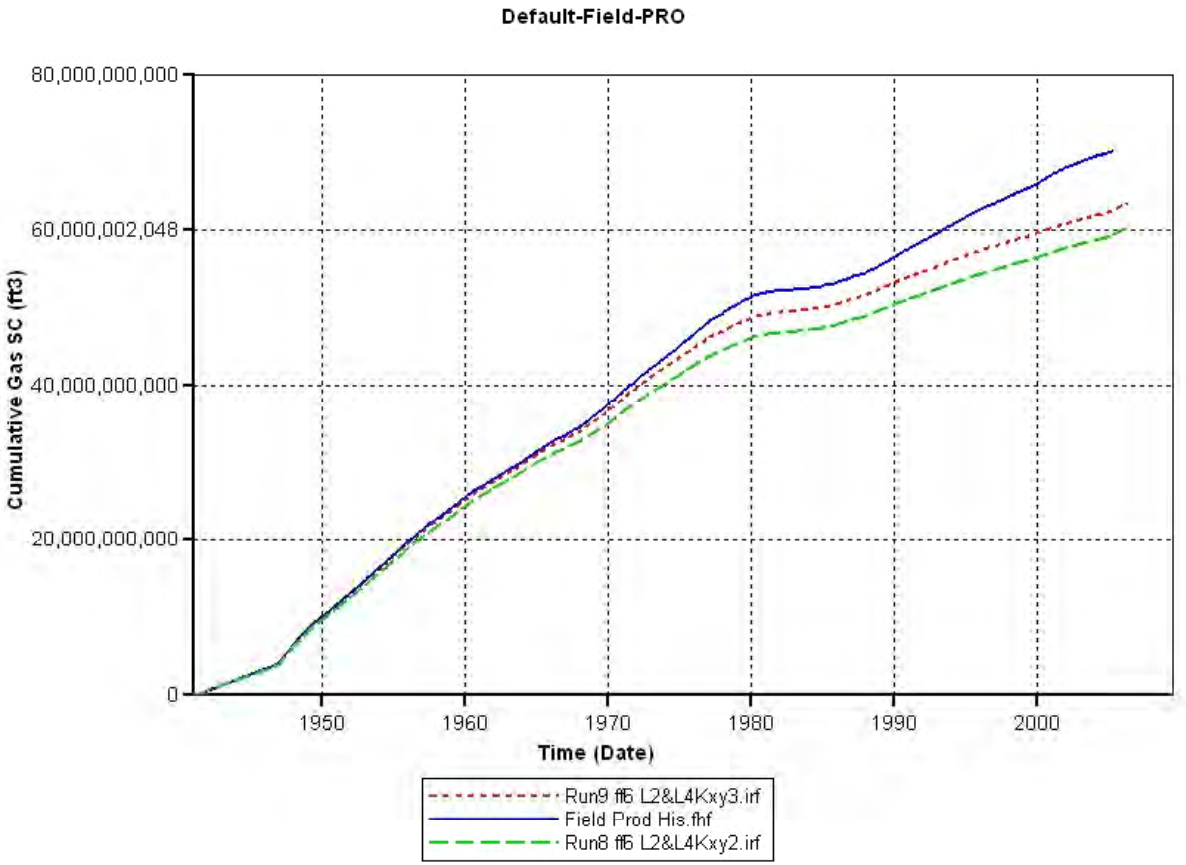

Figure 9.5.28. RUN 4 Results – Simulator-calculated field production from Hoobler area compared to historic volumes and that obtained from RUN 3.

Sim 9: L2 (Krider) and L4 (Winfield) Kxy*3 (on starting multiplier)

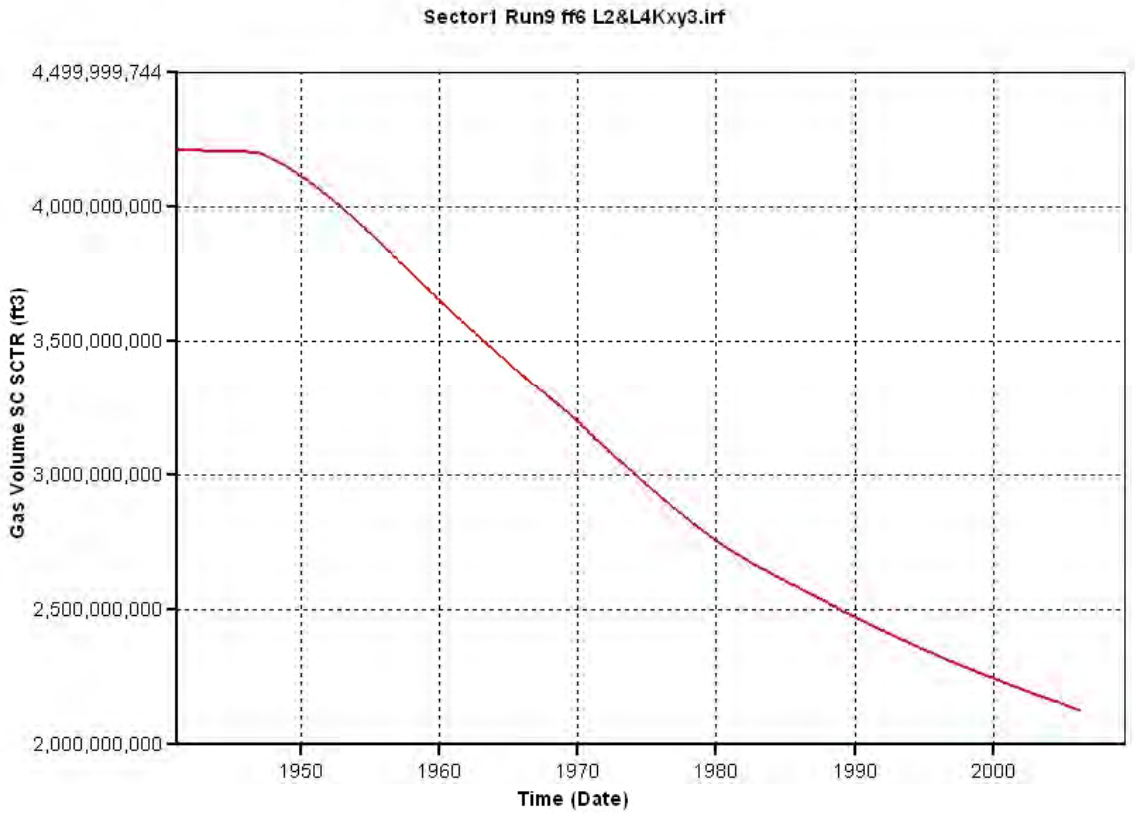

As of 1970, 3.25 bcf gas in place in L1 (Herington).

Figure 9.5.29. RUN 4 Results – Gas-in-place in L1 (Herington) over the production life of the Hoobler study area.

Sim 9: L2 (Krider) and L4 (Winfield) Kxy*3 (on starting multiplier)

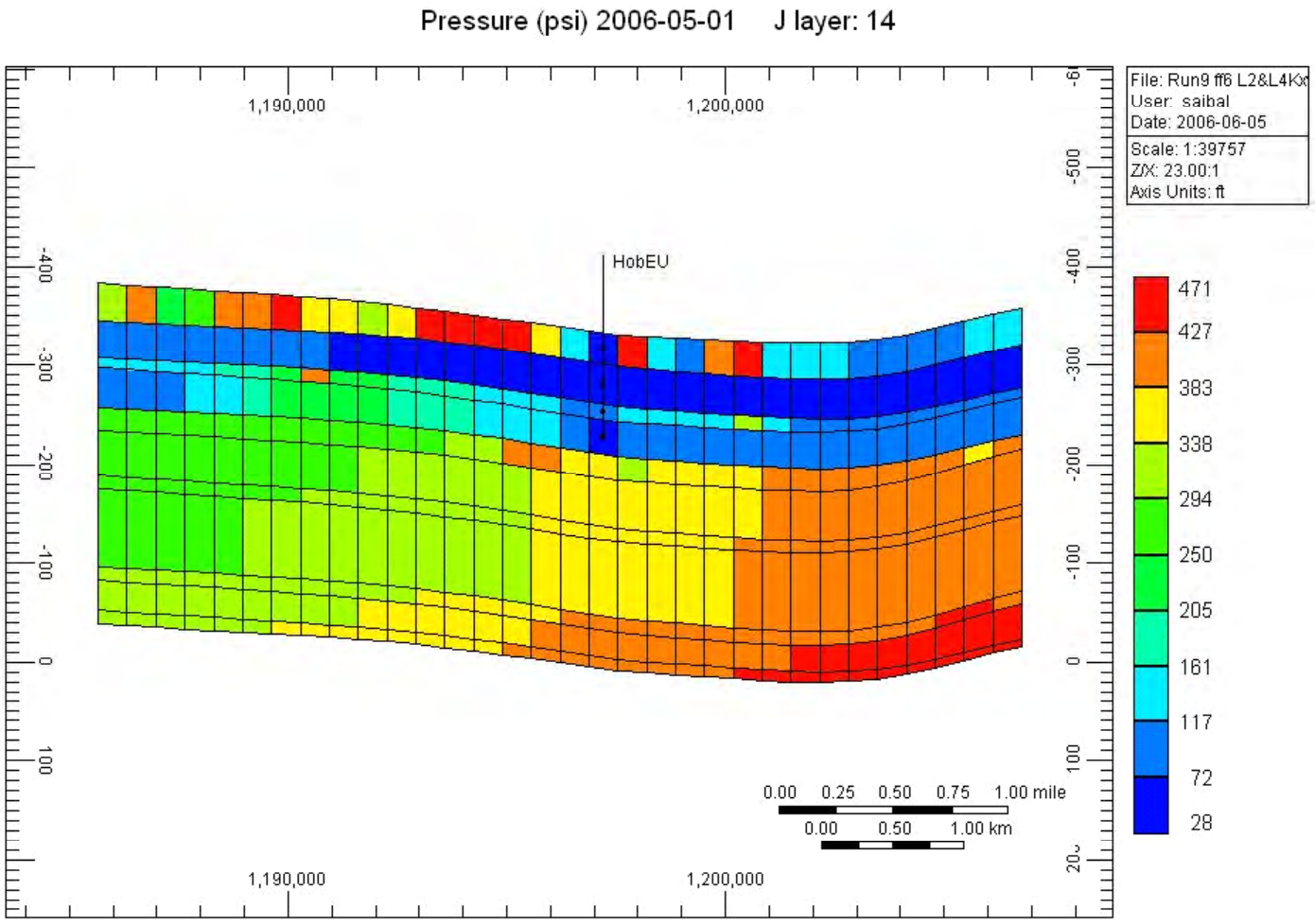

Figure 9.5.30. RUN 4 Results – Simulator-calculated pressure distribution along an east-west cross section through the Hoobler EU well as of May 2006.

Layer	Depth	WC Phi	WC K, md
Herington	2721	14.3	1.2
Herington	2722	14.6	1.37
Herington	2723	13.7	1.46
Herington	2724	12.4	1.46
Herington	2725	10.3	0.54
Herington	2726	10.9	0.19
Herington	2727	8.3	0.08
Herington	2736	6.5	0.01
Herington	2737	6.8	0.03
Herington	2738	7.1	0.05
Herington	2739	6.6	0.02
Herington	2740	5.9	0.06
Herington	2741	5.9	0.06
Herington	2742	5.7	0.02
Herington	2743	5.3	0.01
Herington	2744	5.4	0.02
Herington	2745	6.1	0.02
Herington	2746	6.3	0.02
Herington	2747	6.3	0.02
Herington	2748	6.3	0.02
Herington	2749	6.3	0.02
Herington	2750	6.2	0.03

Herington (1) Av K = 0.305 md

Perm can be multiplied by 3 (over starting multipier)

Figure 9.5.31. Whole-core porosity and permeability measurements from Herington zone in the Chase reservoir measured on core taken at the Hoobler EU well.

Sim 11: L1, L2, and L4 Kxy*3 (over starting multiplier)

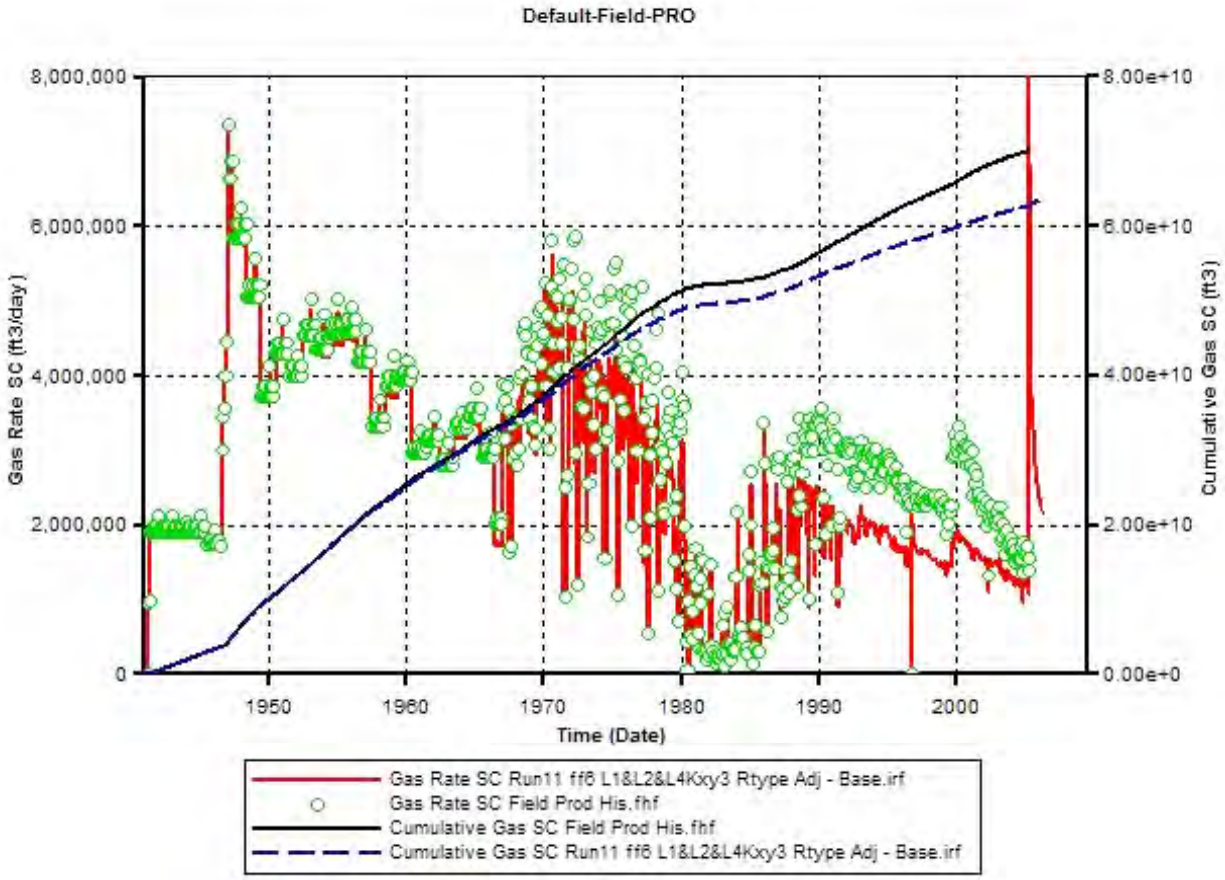

Figure 9.5.32. RUN 5 Results – Simulator-calculated cumulative production and production rate from the Hoobler study area compared with historic volumes.

Sim 12: L1, L2, and L4 Kxy*3, L6 Kxy*2

Field cum pre-1970 almost matched in both cases

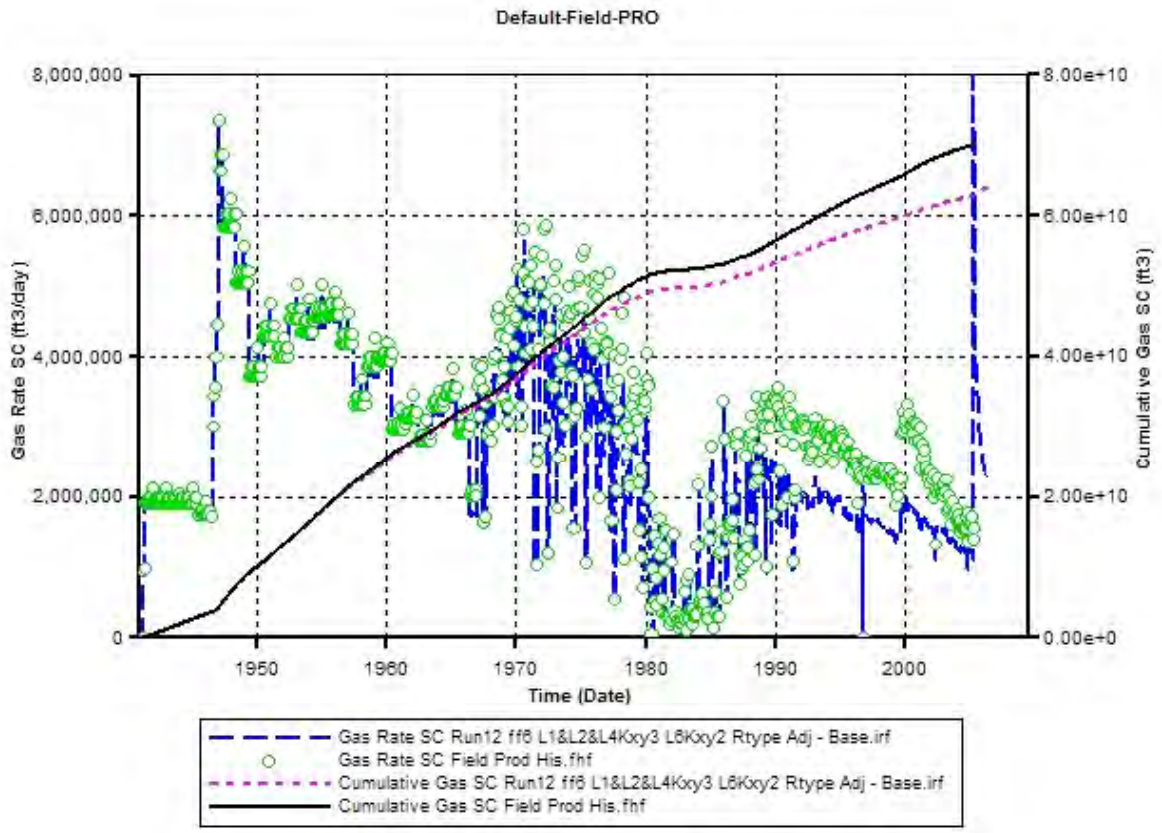

Figure 9.5.33. RUN 6 Results – Simulator-calculated cumulative production and production rate from the Hoobler study area compared with historic volumes.

Sim 11B: L1, L2, and L4 Kxy*4 (over starting multiplier)

Field prod match obtained pre-1970

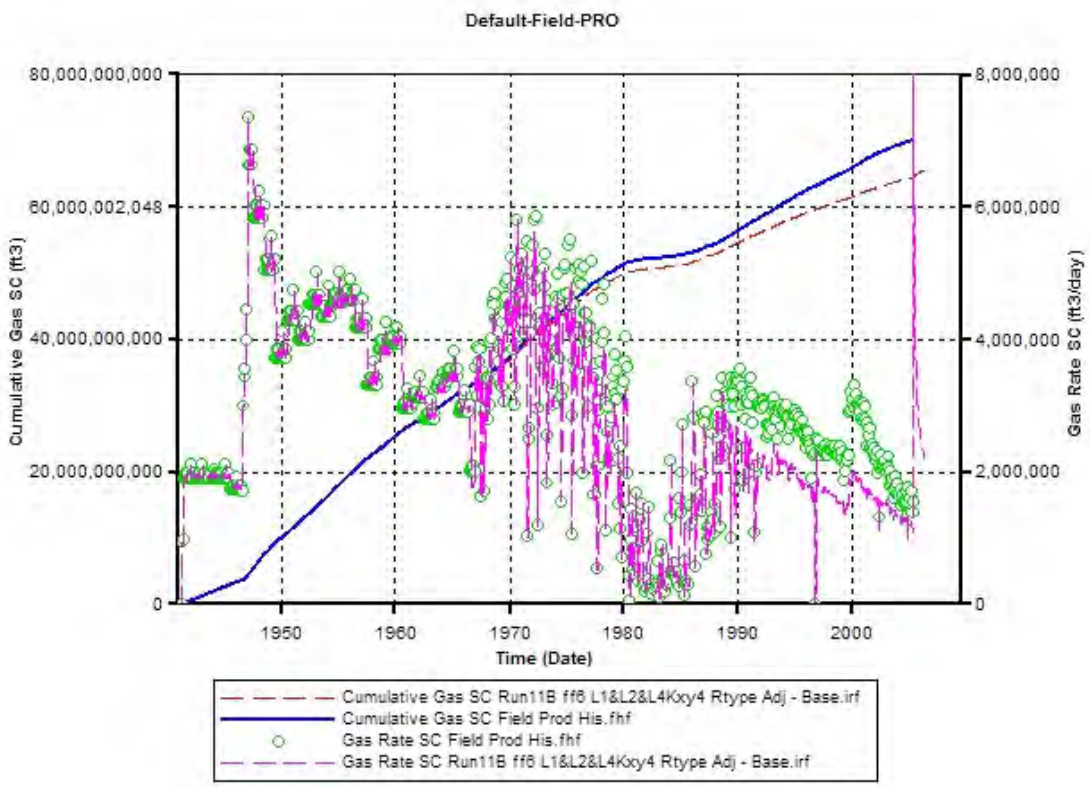

Figure 9.5.34. RUN 7 Results – Simulator-calculated cumulative production and production rate from the Hoobler study area compared with historic volumes.

Sim 11B: L1, L2, and L4 Kxy*4 (over starting multiplier)

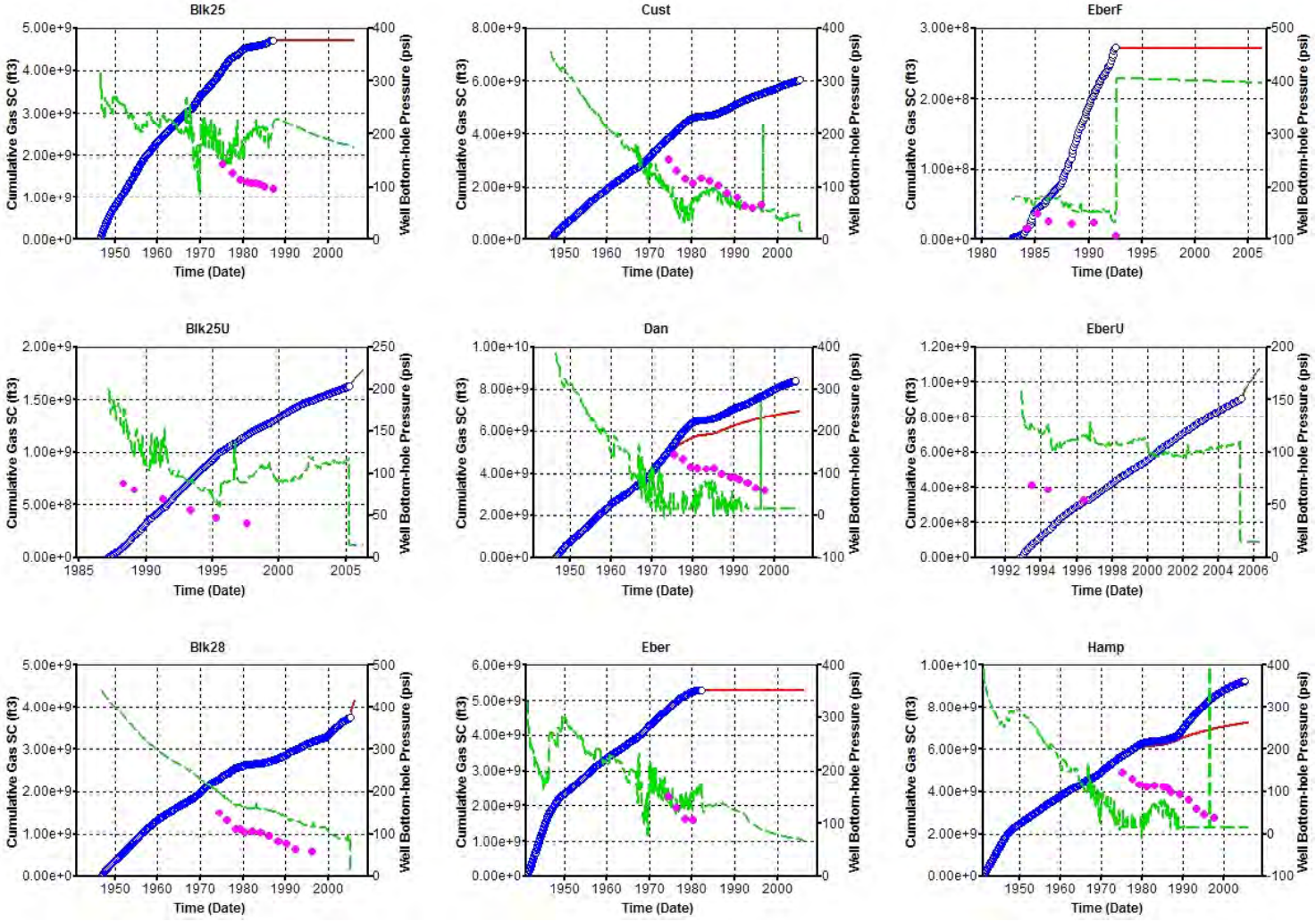

Figure 9.5.35. RUN 7 Results – Cumulative production and flowing-pressure history matches at Chase wells.

Sim 11B: L1, L2, and L4 Kxy*4 (over starting multiplier)

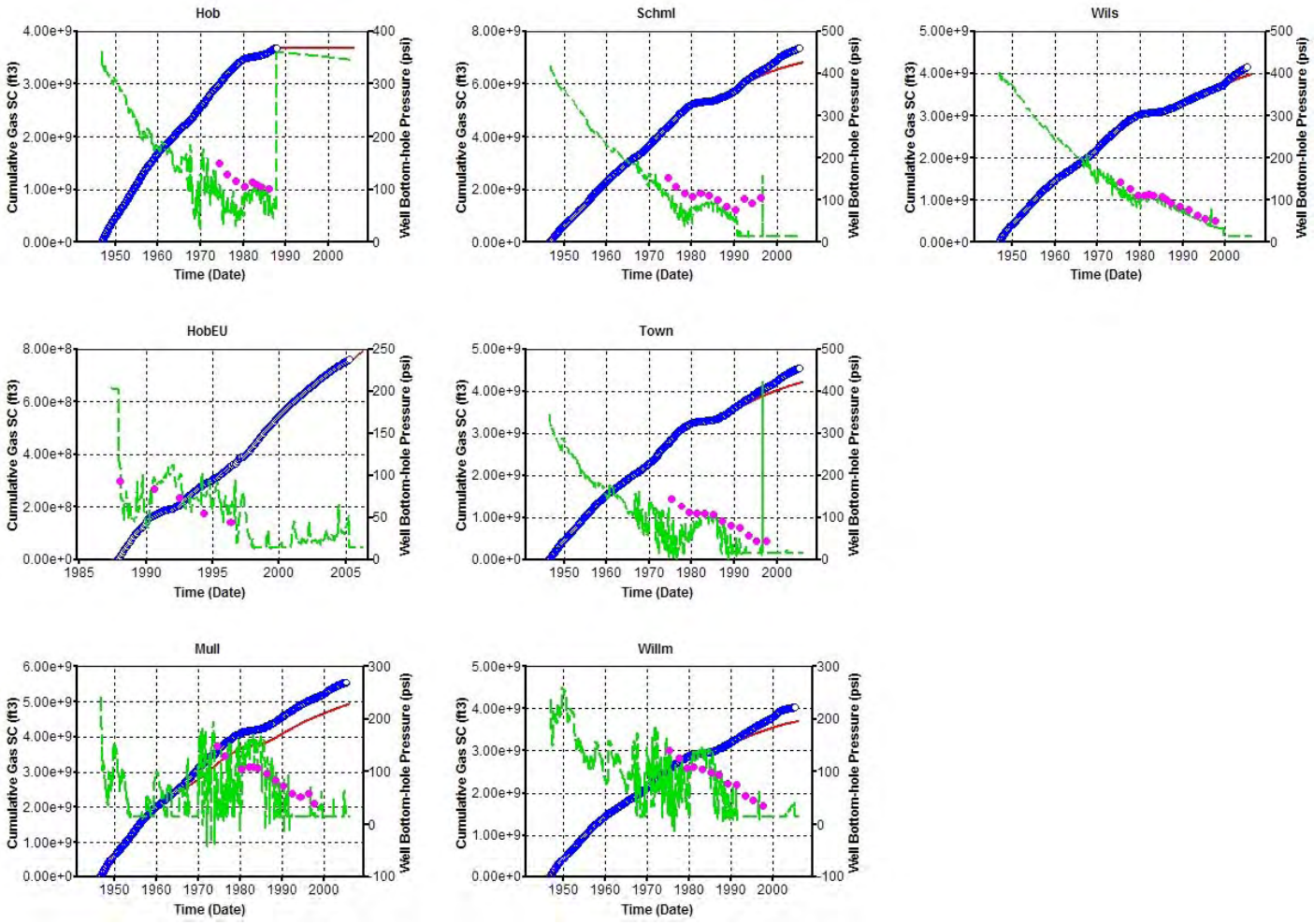

Figure 9.5.36. RUN 7 Results – Cumulative production and flowing-pressure history matches at Chase wells.

Sim 11B: L1, L2, and L4 Kxy*4 (over starting multiplier)

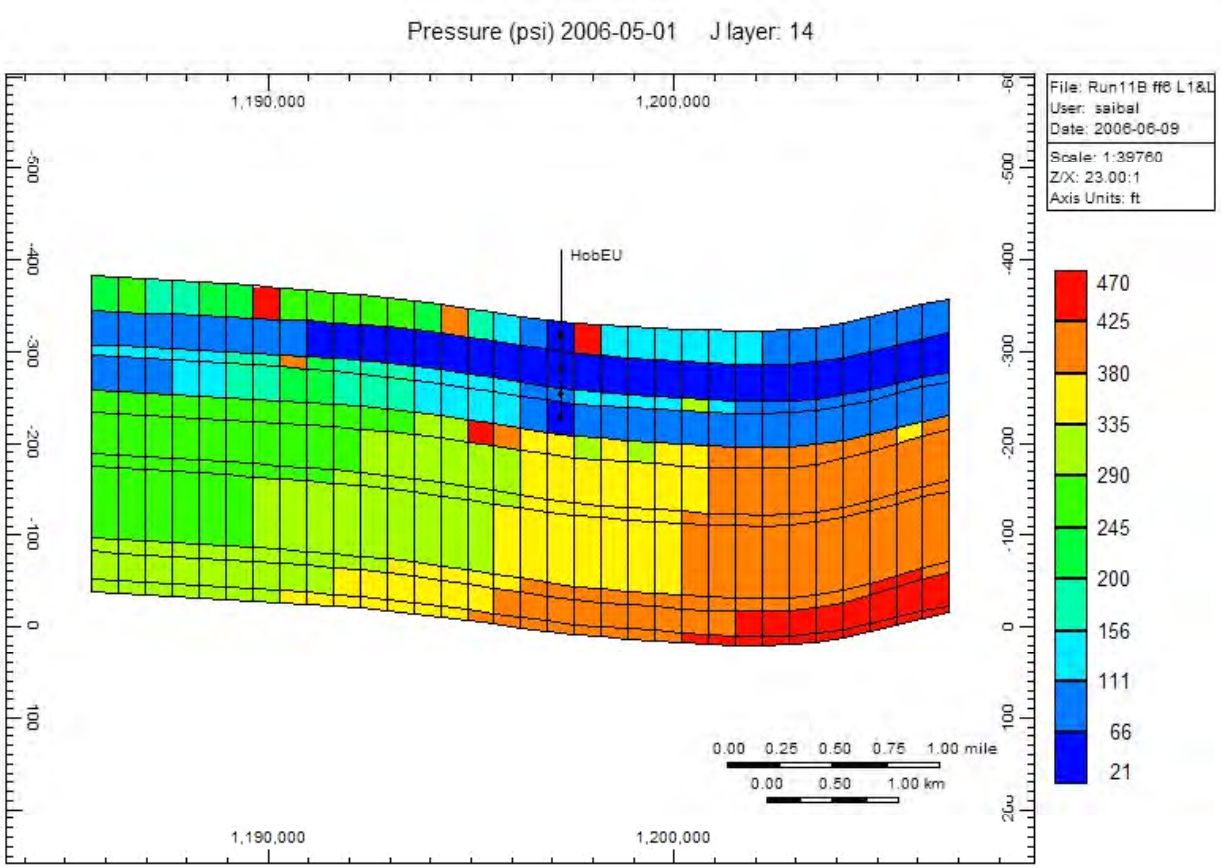

Figure 9.5.37. RUN 7 Results – Simulator-calculated pressure distribution along an east-west cross section through the Hoobler EU well as of May 2006.

Sim 11B: L1, L2, and L4 Kxy*4 (over starting multiplier)

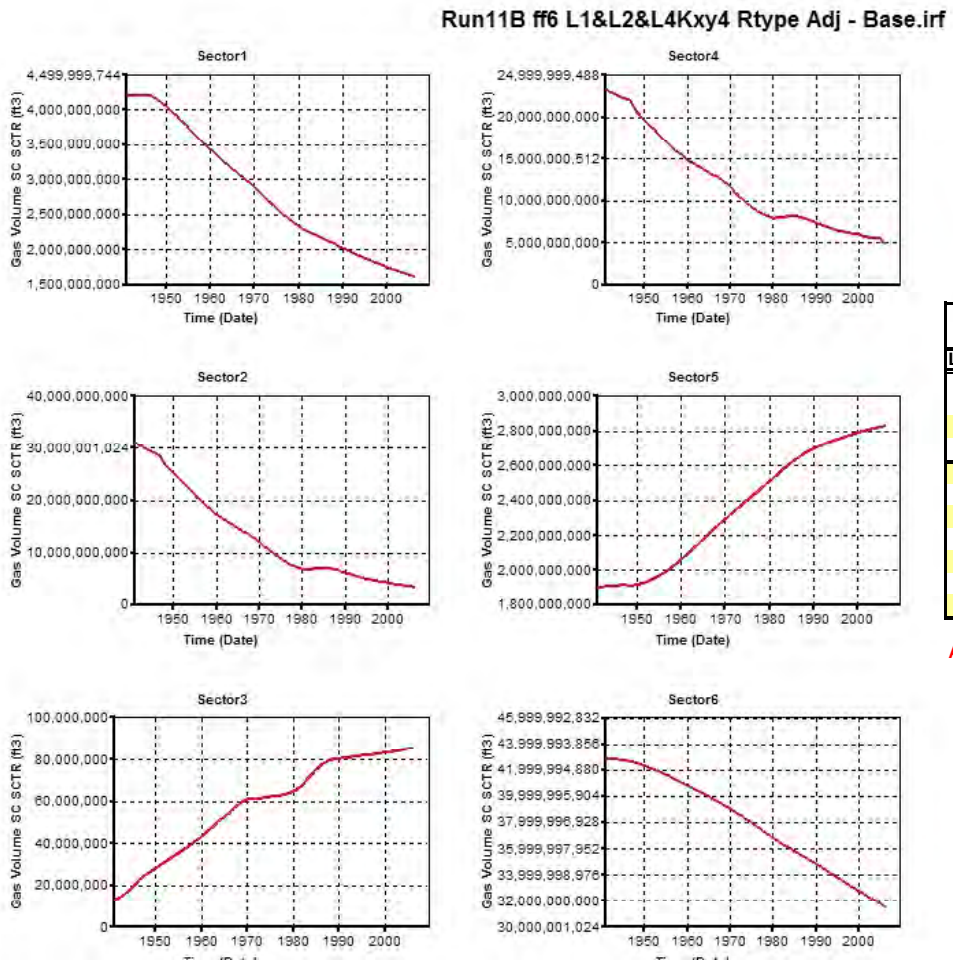

		OGIP in top 4 layers, bcf	58.1
Layer	**Name**	**Marty's OGIP**	**Sim OGIP**
1	Hrngtn	4	4.2
2	Krider	31	30.8
3	Odell	0	0.0123
4	Winf	23	23.1
5	Gage	2	1.89
6	Twnd	42	42.85
7	B/Twnd	3	3.04
8	Ftrly	23	25.19
9	Matfield	0	0
10	Wreford	0	0.0097
11	A1_ SH	0	0
At 450 psi, bcf OGIP		**128**	**131.1**

Figure 9.5.38. RUN 7 Results – Simulator-calculated gas-in-place in the top 6 Chase layers plotted through time.

Sim 11B2: L1, L2, and L4 Kxy*4 (over starting multiplier)
Dan, Hamp, and Town – post-1970, Frac L6, ff = 1, Kxy L6 & L8 *0.8
Black – Run 11B Pwf. Green – Run 11B2 Pwf

Permeability bull's eye around Blk28

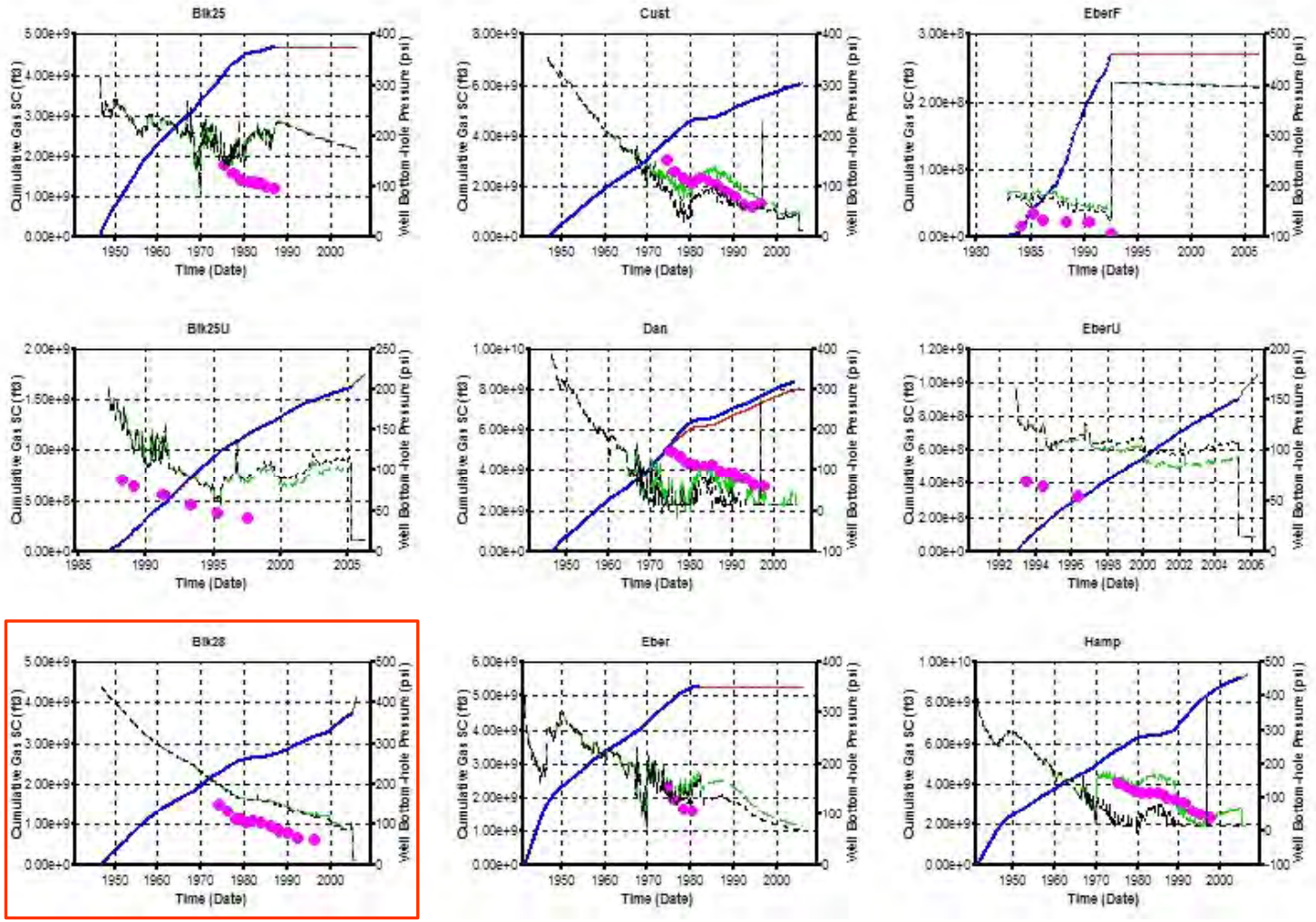

Figure 9.5.39. RUN 8 Results – Cumulative production and flowing-pressure history matches at Chase wells.

Sim 11B2: L1, L2, and L4 Kxy*4 (over starting multiplier)
Dan, Hamp, and Town – post-1970, Frac L6, ff = 1, Kxy L6 & L8 *0.8
Black – Run 11B Pwf. Green – Run 11B2 Pwf

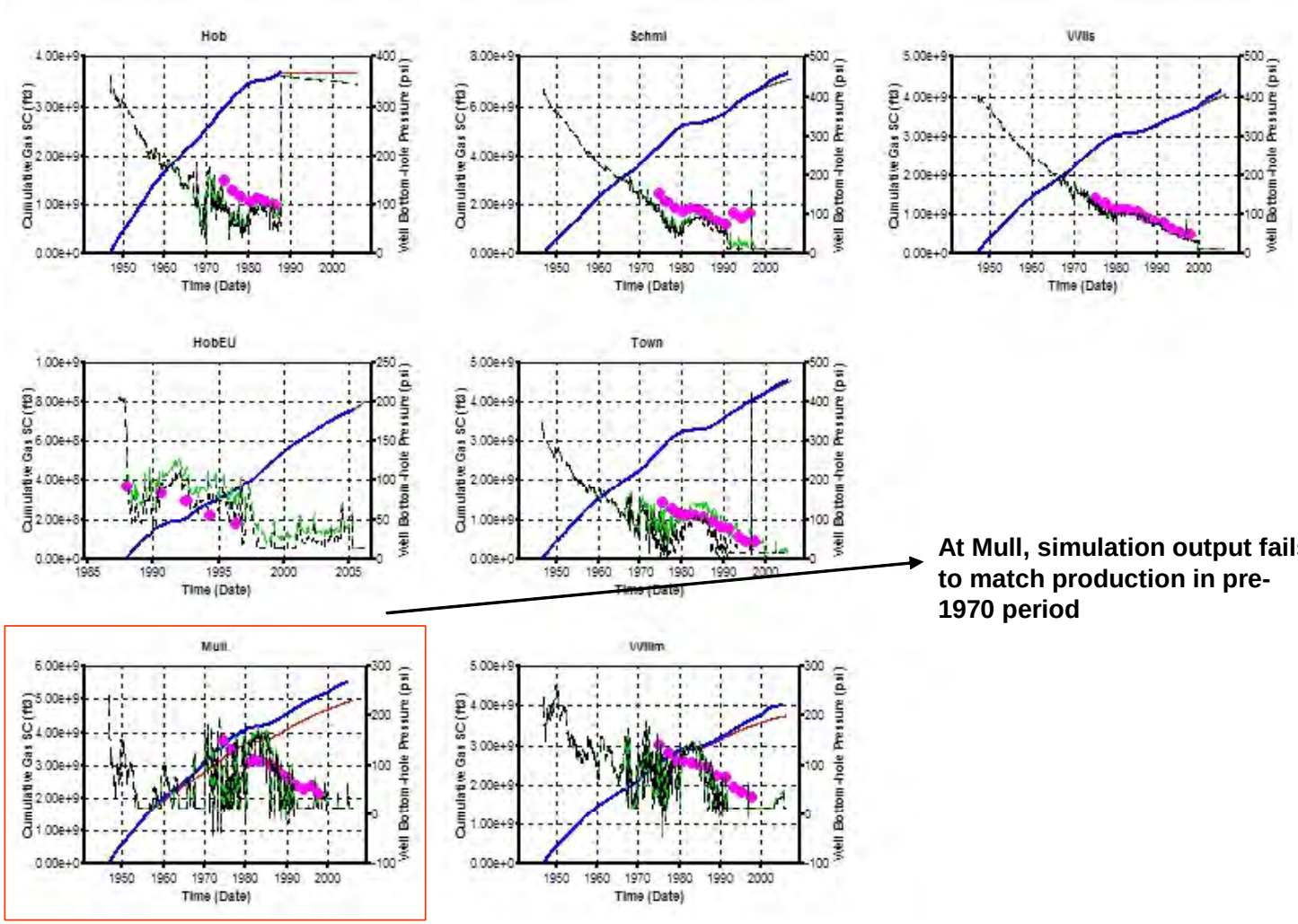

Figure 9.5.40. RUN 8 Results – Cumulative production and flowing-pressure history matches at Chase wells.

Sim 11B3: L1, L2, and L4 Kxy*4 (over starting multiplier)

Dan, Hamp, and Town – post-1970, Frac L6, ff = 1, Kxy L6 & L8 *0.8

Blk28 – L4 Lxy*0.06 (bring Kxy close to that in other wells in L4)

Matches at other wells remain unchanged from Run 11B2

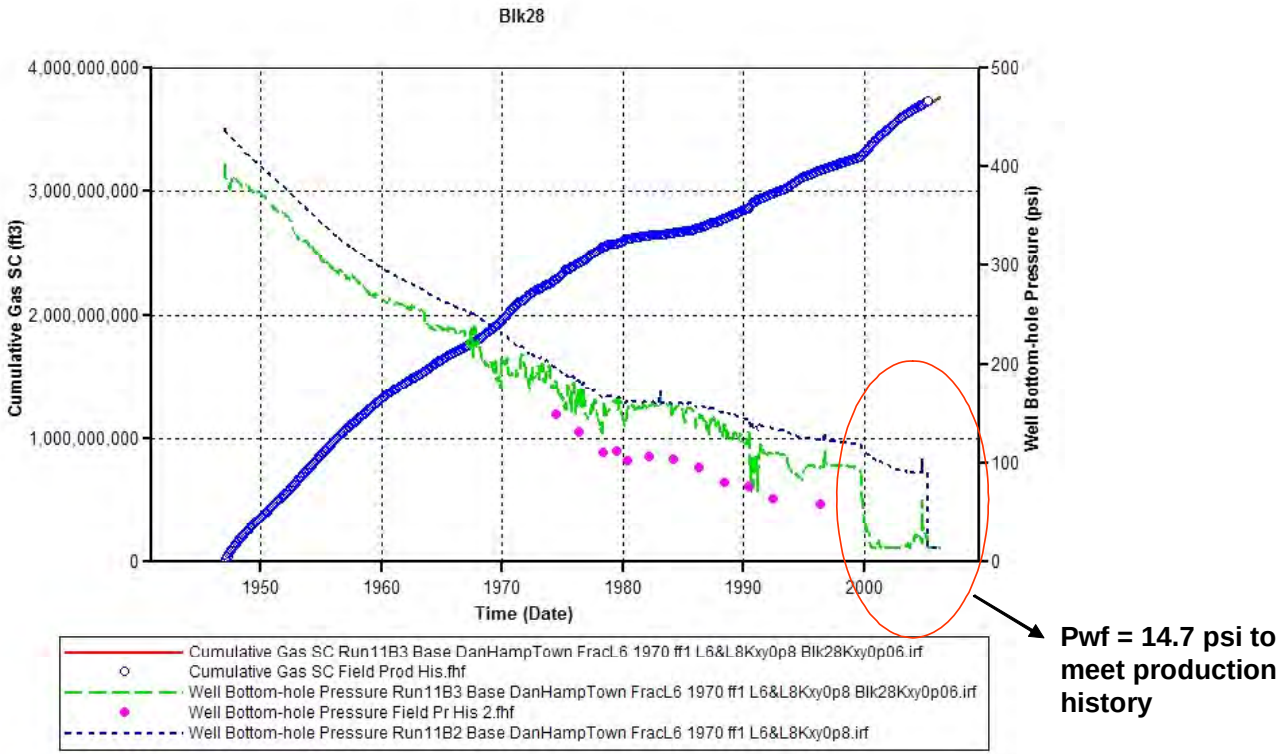

Figure 9.5.41. RUN 9 Results – Cumulative production and flowing-pressure history match at well Blk28.

A.

Model	Formation	Core Kxy (mean)	Model Kxy	Model Kz	Multiplier
1	Herrington	0.286	0.0274	0.000005	10.4
2	Krider	2.246	1.7833	0.036	1.3
3	Odell	0.067	0.0005	0.000007	134.0
4	Winfield	3.348	2.2702	0.00138	1.5
5	Gage	0.359	0.0077	0.0016	46.6
6	Towanda	0.928	1.126	0.0586	0.8
7	B/TWND	0.3	0.0385	0.00323	7.8
8	Ft. Riley	0.215	0.2929	0.0273	0.7
9	Matfield	1.518	0.0032	0.00068	474.4
10	Wreford	0.315	1.21	0.027	0.3
11	A1-SH		0.0029	0.0011	

B.

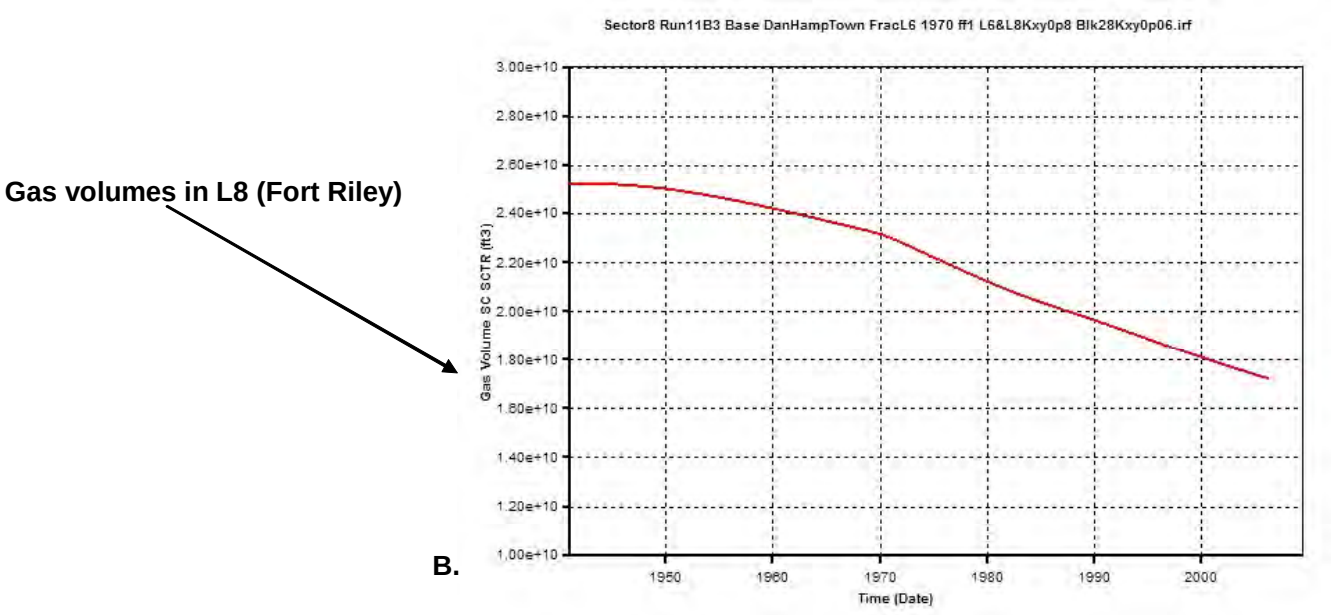

Figure 9.5.42. A) Upscaled vertical permeabilities estimated for each layer in the simulator geomodel. B) RUN 9 Results – Simulator-calculated gas-in-place in Fort Riley through time.

Sim 11B6: L1, L2, and L4 Kxy*4 (over starting multiplier)

Dan, Hamp, and Town – post-1970, Frac L6, ff = 1, Kxy L6 & L8 *0.8

Blk28 – L4 Lxy*0.06 (bring Kxy close to that in other wells in L4)

Dan ff = 4 post-1970, Schm fracL6 post-1970 ff = 1, L7 Kz*0.1

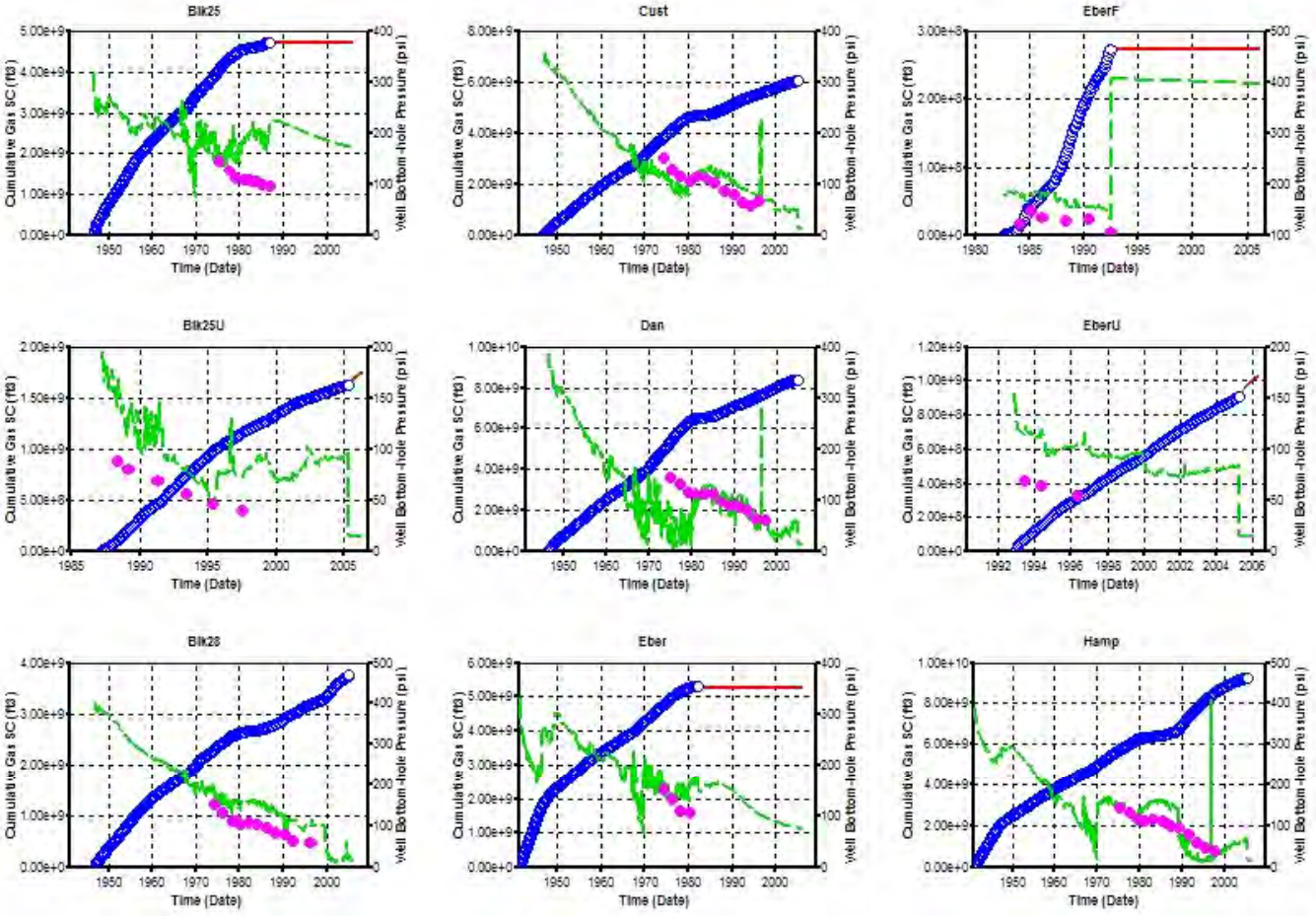

Figure 9.5.43. RUN 10 Results – Cumulative production and flowing-pressure history matches at Chase wells.

Sim 11B6: L1, L2, and L4 Kxy*4 (over starting multiplier)

Dan, Hamp, and Town – post-1970, Frac L6, ff = 1, Kxy L6 & L8 *0.8

Blk28 – L4 Lxy*0.06 (bring Kxy close to that in other wells in L4)

Dan ff = 4 post-1970, Schm frac L6 post-1970 ff = 1, L7 Kz*0.1

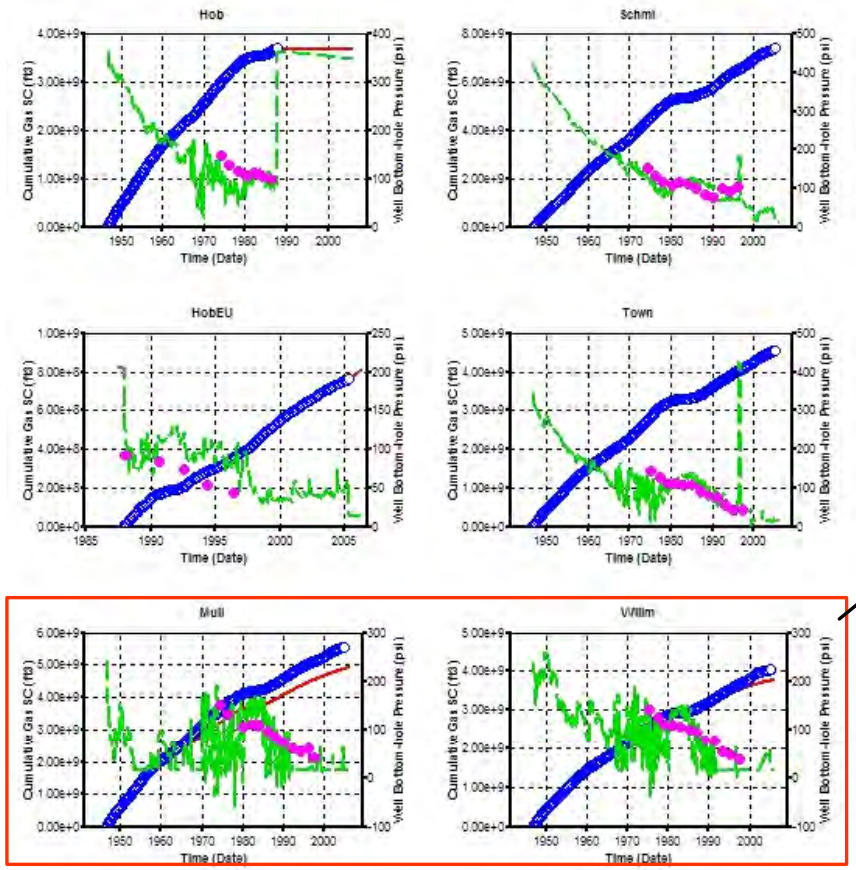

Mull and Willm are adjacent wells and both appear to have a little less gas than required for matching historic production volumes. They are located at the southern border of the study area.

Figure 9.5.44. RUN 10 Results – Cumulative production and flowing-pressure history matches at Chase wells.

Sim 11B8B: Same as Sim 11B6 and plus

Blk28 L4 Kxy*0.67 ff = 3, Blk25 and 25U ff = 1, Eber ff = 2, EberF and EberU ff = 2

HobEU ff = 3

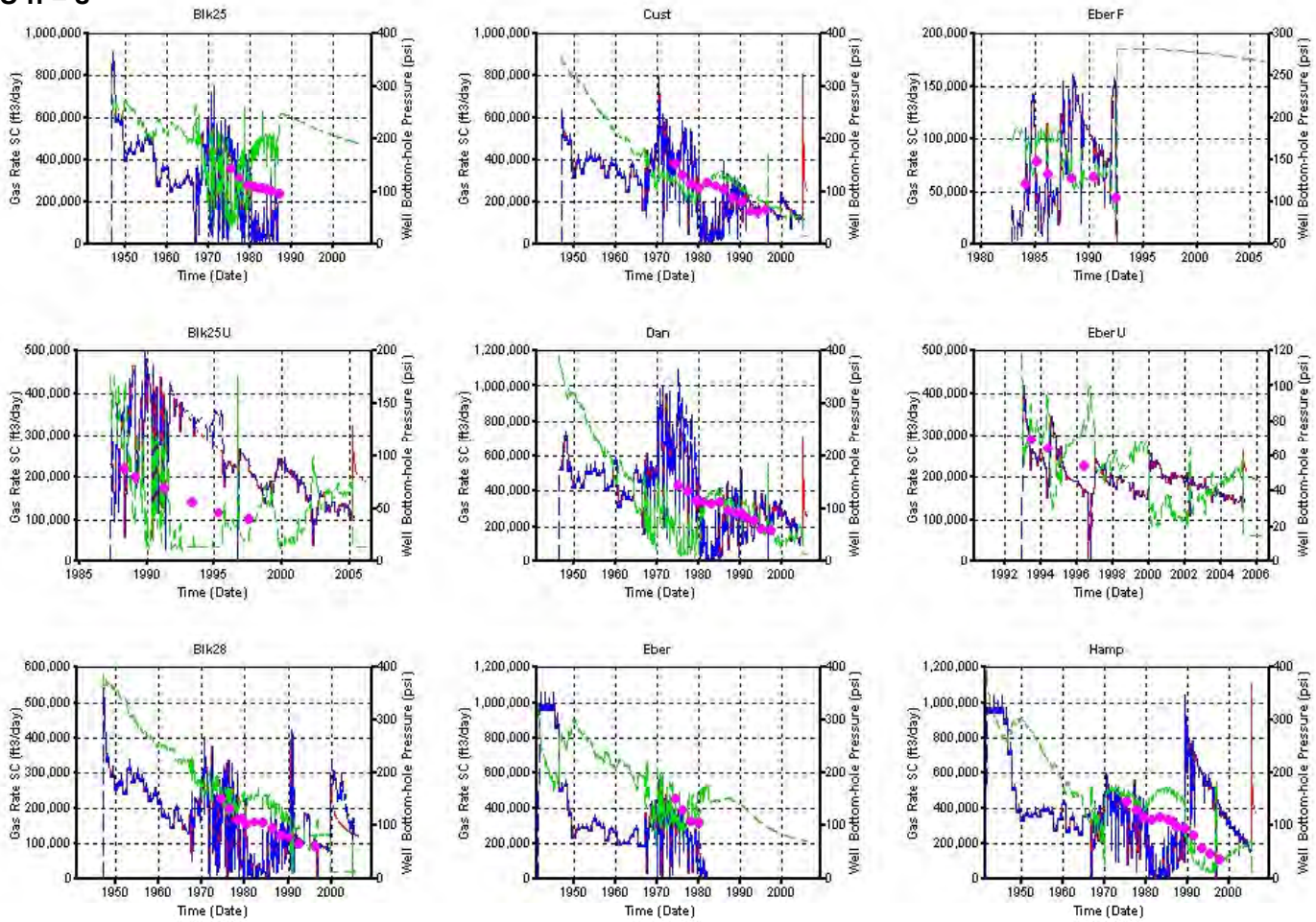

Figure 9.5.45. RUN 11 Results – Production rate and flowing-pressure history matches at Chase wells.

Sim 11B8B: Same as Sim 11B6 and plus

Blk28 L4 Kxy*0.67 ff = 3, Blk25 and Blk25U ff = 1, Eber ff = 2, EberF and EberU ff = 2

HobEU ff = 3

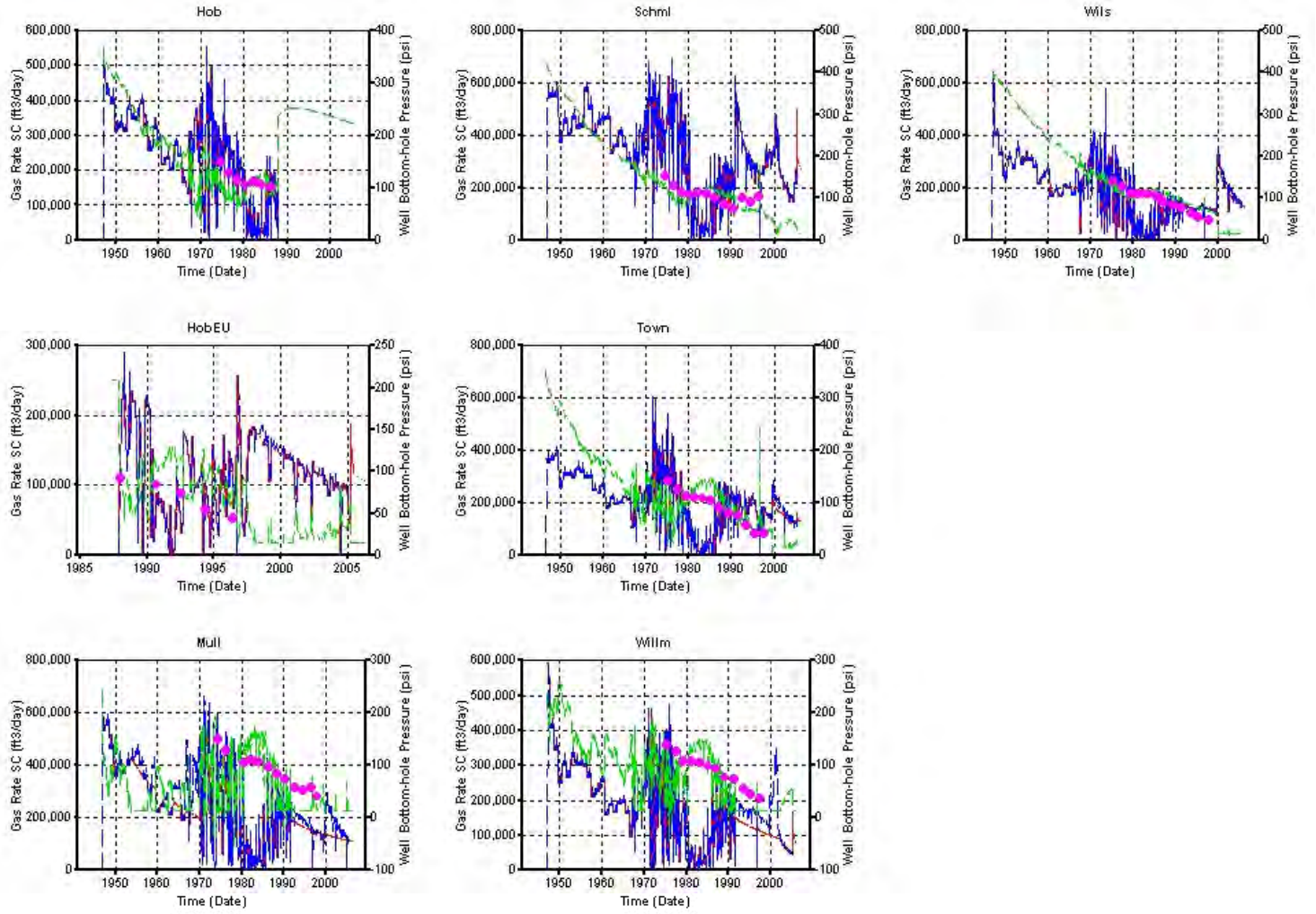

Figure 9.5.46. RUN 11 Results – Production rate and flowing-pressure history matches at Chase wells.

Sim 11B8: Same as Sim 11B6 and plus

Blk28 L4 Kxy*0.67 ff = 3, Blk25 and Blk25U ff = 1, Eber ff = 2, EberF and EberU ff = 2

HobEU ff = 3

Well	Production match	Flowing Pressure match	Production spike when freed of flow constraints
Blackmer 25	**Yes**	**BHFP>WHFP - midway**	**Shut-in**
Blackmer 25U	**Yes**	**Close - but low**	**Yes**
Blackmer 28	**Yes**	**BHFP>WHFP**	**No - unable to match prod from 2000**
Custer	**Yes**	**Yes**	**Yes**
Daniels	**Yes**	**Yes**	**Yes**
Ebersole	**Yes**	**Close**	**Shut-in**
Ebersole F	**Yes**	**Close**	**Shut-in**
Ebersole U	**Yes**	**Close**	**Yes - small**
Hampston	**Yes**	**Close**	**Yes**
Hobbler	**Yes**	**Close**	**Shut-in**
HobbE	**Yes**	**Close**	**Yes - small**
Muller	**Short initally & at end**		
Schmelzel	**Yes**	**Close**	**Yes**
Towner	**Yes**	**Yes**	**No**
Willams	**Short at end**		
Wilson	**Yes**	**Yes**	**No**

Figure 9.5.47. RUN 11 Results – Qualitative estimate of history matches obtained at each well.

Sim 11B8B: Same as Sim 11B6 and plus

Blk28 L4 Kxy*0.67 ff = 3, Blk25 and Blk25U ff = 1, Eber ff = 2, EberF & EberU ff = 2

HobEU ff = 3

A.

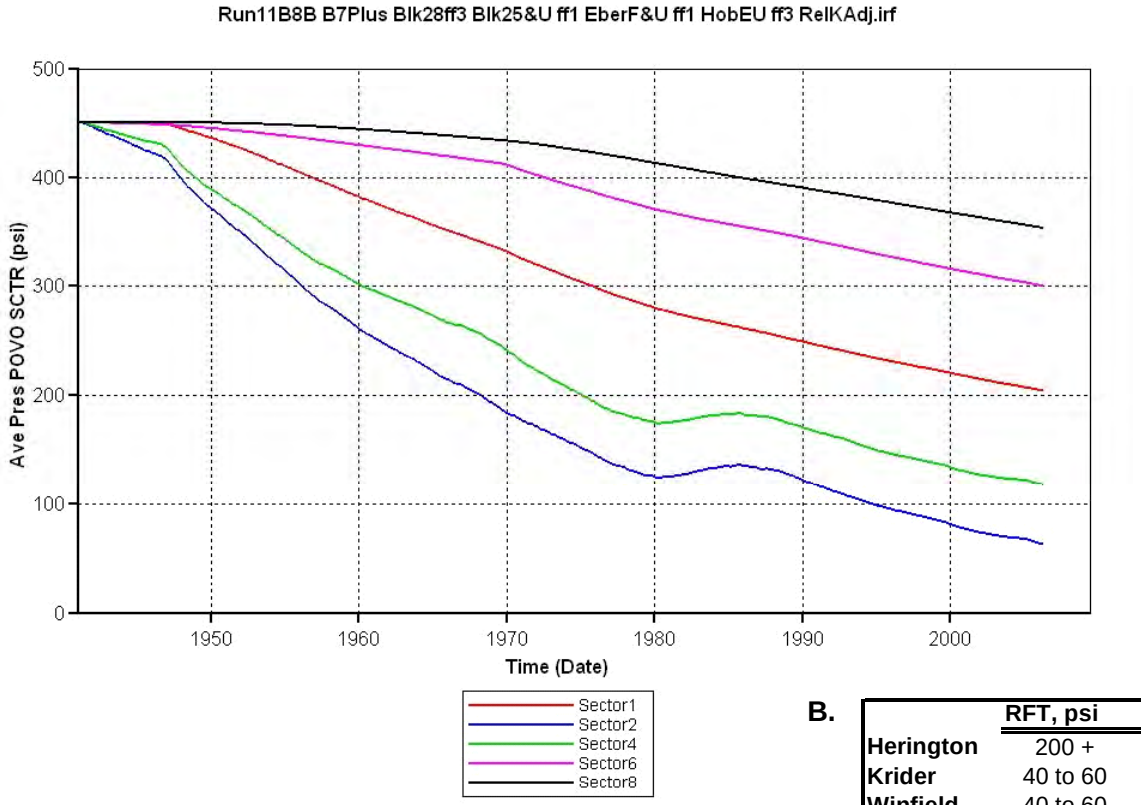

B.

	RFT, psi	PV Avg Sim psi @ May 2006
Herington	200 +	215
Krider	40 to 60	63
Winfield	40 to 60	118
Towanda	150 to 300	300
Fort Riley	450	353

Figure 9.5.48. RUN 11 Results – A) Average pore-volume weighted pressures at Layers 1, 2, 4, 6, and 8 in the Chase reservoir over the production life of the study area. B) Simulator-calculated pore-volume averaged layer pressures as of May 2006 compared with corresponding RFT (best-estimate) data.

Sim 11B8B: Same as Sim 11B6 and plus

Blk28 L4 Kxy*0.67 ff = 3, Blk25 and Blk25U ff = 1, Eber ff = 2, EberF and EberU ff = 2

HobEU ff = 3

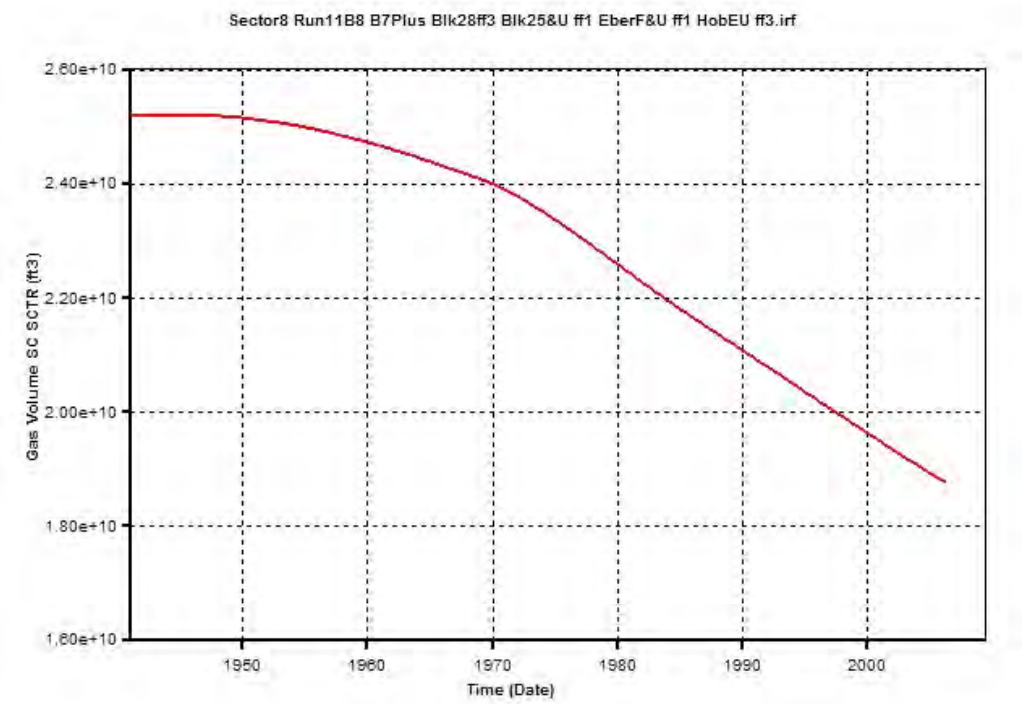

Figure 9.5.49. RUN 11 Results – Simulator-calculated gas-in-place in Fort Riley (Layer 8) through time.

9.6 MATERIAL-BALANCE STUDIES

Saibal Bhattacharya

Introduction

Material-balance (MB) methods, independent of volumetric evaluations, help to estimate original- and remaining-gas-in-place in the reservoir. MB equations are based on the principle of conservation of mass, where the volume of produced fluids (at reservoir conditions) is equated to the expansion of remaining fluids as a result of drop in reservoir pressure due to production. MB methods help estimate gas volumes that are in pressure communication to the well bore, and therefore relate to reserves that might be ultimately recoverable unlike volumetric reserves - part of which may be unrecoverable because they are trapped in reservoir heterogeneities within the drainage area of the producing well(s). Also, MB plots provide insights into the reservoir drive mechanism.

The primary drive mechanism in volumetric reservoirs is through expansion of reservoir fluids, primarily gas, as a result of pressure drop due to gas production assuming negligible expansion of reservoir rock and connate water. Such reservoirs receive no external energy such as from aquifers or from injected fluids into the reservoir. As gases are 100 to 1000 times more compressible than water and oil, reservoirs producing under gas expansion generally have high recoveries, often up to 90% of original-gas-in-place (OGIP).

Assuming a tank-type model and that the reservoir pore volume (PV) in contact with the producing well(s) does not change over the period of MB analysis, the MB equation for a volumetric dry-gas reservoir can be derived by equating the OGIP (under reservoir conditions) to that of remaining-gas-in-place (i.e., RGIP under reservoir conditions) at a later time after gas production that resulted in a decline in reservoir pressure. For a volumetric-driven gas reservoir, a plot of P/z vs. Gp will result in a straight line where P is the average reservoir pressure (psia) at any time (t), z the corresponding gas compressibility factor (dimensionless), and Gp is the cumulative gas produced (mscf) until time t. Subject to availability of sufficient reservoir pressure data (P), and corresponding production volumes (Gp), the above-mentioned line can be fully defined for a reservoir/drainage volume, and, thus, be used to estimate the OGIP and RGIP under some abandonment conditions. However when the plotted data consistently deviate from the expected straight line, it indicates the presence of other energy sources charging the reservoir and/or errors in recording the pressure/production histories. Figure 9.6.1 (from Lee and Wattenbarger, 1996) summarizes the expected shapes of P/z vs. Gp plots under various drive mechanisms.

Material-Balance Plots - Alexander D1 and D2 Wells

Figure 9.6.2A shows the layout of the Hugoton and Panoma fields along with the location of the Alexander wells. Figure 9.6.2B shows the location of the Chase Parent well Alexander D1 (D1) along with that of Council Grove well Alexander D2 (D2). The red broken line approximates the 640-acre drainage area around these two wells. The D1

well is located at the center of this drainage area. However, the D2 well is located close to D1 but is displaced to the northeast of the center. Thus, D2 might be draining from outside the assumed drainage area outlined in Figure 9.6.2B. However, given the general placement of Chase Parent and Council Grove wells in the Hugoton and Panoma fields, it is reasonable to assume that a pair of Chase and Council Grove wells (such as the D1 and D2) is draining 640 acres. Modern logs and a core through the Council Grove section were available from the D2 well.

Figure 9.6.3 shows the plot of P/z versus cumulative gas production (Gp) from D1 until 1975, i.e., until before the start of production from D2. The vast majority of the plotted data follow a linear trend as expected of a gas reservoir producing under volumetric expansion. Based on the above MB plot using pre-1975 production/pressure data, the OGIP in the drainage area of D1 is calculated to be 9.5 bcf.

Figure 9.6.4 plots the P/z data versus Gp data from D1 until December 1990, i.e., before the onset of production from Alexander D3, the Chase infill well which was spudded in February 1991. The pre-1975 data along with the corresponding best-fit trend line are also plotted on Figure9.6.4 as blue points and the blue line. It is apparent from the above figure that the P/z vs. Gp points post-1975 start to stray up and away from the linear trend line (in blue) established by the pre-1975 data. Such a divergence from the linear trend for volumetric gas reservoirs occurs when external energy is added to the reservoir system in the form of gas or water injection (refer to Figure 9.6.1). However, historic records show that no gas or water injection ever took place in the Hugoton and Panoma gas fields.

A previously reported one-section simulation study (Bhattacharya et al., 2004), around the Alexander D1 and D2 wells, has shown that the completions of Council Grove well (i.e., D2) were extended to the Chase layers in order to history match the Council Grove well performance. All Council Grove wells, including the D2 well, were hydraulically fractured upon completion before being put on production. The D2 well came into production as of October 1975. Simulation models from the above-mentioned study show that at the time of completion of the Council Grove wells, the reservoir pressure in the Council Grove was much higher than the Chase layers. The hydraulic fracturing of Council Grove wells in 1975 may have resulted in communication between the Chase and Council Grove reservoirs, and thus the commingled shut-in pressures at the Chase wells, in the post-1975 period, were affected by the higher pressures prevalent in the Council Grove layers. Thus post-1975, the P/z vs. Gp plot of D1 stray up and away from linear trend established by the the pre-1975 data.

Figure 9.6.5 plots the bottom-hole shut-in pressures (BHSP) of D1 and D2. It is apparent from this plot that the reservoir pressure in the Council Grove well (D2) closely tracks that at the Chase well (D1) from May 1976, i.e., about 11 months from the onset of D2 production. The overlap between the shut-in pressures recorded at the D1 and D2 wells suggests that the Chase and the Council Grove reservoirs are in hydraulic communication. Previous studies have shown that in differentially depleted reservoirs, shut-in pressures hover close to that of the most depleted layer(s) that due to their

relatively higher permeabilities are, therefore, at lower pressures. Such overlap between shut-in pressures recorded at the Chase and at the corresponding Council Grove wells, located in the same section, has been observed in other studies on multi-section areas (Bhattacharya et al., 2005; Bhattacharya et al., 2006).

Figure 9.6.4 also shows that the P/z vs. Gp plot for D1 shows a distinct dip in 1992. The Chase Infill well, Alexander D3, was drilled in early 1991, and the interference effects of this well on the performance of the D1 well are evident on the above-mentioned MB plot.

Material Balance Plots – Flower Area Wells

Figure 9.6.6A shows the general location of the Flower area within the Hugoton and Panoma fields, while Figure 9.6.6B details the location of the Chase (Hugoton) Parent wells, the Council Grove (Panoma wells), and the Chase (Hugoton) Infill wells within the Flower area. The Flower area is a nine-section area around the Flower A1 well located in Sec. 25, T. 31 S., R. 38 W.

Figures 9.6.7A to 9.6.7I plot the P/z versus Gp data from the Chase parent wells in the Flower area respectively. The plotted pressure data refer to the surface shut-in pressure recorded at each of the wells at the end of a 72-hr shut-in test because bottom-hole shut-in pressure data were not available. It is not possible to accurately calculate the bottom-hole shut-in pressures at the wells without down-hole pressure gauges or an understanding of the fluid-column composition in each well under shut-in conditions. Also, most Chase wells produce some water and operate with a pump. The shut-in pressures representing reservoir conditions are critical to estimate the OGIP through MB calculations. However, it is reasonable to assume that historically recorded surface shut-in pressures at any Chase Parent well are consistent within themselves (over the years) and should therefore lie on a linear trend in case of a volumetrically driven reservoir. It is recognized that using surface shut-in pressure data to estimate OGIP from MB plots may result in an underestimation. However, it is reasonable to use surface shut-in pressures to test for linearity of P/z vs. Gp lacking subsurface data.

Figures 9.6.7A to 9.6.7I show that sometime in the early 1970's, the P/z vs. Gp data for each of the Chase Parent wells start to stray away and above the linear trend established by the pre-1970 data. The Council Grove wells were hydraulically fractured before start of production, and Figure 9.6.8A tabulates that start-of-production date for the Council Grove wells in the Flower area. Most of the Council Grove wells started to produce in 1970. A loss of linearity occurs in the MB plots of all the Chase Parent wells during a narrow time window extending between 1973 and 1974, and this coincides with the onset of production from the Council Grove wells in the early 1970's. In a volumetric driven reservoir, the upward deviation of the plotted data away from the linear trend indicates addition of external energy to the reservoir system, such as by fluid injection or by an active natural-drive mechanism. In absence of both of the above, the loss in linearity on the MB plots of the Chase Parent wells may be due to establishment of communication between the Chase and the Council Grove reservoirs as a result of the hydraulic fracturing of the Council Grove wells before being put on production. Similar

to the MB plots of Alexander D1 and D2 wells, the shut-in pressure data recorded at the Chase Parent wells in the Flower area may be affected by the higher reservoir pressures prevalent in the Council Grove layers.

Thus, MB plots of the Chase Parent wells indicate hydraulic communication existing between the Chase and Council Grove reservoirs in the Flower area. Previous multi-section simulation studies (Bhattacharya et al., 2005) have demonstrated that completions at the Council Grove wells in the Flower area have to be extended to the Krider zone (Chase reservoir) in order to match the performance of Chase Parent, Council Grove, and Chase Infill wells. The effectiveness of using MB plots of Chase Parent wells to predict the presence of communication between the Chase and Council Grove reservoirs can be tested by plotting the P/z vs. Gp data for Chase Parent wells at an area of the Hugoton field where no Council Grove wells are located in the same section as the Chase Parent wells. MB plots of Chase Parent wells from such an area, like the Hoobler area where there are no producing Council Grove wells, should not show any loss of linearity unlike those of the Chase Parent wells in the Flower area.

An interesting point to note in Figures 9.6.7A to 9.6.7I is that for each of the Chase Parent wells, the P/z vs. Gp plot shows a downward dip some time between 1988 and 1990. It is apparent from Figure 9.6.8B, which lists the dates when production started from Chase Infill wells in the Flower area, that most of these wells went online between 1988 and 1989. Thus, the MB plots of the Chase Parent wells clearly show the interference effects of the Chase Infill wells indicating presence of good lateral communication within Chase layers in the Flower area.

Material-Balance Plots – Hoobler Area Wells

Figure 9.6.9A shows the general location of the Hoobler study area in the Hugoton field, while Figure 9.6.9B shows the location of the Chase wells. The locations circled in red are wells that produce from the Council Grove in the Hooker North field in a downdip position separate from the Panoma field. Figures 9.6.10A to 9.6.10E are the MB plots for the five Chase Parent wells. As in the Flower area, the pressure data plotted is the surface shut-in pressure recorded at each of the wells at the end of a 72-hr shut-in test because bottom-hole shut-in pressure data were not available in the Hoobler area wells. As in the Flower area, we assume that historically recorded surface shut-in pressures at any Chase Parent well are consistent within themselves and should therefore lie on a linear trend in case of a volumetrically driven reservoir.

In the absence of Council Grove wells located in the same section as the Chase wells in the Hoobler area, the P/z vs. Gp plots (Figures 9.6.10A to 9.6.10D) of four Chase wells follow a linear trend until the 1990's. Data plotted on Figure 9.6.10E also follow a linear trend for most of production history of the Custer well. However, some of the plotted points between 1980 and 1986 appear to stray from the previously established linear trend before merging with the trend after 1986. Detailed well-level completion histories were not available to explain this temporary loss of linearity at the Custer well. It is interesting to note that because the post-1986 pressure and production data plots on

to the pre-1980 trend line, whatever caused the loss of linearity as of 1980 was temporary.

Multi-section simulation studies (Bhattacharya et al., 2006) at the Hoobler area have demonstrated that well performances at the above-mentioned five wells were history matched without extending their completions beyond (below) the Winfield (Layer 4 in the Chase reservoir). Detailed completion histories were not available at any of the wells in the Hoobler study area. However, initial completion reports show that these wells were completed to the Winfield zone in the Chase reservoir. Later completions/simulations extending into lower Chase layers would be equivalent to altering (increasing) the drainage pore volume connected to the corresponding well and will result in loss of linearity on the P/z vs. Gp plot. The P/z vs. Gp plots of these five wells followed uninterrupted linear trends until the 1990's, and this validated that the drainage pore volumes connected to each of these wells did not increase as a result of any stimulation or recompletion.

Figure 9.6.11A is the MB plot for the Chase well named Ebersol, one of the earliest wells drilled, in the early 1940's, in the study area. The P/z vs. Gp plot for this well follows a linear trend for most of the well's production life. However, the first three points stray below the established trend line, and the trend when extrapolated to Gp = 0 results in a higher-than-expected P/z value because the P/z value recorded at the previously mentioned five wells hovers between 450 and 500 psi. This indicates that the initial pressure data and/or the cumulative production attributed to the early months are in error. Also, multi-section simulation studies (Bhattacharya et al., 2006) have shown that the completions at this well do not need to be extended beyond the initial completions to the Winfield to obtain a performance history match at this well.

Annual production from the Ebersol well was available from July 1945 onwards, while a cumulative production volume was available (from a different data source) from start of production to June 1945. Available completion records reveal that the well was spudded in May 1940. However, no information was available as to when this well started production. Thus, a production-start date was assumed for this well such that the cumulative production, as of June 1945, when uniformly allocated to the months between the start date and June 1945, resulted in a monthly production slightly greater than that averaged between July 1945 and June 1946. Lack of details regarding the pre-1945 production history at the Ebersol well and use of production data from multiple sources possibly resulted in uncertain Gp values particularly during the early life of the Ebersol well. A slight reduction in the early cumulative production volumes would shift the post-1947 production in the direction of a lower P/z value (less than 500 psi) at Gp = 0. A similar problem occurs for the Hampston well (Figure 9.6.11B). Like the Ebersol, this was one of the early wells spudded in March 1940, and, therefore, had no annual or monthly production data available until mid-1945. The initial cumulative production as of June 1945 was obtained from a different database than that which provided production data from the post-July 1945 period. Mis-match between data from different sources is perhaps the reason why the first two points on the P/z vs. Gp plot for the Hampston well deviate away from the linear trend established by the later data (until 1988). Previously

mentioned multi-section simulation studies on the Hoobler area show that completions at this well have to be extended beyond the initial completion to Winfield (Layer 4 in the Chase reservoir) to Towanda (Layer 6 in the Chase reservoir) in order to history match well performance. The P/z vs. Gp plot for this well shows a loss of linearity at 1988 indicating an increase in pore volume connected to the well.

Figures 9.6.12A to 9.6.12C show the MB plots for three other wells from the Hoobler area whose completions had to be extended to the Towanda (Layer 6 in the Chase reservoir) in the multi-section simulation studies (Bhattacharya et al., 2006) to history match well performance. In the absence of well-level completion/stimulation histories, the completions at these wells were extended to the Towanda in January 1970 in the above-mentioned simulation study. MB plots indicate that a loss of linearity occurs at the wells Daniels, Schmelzel, and Towner during the 1970's. In all these cases, the plotted points stray up and away from the previously established linear trend. Extending completions to deeper pay zones such as the Towanda adds reserve volume to the drainage of these wells and, thus, the MB plot will show a signature similar to adding external energy to the reservoir being drained by each of the wells.

Figures 9.6.13B and 9.6.13C show the production pressure history matches obtained (Bhattacharya et al., 2006) at two wells, namely Muller and Williams, located on the southern boundary (Figure 9.6.13A) of the Hoobler study area. In Figures 9.6.13B and 9.6.13C, the production history is shown by the blue line while the red line is the simulator-calculated production, and the magenta-filled circles represent the historically recorded surface-flowing pressures while the green line represents the simulator-calculated bottom hole flowing pressures. Based on the geomodel used in the previously mentioned reference, the simulator is unable to history-match pre-1970 production at the Muller well and the post-1990 production at the Williams well. Both wells are located on the southern boundary of Hoobler study area. Qualified well logs were available from 3 wells within the study area. The reservoir geomodel used in the simulation study was extracted from a field-wide model built by integrating all available qualified well logs and core data. That model may predict non-representative storage and flow properties in drainage area of these wells, i.e., in the southern part of the study area. MB plot for the Muller well (Figure 9.6.14A) does not show any loss of linearity during its production life, thus indicating that completions at this well, perhaps, did not extend beyond the Winfield (Layer 4 in the Chase zone) into deeper pays zones such as the Towanda. It appears that the reservoir geomodel used in the multi-section simulation study is deficient in storage and/or flow properties in the vicinity of the Muller well, and thus simulator-calculated production rates fail to match pre-1970 historic rates. Figure 9.6.14B is the MB plot for the Williams well. The plotted data follow a linear trend until 1990, which coincides with the time when the simulator-calculated production rate failed to match the historically recorded rates. The MB plot indicates that in the absence of fluid injection, post-1990 recompletion/stimulation resulted in addition of reservoir pore volume to the Williams well. It is, however, difficult to corroborate this hypothesis lacking a detailed recompletion/stimulation history for this well.

Conclusions

Three sets of MB studies were carried out on the a) Alexander D1 (Chase Parent) and Alexander D2 (Council Grove) wells in a single-section area, b) Chase Parent wells in a nine-section area around the Flower A1 well, and c) Chase wells in the 12-section area around the Hoobler well. The choice of study sites for material balance studies is intentional because the sections around the Alexander D1 well and the Flower A1 wells have a pair of Chase Parent and Council Grove wells located in the same section, while the Hoobler area has only Chase Parent wells in operation.

a) The P/z vs. Gp plot at the Alexander D1 (Chase Parent) well indicates that the pressure and production data follow a linear trend until 1975 when the Alexander D2 (Council Grove) well, located in the same section, started to produce. The onset of production from the Council Grove well is marked by a loss of linearity on the P/z vs. Gp data from the Chase Parent well. The post-1975 production and pressure data from the Chase well deviated up and away from the previously established linear trend suggesting addition of energy to the reservoir system drained by the Chase Parent well. However, in the absence of any water or gas injection, this loss of linearity may be explained by communication between the Chase and the Council Grove reservoirs as a result of hydraulic fracturing of the Council Grove wells. Thus post-1975, the shut-in pressures recorded at the Chase wells were affected by the higher pressure prevalent in the Council Grove zones.

b) MB plots for the Chase Parent wells in the Flower area show loss of linearity in the early 1970's, when the Council Grove wells, located in the same corresponding sections, were hydraulically fractured and put on production. The pressure and production data, from the mid- to late-1970's, plot away and above the linear trend established by the previously recorded data at each of the Chase Parent wells. Absent any fluid injection in the Flower area, the post-1975 P/z vs. Gp data indicate that the Chase and the Council Grove reservoirs were in communication as a result of which the shut-in pressures recorded at the Chase parent wells were influenced by the higher pressures prevalent in the Council Grove reservoir.

c) The MB plots for five Chase wells in the Hoobler area continue along a linear trend for most of their production life. Because of the absence of any producing Council Grove wells, located in the same section as the Chase wells, the P/z vs. Gp plots for these wells show a profile typical of a volumetrically driven gas reservoir. Previous multi-section simulation studies in the Hoobler area have confirmed that well performances at these wells were history matched without extending completions beyond that reported in the initial well reports.

d) The interference of the Chase Infill wells on the production of their respective Chase Parent wells (drilled in the same section) is evident on MB plots of Alexander D1 and also the Chase Parent wells in the Flower area, indicating presence of good reservoir communication within Chase layers in the respective study areas.

e) As expected, the MB plots for the Hoobler area Chase wells, which were history matched without extending initially reported completions, show a linear trend that is not disrupted until the 1990's because no Council Grove wells are producing from the same sections as these Chase wells.

f) For the Hoobler area Chase wells, where completions were extended post-1970 into the deeper Chase pay zone to history match respective well performances, the MB plots indicate a loss of linearity in the 1970's. The P/z vs. Gp data during the post-1970 period strays up and away from the previously established trend because recompletions at these wells resulted in increasing the drainage volumes that are in communication with the respective wells.

MB studies have demonstrated that coincident with the start of production from Council Grove wells, the P/z vs. Gp plot of the Chase wells (located in the same section) shows a loss of linearity suggesting communication between the Chase and Council Grove layers as a result of hydraulic fracturing at the Council Grove wells. As expected, this loss of linearity is not observed on MB plots of Chase wells that do not have a Council Grove well producing from the same section. Also, the MB plots of the Chase Parent wells show interference effects due to the start of production from the corresponding Chase Infill well, located in the same section, suggesting good hydraulic communication within the Chase layers in these study areas.

References:

Bhattacharya, S., Dubois, M. K., and Byrnes, A. P., 2004, Multiwell characterization and simulation – Chase/Council Grove reservoir systems, Kansas Geological Survey Open File Report 2004-67.

Bhattacharya, S., Dubois, M. K., and Byrnes, A. P., 2005, Reservoir simulation of nine-section area around Flower A1 well – Chase/Council Grove reservoir systems, Kansas Geological Survey Open File Report 2005-54.

Bhattacharya, S., Dubois, M. K., and Byrnes, A. P., 2006, Reservoir simulation of Hoobler study area – Chase/Council Grove reservoir systems, Kansas Geological Survey Open File Report 2006-27.

Lee, J., and Wattenbarger, R. A., 1996, Gas Reservoir Engineering, Society of Petroleum Engineers, Richardson, TX, p. 349.

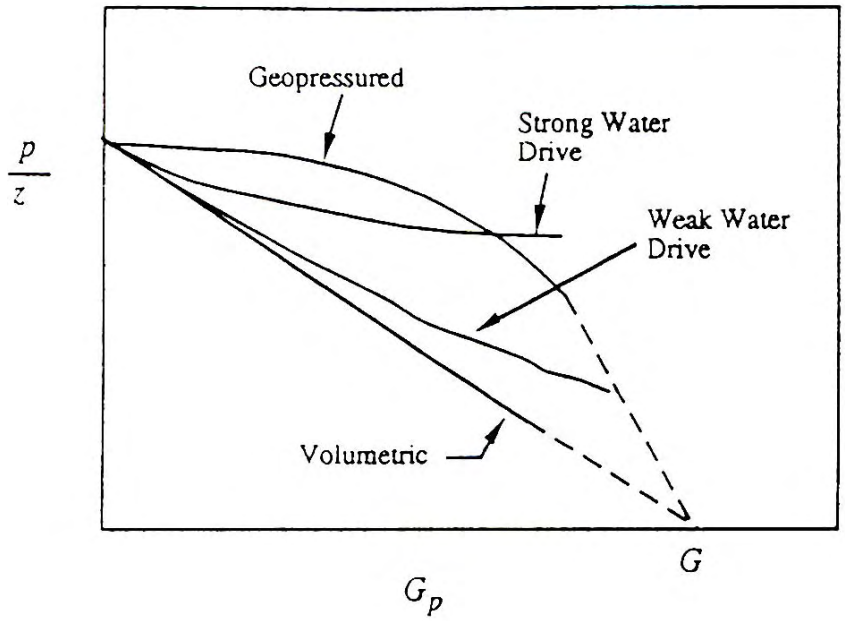

Figure 9.6.1. Expected profiles of P/z vs. Gp curves for reservoirs producing under different drive mechanisms from Lee and Wattenbarger, 1996, p. 236.

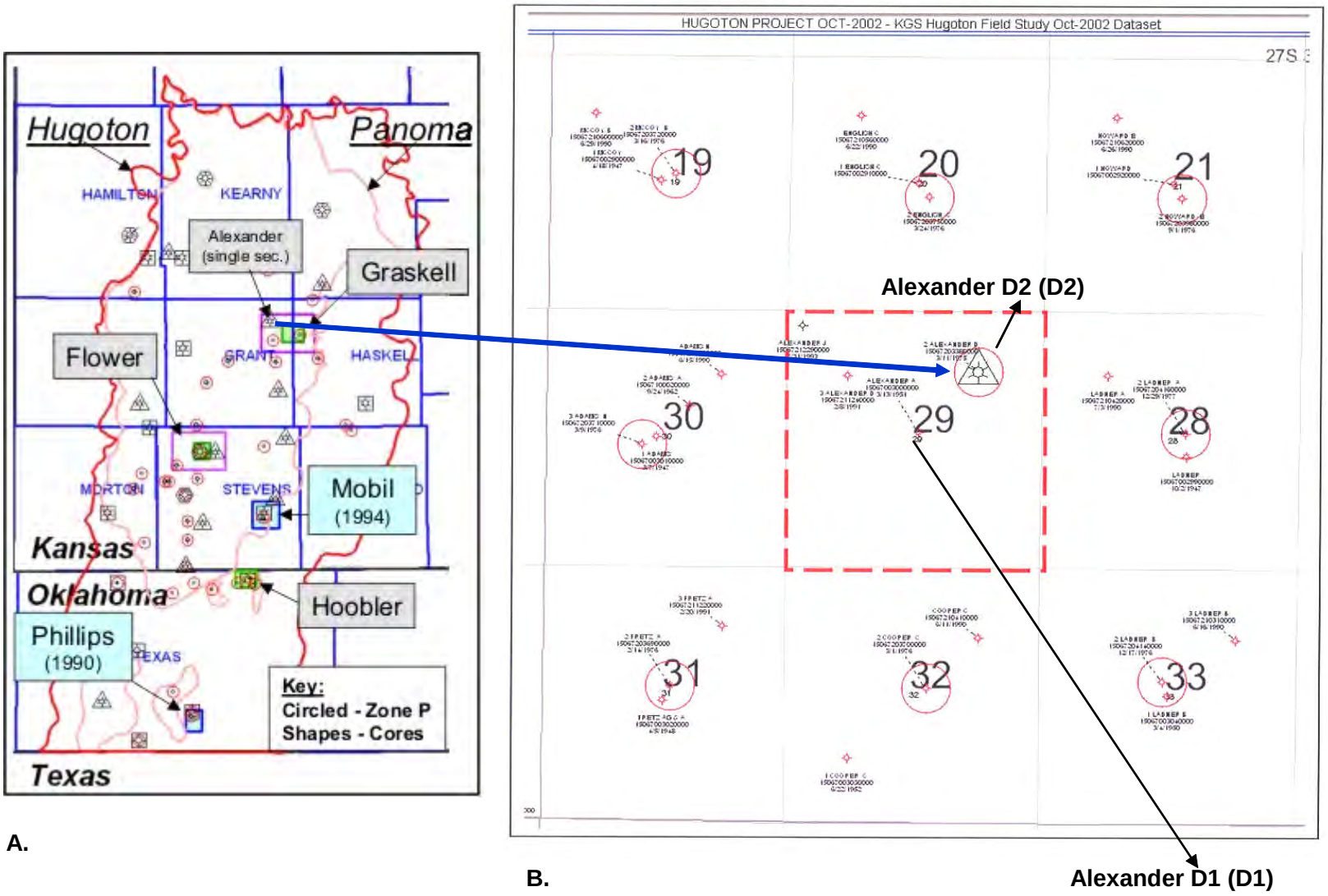

Figure 9.6.2. A) Map showing the layout of the Hugoton and Panoma fields along with the location of the Alexander wells. B) Map showing the relative locations of the Alexander D1 and D2 wells.

Material-balance Studies – Alexander D1

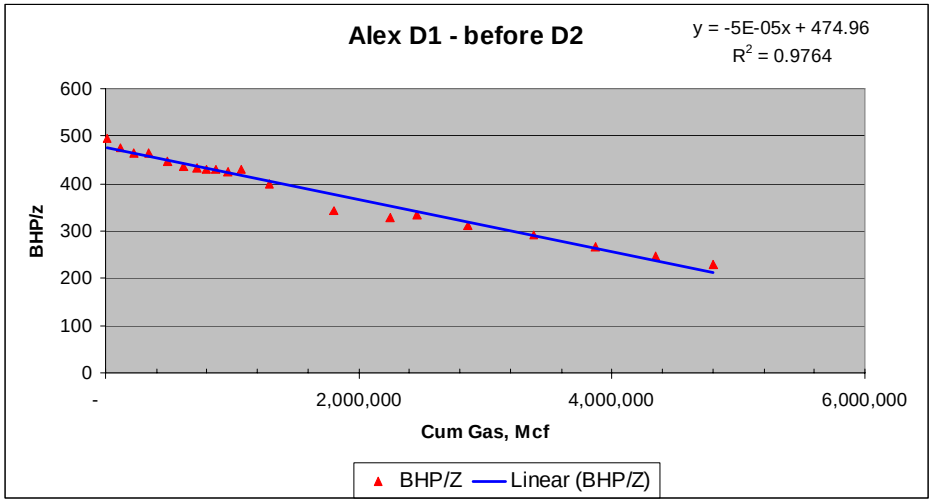

Material balance formulation:

P/z = Pi/zi - (Pi/zi)*(Gp/G)

Total gas reserves:

Pi/zi	474.96 psi	
G	9,499,200 mcf	
Gp	4,803,477 mcf	
RF	0.51	(as of Dec 1990)

Pre-1975 data estimates OGIP to 9.5 bcf.

Figure 9.6.3. Plot of P/z vs. Gp data from Alexander D1 until 1975, and original-gas-in-place calculation from the material-balance plot.

Material-balance Studies – Alexander D1 and D2

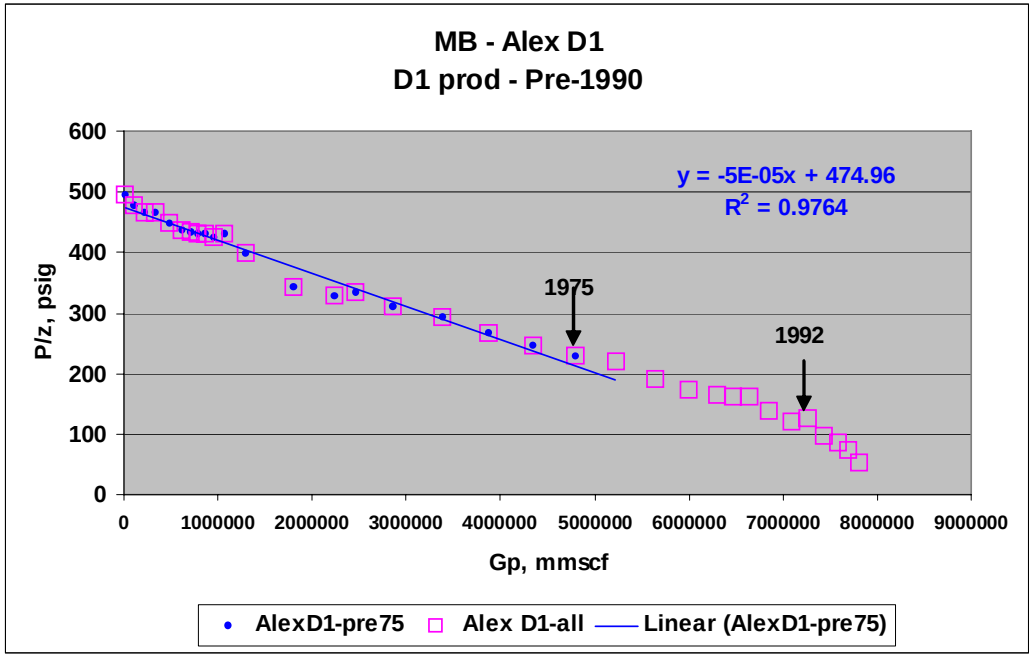

Figure 9.6.4. Plot of P/z vs. Gp data from Alexander D1 until 1990.

Material-balance Studies – Alexander D1 and D2

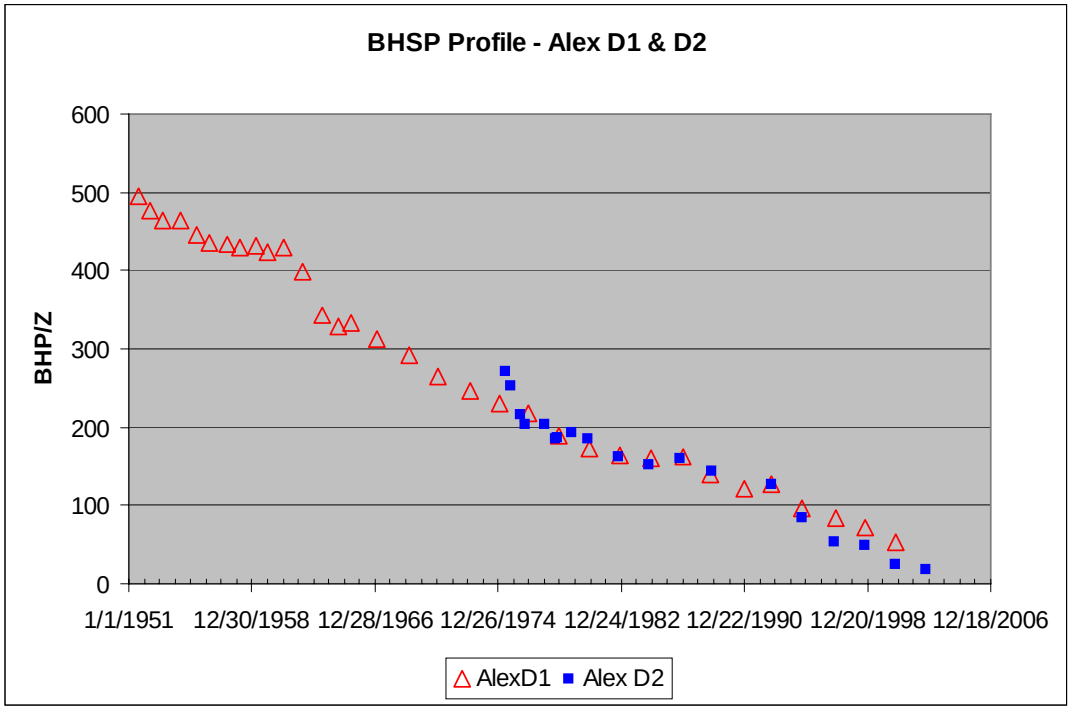

Figure 9.6.5. Plot of bottom-hole shut-in pressures recorded at Alexander D1 and D2 wells.

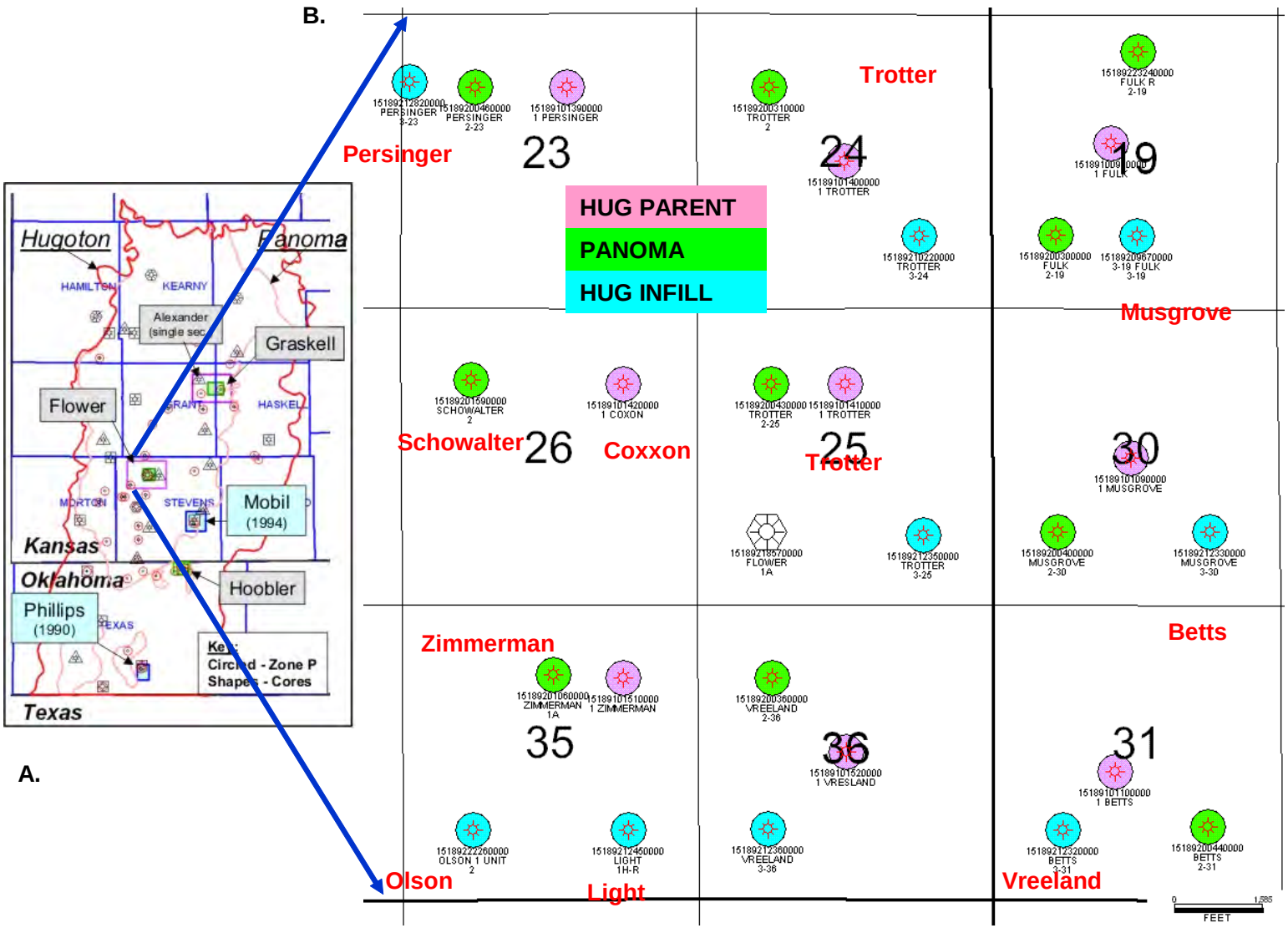

Figure 9.6.6. A) Map showing location of the Flower study area in the Hugoton and Panoma fields. B) Location of the Chase Parent, Council Grove, and Chase Infill wells in the Flower study area.

Material-balance Studies – Flower Area

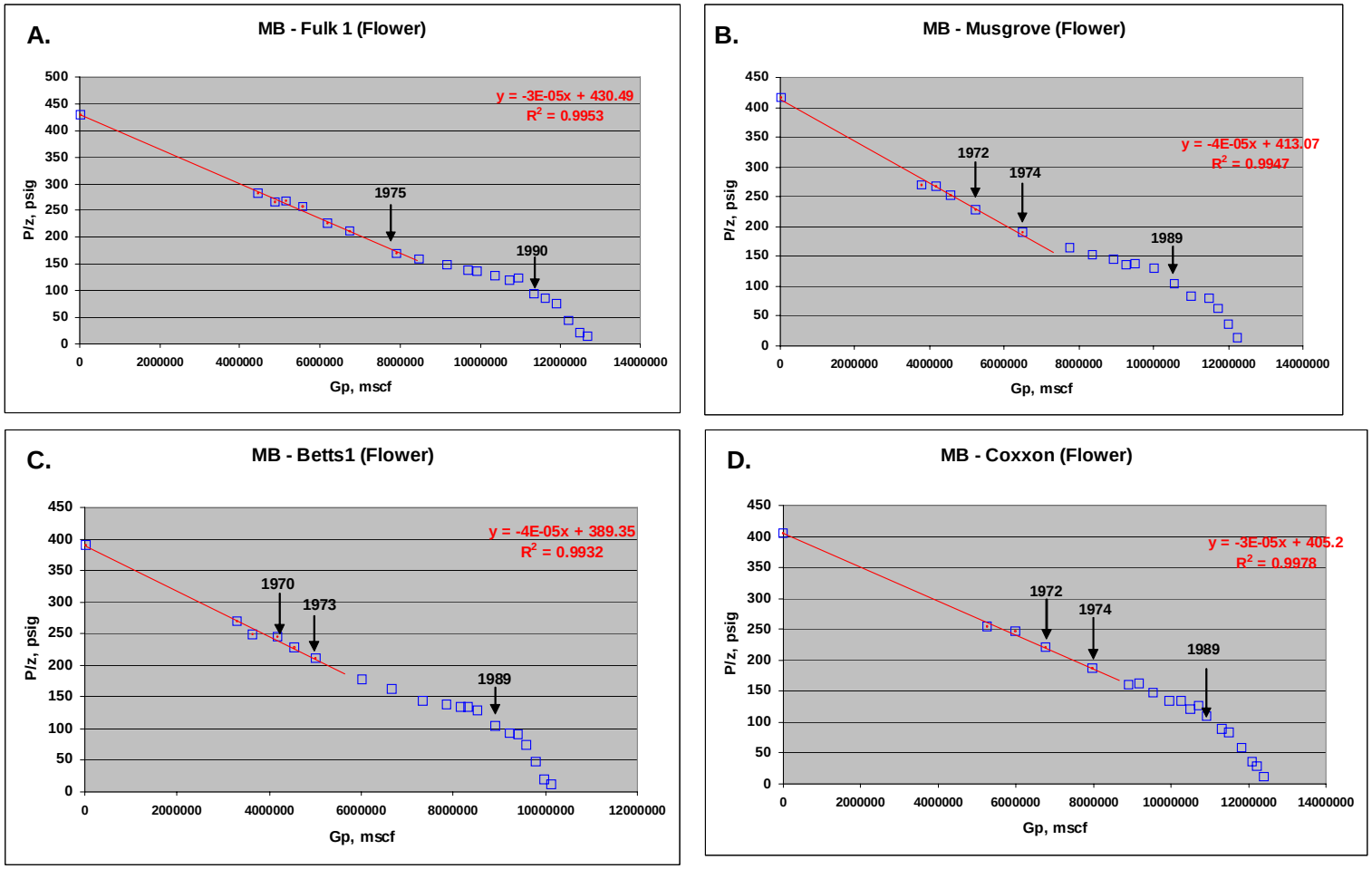

Figure 9.6.7. P/z vs. Gp plots for Chase Parent wells in the Flower study area.

Material-balance Studies – Flower Area

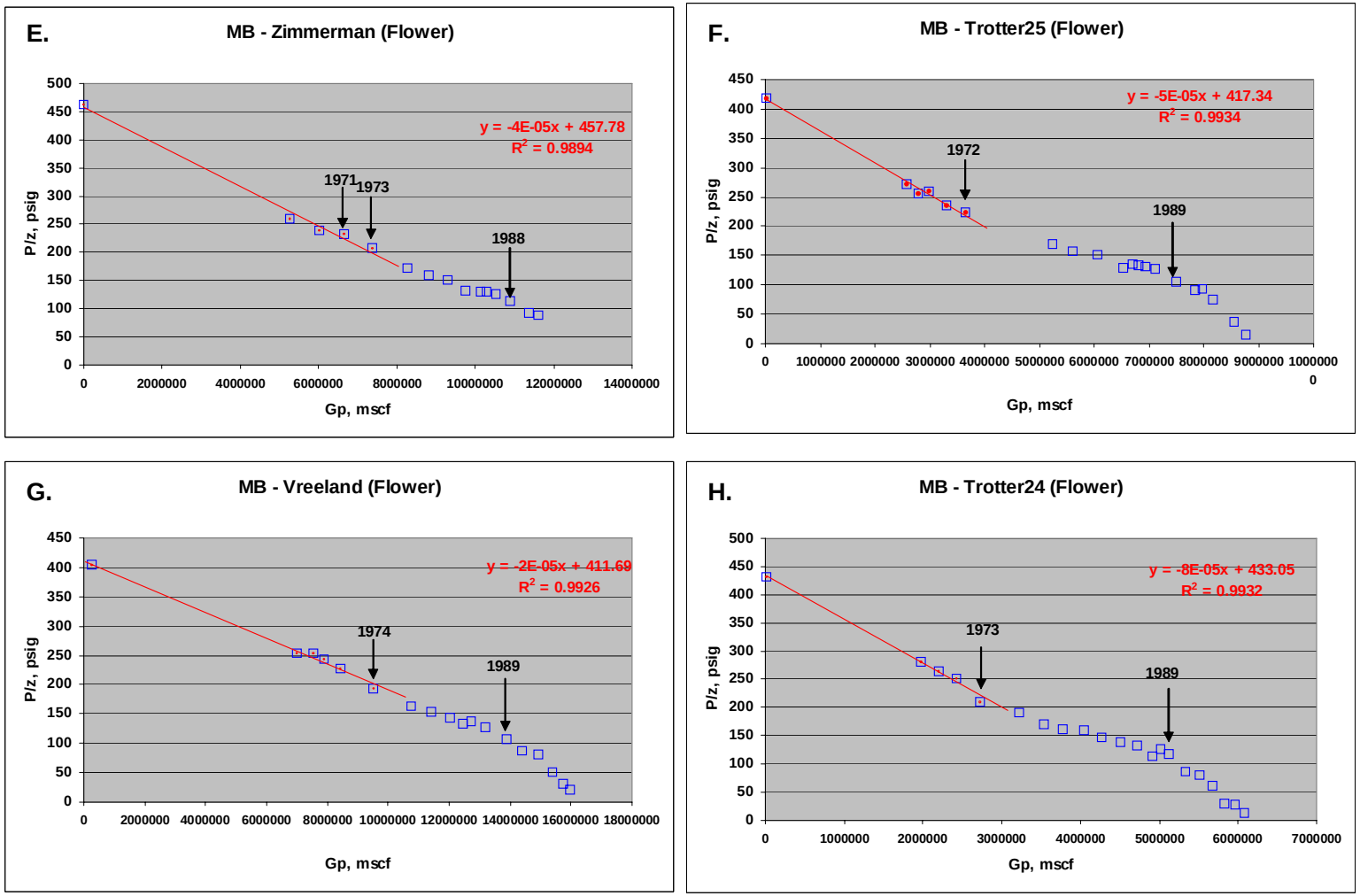

Figure 9.6.7. P/z vs. Gp plots for Chase Parent wells in the Flower study area.

Material-balance Studies – Flower Area

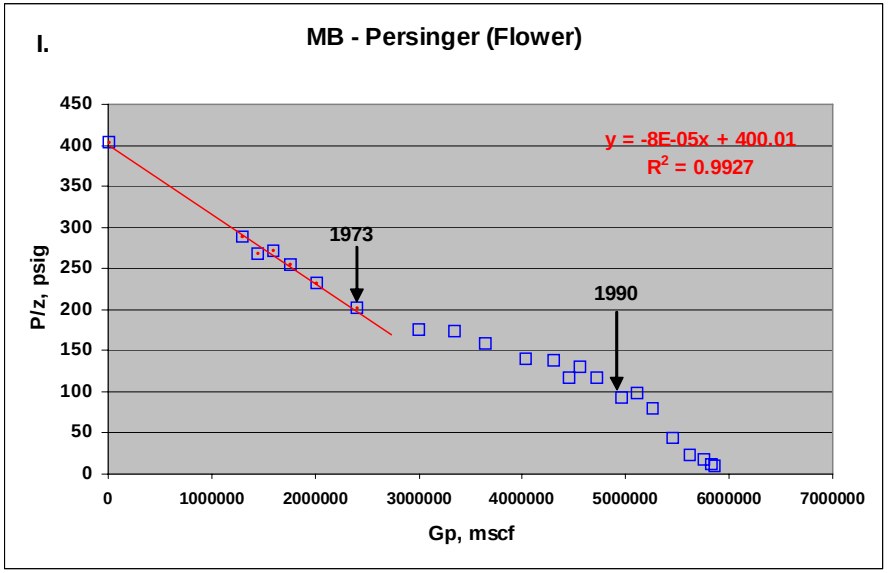

Figure 9.6.7. P/z vs. Gp plots for a Chase Parent well in the Flower study area.

Material-balance Studies – Flower Area

Council Grove wells – Flower Area

	Well	Sim Name	Start Date
1	Trotter2-25	CGTrot25	05/01/1970
2	Schowalter2	CGScho	03/01/1973
3	Zimmerman1A	CGZim	07/01/1972
4	Vreeland2-36	CGVre	05/01/1970
5	Betts	CGBet	06/01/1970
6	Fulk	CGFulk	05/01/1970
7	FulkR	CGFulkR	02/01/2000
8	Muskgrove	CGMus	05/01/1970
9	Persinger	CGPer	06/01/1970
10	Trotter2	CGTrot24	06/01/1970

A.

Chase Infill wells – Flower Area

	Well	Sim Name	Start Date
1	Light	ILigh	10/01/1989
2	OlsonU1	IOlsn	10/01/1997
3	Vreeland	Ivre	12/01/1988
4	Fulk3-19	IFulk	01/01/1988
5	Betts	IBet	11/01/1988
6	Musgrove	IMus	11/01/1988
7	Persinger	IPer	12/01/1988
8	Trotter3-24	ITrot24	01/01/1988
9	Trotter3-25	ITrot25	11/01/1988

B.

Figure 9.6.8. A) List of dates showing start of production at Council Grove wells in the Flower study area. B) List of dates showing the start of production for Chase Infill wells in the Flower study area.

Hoobler Study Area

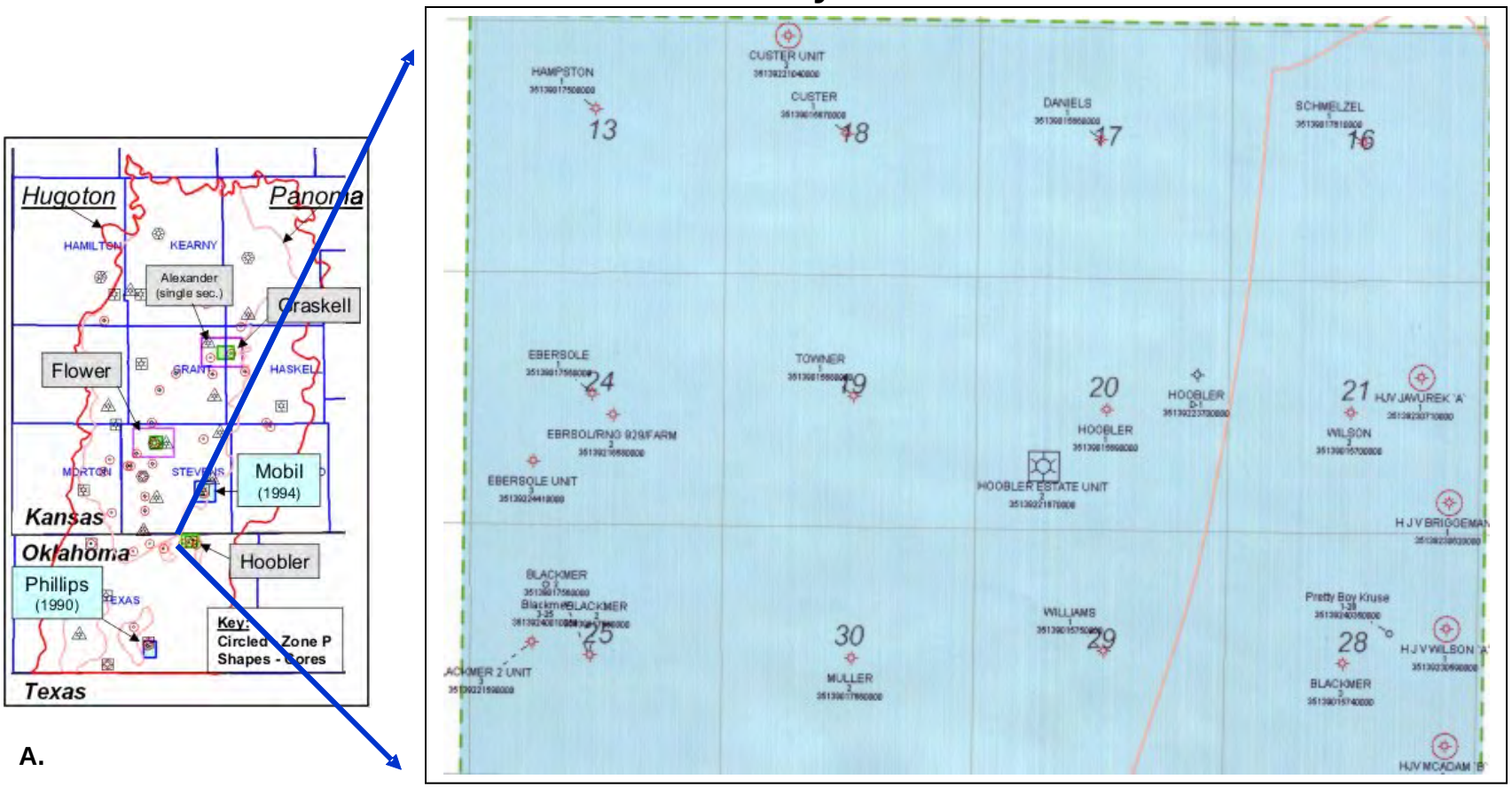

Figure 9.6.9. A) Map showing location of the Hoobler study area in the Hugoton and Panoma fields. B) Location of the Chase wells in the Hoobler study area. Wells circled in red produce from the Hooker North field in a downdip position separate from the Panoma field.

Material-balance Studies – Hoobler Area

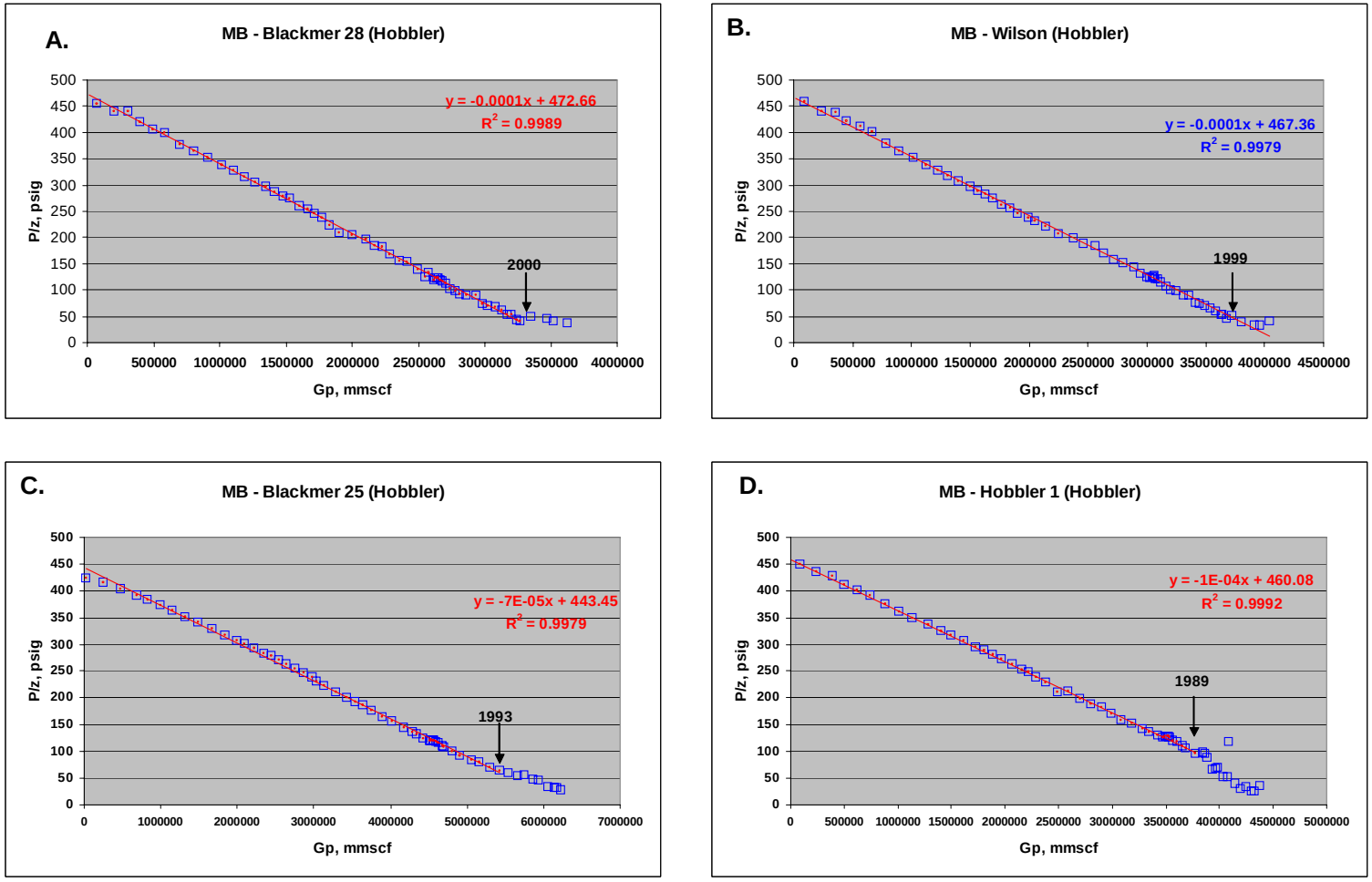

Figure 9.6.10. P/z vs. Gp plots for Hoobler area Chase wells whose completions were not extended beyond Layer 4 during simulation history matching.

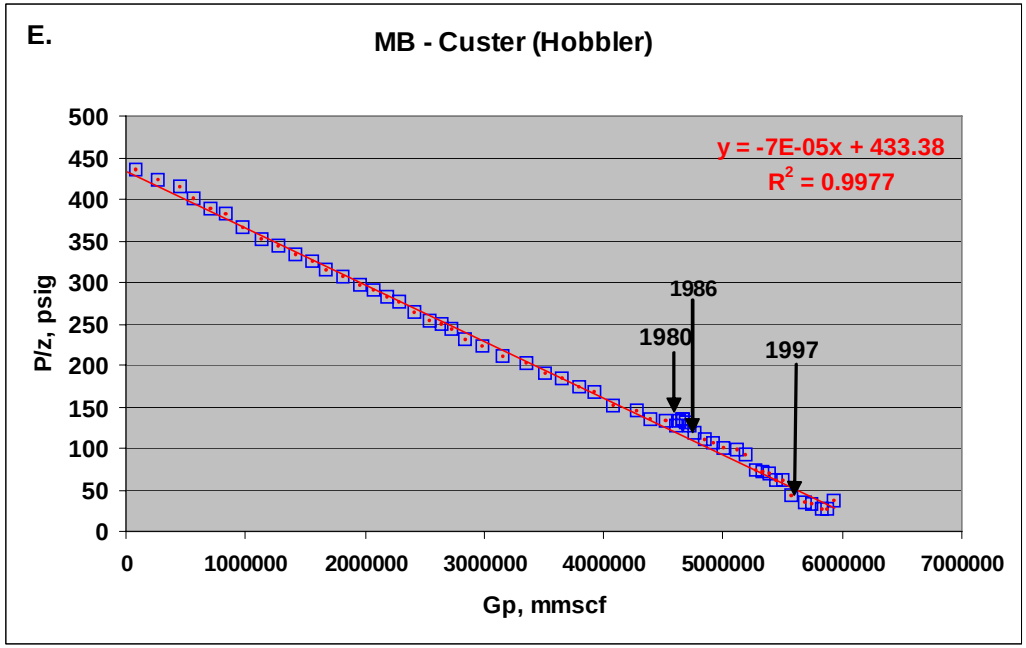

MB trend line indicates that something taking place at the well near 1979 that resulted in a loss of linearity of the P/z vs. Gp data.

Figure 9.6.10. P/z vs. Gp plots for a Hoobler area Chase well whose completions were not extended beyond Layer 4 during simulation history matching.

Material-balance Studies – Hoobler Area

A.

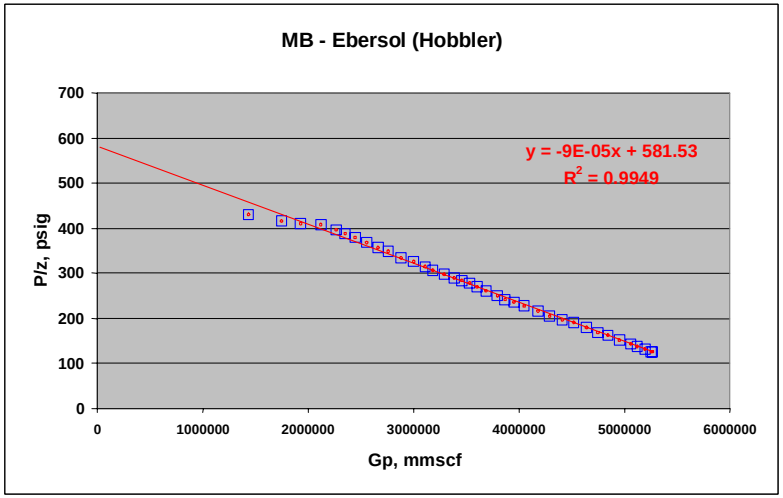

Ebersol did not require completions to extend beyond L4 for history matching.

B.

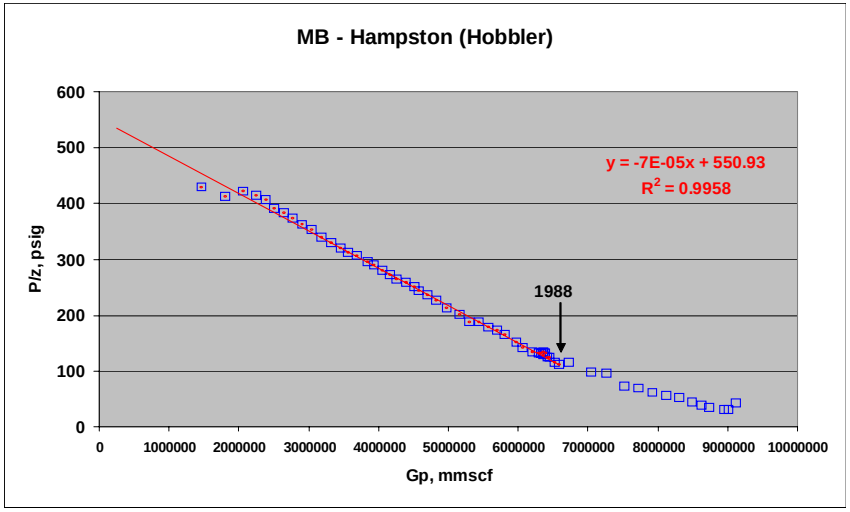

Completions were extended in Hampston to L6 in 1970 for history matching.

Figure 9.6.11. P/z vs. Gp plots for Hoobler area Chase wells with uncertain initial production histories.

Material-balance Studies – Hoobler Area

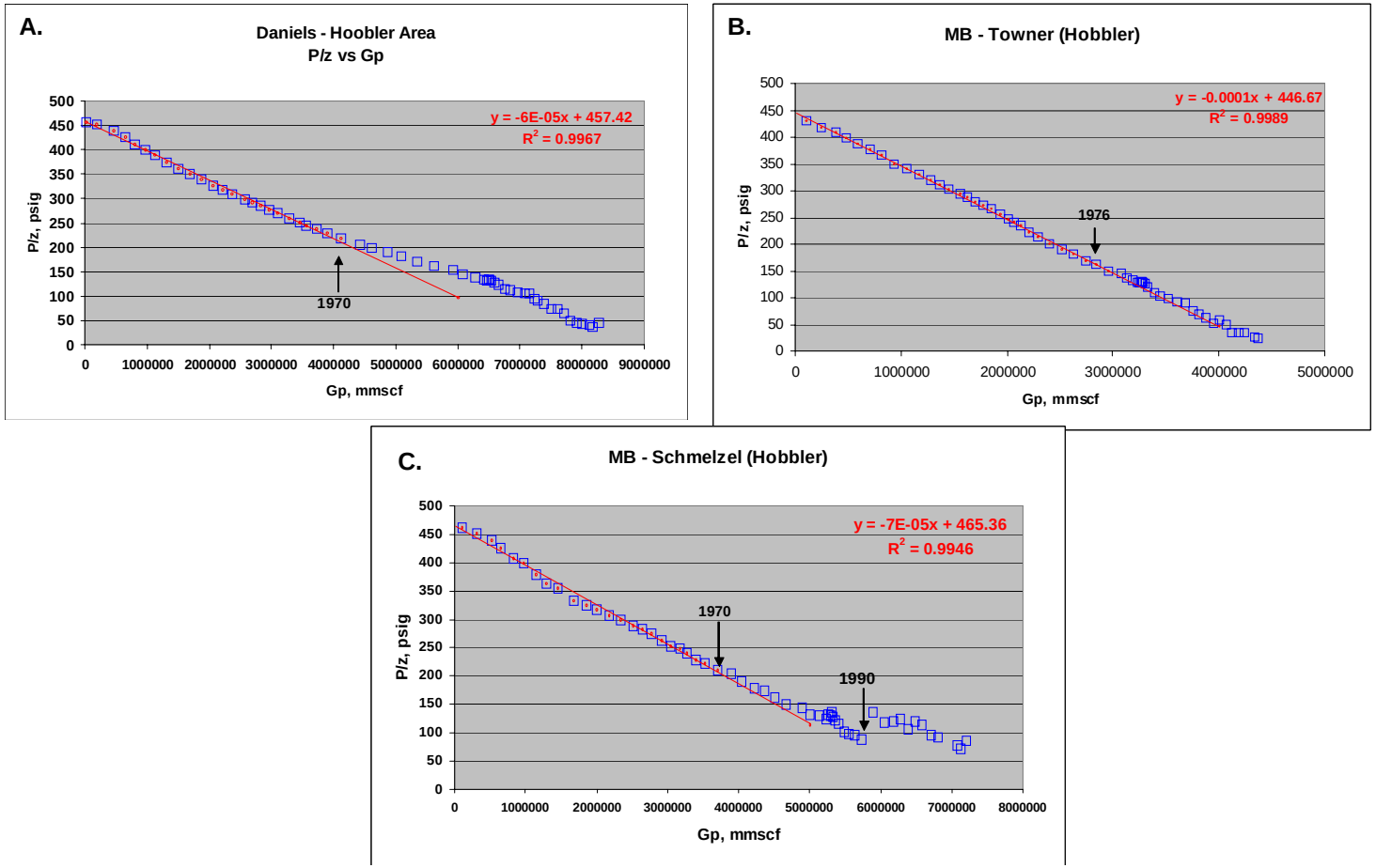

Fractures extended to L6 in 1970 for history matching.

Figure 9.6.12. P/z vs. Gp plots for Hoobler area Chase wells whose completions were extended to Layer 6 after 1970 during simulation history matching.

Material-balance Studies – Hoobler Area

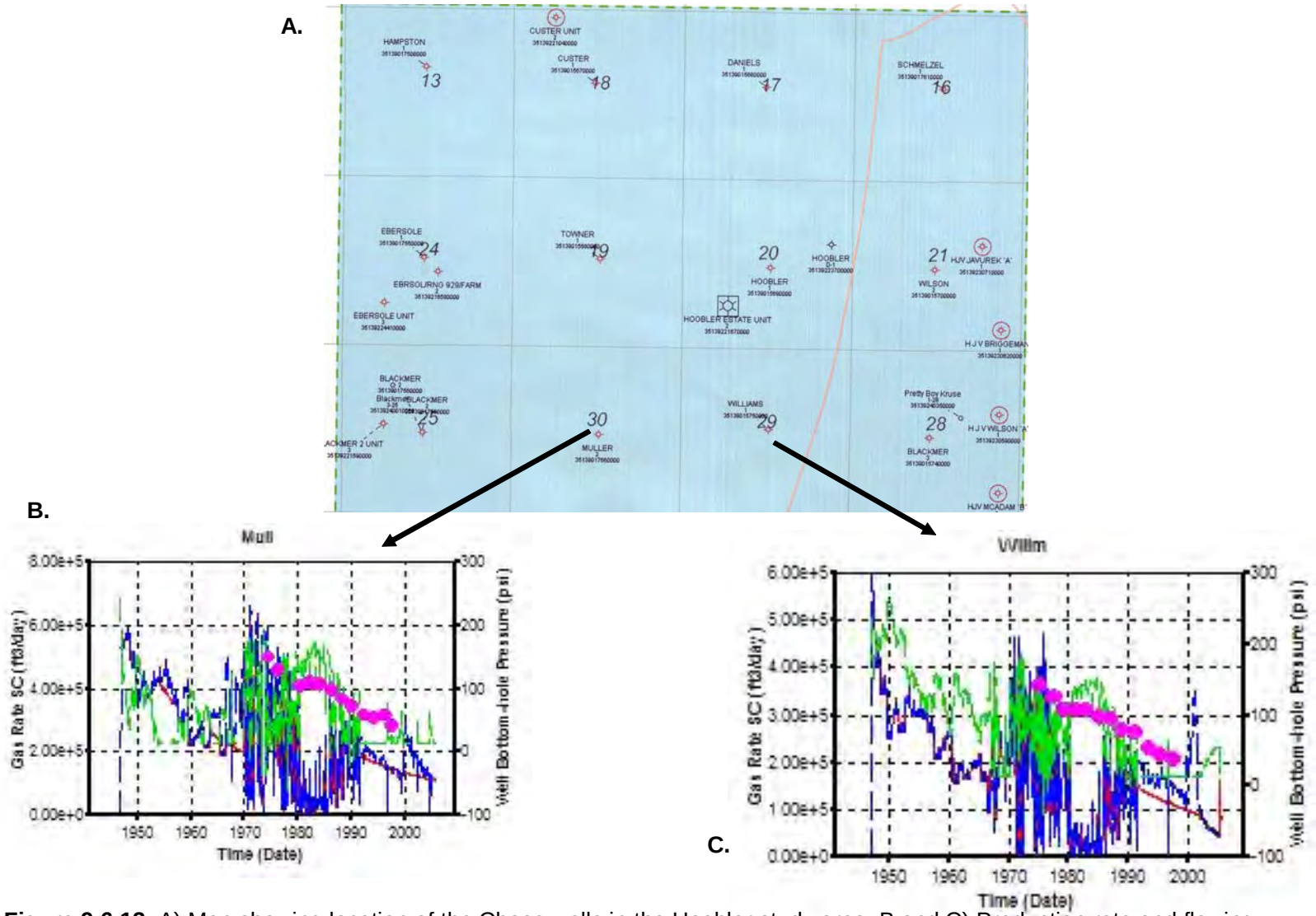

Figure 9.6.13. A) Map showing location of the Chase wells in the Hoobler study area. B and C) Production rate and flowing-pressure history matches at Muller (Mull) and Williams (Willm) wells located in the Hoobler study area.

Material-balance Studies – Hoobler Area

A.

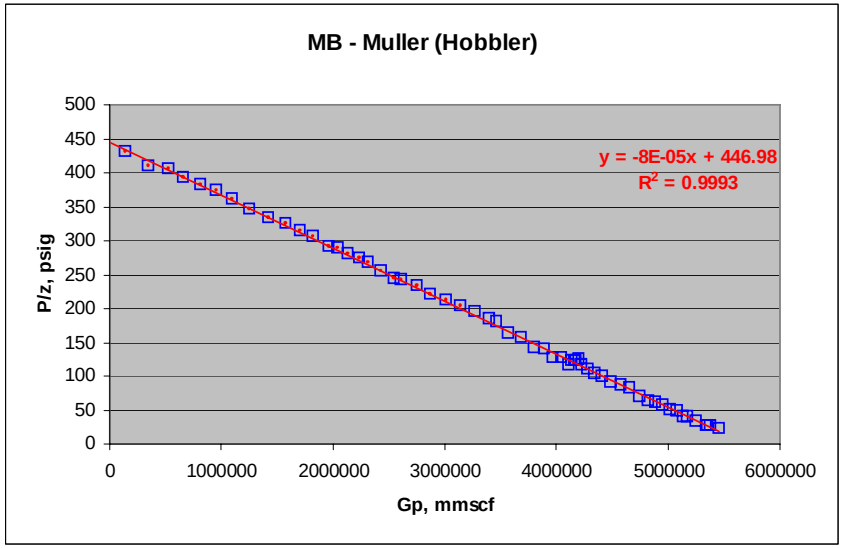

B.

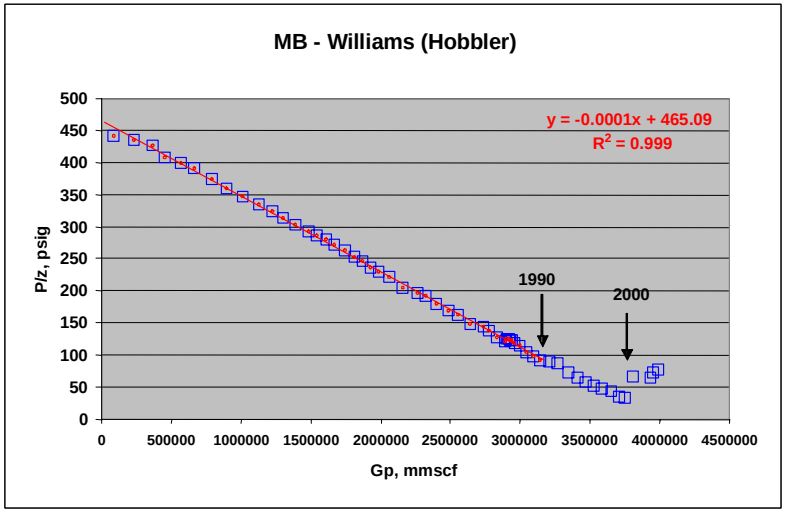

Figure 9.6.14. A) P/z vs. Gp plot for Muller well in the Hoobler study area. B) P/z vs. Gp plot for Williams well in the Hoobler study area.

9.7 LESSONS LEARNED

Saibal Bhattacharya

Introduction

Reservoir simulation and material-balance studies were carried out at different scales and areas of the Hugoton and Panoma fields to validate the full-field geomodel of Chase and Council Grove systems detailed in the previous sections of this report. The primary goal of these engineering studies was to see how close, with minimum modifications, the underlying geomodel came to match well performance. The intent was not to model and simulate the hydraulic fractures at the well to the greatest detail possible or to obtain the most aesthetically pleasing production and pressure history matches. Such tasks need to and will be carried out by workers with goals to evaluate and exploit remaining pockets of reserves using the general framework of the geomodel detailed in this report.

Single-section Simulation Studies – Alexander wells

A 640-acre area around the Alexander D2 (D2), a Council Grove well, was simulated using a 25-layer model. Alexander D1 (D1), a Chase Parent well, located in the same section as D2, was also modeled in this study under the assumption that both D1 and D2 drain from the same 640 acres. This simulation study was carried out until February 1991, i.e., before the completion of Alexander D3 (D3) – a Chase infill well. Each layer in the model was populated with petrophysical properties obtained from wireline logs (recorded at Alexander D2) and from core-analysis data available from the Hugoton and Panoma fields. Within the area simulated, each layer was assumed to have uniform porosity, thickness, and saturation values. Layer porosity and thickness were determined from wireline logs recorded at Alexander D2 while facies-specific capillary-pressure curves were used to estimate the initial fluid saturation based on an assumed free-water level. The Alexander D1 and D2 wells were located centrally in the model area.

Production and pressure history matches at D1 and D2 were obtained when the D1 well was completed in the Chase layers and D2 completions were extended to the Towanda (Layer 6 in the Chase reservoir), and when the volumetric OGIP was reduced by 7.25%. Also, such a model did not show excess flow capacity when D1 and D2 were flowed free of rate constraints. This study showed that completions of the Council Grove well (here D2) had to be extended into Chase layers to history match recorded production at the Council Grove well. Thus, the Council Grove well (D2) produced gas from the Chase intervals. When D2 completions were extended to the Fort Riley (Layer 8 in Chase reservoir), D1 showed excess flow-capacity while D2 showed less than the required flow capacity to match previously established decline trends particularly in the post-1991 period. Fetkovich et al. (1994) and Oberst, et al. (1994) report results from single-and multi-well simulation studies that modeled only the Chase Parent well in the Hugoton field. These studies reported a reduction in volumetric original-gas-in-place (OGIP) to history match Chase Parent well performance. It appears from this study, that such a

reduction of volumetric OGIP was necessary because these studies did not take into account the drainage of Chase gas by Council Grove wells, and also because initial water saturations were calculated from wireline logs especially when fluid invasion is a prevalent problem all over the field.

Multi-section Simulation Studies – Flower Area

A 9-section area around the Flower A1 well (Sec. 25, T. 31 S., R. 38 W.) was simulated. Each section in the study area had a Chase Parent well, a Council Grove well, and a Chase Infill well. Available data included a complete core through the Chase and Council Grove interval and layer-specific DST from the Flower A1 well - a "science well" that was drilled with foam to minimize invasion and was never used as a production well. Core-plug and whole-core porosity and permeability data were available from both the Chase and Council Grove zones and were used to estimate permeability multipliers necessary to convert permeability estimated using facies-specific correlations to effective permeability calculated from layer-specific DST tests. Also, 6 node wells were located within the study area with qualified well logs that were used to build a fine-scale 234-layer regional geomodel from which the relevant 9-section area was extracted and upscaled to 25 layers.

Pressure and production history matches were obtained at the Chase Parent, the Council Grove wells, and the non-border Chase Infill wells when the completions at the Chase wells were constrained to the Chase interval and the Council Grove completions were extended to the Krider (Layer 2 in the Chase interval). Simulation results of such a model also resulted in minimum or no extra flow capacity when wells were released of flow constraints. Also, the simulator-calculated shut-in pressures ranged between 238 to 256 psi at Council Grove wells completed in 1970 in the above-mentioned geo-model. A close match was obtained between simulator-calculated layer pressures to layer-specific DST pressures recorded at the location of the Flower A1 well as of January 1995. Future production rates estimated from the simulation studies indicated a near-term annual decline between 6 to 8% and a long-term decline close to 2% around 2040.

This study clearly showed that the underlying upscaled geomodel with slight modifications, especially by adjusting the core-derived permeability to effective permeability calculated from layer-specific DSTs, resulted in history matches of production and pressure performances at Chase Parent, Council Grove, and non-border Chase Infill wells and also in close matches of layer pressures obtained from layer-specific DSTs. The driver zone in this study area is Krider (Layer 2) in the Chase reservoir.

Multi-section Simulation Studies – Graskell Area

This study was carried out on a twelve-section area (T. 28 S., R. 35 W. to T. 27 S., R. 34 W.) straddling Grant and Haskell counties in Kansas. No cores or layer-specific DST data were available from within the study area. Layer-RFT pressure data were available from 1 well within the study area and from some others outside the study area.

The RFT data showed significant variation in pressures within each pay layer. Cores representative of the Council Grove interval were available from 1 well outside the study area. Thus, porosity and permeability readings measured on core plugs and whole cores from the Council Grove interval were available. No cores representative of the Chase interval in the study area were available. For Council Grove layers, upscaled layer permeability, estimated from facies-specific permeability-porosity correlations, was compared with the core permeability to derive permeability multipliers. Absent a Chase core, the permeability multiplier calculated for the Council Grove layers was applied to the Chase layers. Though 8 node wells with qualified wireline logs were located in the study area, none was positioned in the southwestern or southeastern corner. Like in the Flower area, a Chase Parent well, a Council Grove well, and a Chase Infill well were located in each section in the study area.

The current geomodel for the Graskell study area has insufficient original-gas-in-place (OGIP) and permeability distribution along the southern and southwestern border areas to enable production history matches at Chase Parent, Chase Infill, and Council Grove wells located therein. It is, therefore, imperative that the underlying geomodel be modified to enable successful history matching (of production and pressure) at all wells within the study area. For wells located in the study area and away from the southern or southwestern borders, the simulator-calculated production matches or is close to matching the historic volumes. The simulator-calculated (bottom-hole) flowing pressures are close to and follow the trends set by recorded (surface) flowing pressures particularly at wells where good production matches have been obtained. Production spikes are visible at most wells when released of flow constraints despite production and pressure history matches indicating presence of excess flow capacity in the current model in the drainage areas of the corresponding wells. The best simulation history match was obtained when the Chase Parent wells were completed to the Fort Riley (Layer 8 in the Chase reservoir) and the completions in the Council Grove wells were extended to the Fort Riley. Also, additional permeability multipliers, i.e., 2 for Towanda (Layer 6 in Chase) and Fort Riley and 6 for Herington (Layer 1 in Chase), were employed over and above the initial permeability multipliers discussed above to obtain history matches at a majority of the wells.

Significant intra-layer variation in RFT pressures recorded in and around the study area has been observed leading to doubts about the accuracy and representativeness of RFT recordings. Despite lack of history matches at wells located in the areas where OGIP and permeability distribution were found to be less than the required, the simulator-calculated layer-pressure at the Eliot A6 well is close (within 30 psi) to that recorded by RFT measurements for the two major driver zones in the study area, i.e. Towanda and Fort Riley (Layers 6 and 8 in the Chase reservoir). It is hoped that further refinement of the geomodel, particularly along the southern and southwestern borders, will help to attain history matches at these border wells, and thereby lead to better layer-pressure matches.

Multi-section Simulation Studies – Hoobler Area

Reservoir simulation studies were carried out on a twelve-section area around the Hoobler Estate Unit well (sec. 20, T. 6 N., R. 17 E.). One of the primary reasons, in contrast to the Flower and the Graskell areas, for selection of this study area was the absence of Council Grove or Chase Infill wells in any of the sections. Other reasons for selection of this area are as follows: a) it is located outside the Panoma field and on the edge of the "other" Council Grove production area, b) it has a relatively thick Chase gas column, c) a Chase core from within the study area and nearby Council Grove cores were available, and d) limited layer pressure data from 1995 and 2005 were available. There were 6 node wells with modern log suites and three wells with zonal pressure data from within the Hoobler study area. The RFT layer-pressure data show significant pressure variation within pay layers in and around the study area. Permeability multipliers were estimated by comparing upscaled permeability estimated from facies-specific permeability-porosity correlations with upscaled whole-core permeability for each layer.

Out of 16 wells, good matches with production histories were obtained at 13 wells. Close to good matches were obtained with flowing pressure histories at 12 out of the 16 wells in the study area. Small to high production spikes were visible at seven out of 12 producing wells. Production spikes were not visible at the three wells where the simulator-calculated production fell short of historic volumes. The simulator-calculated pore-volume-weighted average layer pressures in Herington (Chase Layer 1), Krider (Chase Layer 2), Winfield (Chase Layer 4), Towanda (Chase Layer 6), and Fort Riley (Chase Layer 8) matched corresponding estimated pressures from available RFT data. The reservoir appears to be more complex than the model input to the simulator because some of the wells show presence of excess flow capacity while others remain short of gas. Thus, any field-wide increase in layer permeability or layer OGIP to obtain production match will result in excess flow capacity at wells where production history matches have already been achieved. None of these Chase wells has been completed in the Fort Riley (Chase Layer 8) and yet 6.4 bcf of gas flowed out of this layer to layers above and to the wells completed in the Winfield (Chase Layer 4) and Towanda (Chase Layer 6). Based on the layer-specific gas-in-place plots, fluid movement appears to be taking place across the shale layers with vertical permeability playing a critical role in determining the amount of fluid flow into and out of the shale layers.

Material-balance Studies

Three sets of MB studies were carried out on the a) Alexander D1 (Chase Parent) and Alexander D2 (Council Grove) wells in a 1-section area, b) Chase Parent wells in a 9-section area around the Flower A1 well, and c) Chase wells in the 12-section area around the Hoobler well. The choice of study sites for material-balance studies is intentional because the sections around the Alexander D1 well and the Flower A1 wells have a pair of Chase Parent and Council Grove wells located in the same section, while only Chase Parent wells produce from the sections in the Hoobler area.

The P/z vs. Gp plot at the Alexander D1 (Chase Parent) well indicates that the pressure and production data follow a linear trend until 1975 when the Alexander D2 (Council Grove) well, located in the same section, started to produce. The onset of production from the Council Grove well is marked by a loss of linearity on the P/z vs. Gp data from the Chase Parent well. In the absence of any water or gas injection, this loss of linearity may be explained by communication being established between the Chase and the Council Grove reservoirs as a result of hydraulic fracturing of the Council Grove wells. Thus the post-1975 shut-in pressures, recorded at the Chase wells, were affected by the higher pressure prevalent in the Council Grove zones.

MB plots for the Chase Parent wells in the Flower area also show loss of linearity in the early 1970's when the Council Grove wells located in the same corresponding sections were hydraulically fractured and put on production. Without any fluid injection in the Flower area, the post-1975 P/z vs. Gp data indicate that the Chase and the Council Grove reservoirs were in communication as a result of which the shut-in pressures recorded at the Chase parent wells were influenced by the higher pressures prevalent in the Council Grove reservoir.

The MB plots for five Chase wells in the Hoobler area continued along a linear trend for most of their production lives. No Council Grove wells are present in any of the sections modeled. The P/z vs. Gp plots for these Chase wells, therefore, plot along a linear trend uninterrupted as is typical in the case of a volumetrically driven gas reservoir. Also, previous multi-section simulation studies in the Hoobler area confirmed that well performance at these wells were history matched without extending initial completions. Thus the MB plots of these Chase wells showed a linear trend without disruptions until the 1990's. However, MB plots indicated a loss of linearity in the 1970's for the Chase wells, in the Hoobler area, whose completions were extended post-1970 into deeper Chase pay zones to history match respective well performances in simulation studies.

MB studies have, therefore, demonstrated that coincident with the start of production from Council Grove wells, the P/z vs. Gp plot of the Chase wells (located in the same section) shows a loss of linearity suggesting communication between the Chase and Council Grove layers as a result of hydraulic fracturing at the Council Grove wells. As expected, this loss of linearity is not observed on MB plots of Chase wells that do not have a Council Grove well producing from the same section. Also, the MB plots of the Chase Parent wells showed interference effects due to the start of production from the corresponding Chase Infill well located in the same section, suggesting good hydraulic communication within the Chase layers in these study areas.

Take-away Observations

a) The representativeness and robustness of the Hugoton geomodel (Chase and Council Grove systems) is validated through well performance history matches at a majority of Chase and Council Grove wells with minimum modifications to the underlying reservoir model. Invasion effects have plagued initial saturation estimation from wireline logs in Hugoton and Panoma fields. In this study, initial saturations were determined from

facies-specific capillary-pressure curves and an assumed free-water level unlike previously reported multi-section studies which used wireline logs to estimate initial saturations. Also, this study attempted to build a full-field geomodel including the Chase and Council Grove reservoirs for the entire field unlike earlier reported studies that modeled a limited area outside the simulation study. Given the enormity of the area modeled, an automated facies-estimation technique was developed and employed to build the geomodel that served as the basis for 1 single-section and 3 multi-section simulation studies.

b) Permeability predicted from facies-specific correlations needs to be correlated with that estimated from layer-DST or whole cores in order to develop appropriate permeability multipliers for input to the simulator. Multipliers developed with help of layer-specific DST tests, as conducted in the Flower area, worked best for history matching well performance.

c) Storage and flow properties as specified by the field-wide geomodel are sufficient to match production from most Chase wells. However for Council Grove wells, completions have to be extended to the Chase layers in order for the simulator-calculated production rates to match historic volumes. Material-balance (MB) studies on data from Chase (Parent) wells indicate presence of communication between the Chase and Council Grove reservoirs. Current fracture-modeling studies suggest that fracturing carried out at Council Grove wells can result in establishing communication with the Chase reservoir. Previously reported studies mention tracer surveys that show upward and downward extension of hydraulic fractures carried out in Chase wells.

d) Production rates from Chase and Council Grove wells in the Flower area currently decline at annual rates varying between 6 to 8%. Simulation studies show that production-decline rates at these wells will reach 2% by 2040 or later.

e) Current simulation studies show evidence of differential depletion between adjacent zones in the Chase and Council Grove reservoirs and thus confirm observations made in previous multi-section simulation studies. However, previous multi-section simulation studies modeled only the Chase reservoir assuming no cross flow between adjacent layers. In this study, vertical permeability for each layer was estimated from available core data.

References:

Fetkovich, M. J., Ebbs, D. J. Jr., and Voelker, J. J., 1994, Multiwell, multilayer model to evaluate infill-drilling potential in the Oklahoma Hugoton field, SPE Reservoir Engineering, Aug 1994, p. 162 – 168.

Oberst, R. J., Bansal, P. P., Cohen, M. F., and Ryan, T. C., 1994, 3-D reservoir simulation results of a 25-square mile study area in the Kansas Hugoton gas field, SPE Mid-continent Gas Symposium, Amarillo, TX, SPE 27931.